

INSIGHTS INTO THE ANTIOXIDATIVE POTENTIALS OF PLANTS AND SKIN

PhD-Thesis

Dissertation

zur

Erlangung des Doktorgrades

der Naturwissenschaften

(Dr. rer. nat.)

dem

Fachbereich Pharmazie der

Philipps-Universität Marburg

vorgelegt von

Reem Mohamed Alnemari

aus **Taif**

Marburg (Lahn), **2023**

Erstgutachter: Prof. Dr. Cornelia M. Keck

Zweitgutachter: Prof. Dr. Udo Bakowsky

Eingereicht am: 20.01.2023

Tag der mündlichen Prüfung: 14.03.2023

Hochschulkennziffer: 1180

Diese Arbeit wurde verfasst unter der Leitung von

Prof. Dr. Cornelia M. Keck

im Fachbereich Pharmazie am Institut für Pharmazeutische Technologie und Biopharmazie
der Philipps-Universität Marburg.

EIDESSTAATLICHE ERKLÄRUNG

Ich versichere, dass ich meine Dissertation

„INSIGHTS INTO THE ANTIOXIDATIVE POTENTIALS OF PLANTS AND SKIN“

selbständig ohne unerlaubte Hilfe angefertigt und mich dabei keiner anderen als der von mir ausdrücklich bezeichneten Quellen bedient habe. Alle vollständig oder sinngemäß übernommenen Zitate sind als solche gekennzeichnet.

Die Dissertation wurde in der jetzigen oder einer ähnlichen Form noch bei keiner anderen Hochschule eingereicht und hat noch keinen sonstigen Prüfungszwecken gedient.

Marburg, den 20.01.2023



Reem Mohamed Alnemari

To Abdulaziz

My potent antioxidant who fights all the free radicals in my life

To Majed and Farah

My little sweet companions in the PhD journey

To my parents (Safia and Mohamed)

The underline reasons for each achievement in my lifetime

My source of power and determination

Acknowledgements

First of all, I would like to express my sincere gratitude to my supervisor **Cornelia M. Keck** for giving me the opportunity to be a part of her incredible team. Her guidance, expertise and overall insights had given me an inspiring experience. Special thanks for her kind support to me as a working mother, especially during my first two years.

Then, I would like to thank my co-supervisor **Jana Brüßler** for her consistent support and guidance during the years of this project. I'm deeply grateful for her productive and thoughtful comments, recommendations and her valuable assistance during the lab work and the thesis writing. I'm lucky to have had the chance to know and work with her.

I would also like to thank **Henriette Dietrich** for the continuous provision of the animal samples and the technical assistance throughout the research period. She is the spirit of the group with the kindest heart and the warmest smile every morning.

Furthermore, I would like to express my eternal gratitude to **karlsbader weg 5 kindergarten** for all their kindness, love and support over four years. My family was so fortunate to have them by our side. With their assistance, we shared raising two sweet Saudi-German kids. I should not also forget to thank **the city of Marburg** for their exceptional support during the Corona crisis. It was very thoughtful of them to give our family the special attention taking into consideration that one of us is in the front lines, facing Corona every day.

Before the end, I cannot forget to thank **my colleagues**. Thank you to my friend and work partner, Abraham. Thank you to Shashank, Danial, Ralph, Noor, David, Sabrina, Ayat, Christian, Jameera and Laura for the joined work and all the nice memories. You will always be in my mind and heart.

Last but not least, my eternal gratitude is to the **ministry of education** of Saudi Arabia and to my sponsor; **Taif University** for the opportunity to study in Germany.

Finally, I would like to acknowledge my husband: **Abdulaziz** for his unconditional love and support during that very intense academic stage.

Table of content

Chapter 1. Introduction	9
1.1. Oxidation; an eternal reaction in living cells	9
1.1.1. Oxidative stress.....	10
1.2. Antioxidants	11
1.2.1. Current challenges in antioxidant’s delivery	13
1.3. Antioxidants in biology: skin as a model organ	14
1.3.1. Antioxidant skin barrier	14
1.3.2. Oxidative stress in skin.....	15
1.3.3. Effect of the pro-oxidant elements on skin	16
1.3.4. Antioxidants as cosmeceuticals agents	18
1.4. Assessment of oxidative state	20
1.4.1. In plants.....	20
1.4.2. In cosmeceuticals agents	25
1.4.3. In skin and biological tissues.....	26
Chapter 2. Aims of the thesis	28
Chapter 3. Materials and methods.....	29
3.1. Materials	29
3.1.1. List of the used materials.....	29

3.2. Methods.....	31
3.2.1. The plants model	31
3.2.2. The skin model	36
3.2.3. Statistical analysis	40
Chapter 4. Results and discussions.....	41
4.1. The plant model:.....	41
4.1.1. Antioxidative properties of plants and plant formulations	41
4.2. The skin model.....	74
4.2.1. General investigations of skin properties of porcine ears—intact versus impaired skin	74
4.2.2. Skin intrinsic antioxidant capacity	93
4.2.3. Treatment impact on skin antioxidant capacity—topical antioxidants.....	106
4.2.4. Treatment impact on skin antioxidant capacity—UV radiation	158
Chapter 5. Summary	172
Chapter 6. Zusammenfassung	174
Chapter 7. References	176
Chapter 8. Curriculum vitae	202
Chapter 9. Publications.....	203

Chapter 1. Introduction

1.1. Oxidation; an eternal reaction in living cells

The abundant aerobic environment on Earth 2.4 billion years ago resulted in what the scientists have called “The Great Oxidation Event.” It is considered to be the main evolutionary event of all the living entities, as the oxygen-rich atmosphere provided these entities with more energy and increased the ability to metabolise nutrients [1]. Therefore, a huge expansion in kind and nature of the microbes has started and lasted. Yet, the presence of oxygen also brought with it another consequence mostly classified as harmful, the oxidation. This reaction is essential and one of the main eternal life reactions. Generally, it entails the addition of oxygen or the withdrawal of hydrogen or electrons, as well as the generation of free radicals as a by-product [2]. In biological tissue, the damage caused by these radicals begins when they become available in healthy cells, causing molecular and cellular injury and eventually leading to a condition of disease. The production of these free radicals can be endogenous or exogenous, as shown in **Figure 1**.



Endogenous free radicals	Mitochondrial chain
	Phagocytes
	Endoplasmic reticulum
	Enzymes
	Heme protein
	
Exogenous free radicals	UV radiation
	Air pollution
	Ionising radiation
	Smoking
	Processed food
	

Figure 1: Free radical's sources affecting the living cells

Free radicals can be defined as the atoms or molecules that contain an odd number of electrons and are able to exist independently [2, 3]. Reactive oxygen species (ROS), reactive nitrogen species (RON), and reactive sulphur species (RSS) are among the most common species in biology. Examples of the most dominant reactive species (radicals and nonradicals) include the following [2, 4]:

- The hydroxyl radical (OH^\bullet) is a nonselective highly reactive radical, which acts by abstracting the proton from the element or oxidising a metal atom through the electron transfer process.
- Hydrogen peroxide (H_2O_2) is a less active molecule; it can be produced by aerobic metabolism and deactivated by cellular enzymes like catalase.
- The peroxy radical (ROO^\bullet) possesses significant diffusion through biological membranes and has a relatively extended half-life. It can be produced during the lipid peroxidation process, which is begun by the removal of a hydrogen atom from polyunsaturated fatty acids.
- Ozon (O_3) is an exogenous oxidising agent that triggers a degradation cascade in the respiratory system and skin through an electron-transfer reaction, and finally producing the OH^\bullet radical. In contrast, however, it also serves the environment by protecting the Earth from the damaging effects of ultraviolet (UV) radiation, especially UVC.
- The nitric oxide radical (NO^\bullet) is considered to be an essential substance in human biochemistry, as it participates in the neurotransmission and vasodilation processes to lower blood pressure. However, an excess of NO^\bullet is cytotoxic. It can react directly with biomolecules or with ROS to form the peroxynitrite reactive species (ONOO^-).

1.1.1. Oxidative stress

Due to the unpaired electron(s) in the outer orbital, free radicals are highly reactive, unstable, and have a short half-life. Therefore, a consequent reaction with the surrounding cellular components must occur, which has a dual impact in the biological systems, both positive and

negative. The health benefits are observed mainly in the immunological response against the micro-organisms, cellular signalling, and the regulation of cellular redox reactions [3, 5].

However, if the production of these radicals has increased beyond the system capacity for any reason, an imbalance will be initiated, and a series of damages will begin a chain reaction, and if continued, will eventually impact the whole biological system and result in a condition called oxidative stress. A chronic state of the oxidative stress leads to oxidative damage conditions, including DNA modification, lipid peroxidation, and protein carbonylation. Looking at the big picture, these cellular changes manifest into a wide range of diseases and conditions, such as aging, diabetes mellitus, neurodegenerative and cardiovascular diseases, multiple sclerosis, Alzheimer's disease, and various types of cancer [3, 5–7]. In fact, many scientists believe that the oxidative state is a key factor in the development of all the chronic diseases, without exception.

1.2. Antioxidants

Nature always finds a way to maintain balance in its biological systems. Its unique way of fighting free radicals was developed using a protecting group of natural compounds called antioxidants. Similar to the free radical, some antioxidants are produced endogenously, while the consumption of others must be exogenous, primarily derived from plants. **Figure 2** presents multiple groups of individual antioxidants, including enzymatic, non-enzymatic, and synthetic antioxidants [2, 4, 8]. Other means of classification are also available, such as according to their solubility (lipophilic and hydrophilic antioxidants) or according to the origin (endogenous and exogenous molecules).

The antioxidants can be defined as substances with the ability to inhibit the oxidation of other compounds [8, 9]. They are typically reducing agents and hydrogen donors, and they can provide protection from free radicals by two main mechanisms: either by oxidising themselves or by interfering with free radical intermediates [8].

In addition to their vital part in breaking the oxidative cascade, a wealth of research has demonstrated their role in maintaining and improving the well-being of humans. They have shown anti-inflammatory, antiaging, antimicrobial, antidiabetic, anticarcinogenic, as well as hepato-, nephro-, and neuroprotective properties [10, 11]. Moreover, several antioxidant substances, such as ascorbic acid and coenzyme Q10 (CoQ10), are already considered essential nutrients, playing a major role in cellular biochemical processes, functions, and signalling [8, 12].

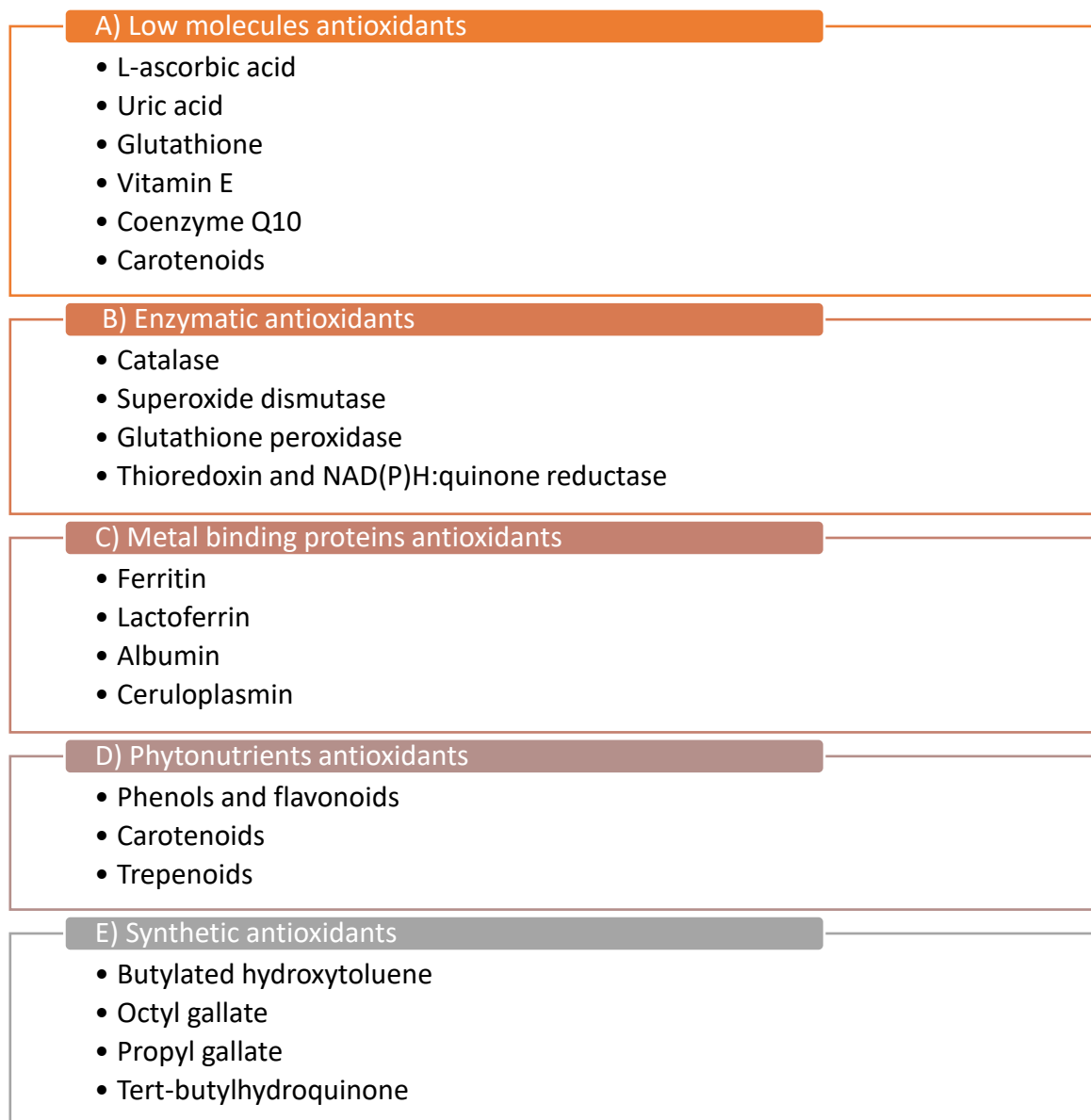


Figure 2: Antioxidants categories in nature

1.2.1. Current challenges in antioxidant's delivery

As discussed earlier, antioxidant health benefits are enormous for various reasons, and thus, their formulation into pharmaceutical preparations is in high demand nowadays. Generally, the pharmaceutical product of a certain antioxidant should provide the recommended dose in a formulation that allows the sufficient bioavailability to the targeted site. Unfortunately, however, achieving this aim is challenging given the complex nature of the biochemical properties of antioxidants, such as poor solubility, extreme lipophilicity, and large molecular weight. Moreover, the antioxidant's stability as an active pharmaceutical agent is a critical issue, as antioxidants can oxidise and subsequently, oxidise the other formulation elements as well [2].

Thus, such issues have been the subject of numerous studies, presenting the antioxidant drug delivery as a promising approach. The solutions provided in the literature can be categorised into two broad spectrums: the chemical modification of the active ingredient or/and the modification of the formulation (e.g., the use of a delivery system).

Considering ascorbic acid a primary example due to its highly challenging formulation, the most classical examples for its chemical modification to improve the bioavailability and the stability is the use of ascorbic acid ester derivatives [13]. This modification resulted in significantly higher cellular levels of ascorbic acid after the topical application of the trisodium ascorbyl 6-palmitate 2-phosphate (APPS) compared to ascorbic acid application in the same study conditions [14].

On the other hand, the development of the delivery systems is among the most successful tactics to modify formulations, such as via the use of nanotechnology and advanced carrier systems. A productive example for the suggested methodologies by researchers for ascorbic acid formulations include the use of spray drying technology with microcapsules [15], microfluidic technique with liposomes [16] and homogenisation in advanced water in oil emulsions [17].

Regarding the delivery of antioxidant plant formulations, extraction is the main process in most production methods, in which the active constituents are isolated primarily using an

organic solvent [18]. However, PlantCrystals has been urged in the recent years as a new concept to overcome the drawbacks of the classical extraction. It is employing a size-diminishing technology aiming to provide more bioavailable and stable plant-based formulations [19, 20]. Further clarification of this novel concept is provided in this thesis.

1.3. Antioxidants in biology: skin as a model organ

Following the presentation of oxidation, free radicals, and the theoretical background of antioxidants, it is crucial now to apply these concepts to one of the biological systems. Skin, as the largest organ in the human body, was selected, and it is the main theme of this thesis.

1.3.1. Antioxidant skin barrier

Skin has a unique anatomy, consisting of corneocytes embedded in a lipid matrix and resembling the brick-and-mortar units to protect the inner organs and prevent the epidermal water loss. It also comprises a complicated system of biochemicals to restore imbalances created by pro-oxidants in the environment. This system, which contains an antioxidant network, is commonly referred to as the epidermal antioxidant barrier [21, 22]. This network is predominantly composed of small-molecule and enzyme-based antioxidants [23].

In addition to preventing the generation of ROS, small-molecule antioxidants serve as free radical scavengers. Their distribution throughout the skin is determined by their solubility. For instance, lipophilic antioxidants are mostly incorporated in the cell membrane and lipid matrix, whereas hydrophilic antioxidants are distributed throughout the extracellular space [2, 24]. Among them are L-ascorbic acid, uric acid, glutathione, vitamin E, CoQ10, and carotenoids.

In contrast, enzymatic antioxidants are often referred to as detoxifying enzymes, and they have a cofactor that is mainly active via electron transfer reaction [2]. The main antioxidants in this category are catalase, glutathione peroxidase, thioredoxin, superoxide dismutase, and

NAD(P)H:quinone reductase [25–30]. In addition, other biomolecules such as bilirubin, melanin, ferritin, L-carnitine, and α -lipoic acid are contributing to the antioxidant skin barrier via their substantial antioxidant activity [2, 31–34].

In comparison, the anti-oxidative properties in the epidermis are more potent than in the dermis, as a gradient concentration is present, particularly for antioxidants with low molecular-weight [2]. Moreover there are several factors that can influence the levels of endogenous antioxidants in skin, such as anatomical site, diet, and stress [35, 36].

1.3.2. Oxidative stress in skin

The term oxidative stress was used for the first time in the 1970s [37]. It can be defined as an impaired oxidative state in living tissue that occurred via the accumulation and/or the over-production of free radicals [38]. As a result, the disruption of this fine oxidant-antioxidant system generates multiple biomolecular deformities, represented in carbonylated protein, lipid peroxidation, and DNA mutations. Eventually, and as recent studies have confirmed, this chronic cellular damage plays a significant part in the development of the organ’s deterioration. For example, several skin disorders found to be associated with the oxidative stress in skin (**Table 1**).

Table 1: Skin diseases associated with oxidative stress

Skin disease	References
Acne vulgaris	[39–41]
Atopic dermatitis	[42–44]
Skin cancer	[7, 45–47]
Psoriasis	[48–50]
Vitiligo	[51–53]

1.3.3. Effect of the pro-oxidant elements on skin

As the outer protective shield, skin often experiences stress from UV radiation and other oxidants. At the cellular level, these pro-oxidants provoke many biological and metabolic processes and trigger a cascade of reactions that can alter DNA, disrupt the antioxidant balance, change signal transduction pathways, impair the immune system, and damage the extracellular matrix.

These deleterious effects are generative conditions of photoaging, photoimmune suppression, and photo carcinogenesis. In the long term, the oxidative stress can play a confirmed role in developing serious disorders and diseases, as outlined above.

Ultraviolet radiation

UV radiation, as a primary pro-oxidant agent, includes several spectral regions. UVC has the shortest wavelengths (100–280 nm) with the highest energy, while UVA has the longest wavelengths (315–400 nm) and the least energy. UVB falls in between. Each UV element has shown variable effects on cells, molecules, and tissues according to its energy and penetration depth into the skin (**Figure 3**) [54].

Accordingly, UVA is the most dominant UV component, making up 95% of the radiation that reaches the Earth, capable of penetrating beyond the epidermis. Therefore, UVA in moderate amount stimulates fibroblast apoptosis, increases oxidative stress, induces ROS production, reduces antioxidant enzyme activity and promotes membrane disruption [55]. However, UVA has less energy than UVB and hence induces carcinogenesis to a lesser extent [56]. On the other hand, UVB radiation directly damages DNA by generating apoptosis or replication defects, triggering inflammatory processes, photo-immunosuppression, melanogenesis, and induces skin cancer [56–58]. For this reason, the sun protection factor (SPF) values only reveal a sunscreen's UVB protection [59].

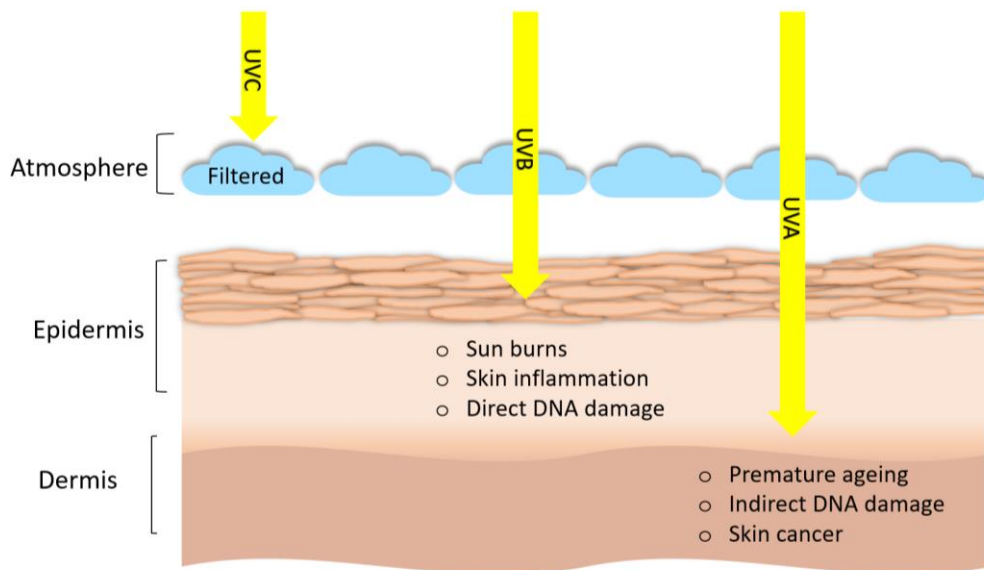


Figure 3: Penetration of UV radiation into the skin and undesired consequences

Visible and infrared light

Recent reports have revealed the ability of the visible and infrared light to trigger skin erythema, pigmentation, thermal damage, and free radical production [60, 61]. Moreover, DNA damage as a result of exposure has been confirmed [2]. Future research in this area is required to provide better understanding and to suggest suitable solutions for skin protection.

Air pollution

Industrial revolution has produced undesired outcomes for human health and environment; according to the world health organisation (WHO), nine out of ten people are breathing polluted air worldwide [62]. Air pollution is defined as a heterogeneous combination of gases and particles originated by humans and nature, such as industrial by-products and windblown dust, and has become an increasingly serious issue in the last decades [63]. Air pollution includes ambient ozone and nitrogen dioxide, traffic-related air pollution, cooking with solid fuels, as well as indoor and outdoor particulate matter (PM).

Several reports have linked air pollution to the oxidative cascade, manifesting as cardiovascular, respiratory, and cancer disorders [64, 65]. This impact is occurring due to the oxidant nature of the ozone, nitrogen dioxide, and airborne particles [63]. Moreover, these components can trigger inflammatory response, which can interfere with the function of the mitochondria and modify the RNA [66, 67].

As the organ in the lifelong direct contact with the polluted air, skin is also a target for significant oxidative changes that affect all the skin's main attributes, such as skin barrier, pigmentation, defence systems, structure, neuroendocrine regulation, and thermoregulation [68, 69]. Compared to skin that is not exposed to pollutants, the exposed skin has higher sebum production and a greater quantity of lactic acid, resulting in a decreased subcutaneous pH. Additionally, cholesterol, vitamin E, and squalene are diminished markedly in people's skin in polluted regions as a result of their mobilisation to counteract oxidative stress in the skin [70]. As the result, growing research has examined the involvement of particulate and gaseous pollution in skin disorders, such as aging, eczema and dermatitis, urticaria, rosacea, and cancer [68, 69, 71, 72].

1.3.4. Antioxidants as cosmeceuticals agents

The use of antioxidants presents a concrete approach to improve overall health. In the case of skin, the benefits of topical antioxidant application have been extensively supported in the last decades. Research has indicated their potential to strengthen the skin barrier, provide photoprotection, repair UV-induced damage, fight photo-oxidative changes, and improve the production and differentiation of the epidermal components [55, 73]. Moreover, they can work as anti-pollution agents by forming a barrier film and eliminating the pollutant's oxidative effects [73]. Screening the literature and the cosmetics market shows the dominance of three antioxidants species for the skin: vitamin C, vitamin E, and CoQ10. Nevertheless, the use of botanical antioxidants is also gaining high popularity. **Table 2** describes the common species of cosmeceuticals antioxidants in addition some phyto-antioxidants that are used with proven efficacy.

Table 2: Common antioxidants species used in cosmeceutical formulation

	Common species	Main efficacy
Vitamin C	<ul style="list-style-type: none"> ○ Ascorbyl 6-palmitate ○ Ascorbyl-2-glucoside ○ Tetra-isopalmitoyl ascorbate 	Photoprotection, anti-inflammatory, anti-melanogenesis, antiaging, anti-pigmentation and wound-healing enhancer [74, 75]
Vitamin E	<ul style="list-style-type: none"> ○ A, β, δ and γ tocopherols ○ Tocopheryl acetate ○ Tocopheryl dimethylglycinate 	Photoprotection, anti-inflammatory activity, anti-melanogenesis, antiaging and humectant agent [2, 76]
CoQ10	<ul style="list-style-type: none"> ○ Ubiquinol ○ Ubiquinone ○ Disodium Ubiquinone 	Anti-inflammatory, anti-tumour, antiaging and anti-pigmentation [77, 78]
Phyto-antioxidants	○ α -Arbutin	Anti-inflammatory, antipigmentation, cytotoxic and wound-healing enhancer [79–81]
	○ Curcumin	Photoprotection, anti-inflammatory activity, anti-cancer, antiaging and wound-healing enhancer [82–84]
	○ Epigallocatechin gallate	Photoprotection, cytotoxic, antiaging and skin hydration agent [85–87]
	○ Resveratrol	Photoprotection, anti-inflammatory activity, anti-cancer, antiaging and wound-healing enhancer [88–90]

1.4. Assessment of oxidative state

1.4.1. In plants

Plants are the major source of natural antioxidants. They are an indispensable constituent that exhibits an extended range of biological benefits, including anti-oxidative, anti-inflammatory, antiaging and anti-carcinogenic properties. For this, their use in nutraceutical, medicinal, and cosmetic applications is fundamental. Phenols are the largest plant derived antioxidant group, containing five sub-groups, as demonstrated in **Figure 4** [91–94]. Each group is characterised with a specific basic chemical structure and includes many substances with substantial health effects. The other active constituents that show significant antioxidant properties are vitamins (vitamin C, vitamin E, and CoQ10), carotenoid and chlorophyll.

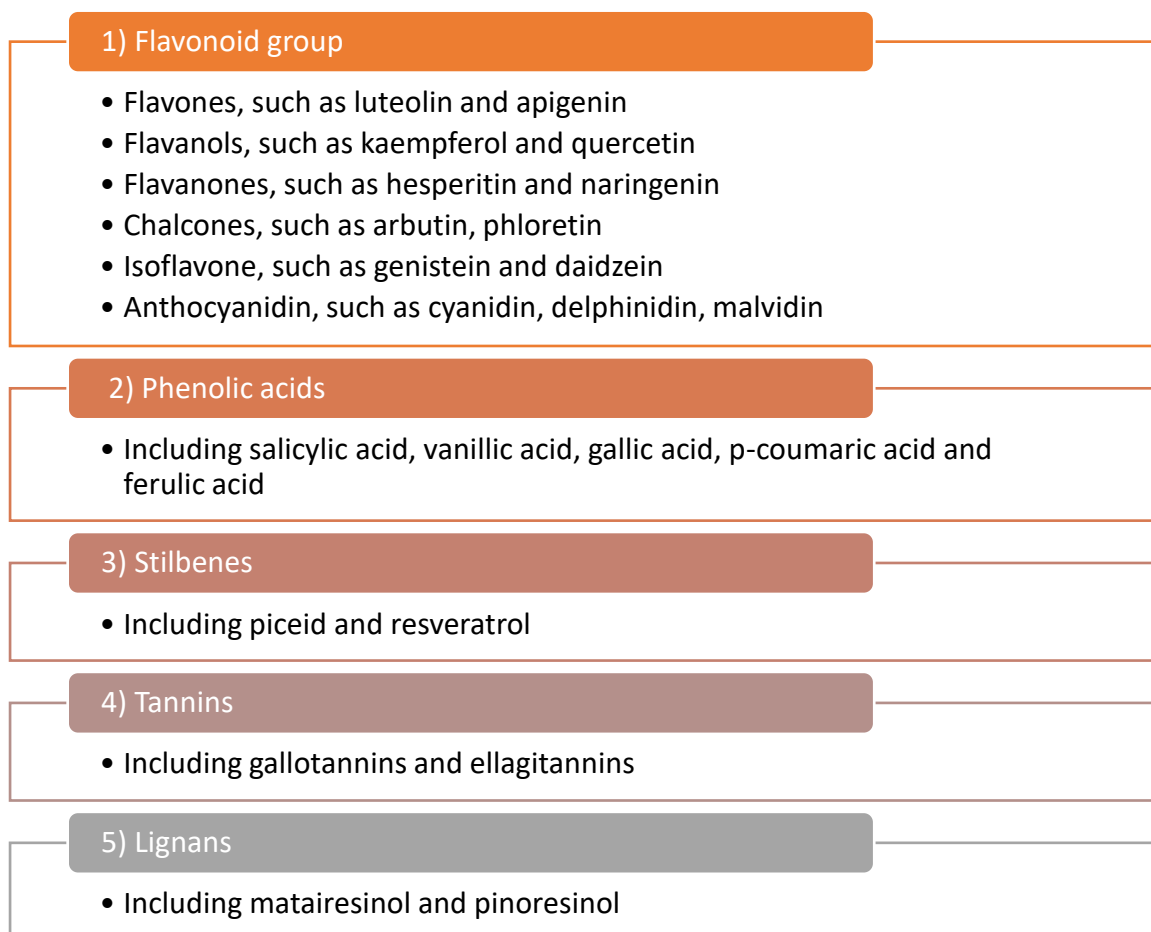


Figure 4: Phenol sub-groups in plants

The estimation of the plant's antioxidative potential is typically done using two main approaches:

1.4.1.1. Direct detection of the plants actives constituents

Phenols can be determined simply by using the Folin Ciocalteu method [95]. Other assays for phenol sub-groups also exist, including:

- Total flavonoid content [96]
- Total monomeric anthocyanin content [97]
- Carotenoid analysis [98]

A more precise analytical method can also be used for determination individual compounds, like the use of HPLC assays [97, 99, 100].

1.4.1.2. Antioxidant capacity (AOC) assays

Due to the complex nature of the dietary and biological composition, isolating each antioxidant component and analysing it separately is typically expensive, inefficient and does not consider the interactions between the antioxidants. Accordingly, the principle of antioxidant capacity (AOC) had developed in chemistry and introduced into the areas of biology, medicine, and nutrition [4]. AOC can be defined as the measured amount of free radicals that can be scavenged by a specific agent [101]. It includes a broad variety of assays, that have been employed to evaluate the potential of nutraceutical and pharmaceutical products (**Table 3**).

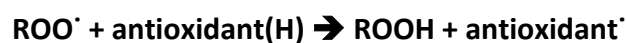
Table 3: Common assays used to determine in-vitro antioxidant capacity

Mechanism	Examples
Hydrogen atom transfer reaction	<ul style="list-style-type: none">○ ORAC (oxygen radical absorbance capacity)○ TRAP (total radical trapping antioxidant parameter)○ Crocin bleaching assay
Electron-transfer reaction	<ul style="list-style-type: none">○ TEAC (Trolox equivalent antioxidant capacity)○ FRAP (ferric ion reducing antioxidant parameter)○ DPPH (2,2-Diphenyl-1-picrylhydrazyl)○ Total phenols assay by Folin Ciocalteu reagent
Other assays	<ul style="list-style-type: none">○ Inhibition of Briggs Rauscher oscillation reaction○ Chemiluminescence○ Electrochemiluminescence

Most of the analytical assays can be classified according to their reaction mechanism [102, 103], as follows:

Hydrogen atom transfer (HAT) based reactions:

In general, HAT-based approaches are composed of a synthetic free radical initiator, an oxidisable probe, and an antioxidant. Their reaction can be described as:



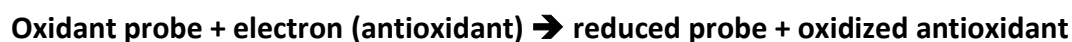
In this reaction, the antioxidant quenches the free radicals (mainly peroxy radicals; ROO[•]) via the hydrogen donation [102].

The majority of HAT-based assays are able to assess the kinetics of competitive reactions, with quantitation obtained from the kinetic curves. The most popular tests belonging to this group include the following:

- **Oxygen radical absorbance capacity (ORAC) assay** was initially developed by Cutler *et al.* in 1993 [104], and since then, it has gained significant popularity. It involves the area under the curve (AUC) kinetics that applies well to antioxidants with a lag phase and those without lag phase. Moreover, it is especially beneficial for food samples, which typically include several components and have complicated reaction kinetics [4]. As a result, the ORAC assay has been widely used in academia, pharmaceutical, and supplement industries to assess antioxidant capabilities.
- **Total radical trapping antioxidant parameter (TRAP) assay** is based on the antioxidant protection for R-phycoerythrin fluorescence decay during the lipid peroxidation process suppressed by AAPH [105]. The TRAP values are determined by defining the lag-phase time of the sample in relation to the standard. Thus, the TRAP assay has good sensitivity; nonetheless, using the lag phase for measurement is the main disadvantage of this method, as not all antioxidants exhibit a lag phase, and the antioxidant capacity profile following the lag phase is entirely ignored [106]. Moreover, it involves a complex and time-consuming process that requires a high level of skill and experience [4]. Accordingly, the application of this assay is limited for the purpose of the routine determination of AOC.

Electron-transfer (ET) reaction

ET-based assays employ a single redox reaction, with the oxidant acting as an indicator of the reaction endpoint. The basic principle can be summarised as:



The probe is an oxidant that removes one electron from the antioxidant, causing the probe to change colour and the degree of colour change is related to the concentration of

antioxidants [102]. The reaction is completed when the colour change ends. Example assays include the following:

- The **Folin Ciocalteu assay**, often known as the phenol determination assay, is commonly used to assess a sample's reducing capacity [95]. Numerous studies have utilised this test and have shown strong linear relationship between the phenolic profiles and the AOC. It is highly applicable, easy, and reproducible. As a result, a vast amount of data has been collected, and the test has become a standard method for analysing phenolic antioxidants.
- Miller *et al.* initially developed **Trolox equivalent antioxidant capacity (TEAC) assay** in 1993 and ABTS (2,2'-azinobis(3-ethylbenzothiazoline-6-sulfonic acid)) was utilised as oxidising agent [107]. Due to its convenience, TEAC test has been used by several laboratories to investigate the AOC, and the TEAC values of numerous substances and food samples have been published.
- The **ferric ion reducing antioxidant power (FRAP) assay** employs a ferric salt as an oxidant that has comparable redox potential to that of ABTS [102]. Therefore, there is a high level of similarity between these two assays, with the only significant difference being that the TEAC assay is conducted at neutral pH and the FRAP assay in acidic conditions [108].
- **Diphenyl-1-picrylhydrazyl radical scavenging capacity (DPPH) assay** utilises one of a few existing stable organic nitrogen radicals with spectral absorption. Although this method is easy and convenient, there are drawbacks limiting its use. DPPH is a long-lived nitrogen radical that is completely different than the extremely reactive and transient ROS. For example, there are numerous antioxidants that respond rapidly with peroxy radicals that may react slowly or even be inert when exposed to DPPH. Thus, the findings of this assay must be supported by other assays that are more relevant to the *in-vivo* conditions. It was previously assumed that the DPPH assay followed a HAT reaction. However, the following data suggested otherwise, like the study by Foti *et al.* which theorise it as an ET reaction based on a kinetic study of the interaction between phenols and DPPH [109].

All the presented assays are varying in the term of substrates, reaction conditions, probes, and quantification techniques. In major cases, it is challenging to compare the findings obtained from different assays as Frankel *et al.* stated [110]. Furthermore, a single assay cannot stand alone to decide the certain potential of an antioxidant system [110]. Hence, the use of multiple approaches and variable conditions to provide for fair assessment is highly recommended.

1.4.2. In cosmeceuticals agents

In the last decade, antioxidants have been anticipated as one of the most valuable ingredients in the cosmetics industry to improve the skin's oxidative state and, moreover, to extend the formulation stability, e.g.; to prevent the lipids peroxidation [2].

Estimating the AOC role of each ingredient in a formulation is not always a practical solution, as the net effects of the ingredient interactions should be considered. Consequently, the evaluation of the antioxidant properties of the final formulation is very often the most crucial step. Beneficially, this purpose can be achieved using the AOC analytical assays included above in **Table 3**. The most commonly applied *in-vitro* AOC investigations for cosmeceutical formulations are the DPPH assay, CUPRAC assay, and ABTS assay; and for a lower threshold of detection, fluorometric methods such as ORAC are applied [111–117].

Throughout the last decade, a particular concept has been established for the indirect determination of the AOC of skincare products; the radical protection factor (RPF) [118]. The RPF measurement defines the scavenging activity of an antioxidant against a certain compound. In this technique, nitroxides are used as the reactive radicals, and the assessment can be performed using electron spin resonance spectroscopy (ESR), which permits the identification of the unpaired electrons species; hence, it reflects the formulation's antioxidant capacity [118, 119]. The advantage of this concept includes the simple classification of antioxidant-containing cosmeceuticals, in addition to its use in monitoring changes in the antioxidant properties over a long period of time. However, it appears that this

method has limited application, probably due to the sophisticated applied procedure and the presence of more efficient and convenient methods.

1.4.3. In skin and biological tissues

Reviewing the literature reveals extensive efforts aimed at providing a better understanding of the antioxidant skin barrier and the influencing factors, such as skin disorders, UV radiation, and particular treatment. In general, the applied approaches can be divided into three basic strategies (**Figure 5**) [120].

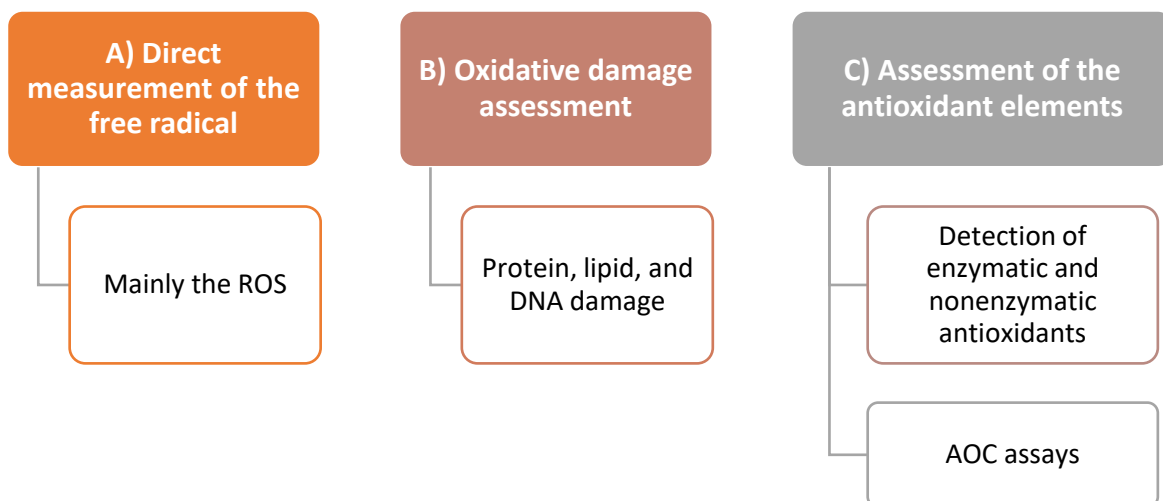


Figure 5: Summarised presentation of current approaches used to evaluate the oxidative state in biological tissue, e.g., skin

The first approach is the quantification of the free radicals in skin as oxidative markers, mainly the ROS. Herrling *et al.* relied on this concept using ESR, aiming to quantify the generated ROS in skin and then use it as a biophysical endpoint to study the impact of and the protection from UV A and B radiation [121]. However, the high reactivity and the short half-life of the ROS have limited its use as a standalone approach, but it is used as a supportive tool in conjunction with much stronger protocols.

The second approach focuses on the assessment of the damaging effects resulting from the oxidative stress in skin tissue. Fujita *et al.*'s study provides a typical example, as they assess the labelled carbonylated protein in the SC using tape stripping and fluorescence microscopy [122]. As well, Nakashima *et al.* have investigated the blue light oxidative effect by studying the skin's lipid peroxidation, in addition to the detection of ROS [60]. Matsumoto *et al.* assessed the expression level of heme oxygenase-1 (HMOX1) mRNA to track the oxidative changes in obese patients after weight reduction surgery [123]. Moreover, Hagens *et al.*, with a novel model, were able to track skin's oxidative elements using the ultraweak photon emission (UPE) system, which detects luminescence phenomena in biological systems [124].

The final approach is the assessment of the skin's antioxidant elements, both directly and indirectly. The direct approach involves applying the detection assays for the enzymatic antioxidant, e.g., catalase and superoxide dismutase [125] and the nonenzymatic antioxidants, e.g., carotenoid and vitamin E [126, 127].

On other hand, the indirect method is based on the estimation of the skin's overall oxidative state, which has a special advantage because it considers the interaction between the various factors and the multiple antioxidants, then it provides a good precise estimation of the tissue state [120]. This can be done using devices such as the electron paramagnetic resonance spectroscopy [128] or by utilising the already known methodologies that have been applied in the fields of food and plants studies, such as AOC assays. Regardless of the simplicity and the versatile possible applications of employing the last specific approach, there is a little research taking full advantages of it, especially in the field of skin research.

Therefore, this thesis is dedicated to establishing and validating a novel model utilising this particular approach to estimate the skin's oxidative state based on a well-established assay in the phytochemistry research.

Chapter 2. Aims of the thesis

The studies in this thesis have been performed aiming to achieve multiple aims. The initial aim was to **optimize** useful methods to assess the antioxidation potentials of specific novel plant formulations. Accordingly, and relying on the first aim, the second aim was to **utilise** some of these already established protocols to assess the skin's oxidative state as a critical skin marker and **develop** a special skin model for the first time. The purpose of the third study was to validate that model in different conditions and to **adjust** its experimental conditions, e.g., storage. After that, the aim was to **characterise** the basic skin biophysical properties and the intrinsic skin antioxidant capacity of the porcine *ex-vivo* skin. The last study was dedicated to **test** the skin model response using several cosmetical elements that produce anti- and pro-oxidative effects.

All the aims were fulfilled successfully, and the results are presented in two main sections: the **plant model** and the **skin model**.

Chapter 3. Materials and methods

3.1. Materials

3.1.1. List of the used materials

3.1.1.1. Plants

- **Dates:** Purchased from a local market in Taif, Saudi Arabia
- **Guava leaves:** Obtained from a local private farm in Taif, Saudi Arabia
- **Taif roses:** Obtained from a local private farm in Taif, Saudi Arabia

3.1.1.2. Active ingredients

- **Coenzyme Q10:** Dr. Rimpler, Wedemark, Germany
- **Dermofeel® Toco 70 (mixed tocopherols):** Evonik Dr.Straetmans GmbH, Hamburg, Germany
- **L-ascorbic acid:** Sigma–Aldrich Chemie GmbH, Steinheim, Germany
- **TPGS (D- α -tocopheryl polyethylene glycol 1000 succinate):** Gustav Parmentier GmbH, Frankfurt, Germany
- **Vitamin A acetate:** Euro OTC Pharma, Bönen, Germany

3.1.1.3. Other chemicals and reagents

- **AAPH (2,2'-azobis(2-amidinopropane) dihydrochloride):** Acros Organics, Geel, Belgium

- **DPPH (2,2-diphenyl-1-picrylhydrazyl):** Sigma–Aldrich Chemie GmbH, Steinheim, Germany
- **Ethanol:** Carl Roth GmbH & Co. KG, Germany
- **Fluorescein:** Alfa Aesar, ThermoFisher GmbH, Kandel, Germany
- **Folin Ciocalteu reagent:** Merck KGaA, Darmstadt, Germany
- **Gallic acid:** Thermo Scientific, Waltham, MA, USA
- **Methanol:** Carl Roth GmbH & Co. KG, Germany
- **Miglyol® 812:** Caesar & Loretz GmbH, Hilden, Germany
- **PEG (polyethylene glycol) 1500:** Caesar & Loretz GmbH, Hilden, Germany
- **PEG (polyethylene glycol) 300:** Caesar & Loretz GmbH, Hilden, Germany
- **Plantacare® 2000:** BASF AG, Ludwigshafen, Germany
- **Purified water:** PURELAB Flex 2, ELGA LabWater, High Wycombe, UK
- **Quercetin:** Biomol GmbH, Hamburg, Germany
- **Trolox:** Santa Cruz Biotechnology Inc., Dallas, USA
- **Tween® 80:** VWR International GmbH, Ismaning, Germany
- **β-carotene:** TCI Deutschland GmbH, Eschborn, Germany

3.1.1.4. List of materials and devices

- **250 W UV hand lamp:** UV Light Technology Limited, Birmingham, UK
- **Adhesive tape:** Tesafilm® crystal clear, tesa SE, Beiersdorf AG, Norderstedt, Germany
- **Edmund BühlerSwip KS-10:** Edmund Bühler GmbH, Bodelshausen, Germany
- **Electrical grinder:** Elta Lizenz GmbH, Oststeinbek, Germany and AR1105 Moulinex, Grenoble, France
- **Glass slide:** Gerhard Menzel B.V. & Co. KG., Germany
- **Homogenizer:** GEA Niro Soavi, Lübeck, Germany
- **Infrared densitometer:** SquameScan® 850A, Heiland Electronic GmbH, Wetzlar, Germany
- **Light microscopy:** Olympus soft imaging solutions GmbH, Münster, Germany

- **Magnetic stirrer:** IKA-Combimag RCT, IKA, Staufen, Germany
- **Mastersizer 3000:** Malvern-Panalytical, Kassel, Germany
- **Multi Probe MPA 10:** Courage + Khazaka electronic GmbH, Köln, Germany
- **NaHCO₃:** Carl Roth GmbH & Co. KG, Germany
- **Plate reader:** FluoStar® Optima plate, BMG Labtech, Offenburg, Germany)
- **Roller:** RENOVO, Brillux GmbH & Co. KG, Münster, Germany
- **Spectrophotometer:** Multiskan GO, Materials 2020, 13, 4368 6 of 21 Thermo Scientific, Dreieich, Germany
- **Ultra Turrax T25:** IKA, Staufen, Germany
- **Yttrium stabilized zirconium oxide beads:** SiLibeads®, Sigmund Lindner GmbH, Warmensteinach, Switzerland
- **Zetasizer NanoZS:** Malvern-Panalytical, Kassel, Germany

3.2. Methods

3.2.1. The plants model

The production and size analysis of the plant formulations were done by Abraham M. Abraham, as described in his publications [129–131].

Summarised scheme for the main studies of this section is presented in **Figure 6**.

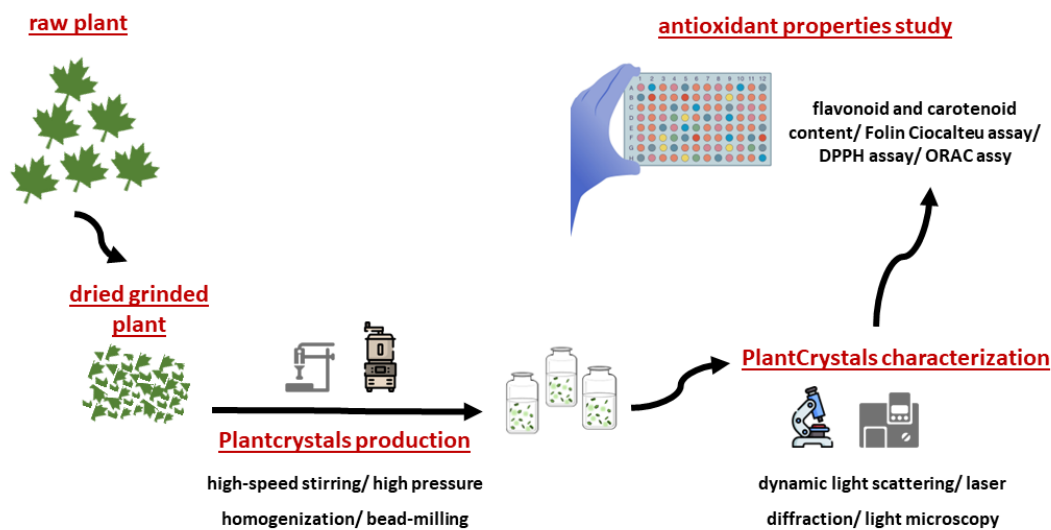


Figure 6: Summarised presentation for the main studies of the plants model

3.2.1.1. Production

The high-pressure homogenization (HPH) or bead milling (BM) was utilised to produce PlantCrystals. But before that process, the plant raw material was grinded using an electrical grinder. After that, the plant powders were dispersed in a surfactant 1% (w/w) solution, as follows:

- Plantacare 2000 with Taif rose
- TPGS with guava leaves
- Tween® 80 with date

All the plant-based suspensions have been prepared to include 1% (w/w) plant material and they were considered as the initial classical control formulations. Then, PlantCrystals were prepared based on these formulations according to the subsequent techniques.

High-pressure homogenization

First, the coarse aqueous suspension had been subjected to high-speed stirring (HSS) to minimize the number of particles > 10 μ m. This pre-treatment step was crucial to prevent the clogging of the gap during high-pressure piston-gap homogenization. After that, the homogenization process was conducted using a LAB 40-piston gap homogenizer in discontinuous mode with a 40 mL batch size at three intervals. It was accomplished at three homogenization phases: the first one was done at low pressure (6 cycles \times 200 bar), the second interval consisted of homogenization at medium pressure; (3 cycles \times 500 bar, 3 cycles \times 750 bar, 6 cycles \times 1000 bar), and the last phase was the homogenization at high pressure of 10 cycles \times 1500 bar [129].

Bead-milling

The other approach to prepare PlantCrystals is the small-scale bead milling approach [132]. In brief, three elements were added into a small vial (12 mm \times 35 mm); the coarse aqueous plant suspension, Yttrium stabilized zirconium oxide beads in a ratio of 60:40, and three magnetic stirring rods (size 6 mm \times 10 mm). Then, the vial has been positioned on a magnetic stirrer plate at room temperature and the mixture was stirred for 24 h at a rate of 1,500 rpm [129].

3.2.1.2. Size characterization

The size analysis of the PlantCrystals was done using three independent methods, including light microscopy, dynamic light scattering (DLS) and laser diffraction (LD).

Initially, the samples were visually examined by the light microscopy. Then, the LD measurements were conducted using a Mastersizer, and data was analysed with Mie-theory using a real refractive index of 1.5 and an imaginary refractive index of 0.01. Later, and using

the Zetasizer NanoZS, the DLS measurements were performed at 20 C°, and the data was analysed using the instrument's built-in general-purpose mode [129].

3.2.1.3. Antioxidant properties investigation

Determination of flavonoid and carotenoid content

The flavonoid content was determined utilising the aluminium complex reaction [133]. In 96-well plate, 100 µL of each suspension has been combined with 100 µL of 2% (w/v) AlCl₃ ethanolic solution and kept in the dark for 1 h. Followed by the absorbance evaluation at 420 nm. The flavonoid content was calculated with respect to the quercetin calibration curve and expressed as quercetin equivalent (QE µg).

On the other hand, the carotenoid content was assessed using Rodriguez-Amaya *et al.* approach [98]. Each sample's absorbance was measured at 450 nm, and calculations were performed in relative to the standard curve of the β-carotene. Results are expressed as β-carotene equivalent (β-CE µg).

Determination of antioxidant capacity

Folin Ciocalteu Assay

Folin Ciocalteu (F-C) colourimetric test was employed to evaluate the total polyphenol content and the AOC [103]. To perform the assay, 100 µL of each suspension was added to 200 µL of F-C reagent and 2 mL of purified water. After incubation at room temperature for 5 min, 1 mL of 20% (w/v) Na₂CO₃ solution was placed into the reaction vial, and the mix was incubated again for 1 h in the dark. The resulted mixture was subsequently evaluated spectrophotometrically at 765 nm, the content was calculated in relative to gallic acid as standard and expressed as gallic acid equivalent (GAE mg).

DPPH Assay

As another assay for AOC determination, methanolic DPPH (1,1-diphenyl-2-picrylhydrazyl) was used by applying the detailed protocol published previously [129, 130]. Briefly, 100 μL of 0.2 mM DPPH solution was added to 100 μL of each antioxidant serial solution into a 96-well plate and kept in dark for 30 min. Next, the absorbance was detected spectrophotometrically at 517 nm, and the IC 50 was obtained by plotting the sample concentrations versus its corresponding percentage of the radical scavenging activity (% RSA). The % RSA has been calculated according to the following equation:

$$\text{radical scavenging activity (\%100)} = (A_{\text{DPPH}} - A_{\text{sample}} / A_{\text{DPPH}}) \times 100$$

Where A_{DPPH} is DPPH absorbance and A_{sample} is the sample absorbance. Results are expressed as IC 50 value (mg/ml), which is the required amount of the antioxidant to scavenge 50% of the amount of the free radical.

ORAC Assay

The modified ORAC (oxygen radical absorbance capacity) method developed by Ou *et al.* was applied to plant and skin samples [129, 134, 135]. The used chemicals include Trolox (6-Hydroxy-2,5,7,8-tetramethylchroman-2-carboxylic acid) as the external standard, AAPH (2,2'-azobis(2-methylpropionamide) dihydrochloride) as the source of free radicals, and fluorescein as the employed fluorescent probe. The preparations were in concentrations from 22.2 to 100 μM for Trolox standards, 125 mM for AAPH and 1 μM for fluorescein. To mimic the normal physiology, all materials were produced in a physiological buffer (pH = 7.4).

The reaction was initiated by placing 20 μL of each standard/sample in a black 96-well plate, in addition to 150 μL of the fluorescein solution. Upon incubation at 37 $^{\circ}\text{C}$ for 10 min, 90 μL of the freshly prepared AAPH solution was added to each well. Afterwards, the plate was immediately inserted into the plate reader, and the measurement detection was started using excitation of 485 nm and emission of 520 nm for 100 min.

After the required period, the area under the curve (AUC) of each standard/sample was computed by plotting the relative fluorescence intensity versus time. After that, the calibration curve and its regression equation were generated using the concentration of Trolox standards and their AUC values, and the concentration of Trolox corresponding to the AUC of the samples was given as μM Trolox equivalents ($\mu\text{M TE}$). Finally, the fluorescence intensity of each sample was utilized to calculate the AOC values.

All measurements were carried out in triplicate, and the findings are shown as means \pm standard deviation.

3.2.2. The skin model

This model represents the bulk part of the current thesis, aiming to study the biophysical and antioxidative properties of the skin, and then to establish a novel viable *ex-vivo* model for skin-antioxidant's research. A summarised scheme for the main experimental outlines of skin section is presented in **Figure 7**.

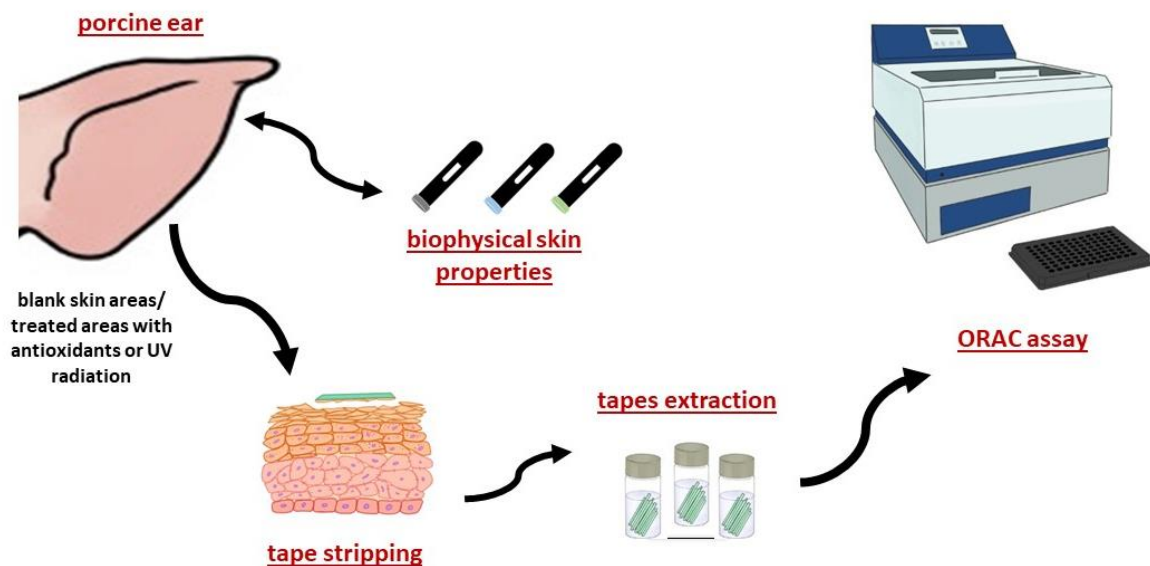


Figure 7: Summarised presentation for main studies of the skin model

3.2.2.1. Porcine ear handling

Porcine ears have been generously given by a local slaughterhouse nearby Marburg, Germany. As soon as they were received, they were rinsed with cold tap water, dried gently using clean paper towels and then hair was removed properly without damaging the skin surface. At that point, multiple intact areas of $1.5 \times 2 \text{ cm}^2$ were marked and used for the experiments and the subsequent tape stripping (**Figure 8**).

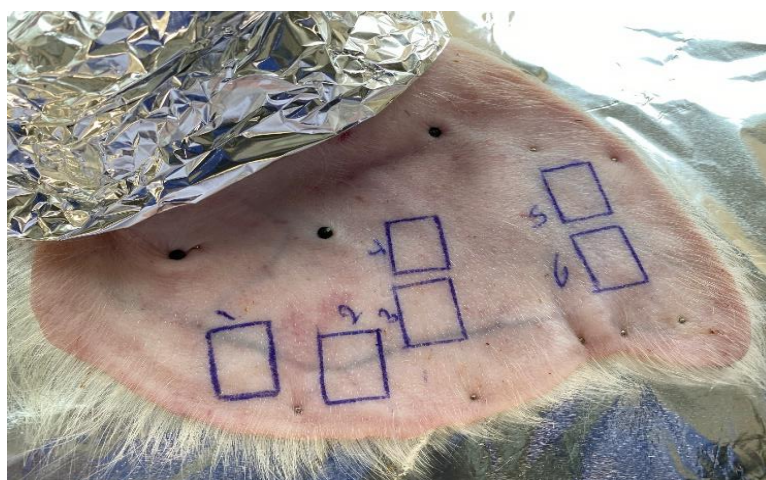


Figure 8: Ready to use porcine skin

3.2.2.2. Skin assessment and treatment

Study of the biophysical porcine skin properties

The skin parameters including trans epidermal water loss (TEWL), hydration, stiffness, surface pH and colour were evaluated with the Multi Probe Adapter MPA 10. The used skin probes are Tewameter® TM 300, Corneometer® CM 825, Indentometer IDM 800, Skin-pH-Meter PH 905 and Mexameter® MX 18, consequently. All of them were calibrated periodically according to the manufacturer operating instructions and the measurements were done at least in

triplicate, at room temperature of (23 °C ± 0.6 °C) and in a room with a relative humidity of 44–63%.

Skin treatment

After the establishment of the *ex-vivo* porcine skin model, multiple treatments had been applied to explore its potential and expand its applications.

The initial experiment has been intended to assess the anticipated antioxidative effect. This step was accomplished utilising finite doses of 6.3 µL/cm of the following active ingredients:

- Ascorbic acid aqueous solutions (1 - 30% (w/v))
- Ascorbyl palmitate (1 - 30% (w/v)) in Miglyol® 812
- Vitamin E (1 - 30% (w/v)) in Miglyol® 812
- CoQ10 (0.5 - 5% (w/v)) in Miglyol® 812
- TPGS aqueous solutions (0.5 - 5 % (w/v))
- Vitamin A acetate (0.5 - 5% (w/v)) in Miglyol® 812
- PEG 300
- PEG cream (1:1 of PEG 300 + PEG 1500 [136])

Solutions and blank solutions (solvent only) were applied and incubated for 2 h at 32 °C. Then, the residuals were wiped off softly by wet and dry paper tissue. Consequently, tape stripping protocol was applied.

The following application was performed utilizing UV radiation as a pro-oxidative agent. The porcine ears had been exposed to the radiation of a 250 W UV hand lamp for 1 and 2 h inside a metallic box (**Figure 9**). The controlled ear undergone to the same conditions inside the metallic box but was covered with an additional paper box to prevent the radiation.



Figure 9: UV radiation source inside metallic box for exposure of the porcine skin

Tape stripping

Tape stripping performed by placing adhesive tape on skin using a defined pressure with a roller, followed by a quick tape removal with a layer of stratum cornea (SC) [137]. A total of 30 SC layers were removed from the skin area for all the samples. According to the specific experimental design, tapes have been collected in one set (30 tapes) or three sets where each set contains 10 tapes and subsequently, 10 SC layers. Each set was then extracted with 70% (v/v) ethanol in purified water, and after that subjected to shaking for 1 h at 160 rpm. Eventually, the obtained SC extracts have been analysed using ORAC assay.

Quantification of protein content

Directly after the tape stripping, the absorbance of each individual tape was determined using an infrared densitometer (IR-D) to identify the optical pseudo-absorption at 850 nm. According to known data, the detected absorbance showed a linear correlation with the protein content in tapes [138, 139] and it is considered a reliable, simple and non-invasive technique to quantify the amount of skin corneocytes [122, 138]. Results are expressed as an average cumulative protein absorption (%).

Storage and extraction of tapes

The tapes were placed in tightly secured glass vials and stored according to the specifications of the study outline. Before the adjustment of the storage conditions, tapes were stored in the refrigerator and analysed within 24 h. Then, multiple storage conditions were studied, including storing at room temperature (20 ± 2 °C), in the refrigerator (4 ± 1 °C) and the freezer (-20 ± 2 °C). At last, and according to the obtained findings, tapes were stored immediately at -20 ± 2 °C and analysed within 10 days.

3.2.3. Statistical analysis

Excel (Microsoft 365 Redmond, WA, USA) has been used for graphs and descriptive analysis, and GraphPad Prism (version 9–9.4.1, GraphPad Software, San Diego, CA, USA) was utilised for ORAC calculation and statistical analysis. Each dataset was assessed for normality, and after that t-test or ANOVA and post hoc analysis (Tukey and Dunnett's) were employed for comparison. Pearson's r was applied for the correlation analysis. Experiments were performed in triplicate; results were expressed as mean \pm standard deviation (SD) and p values < 0.05 were considered statistically significant.

Chapter 4. Results and discussions

4.1. The plant model:

4.1.1. Antioxidative properties of plants and plant formulations

This section focuses on the optimisation of several assays designed to effectively evaluate the antioxidant properties of plant formulations. The optimised assays were applied to multiple plant parts, including flowers, leaves, and fruits, which were prepared using two different techniques: in classical extract form and PlantCrystals formulations. The following sections present the assay optimisation and validation, followed by a description of the application to plants, as shown in **Figure 10**.

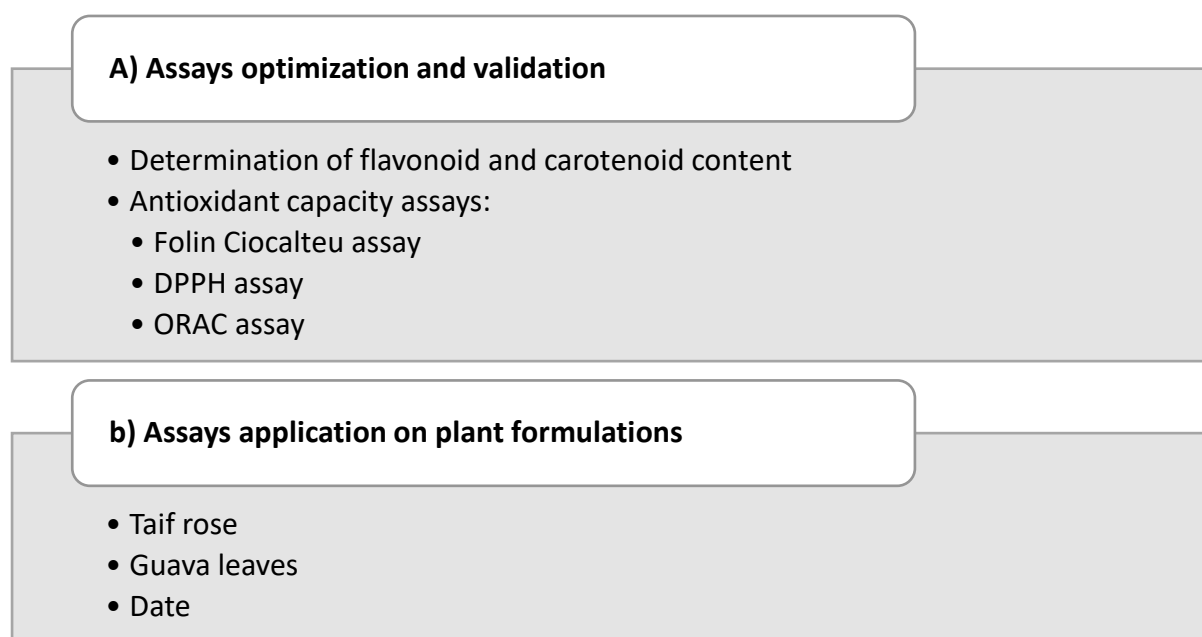


Figure 10: Study outline of current section

4.1.1.1. Assay optimisation and validation

Determination of flavonoid and carotenoid content

Flavonoid content was determined through flavonoid reactions with AlCl_3 as a complexing agent. Such a reaction leads to the production of a coordination complex product that can be evaluated spectrophotometrically. This method is based on the strong flavonoid affinity to bind metal ions like aluminium due to their many hydroxyl and oxo groups [140]. **Figure 11** illustrates this reaction using quercetin as a reference flavonoid, while **Figure 12** presents a quercetin calibration curve that was used as a quantitative standard reference.

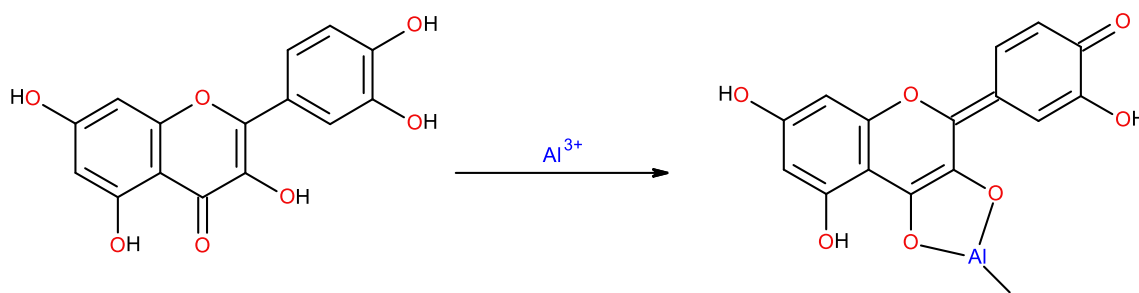


Figure 11: Scheme for the complex reaction forming Al (III)-quercetin chelate resulting in detectable measurement at 420 nm

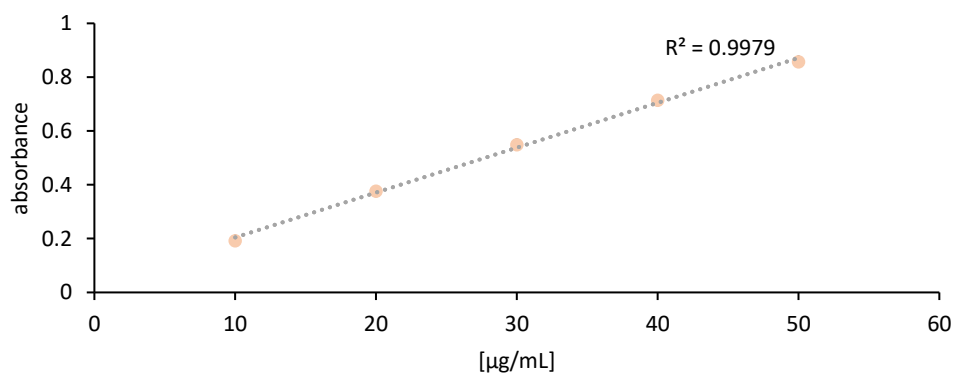


Figure 12: Standard calibration curve of quercetin [$\mu\text{g/mL}$] upon the reaction with AlCl_3

To assess carotenoid content, the most popular and straightforward means of estimation is to detect the ultraviolet-visible spectrum in the area of 444–502 nm [98]. Therefore, the method outlined by Rodriguez-Amaya *et al.* [98, 141] was applied with respect to a standard calibration curve of β -carotene, as shown in **Figure 13**.

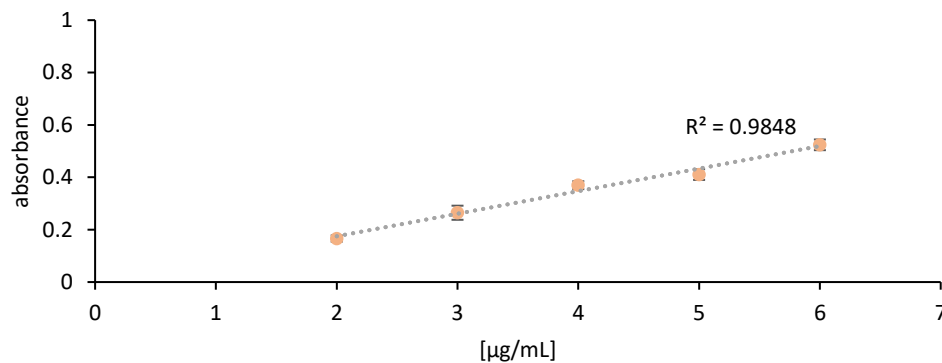


Figure 13: Standard calibration curve of β -carotene [µg/mL]

Although these procedures are rapid, simple, convenient, and extensively applied in the literature [98, 129, 142, 143], they have one main flaw—the possible differences in absorption maxima (λ_{\max}) of the various substances that are present in plants compared to the standards (quercetin and β -carotene) due to the differences in their chemical structures. Subsequently, the final content estimation may show a false positive or negative result [140].

However, in the present work, this drawback can be considered insignificant, as the main aim here is to compare the content of an individual plant before and after being processed via a specified process and not to compare one plant to another. This means that the effect of the false value could be balanced by the comparison.

The other main challenge in carotenoid and flavonoid analysis develops from their instability during analysis, as they are sensitive to oxygen, heat and light [98, 144, 145]. Therefore, precautions had been made to provide the greatest protection possible during the study. However, during the production of the PlantCrystals, considerable exposure to heat and

oxygen might occur even with the use of an ice bath, which may eventually have affected the final contents in some cases [129].

Determination of AOC

Folin Ciocalteu assay

This approach depends on the specific reaction between the Folin Ciocalteu (F-C) reagent and the phenols in plants, which form a mixture that can be spectrophotometrically detected. The F-C reagent is composed of phosphomolybdate and phosphotungstate, and upon its reduction via electron transfer from a phenolic compound, a blue colour appears (**Figure 14**).

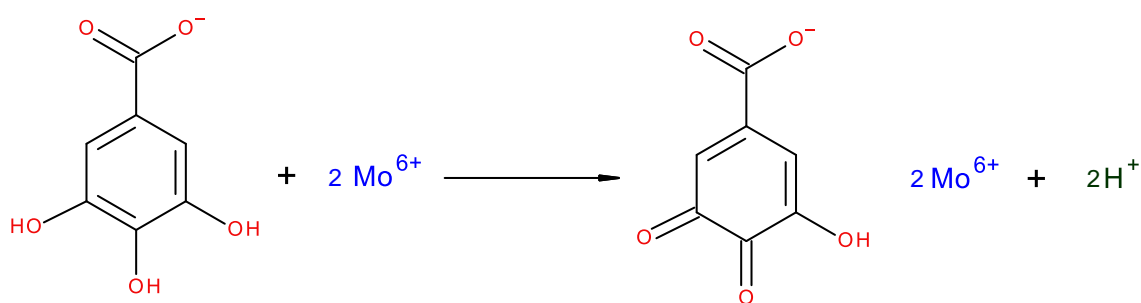


Figure 14: Electron transfer from the phenol compound (e.g., gallic acid) to the molybdate complex of Folin Ciocalteu reagent in alkaline condition, which resulted in detectable blue colour at 765 nm

This technique is highly popular and has been described in the European Pharmacopoeia [146]. It is also considered an excellent approach for determining the AOC due to its nature as a redox reaction where any molecule with a reducing ability can progress the reaction [103]. However, the reducing abilities of most plants are a result of their phenols; thus, the current method has become known as effectively able to determine the total phenol content

of plants [147]. As a reference substance in the present work, gallic acid was used in the range of 25–500 mg/mL, with the calibration curve shown in **Figure 15**.

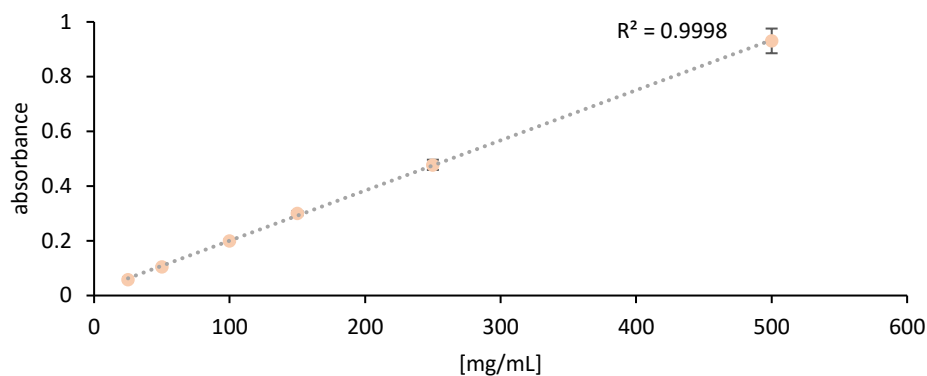


Figure 15: Standard calibration curve of gallic acid [mg/mL] using Folin Ciocalteu assay

The advantages of this assay include rapid performance, low cost, and high suitability for routine work. Moreover, it is largely accurate and has achieved a very good correlation with ORAC [95, 103]. On other hand, the colourimetric interference with some substances like sugars and aromatic amines is the main disadvantage of the F-C assay [103].

DPPH assay

As one of the most common tests to determine the AOC, the DPPH assay, utilises the nitrogen-stable free radical 2,2-Diphenyl-1-picrylhydrazyl (DPPH) as an indicator of the antioxidant reaction. This assay measures the antioxidant-reducing capacity towards DPPH^{\cdot} , which can be spectrophotometrically evaluated by the proportional decrease in the purple colour and the antioxidant concentration (**Figure 16**).

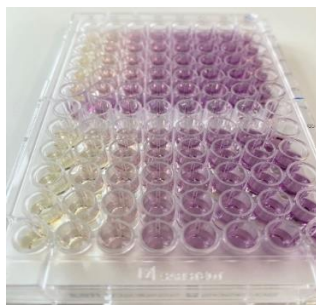


Figure 16: Colour of the DPPH solution in 96-well plate which vanished gradually by the increased antioxidant concentration in the sample (from right to left)

DPPH assay is classified mainly as an electron transfer (ET) reaction, but the hydrogen-atom transfer (HAT) reaction is also considered a marginal mechanism [102]. The reaction proceeds by the proton donating antioxidant which reduces the stable free radical reduction to DPPH-H and results in the disappearance of the DPPH deep purple colour in the concentration-dependent pattern (**Figure 17**).

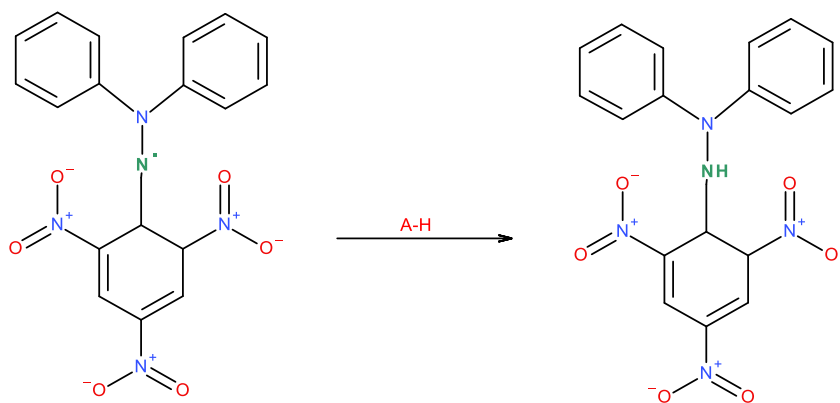


Figure 17: Conversion of DPPH radical to the DPPH-H in the presence of a proton donating antioxidant (A-H), which resulted in the disappearance of its purple colour

DPPH assay has been extensively applied for antioxidant screening and has several advantages, including its simplicity, rapid performance and easy application, in addition to its good sensitivity and accuracy. However, its major drawback is the spectral interference with high-absorption groups around the measurement area (500–550 nm), such as carotenoid and chlorophyll [103, 129]. The other drawback is caused by the employment of the nitrogen-free radical which does not bear any similarity to the most common radical in biological systems; the highly reactive peroxy radicals (ROO[•]). Accordingly, the antioxidant reaction may proceed differently with DPPH[•] than with ROO[•], yielding data that cannot be meaningfully interpreted [103].

For these reasons, there was an insistent need to apply another AOC assay to be used in addition to the F-C and DPPH assays to support the results and gain a deeper knowledge of the tested substances.

ORAC assay

This ORAC assay is based on the HAT mechanism. The reaction depends on the competition between the radical generator and antioxidant on a fluorescent probe over time, that eventually produces a nonfluorescent product, as illustrated in **Figure 18**. The free radical used here is 2,2'-Azobis(2-methylpropionamide) dihydrochloride (AAPH), which generates peroxy radicals, the most biologically relevant free radicals.

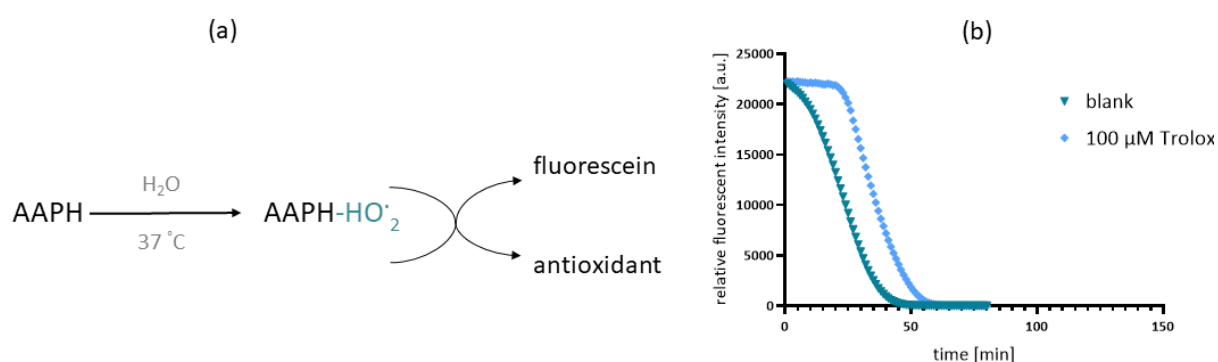


Figure 18: (a) The basic reaction of ORAC assay and (b) time-dependent fluorescence decay curve with and without antioxidant

To adjust the assay for the chemicals and device in the present study, several steps were followed to optimise the experimental conditions before validation.

ORAC assay optimisation

- The first step involved adjusting the gain, which is the specific value used to modify the photo multiplier tube sensitivity in the fluorimeter. It is the most critical device-related factor that can influence the measurements, as a higher gain means greater sensitivity and thus higher relative fluorescence intensity that can be detected, and versa vera. Therefore, three different gains were selected and used to detect the intensity of the fluorescein solution as follows: 396, 963, and 2000. As shown in **Figure 19**, the 2000 gain resulted in the maximum detected intensity via the device (65000 au) and the lowest gain resulted in extremely low values, around zero. While the middle gain identified values around 25000 au, which is properly sensitive and far enough from the minimum and maximum reading values.

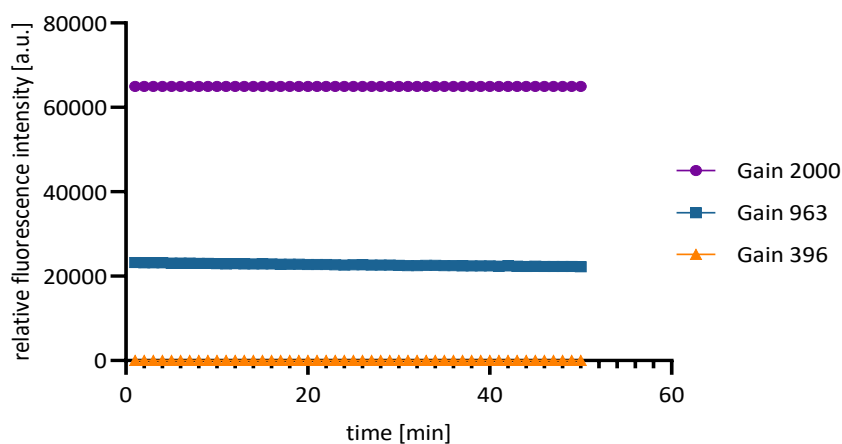


Figure 19: The detected fluorescence intensity using three different gains

- The second step focused on selecting the suitable concentration of the employed free radical, AAPH. Literature screening revealed multiple possible concentrations that could be used [148–150], accordingly, 400 μM and 125 mM (high and low concentrations) were selected for investigation. They were tested with the fluorescein solution, and the results revealed that the higher concentration was able to initiate fast and complete curve decay while the other was not; thus, it was selected for the experiment (**Figure 20**).

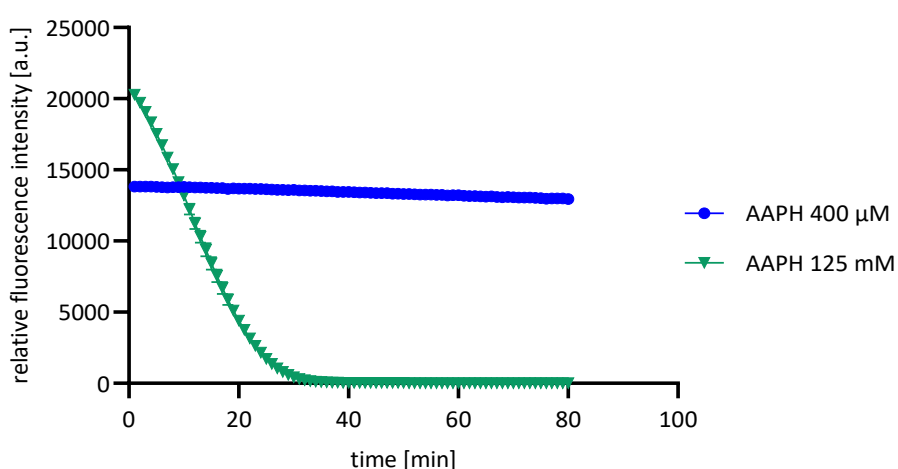


Figure 20: Curve decay of the fluorescent probe over time using two different concentrations of the AAPH

- Upon optimisation of the basic conditions, Trolox stock was prepared. A Trolox range of 12–150 μM has been identified as the external standard and was used in the present work. Outcomes suggested that the concentration range of 22.2–100 μM was the most suitable range for the assay, showing a very good response with the free radicals and achieving an excellent linear relationship in the calibration curve, as illustrated in **Figure 21** and **Figure 22**. This wide range covers variable samples and is

comparable to the ranges used in multiple published studies in the literature [134, 151, 152].

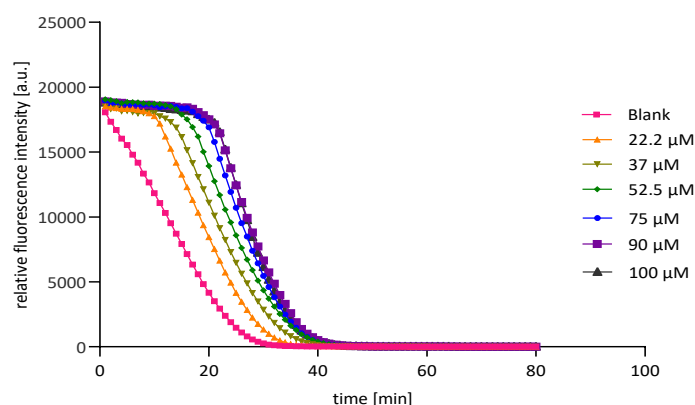


Figure 21: Fluorescence decay curves induced by AAPH for multiple Trolox concentrations

Validation

After the adjustment of the assay conditions, it was crucial to validate the method before regular usage in the AOC studies. Therefore, the modified assay was independently performed for five runs. The calibration curve was calculated by plotting the Trolox concentrations versus their corresponding AUC values (**Figure 22**). The correlation coefficient for each run is described in

Table 4, showing a cumulative r of 0.99 ± 0.005 , thus, the linearity of the method was ensured.

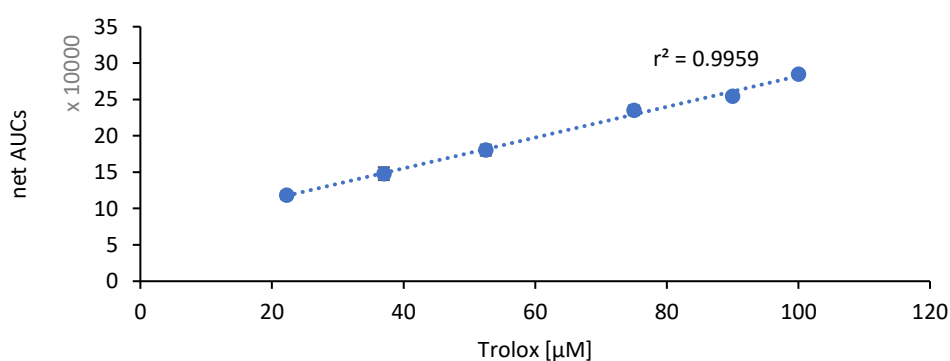


Figure 22: Trolox calibration curve

Table 4: The correlation coefficient, slope and intercept of the Trolox standard curve for each run

Run	r ²	Slope	Y-intercept
1	0.98	2226.00	76441.00
2	0.99	2598.00	45345.00
3	0.99	2604.00	46632.00
4	0.99	3070.00	26512.00
5	0.99	3634.00	31737.00

Furthermore, the relative standard deviation (%RSD) and the relative error (%RE) were used to express precision and accuracy. As summarised in **Table 5**, the method showed that the %RSD was < 10% and the %RE was within $\pm 10\%$; thereby, it was clearly demonstrated that the validated assay was specific, precise, and accurate within high criteria.

Table 5: Precision and accuracy of the ORAC assay for 5 runs, expressed as relative standard deviation (% RSD) and relative error (% RE)

Nominal Trolox concentration		37.5	90
Run 1	Intra-mean	36.5	86.8
	% RSD	5%	2%
	% RE	97%	96%
Run 2	Intra-mean	37.3	91.2
	% RSD	6%	2%
	% RE	100%	101%
Run 3	Intra-mean	39.1	91.4
	% RSD	5%	3%
	% RE	104%	102%
Run 4	Intra-mean	39.1	91.4
	% RSD	5%	3%
	% RE	104%	102%
Run 5	Intra-mean	34.8	90.9
	% RSD	4%	4%
	% RE	93%	101%

The ORAC assay has several advantages over other assays, making it a powerful tool in antioxidant screening. First, and unlike the previously used assays in this section, it integrates the lag time and the initial rate approach, which is especially helpful for plant samples since they include several substances and have complicated reaction kinetics [102]. It also provides a measurement for both lipophilic and hydrophilic antioxidants [102, 103] Moreover, this

assay applies the most biologically relevant free radical; the peroxy radical (OH^\bullet), and is based on fluorometry, which is more sensitive and specific than spectrometry and does not interfere with plant constituents [153–155]. Thus, the outcomes can be more meaningfully correlated to the *in-vivo* setting.

For reasons outlined above, ORAC has been widely used in the food research community as the AOC assay of choice and was applied to generate the AOC database alone [156] and with the F-C assay [157]. The challenges of performing the ORAC assay include the longer preparation and analysis times, as well as the fluorometer requirement, as this device may not be as readily available to researchers as a spectrometer. In addition, the samples in the 96-well plate were maintained at a temperature of around 37 °C, which was essential given that the reaction is temperature sensitive. This step required avoiding the use of all external wells of the plate to guarantee the accuracy and reproducibility of the results.

Following the earlier prescribed steps, an applicable, accurate, and precise ORAC was established and ready to be employed with the prepared plant formulations, along with the other mentioned assays.

4.1.1.2. Assays application on plant formulations

Three plants from Saudi Arabia—resembling roses, leaves, and fruit, as shown in **Figure 23**—were selected for this study. These plants included Taif roses (*Rosa damascena trigintipetala* Dieck), guava leaves (*Psidium guajava* L.), and dates (*Phoenix dactylifera*), which were tested for the activity upon their preparation into the two formulations: classical hydrophilic extract and PlantCrystals.



Figure 23: Macroscopical images of the plant used to produce the plant formulations; (A) Taif roses, (B) guava leaves and (C) dates

The plant formulations were prepared using high-speed stirring (HSS), homogenisation (HPH) and bead-milling (BM); these techniques allow for the downsizing of the plant materials into micro- or even nano-sized particles without the use of any organic solvent or bio-waste. Thus, the produced formulations were called PlantCrystals, and as a novel plant concept, they have multiple advantages in addition to being an eco-friendly technology [129]. PlantCrystals, compared to the conventional plant extracts, have higher amounts of readily available active ingredients due to the cell disruption that occurs during processing. While conventional plant extracts provide only a limited fraction of plant constituents depending on the constituents solubility. The feasibility of the PlantCrystals concept was proved in prior work, where the improved antibacterial and antifungal activities of multiple plant materials have been demonstrated [19, 20, 158]. However, this section was devoted to exploring their potential to enhance the AOC, as this particular activity has not been investigated extensively yet. Therefore, a systematic study to examine the effect of plant material and the different processes on PlantCrystals sizes and properties was done.

Hence, Taif rose, guava leaves and date were selected for their well-recognized role as antioxidative agents and their known ability to prevent and treat oxidative stress and related diseases. Moreover, they are widely exploited as food, nutraceuticals, phytomedicines, skincare and cosmetics.

In the following section, these plants were prepared into PlantCrystals, in addition to ordinary extracts as control samples.

Taif rose

Taif rose belongs to the *Rosaceae* family, and it is one of the most important crops of the Taif governorate in Saudi Arabia, where there is a special annual festival dedicated to celebrating the harvest season with art, food, as well as locally made cosmetics and perfumes (**Figure 24**). Several crude materials using this plant are also produced, such as rose oil, rose concrete, rose water, and dried rose petals, which are used afterwards in the perfume, cosmetics, and food industries.



Figure 24: Taif rose trees (*Rosa damascena trigintipetala* Dieck) during the spring of 2022

The Taif rose is rich in many valuable components like essential oils and multi-group antioxidants, justifying its popularity as a natural remedy (**Table 6**). Modern research has confirmed the Taif rose's well-known traditional benefits as an antitussive, relaxant, and for topical antiaging [159]. It demonstrates significant antioxidant, anti-inflammatory, antimicrobial, anti-tumour, and antidepressant activity [160, 161], in addition to providing

migraine relief through aromatherapy treatment [162]. Accordingly, it is a promising candidate to be the plant of choice to be formulated into the novel PlantCrystals formulation.

Table 6: Main phytoconstituents of *Rosa damascena*

Phytochemical group	Major constituents
Essential oils	Citronellol, geraniol, nonadecane, nerol and linalool [163]
Phenolic compounds	Gallic acid, catechin, quercetin, gallic acid, rutin and apigenin [164]
Alkaloid compounds	Berbamine, jatrorrhizine, palmatine, reticuline, isocorydine and boldine [165]
Carotenoid degradation products	β -damascenone, β -damascone and β -ionone [166]
Mineral contents	Phosphorus, potassium, calcium, magnesium, sodium, iron, copper and manganese [159]
Vitamins	Vitamins C, A, B1, B2, B3 and K [167]

Size characterisation of PlantCrystals

In the current study, the use of HSS and then HPH on the Taif rose plant successfully produced PlantCrystals, with the main particle size of $> 5 \mu\text{m}$ (z-average = $4704.33 \pm 919.93 \text{ nm}$) as analysed by dynamic light scattering. **Figure 25** illustrates the findings obtained using laser diffraction, which had a wide volume distribution within the range of 5–220 μm . In comparison to the bulk suspension, these sizes appeared to be smaller and the liberation of the active constituents of the plant was assumed to occur during the grinding process.

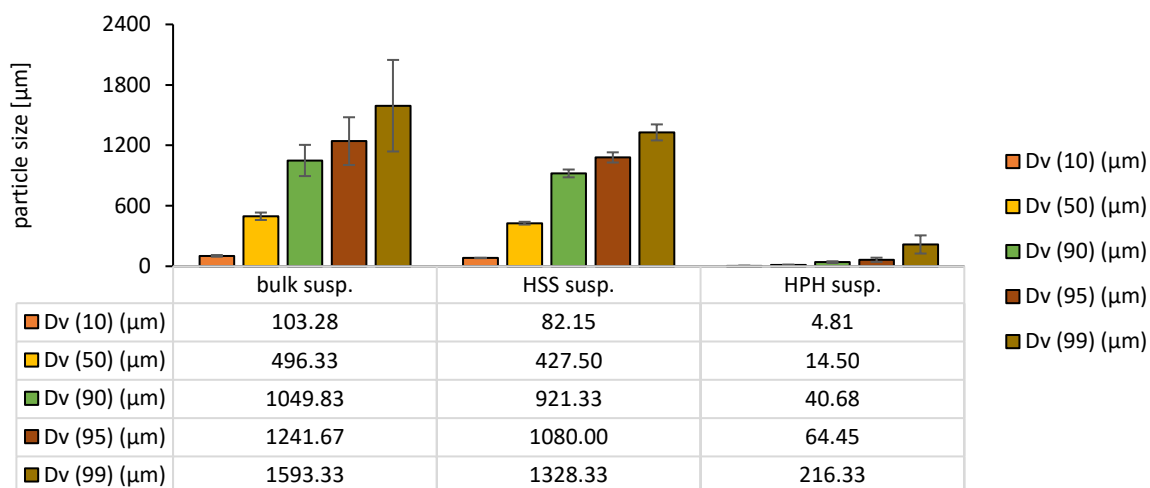


Figure 25: Taif rose particle sizes analysis by laser diffraction obtained before processing (bulk susp.), after processing with high-speed stirring (HSS susp.) and high-pressure homogenisation (HPH susp.)

The last size inspection was done using the light microscope, which agreed with the previous results. The HPH suspension (susp.) showed much smaller particles compared to those in the bulk and HSS suspension; nevertheless, large micro-particles were still observed (**Figure 26**). Thus, the Taif rose PlantCrystals included particles in the micro range, and they are still forming a more effective and stable formulation than the initial suspension. However, the use of another grinding method (e.g., BM or smart technology) may generate smaller particles and probably higher activity [129].

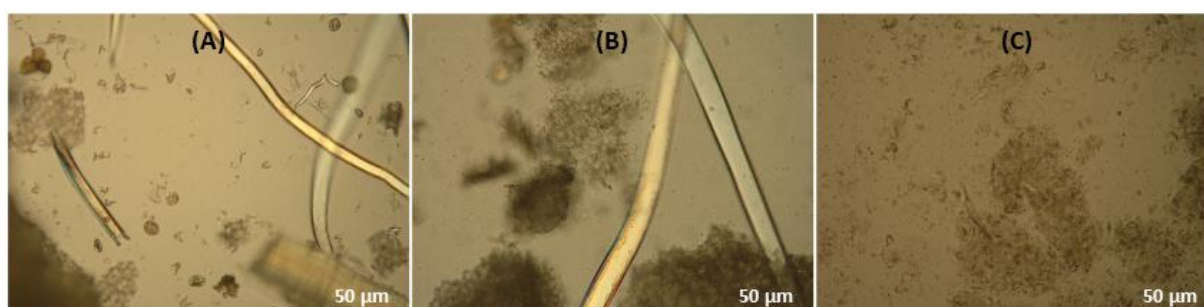


Figure 26: Microscopical images of Taif rose formulations; (A) bulk plant suspension, (B) processed plant with HSS, and (C) PlantCrystals. (Magnification: 200-fold)

Determination of AOC

The previously developed assays within the present study were utilised to investigate the influence of the grinding process on the Taif rose bio-actives, particularly antioxidants. The studies were done using the initial sample (bulk susp.), the intermediate formulation (HSS susp.), and the PlantCrystals.

Overall, as presented in detail in the following part, the release of more active components was achieved, resulting in a highly improved formulation with a significance value of < 0.0001.

Determination of flavonoid and carotenoid content

The content analysis of the samples is described in **Table 7** and it revealed the remarkable success of the HPH processes to liberate the flavonoid and carotenoid materials. For flavonoid, the content significantly increased by more than four-fold, while for carotenoid, the improvement was more than eleven-fold. These results confirmed the maximised pharmacological potential of the Taif rose PlantCrystals.

Table 7: The flavonoid and carotenoid content of Taif rose plant formulations

Formulation	Flavonoid content	Carotenoid content
	QE [μg]	β -CE [μg]
Bulk suspension	88.81 \pm 3.17	2.97 \pm 0.58
HSS suspension	104.67 \pm 1.24	4.49 \pm 0.23
HPH suspension	372.81 \pm 28.10	34.49 \pm 0.50

Folin Ciocalteu assay

This assay was used to estimate the total phenolic content and to determine the AOC of the samples. Compared to the initial bulk suspension, the obtained homogenised sample showed activity improvement by almost 200%, as it was 573.33 ± 3.03 and reached 1031.56 ± 15.33 mg GAE, as shown in **Figure 27A**.

This finding confirmed the higher phenol content of the PlantCrystals, and also provided vital evidence that the compounds in the processed formulations still have significant AOC after HPH.

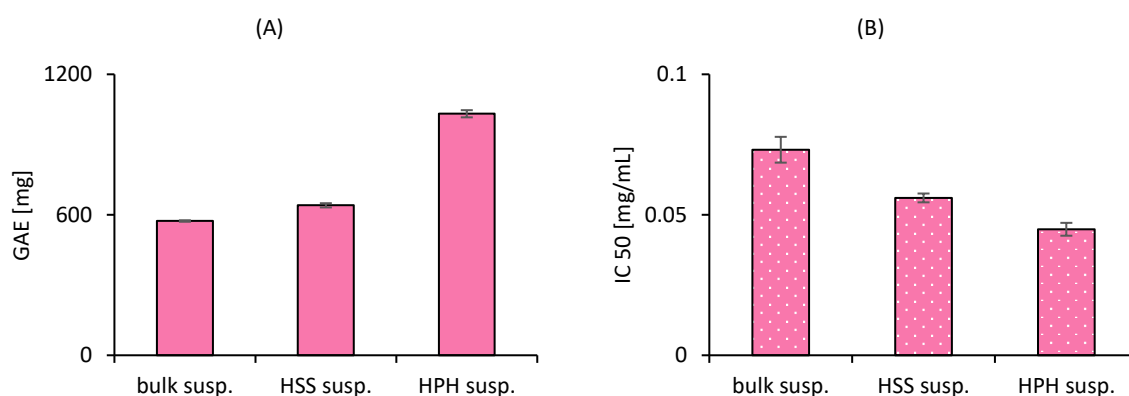


Figure 27: Antioxidant capacity of Taif rose plant formulations, (A) using Folin Ciocalteu assay expressed as GAE [mg], and (B) using DPPH assay, expressed as IC 50 [µg/mL]

DPPH assay

For further proof of concept, the plant formulations were analysed using DPPH assay. The results are shown in **Figure 27B** and expressed using IC 50, which is the amount necessary to scavenge 50% of the existing free radicals; a lower IC 50 indicates a higher AOC. The DPPH values were in total agreement with the F-C assay findings. The AOC increased with decreased particle size, eventually reaching 200% AOC improvement for the PlantCrystals sample (0.07 ± 0.004 to 0.04 ± 0.002 µg/mL).

Thereby, Taif rose PlantCrystals can be employed as a useful formulation for greater efficiency and safety in cosmetics and food instead of the classic extract. In addition to the improved bio-active content, this formulation is expected to achieve better bioavailability when applied *in-vivo*; for example, in topical application, because the small particle sizes enhance bio-active penetration and skin adhesion [168].

The presented data verifies two points: first, the suitability of the selected assays for investigating the impact of the grinding process on plant micro-nutrients. Second, it confirms the superiority of the PlantCrystals over the traditional plant formulation in terms of the AOC, using the Taif rose as a model plant. Therefore, this novel formulation could be the aqueous formulation of choice, providing the highly active suspension of Taif roses with zero organic solvents and waste. A suggested practical application for this technology can be obtained using rose waste resulting from distillation, such as in the rose oil industry, which is produced in tremendous amounts every year [169] and expected to be recycled effectively. The rose waste PlantCrystals is anticipated to have very good AOC activity, as published studies have indicated remarkable activities using plant waste (e.g., black tea waste PlantCrystals) [130, 170]. The pruning rose waste also seems to be another good candidate to be formulated using this interesting concept, as its substantial bio-potential has been proven; thus, further active and economical formulations could be effectively produced [165].

Date

Date is the fruit of the date palm tree (**Figure 28**), which is among the oldest known plants that have been consumed by humans for more than 6,000 years. There are over 200 date cultivars worldwide with differences in taste, texture, and nutritional value. The top production countries of dates are Egypt, Saudi Arabia, and Iran [171]; the date in these countries has special value and is deeply connected to communities' history and religious beliefs.



Figure 28: The date palm tree (*Phoenix dactylifera*)

Traditionally, in the Arabian Gulf area, date is considered to be a wholistic staple food; so, it can be the single element in a meal accompanied by milk or water. Recent studies have confirmed this, finding this fruit to contain all nutrients essential for survival, including carbohydrates, proteins, lipids, vitamins, minerals, and dietary fibres (**Table 8**). Additionally, and unlike most fruits, the matured date (tamer) can be self-preserved for a long time due to its high sugar and low moisture content [172]. Much data has corroborated the numerous health benefits associated with date consumption, such as its antioxidant, hepato- and nephroprotection, antimicrobial, anti-diabetic, and anti-tumour properties [173–177].

Table 8: Main phytoconstituents of date

Phytochemical group	Major constituents
Sugar and organic acid	Glucose, fructose, sucrose, oxalic and malic acid [178]
Amino acids	Proline, glycine, lysine, histidine, alanine and arginine [178]
Phenolic and flavonoid compounds	Vanillic acid, gallic acid, syringic acid, coumaric acid, caffeic acid, ferulic acid, apigenin, luteolin, quercetin and rutin [178, 179]
Phytosterols	β -sitosterol, stigmasterol and isofucosterol [177, 180]
Phytoestrogens	Formononetin, daidzein, genistein, glycitein, matairesinol, pinoresinol and coumestrol [177, 181]
Mineral contents	Potassium, phosphorus, magnesium and sodium [178]
Low molecules antioxidants	Glutathione, vitamin C and E [178]

Size characterisation of PlantCrystals

The concept of PlantCrystals using the BM technique was utilised to maximise plant benefits. Size analysis by dynamic light scattering revealed satisfying results, as this process was successful to ensure nano-sized particles (z-average = 348 ± 8 nm). Laser diffraction data is provided in **Figure 29**, reflecting the existence of small particles in the range of 3–121 μ m in the PlantCrystals suspension. It also indicated the mechanism that facilitates the production of this fine formulation; the small particle volume of the original bulk suspension, ranging from 44–574 μ m. The soft texture of this fruit and the high content of soluble fibres is the most likely explanation for this result. However, the effects of BM cannot be neglected, as this method showed higher efficiency in milling the plant mixture in the previously published studies, and resulted in a lower z-average compared to the homogenised sample [129].

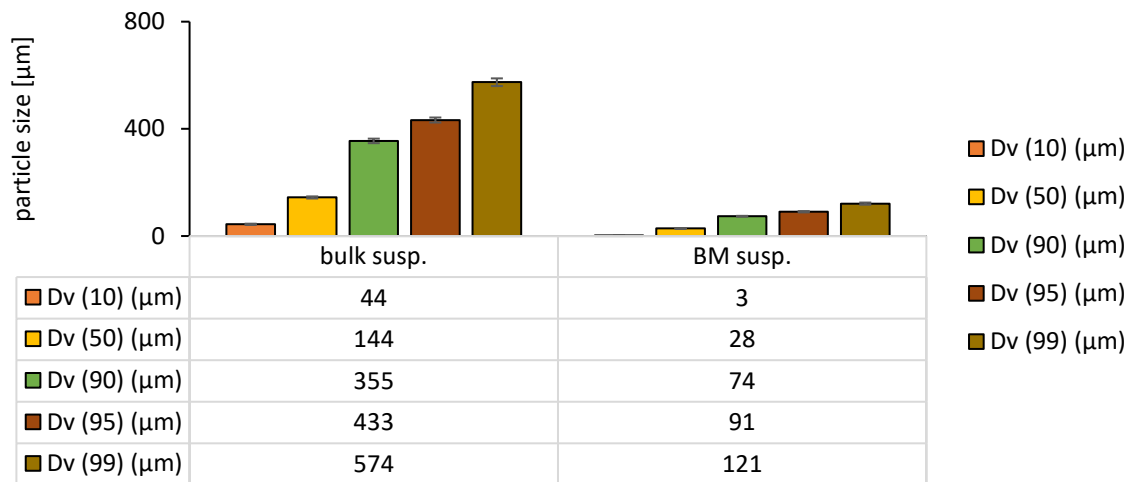


Figure 29: Date particle sizes analysis by laser diffraction obtained before processing (bulk susp.) and after processing with bead-milling (BM susp.)

As expected, the light microscopic images had provided the same conclusion (**Figure 30**). The bulk-suspension image shows the unprocessed particles and date fibres, while the clear field in the other image implies the presence of much smaller particles. As mentioned previously, the successful nano-sizing of this plant occurred due to the technique used and the nature of the date plant. Therefore, it might be assumed that any plant with a similar nature could be ground effectively using BM (e.g., raisins).

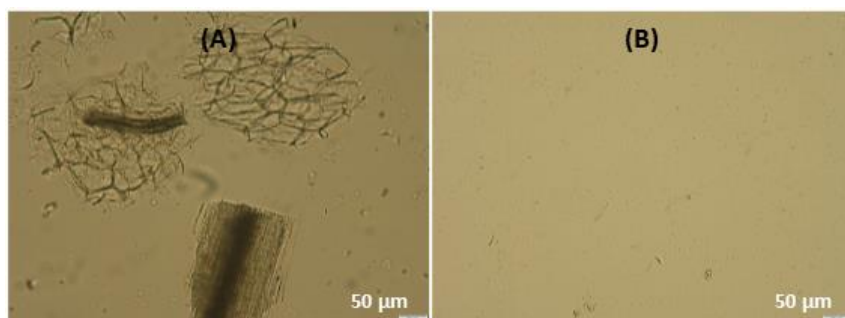


Figure 30: Light microscopic images of date formulations; (A) bulk plant suspension, and (B) PlantCrystals. (Magnification: 200-fold)

Determination of AOC

The established assays also reflected the evident success of BM to improve the potential of the formulation, with $p < 0.0001$.

Determination of flavonoid and carotenoid content

The BM process effectively released the plant constituents, as the flavonoid increased dramatically, from 6.13 ± 0.90 to 36.12 ± 0.73 μg QE. However, the carotenoid content was undetectable in both the initial and final samples. Reviewing the literature revealed that the date contains carotenoid but only in minute amounts [182]; therefore, detecting them was not possible using the spectrophotometer. A more advanced method is needed to detect these active constituents, such as liquid chromatography-mass spectrometry (LC-MS).

Folin Ciocalteu assay

The obtained values are described in **Figure 31A**, revealing activity enhancement from 184.43 ± 1.83 mg GAE (bulk suspension) to 246.28 ± 2.76 mg GAE for the PlantCrystals.

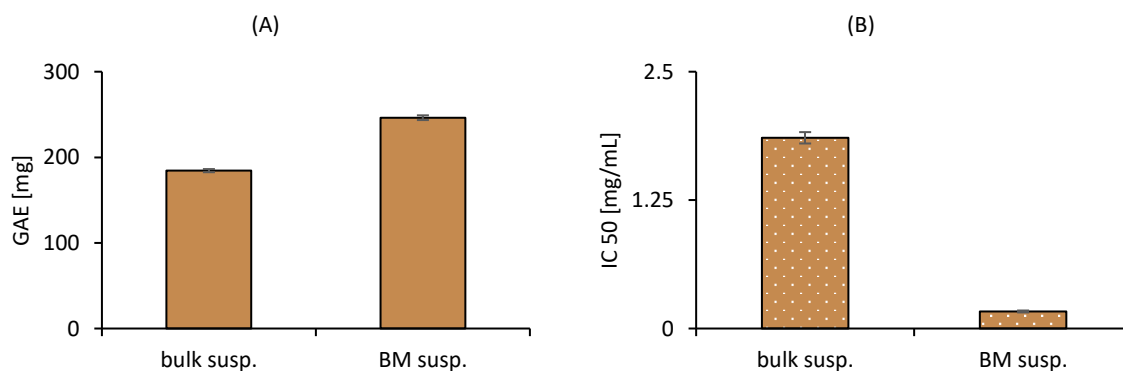


Figure 31: Antioxidant capacity of date plant formulations, (A) using Folin Ciocalteu assay expressed as GAE [mg], and (B) using DPPH assay, expressed as IC 50 [$\mu\text{g}/\text{mL}$]

DPPH assay

The AOC study by DPPH showed the outstanding capability of the PlantCrystals to scavenge free radicals, as the IC 50 had dropped from 1.85 ± 0.055 to 0.16 ± 0.01 $\mu\text{g}/\text{mL}$ (**Figure 31B**). However, the AOC values of both formulations had achieved higher activity than in the date sample outlined in the study of Hamad *et al.*, as their date extract of the same cultivars (Rashodia date) had IC 50 around 2.8 mg/mL [178]. This emphasises the benefits of using the whole plant in the formulation instead of using the extract and limiting the extracted elements according to their solubility. Therefore, the use of PlantCrystals enables the better availability of the phyto-actives in the formulation in addition to the synergistic effects of the plant constituents.

Based on the study results, it could be concluded that BM is highly applicable for use with fruits; mostly soft fruits. The significant improvement in the number of nutrients makes the date PlantCrystals a highly practical formulation to be used, for example, with hospitalised patients who need enteral nutrition (tube feeding) as a simple and rich food formula. For patients with digestive disorders, PlantCrystals also can be helpful in providing a source of readily absorbed natural food instead of synthetic formulations containing artificial ingredients and sweeteners.

Guava leaves

Since the ancient times, *Psidium guajava* L. (**Figure 32**) has been consumed as a traditional remedy in many countries to treat multiple conditions such as caries, wounds, diabetes, and gastrointestinal disorders [183]. In Saudi Arabia, the most used part of the plant is the leaves, which are thought to be particularly effective for respiratory disorders as an anti-inflammatory and cough suppressant when used as herbal tea (aqueous extract). Recent research has confirmed these traditional claims, not only for the respiratory system but also regarding the plant's antioxidant, cytotoxic, antimicrobial, antidiabetic, antispasmodic, and antiplatelet properties [184–188].



Figure 32: Guava tree (*Psidium guajava* L.)

Several studies have investigated the phytochemical nature of this plant, which has been found to comprise a unique mixture, including essential oils, polysaccharides, phenols, chlorophyll, vitamins, and minerals, as presented in **Table 9**.

Table 9: Main phytoconstituents of Guava leaves

Phytochemical group	Major constituents
Polysaccharides	Unsulfated and sulphated guava leaf polysaccharides [189]
Phenolic compounds	Quercetin, avicularin, apigenin, gallic acid, catechin, epicatechin, rutin, gallic acid and guaijaverin [190, 191]
Essential oils	Pinene, cymene, limonene, cineole, ocimene and terpinene [192, 193]
Mineral contents	Calcium, potassium, sulphur, sodium, iron and magnesium [194]
Vitamins	Vitamins C, A, B, E, and K [192]

Size characterisation of PlantCrystals

The application of the diminishing size technology was aimed to improve the leaves' dietary values with the advantage of having a natural and eco-friendly formulation. This aim was fulfilled, and thus HPH was effectively utilised as the dynamic light scattering study reflected the presence of small particles with a z-average of only $1.50 \pm 0.18 \mu\text{m}$. The laser diffraction investigation also revealed the success of the process, and particles in the range of 2.4–130 μm were detected in the PlantCrystals (**Figure 33**). Moreover, the microscopic images were consistent with the other results, showing a well-dispersed suspension with very small particles (**Figure 34**).

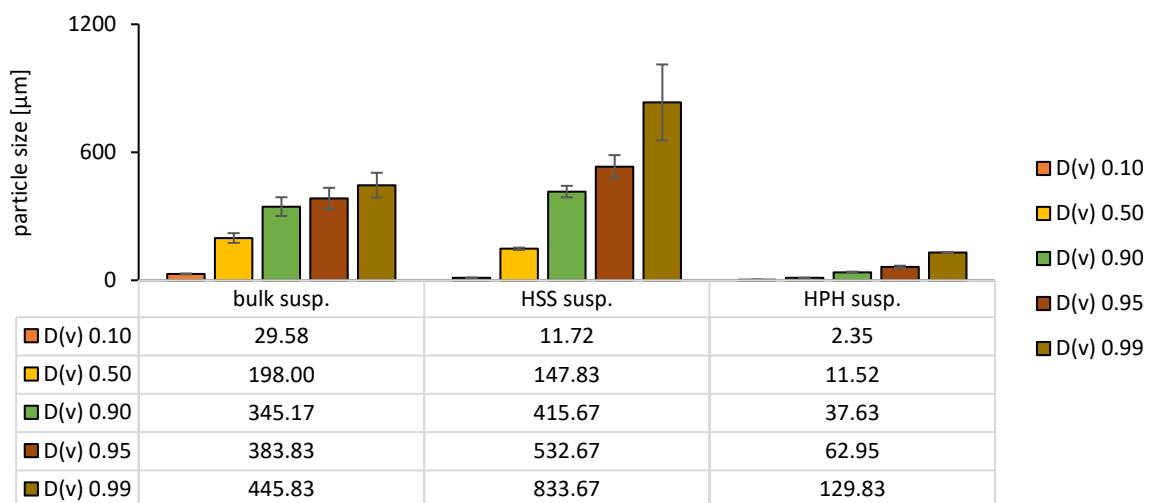


Figure 33: Guava leaves particle size analysis by laser diffraction obtained before processing (bulk susp.), after processing with high-speed stirring (HSS susp.) and high-pressure homogenisation (HPH susp.)

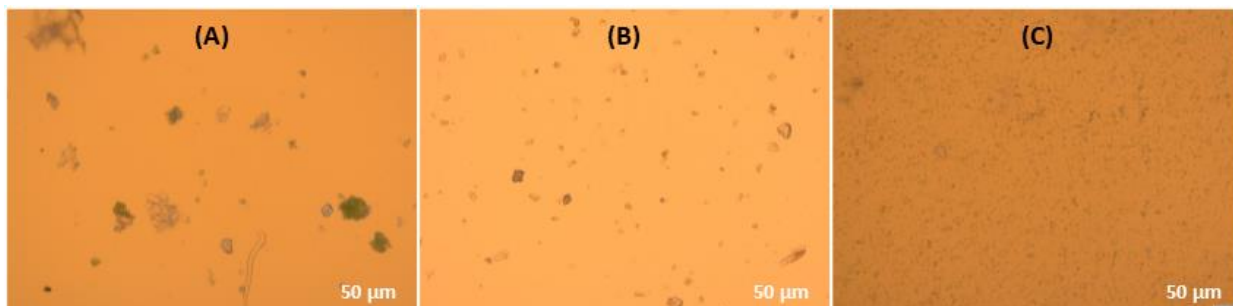


Figure 34: Light microscopic images of guava leaf formulations; (A) bulk plant suspension, (B) processed plant with HSS, and (C) PlantCrystals. (Magnification: 200-fold)

Determination of AOC

As expected, the positive impact of the HPH technology was reflected in the content analysis and the AOC, with a statistical significance of < 0.0001 .

Determination of flavonoid and carotenoid content

As demonstrated in **Table 10**, flavonoid availability was improved by almost five-fold, while the spectrophotometer measurements indicated a carotenoid increase of more than fourteen-fold compared to the bulk suspension. Nevertheless, the other studies did not specify the presence of a significant amount of carotenoid in this plant [195], therefore, the detected chromophores can be due to other plant constituents in guava leaves that have high absorption in the same area, like chlorophyll and β -caryophyllene [196, 197].

Table 10: The flavonoid and carotenoid content of guava leaves formulations

Formulation	Flavonoid content	Carotenoid content
	QE [μg]	$\beta\text{-CE}$ [μg]
Bulk suspension	115.86 \pm 14.81	6.88 \pm 0.26
HSS suspension	114.71 \pm 10.10	6.93 \pm 0.30
HPH suspension	500.88 \pm 42.33	99.26 \pm 5.54

Folin Ciocalteu assay

The results are shown in **Figure 35A**; significant improvement in activity was detected, increasing from 1229.00 \pm 2.97 to 2385.93 \pm 12.92 mg GAE for the PlantCrystals.

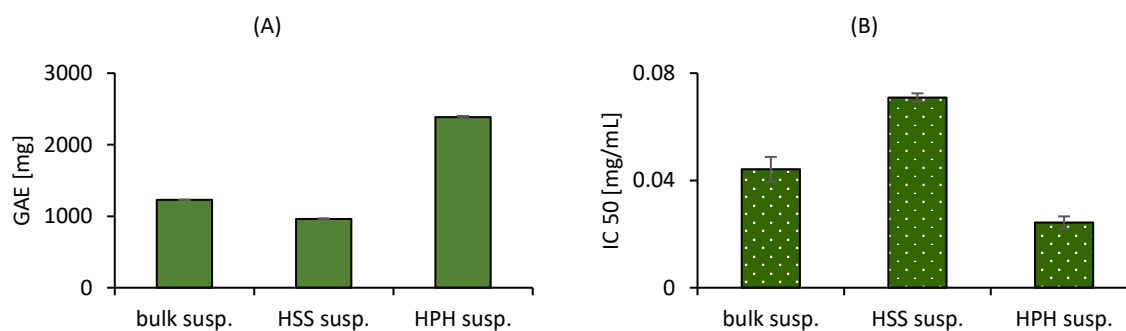


Figure 35: Antioxidant capacity of guava leaves formulations, (A) using Folin Ciocalteu assay expressed as GAE [mg], (B) using DPPH assay, expressed as IC 50 [$\mu\text{g}/\text{mL}$]

DPPH assay

A similar trend was observed using the DPPH assay, where the AOC was enhanced to almost double the activity, and the IC 50 dropped from 0.04 ± 0.001 to 0.02 ± 0.002 $\mu\text{m}/\text{mL}$ (Figure 35B).

In both AOC assays, the poor impact of the HSS process was observed. This phenomenon can be explained by the massive induction of oxygen that occurs during this procedure, which is prone to degradation of the vulnerable antioxidants after being released, such as vitamin C. A comparable scenario occurred during the production of the jasmine tea mixture in the study of Abraham *et al.*, as the HHS decreased flavonoid and carotenoid content, as well as the AOC [129]. Even the final PlantCrystals formulation was impacted [129]. On the contrary, this situation did not occur in the current study, as the further milling effectively allowed for the extraction of more valuable active phytoconstituents that tolerated the HPH protocol well.

The other leaf-based PlantCrystals that were formulated during the course of the study by Abraham *et al.* also showed remarkable success. Sage and laurel leaves had a small z-average upon HPH (≈ 650 nm), with elevated available content and AOC for the final samples. While grape leaves using BM had smaller sizes, but unexpectedly, the process did not produce a significant increase in the AOC [129]. Nettle PlantCrystals in the other study exhibited tiny sizes with good elevated flavonoid content and AOC activity via F-C assay [168]. In addition, it accomplished a more consistent and viable layer on the SC.

Therefore, HPH is a valuable method for producing guava leaf PlantCrystals; however, the use of BM is expected to produce smaller particles, but the net effect on the AOC is questionable.

Notably, guava leaves contain a significant amount of chlorophyll, which might spectrophotometrically interfere with the content analysis assays and the DPPH measurement at 400–700 nm [196]. Accordingly, the ORAC assay was further utilised to ensure the previous findings and roll out the possibility of obtaining inaccurate data.

ORAC assay

Interestingly, the AOC values determined by ORAC emphasised the same findings demonstrated in **Figure 36**. As the highly improved activity of PlantCrystals formulation was observed ($3883.35 \pm 51.74 \mu\text{M TE}$) compared to the bulk ($1074.94 \pm 229.19 \mu\text{M TE}$), in addition to the negative effect of the HSS on the AOC ($780.61 \pm 85.32 \mu\text{M TE}$). Ultimately, the ORAC can be a useful addition to the assay set to investigate the formulation AOC in a more accurate and interference-free way that works in a totally different mechanism. Indeed, the use of this assay added more value to the results, as it is a major AOC for plant studies with several advantages as described earlier in this section. Accordingly, the ORAC assay was effectively used to assess the guava leaf formulations in the current study, as well as for other plants in earlier published studies [129, 130].

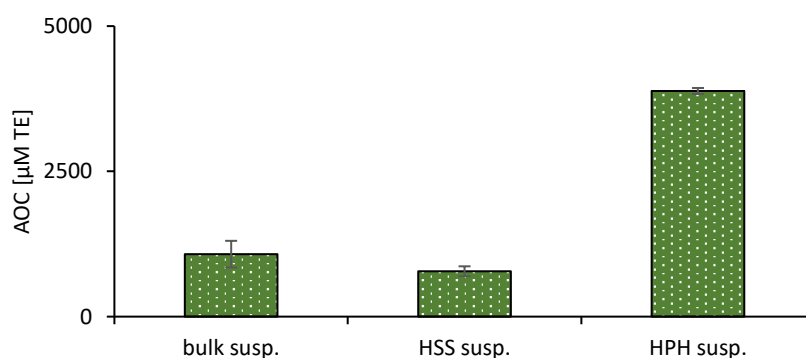


Figure 36: Antioxidant capacity of guava leaves formulations using ORAC assay, expressed as $\mu\text{M TE}$

Based on the obtained findings, the PlantCrystals concept has proven itself again to be a highly effective technique able to maximise the plant's sample value, particularly guava leaves. One example for the possible application is the use in dermal drug delivery as a wound-healing enhancer or as an antiaging ingredient in cosmetics. This potent, eco-friendly and natural

preparation can be used in many areas, and it will have a superior economical value since leaves are mostly wasted.

Summarising this study, the data revealed the advantage of PlantCrystals in terms of the antioxidative properties. In addition to the applied downsizing technique, several factors are estimated to influence the extent of the detected AOC in PlantCrystals, including:

1. The amount of the active constituents in the plant material, e.g., guava leave PlantCrystals showed the highest improvement of the AOC due to its higher original content of antioxidants.
2. The nature of the antioxidants, as the presence of hydrophilic active constituents, can be affected by the aqueous vehicle (stability issue) and by the applied method, i.e., if it includes heat and oxygen induction.
3. The presence of the UV-absorbing chromophore in the plant phytochemicals, which may interfere with the spectrophotometric measurement and give misleading data.

Nevertheless, this unique production method has been applied using many other plants from all over the world by Griffin *et al.* [19, 170] Sarfraz *et al.* [20], Abraham *et al.* [129–131], Knoth *et al.* [168] and Yassen *et al.* [198]. The tremendous enhancement of plant bioactivity has been observed, as well as antimicrobial, antifungal, and antioxidant activity.

The AOC characterisation was done using the assays listed in this study (flavonoid and carotenoid content determination, Folin Ciocalteu, DPPH and ORAC assays) and some published data sets are already released, all of which are cited in this section [129, 130, 168].

Comparing the obtained findings in this work did reveal that the Guava leaves PlantCrystals can be selected as the formulation of choice to be used in as novel cosmeceutical product, as the skin is the organ of focus in this thesis. Guava leaves PlantCrystals has shown the highest AOC, in addition to the presence of high amount of the natural vitamin C and the other multiple components that have proven efficacy when applied topically (e.g., quercetin). The development of such formulation is a promising approach, but in order to establish a suitable method that is able to assess the antioxidative impact of a certain formulation, a feasible and novel model must be developed and validated. This work has been done and presented in the coming section: the skin model and the current research on PlantCrystals had provided the backbone for those prospective studies.

4.2. The skin model

4.2.1. General investigations of skin properties of porcine ears—intact versus impaired skin

The study of the skin model in this thesis began with the measurement of the skin's biophysical properties, including barrier function, hydration, stiffness, pH and colour, using a multi-probe adapter MPA 10 device.

Fifty porcine ears were utilised in this study, which aims to define the standard values for the intact skin of the porcine ear *ex-vivo* model during a period of seven weeks. Furthermore, an extensive investigation of the impaired skin features was performed, using three to four distinct areas of each ear. Eventually, 194 skin spots were obtained and examined.

Five probes were used in this study; each one was applied to study a specific skin characteristic, as illustrated in **Figure 37**.

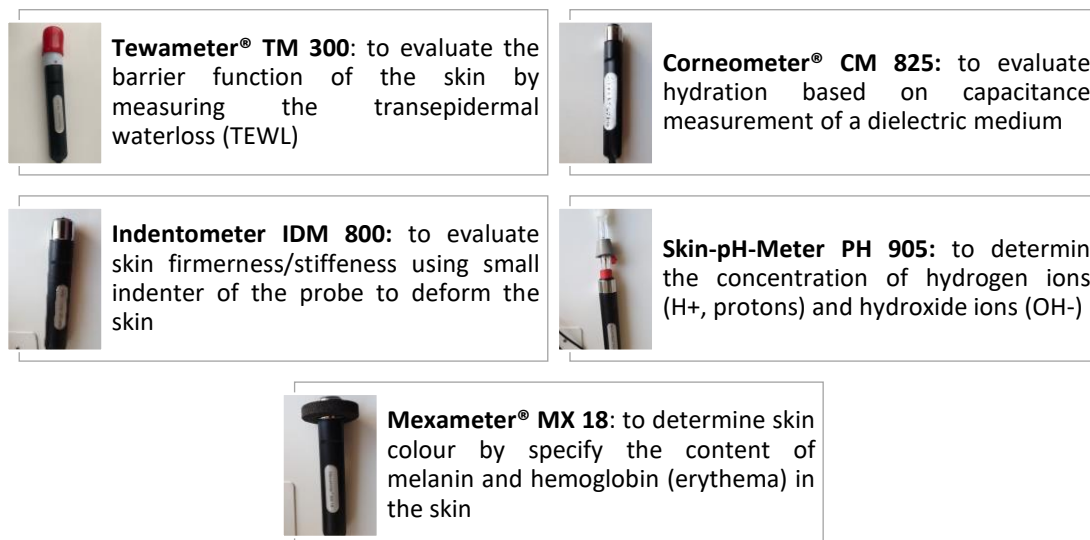


Figure 37: Skin probes used in current study

The concept of using a topical device on skin to estimate its character is an old protocol, and still, in rising popularity nowadays. The modern devices are providing fast, accurate and non-invasive measurement of skin properties via simple application. The more we know about these skin properties, the more we understand about skin physiology and pathology. Moreover, additional knowledge will be available regarding the associated factors (positive or negative) with these biophysical properties.

Historically, skin colour might be the first studied skin related factor (1953), and consequently, seven skin types were categorised using spectrophotometers and microscopes [199]. “Melanin granules” were determined to be the single factor defining skin colour. Later, the advanced research showed further chromophores that are present in the skin to identify its natural colour. They include; melanin (brown), oxyhaemoglobin (red), and deoxygenated haemoglobin (blue), in addition to carotene, as an exogenous pigment (yellow-orange) [200]. Skin colour determination is a valuable tool in medical science, not only to ascertain race - which is associated with multiple health factors- but also to understand, diagnosis, and treat many pigmentary disorders, e.g., hyperpigmentation and leukoderma [200]. In addition to the Mexameter® MX 18, several devices are available to assess skin colour, such as hyperspectral imaging [201], noncontact SIAscopy [202] and chromametry [203].

Skin surface pH as another crucial feature, was also among the early factors mentioned in the literature [204–206]. The skin’s buffering system was called “the protective acid coat” [207], and its relevance to the other body disorders was recognised [208]. Now, this parameter is not only of historical value, but it is also of a clinical significance in estimating the skin’s overall health, as it is vital to maintaining proper skin functions, like lipid synthesis and aggregation, permeability and antimicrobial defence [209, 210]. In this context, pH can be defined as “the negative logarithm of the concentration of free hydrogen ions in aqueous solution” [209]. The natural pH- range on skin is 4.1–5.8 [210], and its elevation is a sign of a disturbed general or localised health, as in the case of the irritant contact dermatitis, atopic dermatitis, and kidney disorders, among other conditions [208, 209]. It can be affected by endogenous factors (site, age, and sweat) and exogenous factors (cosmetic products and topical antibacterials) [209, 211].

The third skin property that has attracted considerable attention over the last decade is epidermal barrier health. The most significant research documenting its indirect evaluation was done by measuring the water in skin in 1980s, depending on the dielectric constant of water, expressed as transepidermal water loss (TEWL) and skin capacitance measurements (hydration) [212, 213]. Since then, the accumulated common knowledge has confirmed the implication of these two parameters, connecting both to clinically related pathogenesis, such as the link between the dry skin of elevated TEWL with psoriasis and atopic dermatitis [214–216]. Furthermore, long-standing methods have since been developed to provide more accurate and rapid status estimation. Several devices are currently available to estimate TEWL, like the Evaporimeter®, Vapometer®, and AquaFlux AF200® [217]. However, the most extensively used device is the Tewameter® TM 300 [217], which was used in this study. To assess hydration based on skin conductance, Corneometer® CM 825, DermaLab Moisture Unit® and Skicon 200 EX® are used [218]. Based on the same principles, another method has recently been published in scientific reports combining a smartphone, hydration probe and bio-display to provide instant, accurate, and portable skin hydration reporting [219].

The last area of interest is skin stiffness, which was also mentioned in the early 1980s as a skin marker linked to other health statuses, e.g. diabetes mellitus and stiff skin syndrome [220–222]. It gained attention as “the skin’s mechanical behaviour”, manifested in decreased skin elasticity affecting both the epidermal and subcutaneous tissues. It was measured using tensile testing, and the difference in skin stiffness was observed according to age, sex and anatomical site [223]. The updated methods to assess this feature include the use of a torquemeter [224], atomic force microscopy [225], ultrasound shear wave elastography [226] and the Indentometer IDM 800, which has the advantages of the simple and fast evaluation.

Therefore, the current study was done employing the multi-probe adapter (**Figure 37**) to provide the deeper understanding of the normal and abnormal skin of the porcine ear *ex-vivo* model. Although this model has been used extensively in skin and cosmetics research to date, particularly with the EU banning cosmetics testing on animals in 2009, most of the porcine biophysical properties and their subsequent comparison to human skin have not yet been determined. Accordingly, the skin investigations in this section were dedicated to fill this gap.

4.2.1.1. Definition and classification

Intact and impaired skin areas were defined on each porcine ear, initially according to the visual check-up, and then, using the Mexameter® assessment. After that, they were classified according to the erythema level, because all the impaired areas were subjected to erythema in variable extend.

Intact skin was specified as being free of scratches, redness and discoloration. Close observation of the impaired skin specified the presence of multiple deformities in the porcine ear skin, including erythema at multiple levels, wounds with different depths and sizes, brown discolorations and dry crusts.

The visual assessment revealed that most of the impaired areas displayed erythema and wounds of variable severity. Other manifestations like scars and crust were also present, but they did not meet the minimum required sample size (three replicates) and thus were excluded and considered as non-dominant skin impairment conditions.

Accordingly, the presentation of the results in this section is organised according to the classifications of erythema and wounds. Erythema cases were further sub-grouped according to the identified erythema level (**Figure 38**), while wounds were divided according to the visual inspection into penetrating (deep) and non-penetrating (superficial) wounds, in addition to the erythema level, as described in **Figure 38**.



Figure 38: Classified skin erythema level using Mexameter®

Figure 39 provides a photo documentation of four different ears, showing the marked areas, first tagged by number and then categorised as described earlier.

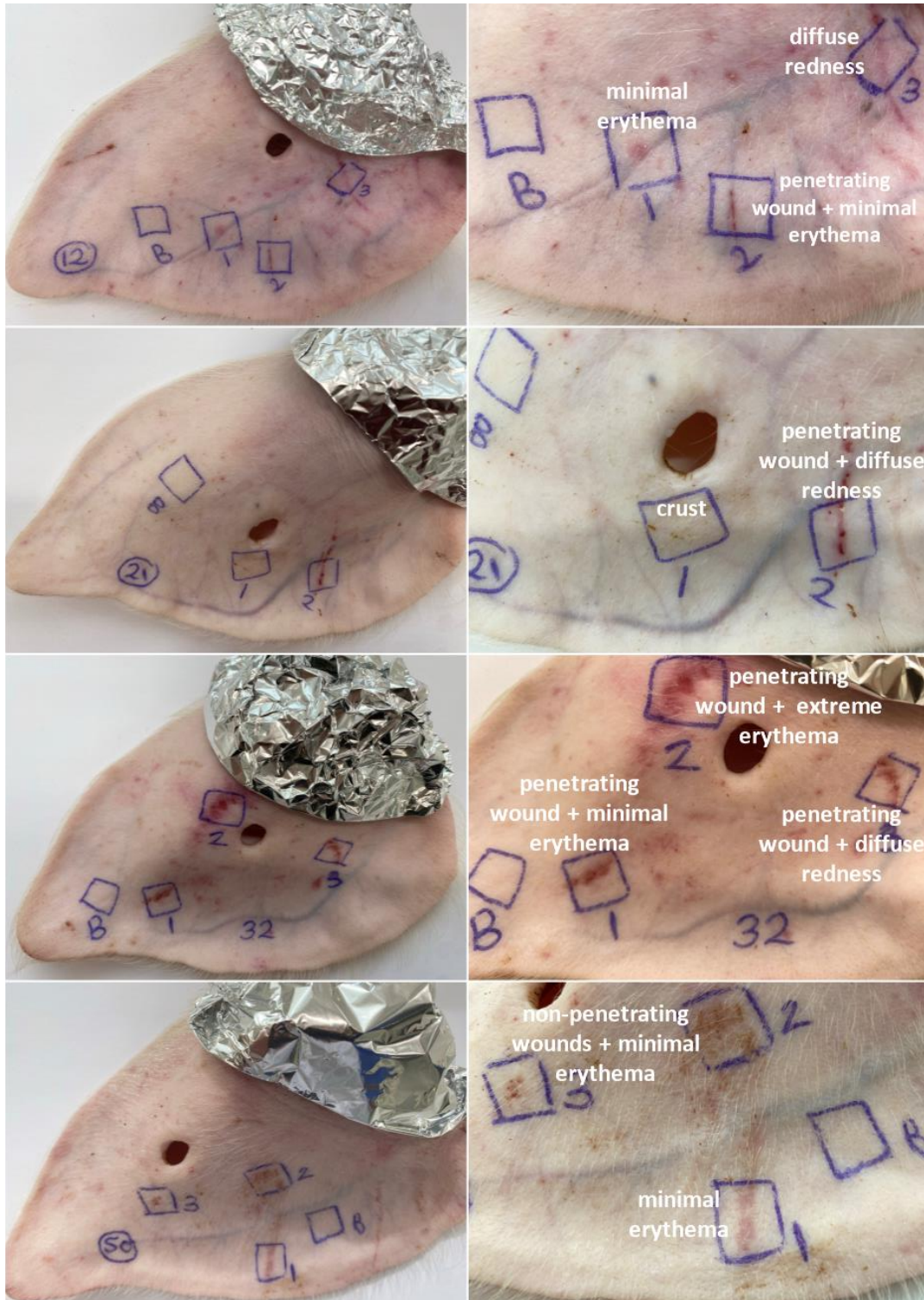


Figure 39: Examples of included ears in this study; left column shows the whole ear with the marker areas where (B) on each ear referred to the blank-intact area, while the impaired areas were numbered and then classified as shown in the right column

4.2.1.2. Intact skin

Investigation of the intact skin was done using 49 different porcine ears; the results are presented in **Table 11**. One intact area was excluded because it showed minimal erythema.

The detected TEWL was 10.64 ± 2.28 g/hm², reflecting a healthy skin barrier with proper function that was able to prevent epidermal water loss. On the other hand, the average measured hydration was 24.60 ± 9.44 , which is considered very dry according to the device manual. However, the acknowledgeable standard reference for healthy skin (> 40) has been specified for human studies; therefore, lower hydration values are commonly considered acceptable in *ex-vivo* porcine skin studies [227] and the obtained values in the current study confirmed this conclusion. Skin stiffness, another important skin parameter, was found to be 0.66 ± 0.23 mm, indicating the low penetration distance of the probe indenter into the skin, as the stiffer the skin, the less displacement depth will be found. Furthermore, the surface pH evaluation suggested neutral skin (6.38 ± 0.57) compared to the known acidic skin range. Finally, the Mexameter® studies indicated normal skin colour, which was classified as photo type I: extremely white skin.

Table 11: Skin biophysical properties for intact skin areas

Skin property	Value
TEWL (g/hm ²)	10.64 ± 2.28
Hydration	24.60 ± 9.44
Stiffness (mm)	0.66 ± 0.23
pH	6.38 ± 0.57
Melanin	49.67 ± 37.95
Erythema	63.17 ± 36.37

The acquired findings were compared to the published data to better interpret the porcine skin properties. The comparison showed similar results to many existing studies, while the impact of the biological variations was obvious in relation to other studies. Regarding the investigation of stiffness, inadequate research on porcine skin was found in the literature using the Indentometer; therefore, the complete assessment was limited.

The first study is that by Keck *et al.*, which was performed in the same lab as in the present study. Their TEWL measurement was ≈ 10 g/hm², while hydration was ≈ 29 , and stiffness achieved 0.9 ± 1 mm into the *ex-vivo* porcine skin [228]. The barrier functions and hydration parameters were almost identical, but a softer skin was noted (higher stiffness value). The most reasonable explanation is the natural variation among the biological samples. It is worth mentioning that the skin in their experiment became even more softer due to the effects of time. The authors explained this phenomenon by the effect of rigor mortis, which was combined with increased TEWL and hydration. However, the low sample size in their investigation compared to the current study also limits the possibility of a direct comparison of the findings.

Other research was also conducted at the same institution by Kaushik *et al.* They documented healthier parameters with lower TEWL values (≈ 6 g/hm²), and well hydration state (≈ 35) [229]. Their sample size was also low; however, more hydrated skin was detected in other studies in this thesis, up to 34.7, due to the seasonal effect (more hydrated skin was detected in winter/spring than summer/autumn) and the 24 h storage in fridge before the experiment. Moreover, another publication also documented high hydration value (≈ 50), but they were utilising defrosted and cartilage-free skin [230], So, the skin integrity was impacted by the freezing and the process of cartilage removal, which was reflected on changed biophysical properties.

Several factors can cause the fluctuation in skin parameters during a study, such as the lab's relative humidity (high or low), skin storage method (closed or open chamber), and storage duration (fresh skin versus skin stored in a refrigerator or freezer) [217, 228]. Other additional factors may also directly impact skin status, such as animal age and sex, water exposure,

environmental conditions, temperature changes, and pre-slaughter stress [231, 232]. For these reasons, the current work was done using fresh intact porcine ears, in controlled conditions (temperature of 23 ± 0.6 °C and relative humidity of $54.49\% \pm 5.77\%$) at a particular season: summer of 2021.

Reviewing the literature had revealed a clear lack of data on the skin properties of *ex-vivo* porcine skin; on the contrary, there have been many reports on the properties of human skin due to the simple and non-invasive use of the measurement protocol.

Therefore, a comparison of the porcine ear model to human skin is feasible and highly valuable in highlighting the potential similarities and differences. Although the *ex-vivo* porcine skin model has already been established as a substitute with confirmed similarity to human skin, most of the obtained values regarding its properties have been markedly different among studies.

In general, human skin has stronger barrier functions, is more hydrated and softer, with an acidic -not neutral- surface. The estimated values are as following:

- TEWL range of 6 - 10 g/hm² [232–234]
- Hydration range of 40 - 64 [232–235]
- Stiffness range of 1.4 – 1.8 mm [236]
- pH range of 4 – 6 [234, 235]

One of the main possible hypotheses for these variable values between human and porcine skin is the fact that living and non-living skin is being compared; an *in-vivo* model to *ex-vivo* tissue that no longer has active biochemical reactions and blood circulation. The only way to confirm or reject this hypothesis is to measure the skin properties of a living porcine animal.

Taking skin pH as a main example, reviewing the literature showed few relevant studies, such as the one that showed pigs with skin pH of 7.22 ± 0.28 by Ajito *et al.* [237]. They also demonstrated the tendency of the animal's skin to be within the basic range, as they recorded values of 7.07 ± 0.13 in cats, 7.75 ± 0.71 in dogs and 8.46 ± 0.57 in calves [237]. Thus, in the

pH comparison, the acquired pH range for the animals involved higher values than the human skin due to some differences between the humans and the animals, e.g., environmental impact and the lack of eccrine glands in pigs [238]. Regarding the study's findings, the obtained pH for the intact porcine skin now seems lower than that mentioned in published data (6.38 versus 7.22). The expected reason is the rigor mortis changes that involve the production of acetic acid, which has a very low pH [228].

Regarding barrier function measurement, old studies had examined the TEWL in living pigs, and interestingly, their reported values were highly similar to those of human skin; 6.29 ± 1.25 [239] and 7.56 ± 2.90 g/hm² [240]. Therefore, the conclusion could be drawn that the mild deterioration in the barrier function in the *ex-vivo* samples of this study was also due to the rigor mortis process (i.e., post-mortem contraction) [228].

In the term of stiffness, human skin has been found to be much softer than porcine skin [236]. This can be further generalised, as it is also supported by other research comparing the mechanical response of *ex-vivo* human and porcine skin, finding a marked change, explained by potential structural differences [241].

Although the current study has determined some differences in the biophysical properties of *ex-vivo* porcine skin, the suitability of this model has been proven in numerous research due to the common anatomical and physiological similarities to the human skin, such as SC and epidermal thickness, immunological components, protein and lipid compositions, and hair follicle distribution [238, 242]. Therefore, its application as a skin model has been recognised for wound healing, transdermal penetration, burns, radiation impact, infectious and inflammatory diseases [242, 243].

According to the findings of the present study, the normal values of the biophysical properties for *ex-vivo* porcine skin were determined and hence can be used as reference values in future studies. Their determination is of high value, as this model is widely used in the scientific research, mainly in the field of dermatology and cosmetics, and as mentioned previously, there is a scientific gap in this area and an absence of valid reference values. The

measurements using this convenient, rapid and non-invasive tool can reveal skin changes that might occur during a given condition or treatment.

4.2.1.3. Erythema

Erythema is manifested by a visible skin redness. It can be developed due to physical injury or as a part of the inflammation reaction that can result from skin disorders or overexposure to ultraviolet (UV) radiation [244]. This skin response has been utilised extensively in skin research to indicate skin status, for example, to evaluate the damage extent of a particular treatment and to determine the sun protection factor (SPF) of sunscreen products [59, 244]. In a similar way, erythema level was considered to be the primary marker of impaired skin in the current study.

In total, 37 single erythema spots were detected. They included minimal erythema (27 areas), slight erythema (5 areas), and diffuse redness (5 areas). Their measured biophysical properties are presented in **Table 12**.

Table 12: Skin biophysical properties for the skin areas with erythema

	Slight erythema (x = 5)	Minimal erythema (x = 27)	Diffuse redness (x = 5)
TEWL (g/hm ²)	11.98 ± 1.65	12.56 ± 2.50	11.84 ± 2.31
Hydration	13.78 ± 7.70	22.71 ± 10.10	23.41 ± 9.57
Stiffness (mm)	0.51 ± 0.21	0.67 ± 0.33	0.75 ± 0.41
pH	6.30 ± 0.41	6.55 ± 0.50	6.20 ± 0.74
Melanin	46.69 ± 25.51	53.44 ± 26.11	97.71 ± 31.40
Erythema	128.40 ± 27.35	236.28 ± 57.32	376.56 ± 22.42

Compared to the parameters of the intact skin, a mild change in the TEWL was detected, while the hydration and stiffness values reflected clear differences with specific patterns; higher hydration was positively correlated with higher erythema levels (Pearson $r = 0.8610$), and both resulted in reduced skin stiffness (softer skin; Pearson $r = 0.9650$). For surface pH, no marked differences were found among the samples.

A logical and simple explanation for this alteration in skin properties can be established by understanding the process of inflammation, wherein the localised vasodilation and oedema are developed to improve the blood circulation as an immediate response in the affected areas. Initially, the vasodilatation begins to enable the local supply of the inflammatory mediators [245]. Then, oedema is formed due to the flux of the rich plasma from the intravascular tissue into the interstitial compartment in order to deliver antibodies and proteins [245].

These processes change the function and permeability of the small blood vessels, which eventually also changes the physiological functions of the affected organ. In this context, skin increased erythema means increased vasodilatation and oedema, thereby elevated the bound water in the tissue and softened the skin. Similar observations were the basis of a study applying a porcine contact dermatitis model, wherein they graded the inflammatory areas according to the visual check-up of the erythema and oedema [246].

Although TEWL is considered to be a gold standard for the determination of skin health as shown in several reports [217, 232, 247], this erythema study showed otherwise. There was no significant difference in this value between skin with erythema and intact skin. However, further samples with higher erythema values are needed to identify that impact. Accordingly, the use of Tewameter® alone for skin assessment is not recommended to evaluate skin health.

To provide deeper understanding, further analysis using another graphical presentation was applied, comparing each impaired area to the intact area of the same ear and calculating the % of change. This method can provide more precise comparison from a different perspective.

As shown in **Figure 40**, higher TEWL variation was found. All the values were higher than those of the intact skin, indicating affected barrier function. However, this impairment did not exceed 116% and 121% in areas with slight erythema and diffuse redness, respectively, but it reached 131% for the areas with minimal erythema. It appears that the larger sample size for this category succeeded in reflecting the real biological sample differences. Nevertheless, the reasons for erythema are numerous, and their impact on the skin barrier is predicted to be highly variable. For example, the physical injury resulting from an animal fight will probably affecting the mechanical skin integrity more aggressively than the inflammatory response, e.g., due to UV exposure.

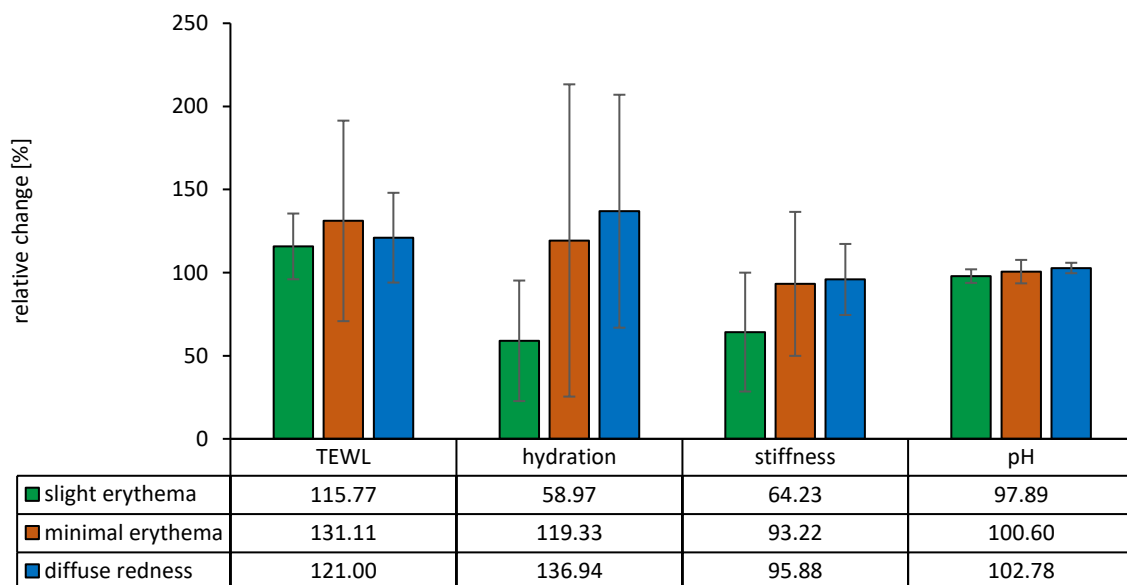


Figure 40: Relative change in biophysical properties for skin areas with erythema, expressed as relative change [%] in relation to intact skin off the same porcine ear

In the studies using Corneometer® and Indentometer (**Figure 40**), as emphasised above, hydration and softness increased with elevated erythema levels. Moreover, the comparison to the intact skin areas led to interesting findings; their values were markedly lower for slight erythema (59% and 64%); with more erythema, the values increased closer to the intact skin

(119% and 93%); and eventually, the values increased to 137% and 95% in the samples with diffuse redness, respectfully. Therefore, these findings clarified that skin properties changed in relation to the severity of the inflammation process, indicated by the erythema level. Mild inflammation resulted in less hydrated and stiffer skin, but with increased severity, the process became more serious and higher vasodilatation and oedema were produced, and thus elevated the hydration and softness. However, at a certain point, the extreme fluid accumulation in the tissue is expected to decrease the softness and make the skin stiffer and firmer. Further studies using more samples are required to confirm this hypothesis.

The surface pH levels revealed minor incremental changes following the same pattern observed previously. The expected reason for are the chemical changes of the skin tissue, which impact the buffering system, e.g., the dilutional effect of the oedema on the hydrophilic constituents, which play a major part in the skin buffering system, including lactic acid, amino acids and keratin [248].

Evaluating skin erythema is a critical measurement in the field of dermatology. In fact, the establishment of the porcine erythematous skin properties could provide the background for future studies employing these skin areas as *ex-vivo* impaired skin model. The value of this concept is worthwhile, especially considering the recent clinical study of skin irritation from the use of facial masks during COVID-19 pandemic [249]. Their data has disclosed a trend that is comparable to our findings: elevated redness associated with decreased hydration and TEWL compared to the baseline.

Accordingly, the current research presents an initial erythematous porcine skin model as promising prospective approach that is biomimetic, applicable and viable as impaired skin model.

4.2.1.4. Wounds

Skin wounds can be defined as the damage to or break in tissue integrity [250], mostly occurring on skin and mucosal membranes. There are multiple ways to classify wounds, for

example, open or closed, chronic or acute and penetrating or non-penetrating [251]. As the main focus of this thesis is the outer skin layers, the classification according to wound depth was applied. Accordingly, the wounds in the porcine ears were examined and categorised as penetrating and non-penetrating wounds. Otherwise, all the included wounds were open, acute, and contaminated with soil.

Penetrating wounds

Penetrating wounds include open, fresh wounds that have resulted from a stab or cut through the skin thickness. During the course of the study, 67 areas with variable erythema levels were identified and evaluated, as shown in **Table 13**.

Table 13: Skin biophysical properties for skin areas with penetrating wounds

	Slight erythema (x = 3)	Minimal erythema (x = 24)	Diffuse redness (x = 19)	High erythema (x = 10)	Extreme erythema (x = 9)
TEWL (g/hm ²)	14.67 ± 0.38	16.53 ± 6.81	19.43 ± 4.98	17.33 ± 5.22	21.76 ± 8.78
Hydration	25.65 ± 8.41	15.45 ± 10.30	18.4 ± 11.34	19.34 ± 10.71	19.00 ± 12.27
Stiffness (mm)	0.62 ± 0.25	0.60 ± 0.42	0.60 ± 0.29	0.88 ± 0.43	0.93 ± 0.24
pH	6.74 ± 0.60	6.54 ± 0.47	6.28 ± 0.70	6.34 ± 0.63	6.68 ± 0.19
Melanin	103.41 ± 65.65	127.66 ± 111.48	129.52 ± 52.45	228.10 ± 138.50	222.49 ± 109.80
Erythema	117.85 ± 50.10	248.16 ± 40.12	366.32 ± 38.61	473.08 ± 58.48	702.37 ± 119.86

Expectedly, and as a direct result of mechanical injury, the Tewameter® measurements indicated the impaired skin barrier, which were positively correlated with the extension of the erythema (Pearson $r = 0.9017$). Compared to the intact skin, a significant difference was found for all the skin areas except for skin with slight erythema ($p < 0.05$).

Regarding hydration, most areas had drier skin, except for the wounds with slight erythema, as that level of erythema revealed wounds of less severity and thus less barrier damage and water evaporation. This dryness was significant in the case of minimal erythema ($p < 0.0001$) and diffuse redness ($p = 0.0013$). The nature of the injury led to loss of the skin's bound and free water, even though with the concurrent vasodilation and oedema resulted by the physical injury. However, looking into stiffness values, the inflammation processes were intense enough in the high and extreme erythema samples to soften the skin (0.88 ± 0.43 and 0.93 ± 0.24 mm). The pH levels mildly fluctuated with no particular pattern.

Calculation the % of change comparing to the intact skin of the same ear had implied comparable findings (**Figure 41**). Indeed, the barrier functions were impacted and strongly associated with the extension of erythema. On the other hand, hydration was found to be lower in the injured areas, except in the wounds with extreme erythema, where the oedema was able to compensate for the water loss even with the presence of the injury. Closer to what was shown earlier, stiffness was also improved with the compensating high and extreme erythema.

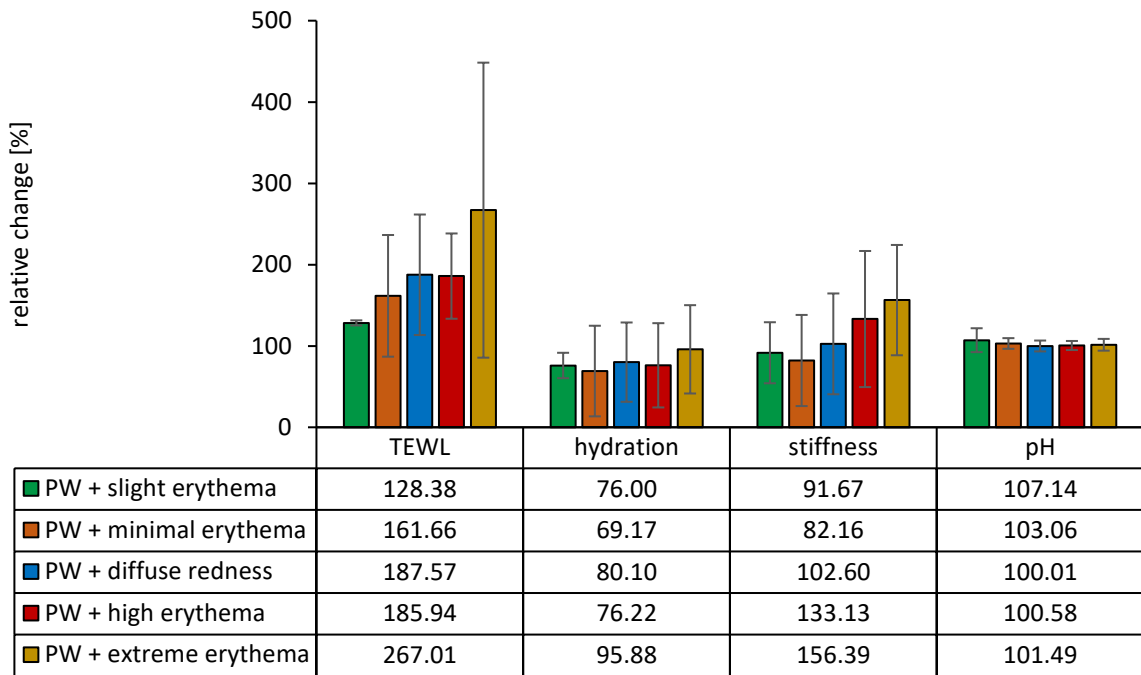


Figure 41: Relative change in biophysical properties for skin areas with penetrating wounds (PW), expressed as relative change [%] in relation to intact skin off the same porcine ear

Non-penetrating wounds

The extension of the non-penetrating wounds was limited to the skin surface and could be caused by friction trauma, e.g., with farm soil. In the current study, 19 samples were identified in this category, and the included areas showed minimal erythema (x = 8), diffuse redness (x = 6), and high erythema (x = 3), as illustrated in **Table 14**.

Table 14: Skin biophysical properties for skin areas with non-penetrating wounds

	Minimal erythema (x = 8)	Diffuse redness (x = 6)	High erythema (x = 3)
TEWL (g/hm ²)	11.09 ± 5.91	17.73 ± 5.34	26.77 ± 7.45
Hydration	14.11 ± 8.08	19.82 ± 12.00	7.83 ± 5.46
Stiffness (mm)	0.60 ± 0.31	0.78 ± 0.47	0.93 ± 0.45
pH	6.29 ± 0.57	6.34 ± 0.37	6.39 ± 0.30
Melanin	82.25 ± 39.21	115.69 ± 39.83	188.04 ± 89.32
Erythema	231.66 ± 40.68	356.17 ± 39.49	503.04 ± 26.92

As expected, TEWL was elevated in all samples compared to the intact skin, with significantly meaningful difference in areas with diffuse redness ($p = 0.0156$) and high erythema ($p < 0.0001$). Moreover, the erythema was positively associated with the degree of barrier impairment (Pearson $r = 0.9992$ with $p = 0.0259$), as more damaged skin surfaces meant more vascular injuries and higher erythema.

Examining the hydration readings revealed lower hydration than normal, mainly in the high erythema samples, which had the driest detectable hydration overall in the study ($p < 0.0001$). No specific pattern was determined due to the absence of the minimal and extreme erythema samples, but it appears that hydration values were associated with erythema except for the severe injuries that developed high and extreme erythema, where the acute epidermal damage countered the oedematous effect.

Furthermore, stiffness measurements showed a trend similar to the TEWL findings, with positive correlation with erythema (Pearson $r = 0.9950$). This result was a typical example of the possible false-positive measurement. The oedema and defective barrier in the wounded skin enabled the Indentometer indenter (pin) to rotate deeper in the skin, suggesting its softer

nature. Therefore, the biophysical skin studies should always be combined with the visual investigation to rule out any possible misinterpretation.

Another trend was also observed in the mild increase of the skin pH along with the erythema. A possible reason for this could be the vascular rupture, leading to a slight change, as the blood has a slightly basic pH (7.36 - 7.44) [252].

The calculation of the % of change is demonstrated in **Figure 42**, indicating additional findings, largely regarding the Indentometer readings, where a positive trend was noticed between hydration and stiffness. Subsequently, the samples with diffuse redness had the most soft and hydrated skin spots. The rest of the results indicated data comparable to that in **Table 14**.

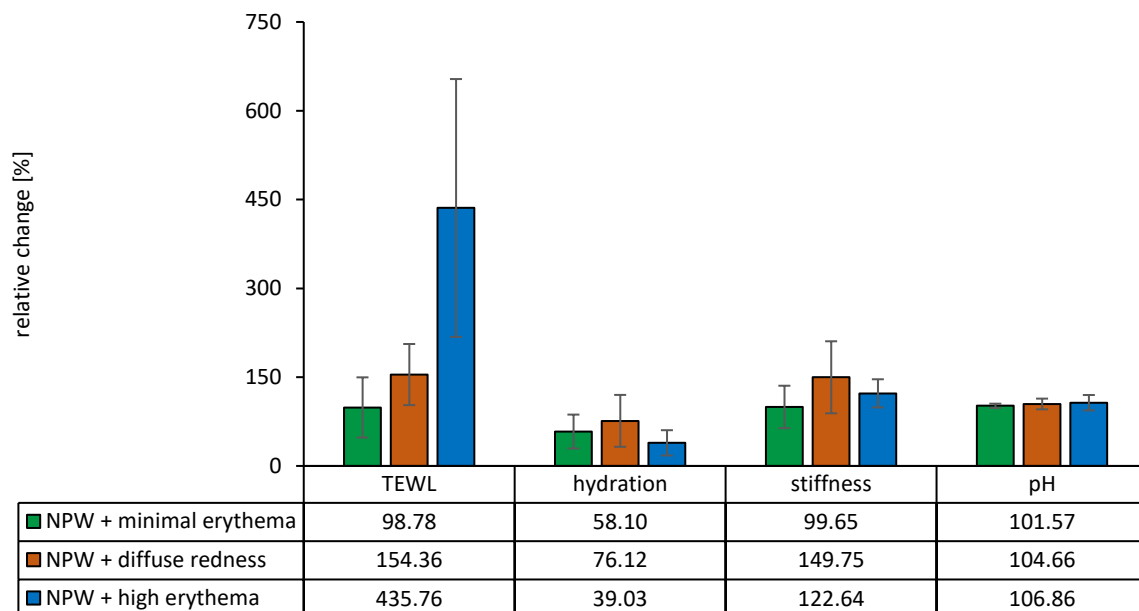


Figure 42: Relative change in biophysical properties for skin areas with non- penetrating wounds (NPW), expressed as relative change [%] in relation to intact skin off the same porcine ear

These changes in skin properties were in agreement with all the expected consequences of the acute physical injury in skin [247, 253]. In matter of fact, this trend (elevated TEWL and

decreased hydration) has been observed in many skin disorders, such as stable plaque psoriasis [254], scalp seborrheic dermatitis (with no differences in skin surface pH and roughness) [255], Werner syndrome and aged skin (with mild elevated pH, skin roughness) [256], as well as the skin after treatment with isotretinoin (with elevated erythema and pH values) [257]. As a result of skin changes, the SC diffusivity is increased, and higher drug permeability is anticipated due to the disturbed barrier function [258].

Thus, by characterising wounds in the *ex-vivo* porcine skin, a useful model can be established by employing these naturally occurring wounds. For example, as a wound-healing model or for penetration studies of the damaged skin. This model, as in the erythema model, may offer a more realistic and natural model that can be easily classified according to erythema level. However, a more precise method to classify the wounds (e.g., using Ultrascan UC 22 or histological studies) might be needed to distinguish the wound according to the depth of injury into the skin. Such a model can be used instead of skin damages induced by tape stripping [247], microneedles [253] or acetone treatment [258].

Therefore, the results of this study had demonstrated the references values for the intact skin of the porcine ear model, along with the values of the most common impaired skin deformities, including erythema and wounds samples. The classification according to the erythema level using Mexameter® was followed, and was successfully able to differentiate between the different samples. Moreover, as a one of the kinds, this study can be considered a validation study for the skin-probe assessment of the bio-physical parameters of skin to characterize different skin conditions.

Accordingly, a biomimetic model using the naturally occurring impaired skin areas was suggested for prospective studies. Additionally, further skin investigation for elasticity, roughness and friction can be off additional interest.

4.2.2. Skin intrinsic antioxidant capacity

As ORAC assay has been used successfully to evaluate the plant's AOC, the study to investigate another application of this valuable assay is presented in this section, which is its employment to assess the oxidative state of the intact skin. Thereby, the term; intrinsic antioxidant capacity (iAOC) has been introduced and used to describe the capability of the skin's antioxidant barrier to scavenge free radicals. The porcine ear was used as an *ex-vivo* model, and the skin was removed via tape stripping technique.

The essential aim was to define the normal range, and to determine the impact of the various conditions on the skin's iAOC. Therefore, in addition to the re-validation of the assay to be adjusted to skin samples, the study had been done in three stages, as illustrated in **Figure 43**.

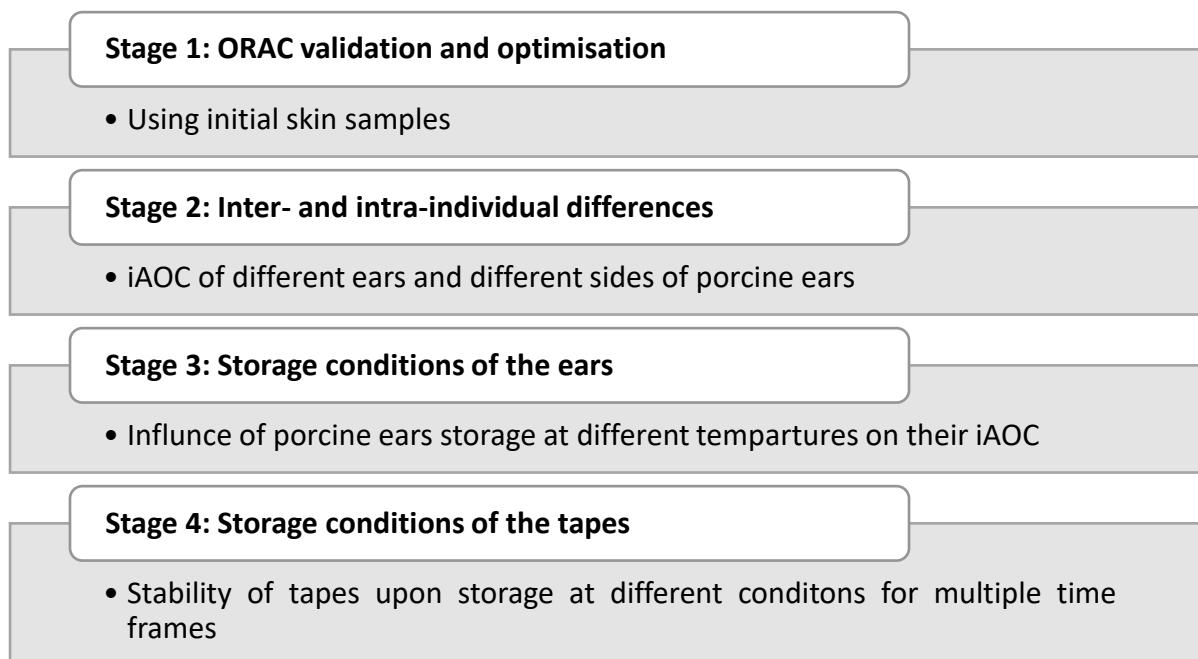


Figure 43: Study outline of current section

ORAC optimisation and validation

The specificity of the ORAC test has already been demonstrated in the scientific literature [134], and the optimal assay conditions were established previously in this thesis. Thus, the subsequent phase was adjusting the ORAC response with skin samples. Accordingly, the assay was applied to preliminary samples, and the findings demonstrated that the reaction needed around 100 minutes to reach the complete decay curve after the addition of skin samples, as shown in **Figure 44**. This period was longer than the required duration to obtain a complete decay curve for Trolox and plant samples. The reason is attributed to the complex nature of antioxidants in the skin, with variable response rates (rapid and slow-reacting antioxidants). Tocopherol, for example, is one of the primary lipophilic antioxidants and it is a fast-acting antioxidant, but glutathione, another crucial skin component, needs a longer response time and it is classified as a slow-acting antioxidant [259].

This interesting result highlights the superior advantage of ORAC when used to analyse biological samples that include several antioxidants. It combines initial rate and lag time mechanisms [102], which is eventually highly suitable for AOC detection of both; slow- and fast-acting antioxidants. In addition, this protocol provides a direct evaluation of both hydrophilic and lipophilic AOC [102].

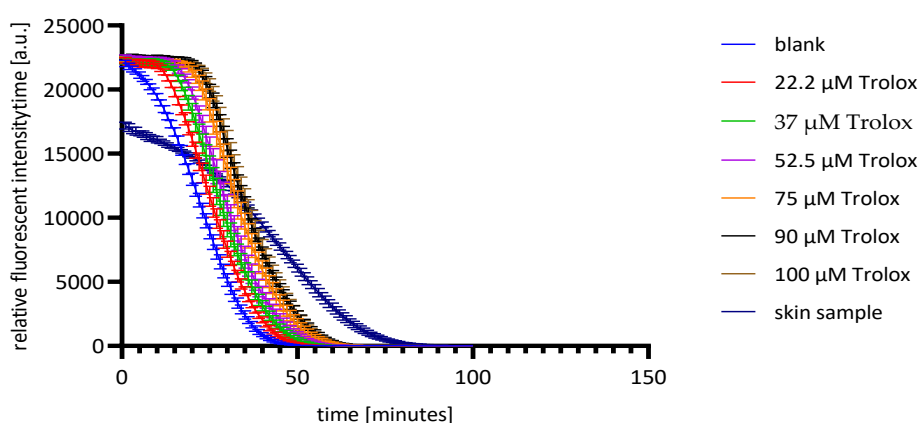


Figure 44: ORAC assay decay curves for Trolox and skin sample

Following this step, the assay was validated and a relative standard deviation (% RSD) of $\leq 9\%$ verified the method's excellent precision. Accuracy was measured as the relative error (%RE) and it was $100\% \pm 9\%$ for the Trolox samples while the correlation coefficient of the calibration curves was 0.99.

Therefore, ORAC was mildly adjusted, and successfully used to estimate the initial iAOC of porcine skin, demonstrating its applicability for the intended use.

inter- and intraindividual differences

As mentioned earlier, this part aimed to investigate the skin AOC of different ears and different areas of the same ear. So, the skin iAOC of seven independent ears was tested, in addition to both sides of all ears, as shown in **Figure 45**. A combined protocol including ORAC assay and tape stripping had been applied, besides the use of two supporting tools: the infra-red densitometer (IR-D) and the light microscope.

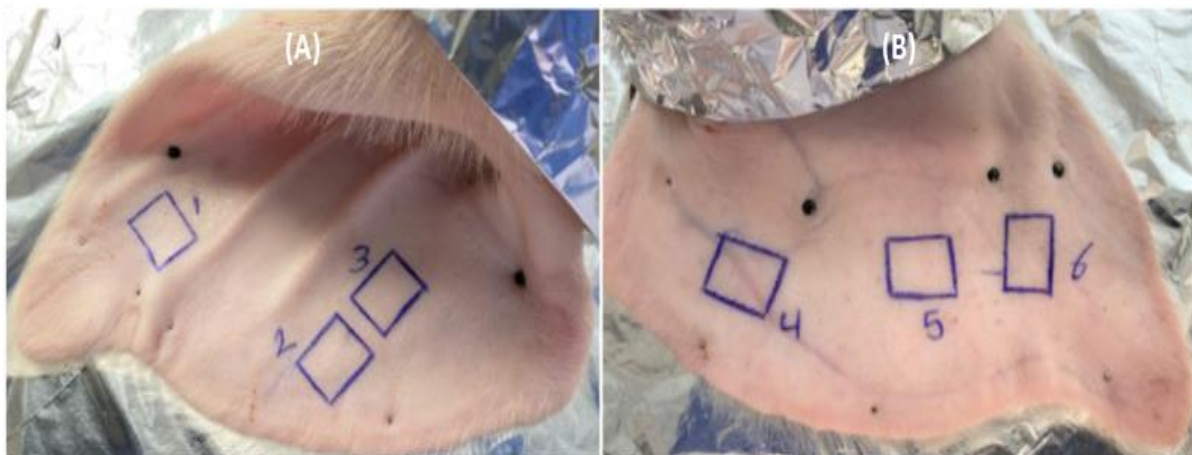


Figure 45: (A) The ventral side of the porcine ear, and (B) the dorsal side of the same ear that were used in the intra-individual differences study

study of the removed SC by tape stripping

Via IR-D

This useful device was employed to indirectly estimate the amount of the removed corneocytes from stratum cornea (SC) via tape stripping, as it has been used in multiple research reports [122, 138, 139, 260]. In the current study, all the tapes that were obtained had been examined by IR-D, and the results are demonstrated in **Figure 46**. The measurements revealed that more corneocytes were removed from the dorsal side than the ventral side, with $p = 0.0016$.

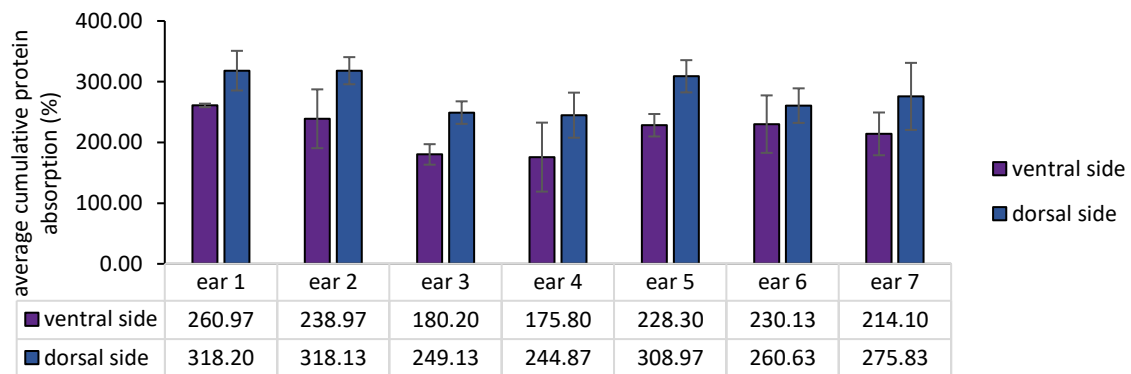


Figure 46: Average cumulative protein absorption (%) for dorsal and ventral sides of different ears

The average cumulative protein absorption for all the samples was $282\% \pm 48\%$ for the dorsal side and $218\% \pm 43\%$ for the ventral side. According to the literature, these values represent $86\% \pm 15\%$ and $67\% \pm 13\%$ of the removed SC, respectively, in comparison to the values obtained for the total SC (IR-D value of $327\% \pm 133\%$) [138]. Using the following equation that has been provided by Klang *et al.* [138] and others [261] to compute the thickness of the excised SC, more accurate data could be predicted from the IR-D measurements.

$$SC \text{ mean thickness} = \frac{A}{0.41} \mu\text{g}/\text{cm}^2$$

Therefore, the SC thickness (calculated from protein mass) was calculated as $6.88 \pm 1.18 \mu\text{m}$ for the dorsal side and $5.33 \pm 1.06 \mu\text{m}$ for the ventral side.

The primary reason for the difference in the number of removed corneocytes is the skin's nature of each side, which allowed the 30 tapes to take more cells from the dorsal side than from the ventral side.

In relevance to the current study, a previous report by Turner *et al.* [262] has described in detail many differences between the porcine skin regions. Their research revealed significant histological differences in the collected skin from several areas, including the two ear sides. Interestingly, there were major changes in the amount of different cell types in each layer, such as melanocytes and Langerhans cells, as well as the thickness of the dermis layer. A larger number of melanocyte cells was found in the dorsal side, which can be considered a crucial factor to increase its iAOC, since they have marked AOC [263]. Additionally, that side exhibited greater hair density than skin from all the other body regions [262]. From a physiological point of view, the ventral side is susceptible to ear discharges, and these oily secretions may inhibit the optimal removal of the horny layer by forming a film on the skin. Even though the film will be removed after a few strips, the total quantity of removed SC will be impacted.

Via light microscope

The microscopical examination of the tapes after tape stripping shows the skin furrows and the corneocytes removal pattern. In a similar pattern observed by Klang *et al.* [138], there were clusters in some areas, and other areas on the tape were semi-empty (**Figure 47**). However, the images confirmed the earlier obtained data by the IR-D, as the tapes of the ventral side had lesser cell density and fewer clusters.

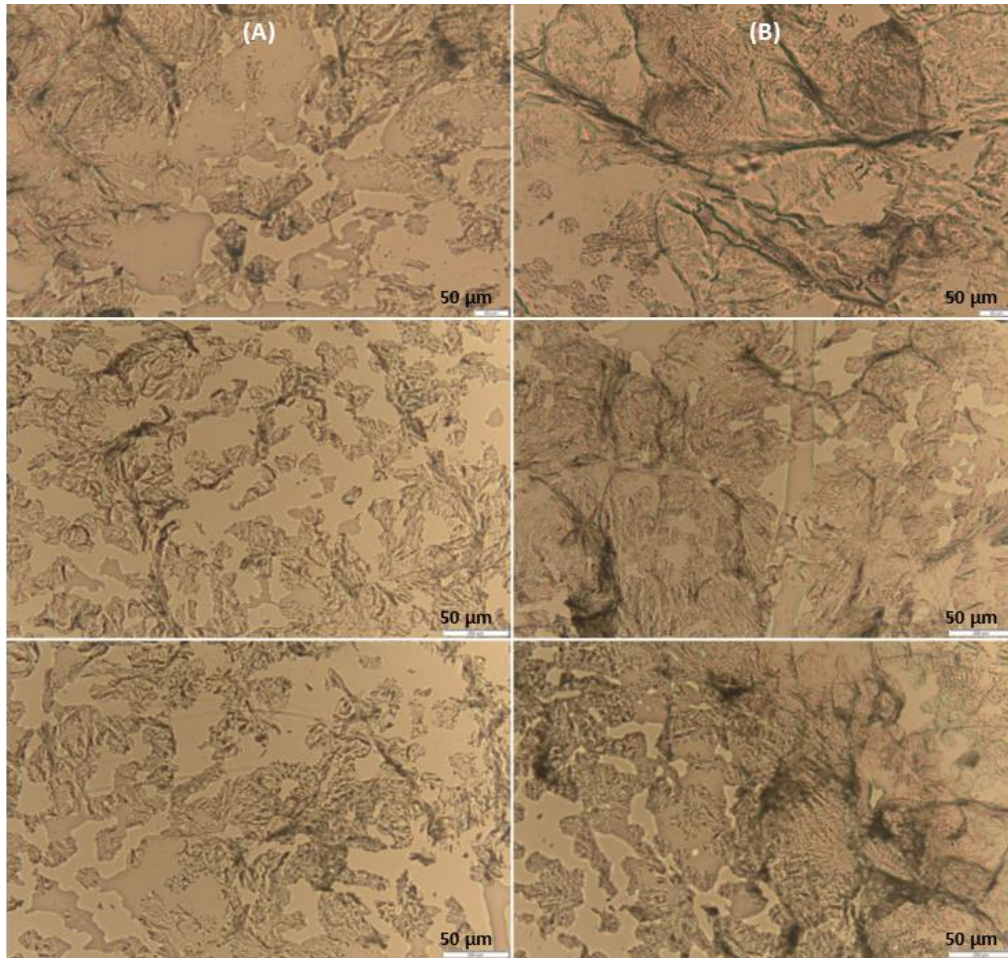


Figure 47: Images of the different tape strips obtained via light microscopy; (A) removed SC from the ventral side, while (B) removed SC from the dorsal side of porcine skin (Magnification: 200-fold)

Skin AOC

Initially, the variability of iAOC was examined using skin from seven ears, and assessed at six spots per ear (inter-individual). So, **Figure 48** shows the average iAOC, which ranged from 150 to 129 μM TE. No statistical difference was found between the average iAOC of the tested ears.

This result is logical and expected, as the used skin was taken from porcine animals that lived in the same conditions; i.e., weather and ultraviolet (UV) exposure. Moreover, they were of

the same breed and obtained from one farm during a particular season. The maintenance of these factors is critical, as the study of Maibam *et al.* indicated the difference in the oxidative markers among different season in cattle skin [264]. In all breeds, significant higher levels of the variable oxidative markers were detected during summer, then in winter and spring.

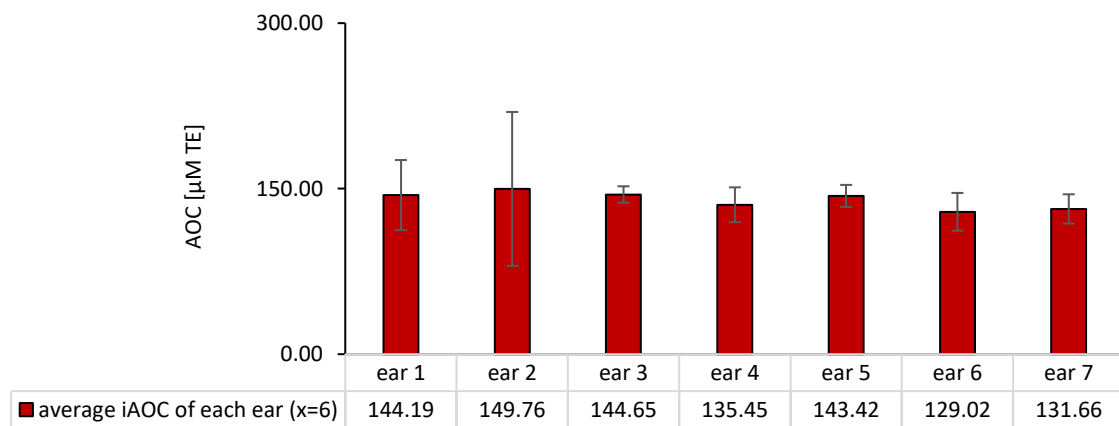


Figure 48: Average iAOC of different ears

Additional extensive evaluations of the iAOC were conducted within the same ears (intra-individual). So, the dorsal and ventral sides of each ear were assessed individually. Remarkably, higher values were found from the dorsal side, as illustrated in **Figure 49** ($p = 0.0016$).

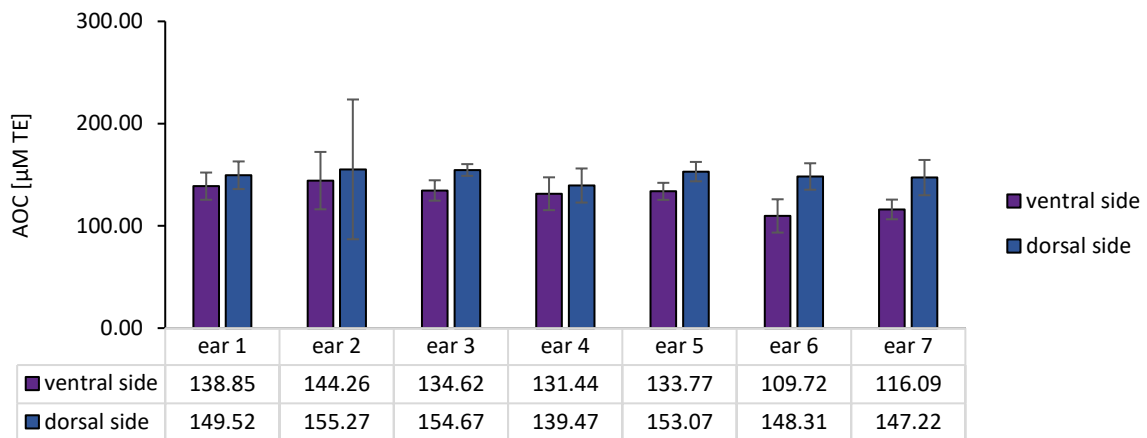


Figure 49: Average iAOC for dorsal and ventral sides of different ears

The previous investigations using the IR-D and the light microscope had clearly reflected the reason behind these results, which is due to the extraction of more corneocytes from the dorsal side than the ventral side. Therefore, and to connect all the data, the correlation between the average cumulative protein absorption and its corresponding iAOC was computed for every analysed sample (42 areas). With a Pearson's r value of 0.49 and a significance level of $p = 0.0011$, the calculation provides a statistically significant positive correlation.

Thereby, the normalised iAOC for each group was calculated using the following equation:

$$\text{normalised iAOC } [\mu\text{M TE}] = \frac{\text{iAOC } [\mu\text{M TE}]}{\text{average cumulative protein absorption } (\%)} \times 100$$

As shown in **Figure 50**, the findings revealed higher values for the majority of ventral side samples.

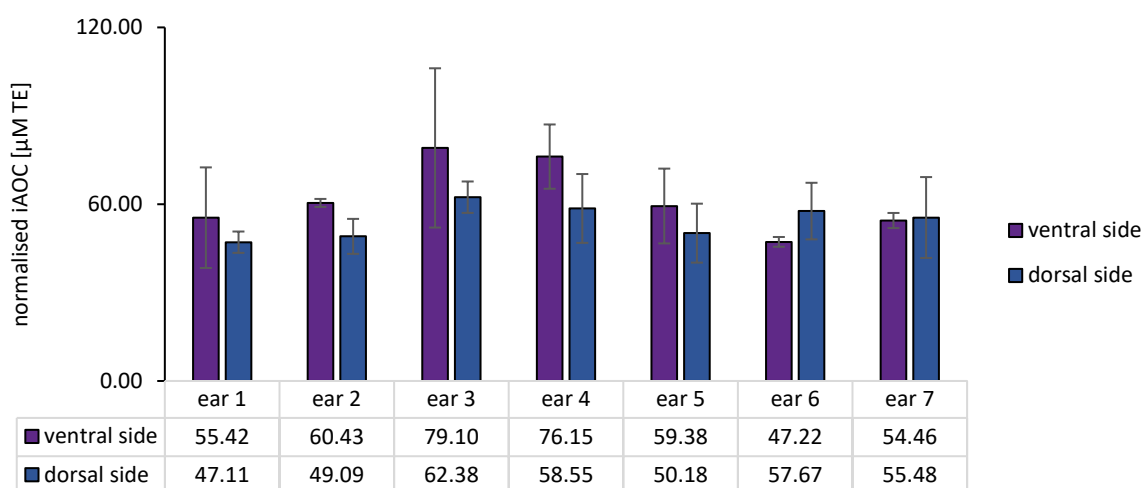


Figure 50: Normalised skin iAOC for dorsal and ventral ear sides

This positive correlation means removing more cells will acquire more antioxidants to be detected via the ORAC assay. However, the analysis of each data set for each ear separately, revealed a broad correlation range; from 0.3 to 0.7. This variance can be justified by the impact of the tape stripping procedure on the IR-D. As was already shown in the microscopical images, tape stripping strips off the porcine corneocytes in an irregular pattern, i.e., it does not remove the skin layer by layer in a consistent manner. Thus, the IR-D values may have been affected by this irregularity, exhibiting occasional imprecise protein absorption [138]. However, according to a massive amount of research, the use of this device for the purpose of quantifying the removed SC, is of high credibility [122, 138, 139, 260].

To summarise this stage, it can be stated that the ORAC assay has been successfully employed, and accordingly, the baseline for the iAOC of porcine skin was determined. Moreover, this method was able to provide distinguished results, e.g., for the different sides of the ear.

Hence, further studies to identify the best conditions for this model had to be done to regulate the routine use in the prospective studies.

4.2.2.1. storage conditions of the ears

In the third part of this study, the influence of ear storage conditions on the skin's iAOC was investigated. The findings are expressed in relative to the iAOC value of freshly analysed samples. As demonstrated in **Figure 51**, the storage at ambient temperature for 24 h had increased the values by up to 129% ($p = 0.0001$). But, the storage in the refrigerator for up to 48 h did not have any impact.

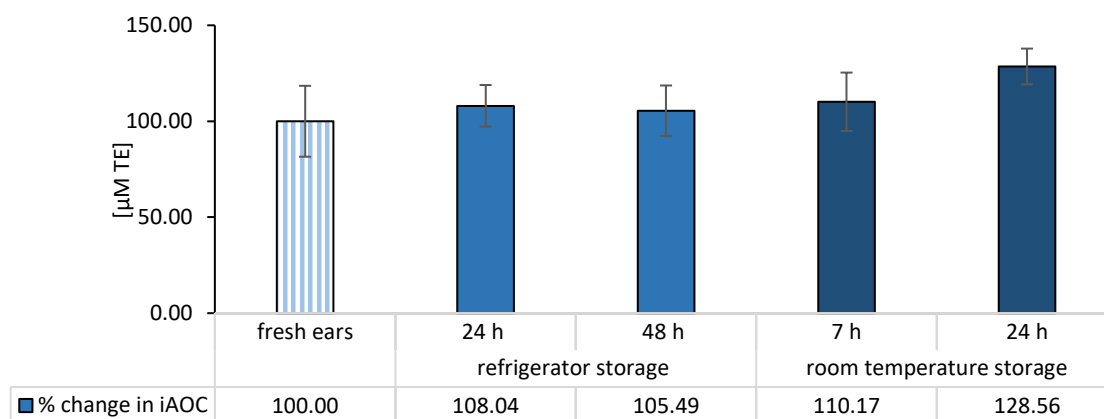


Figure 51: Influence of ears storage on the iAOC, for up to 48 h

The obtained findings highlighted the stability of the antioxidants in skin tissue in the refrigerator since the storage of the whole ear did not compromise the cell's integrity or expose its biochemicals. Tocopherol, for example, remained localised in the mitochondrion and endoplasmic reticulum of the cells, and melanin was still in its typical storage location; the melanosomes [2]. While the ascorbic acid was kept as it is; freely available in the mitochondrion and also in the extracellular space due to its hydrophilic nature [24]. This stability of skin antioxidants after storage at 4 ± 1 °C (refrigerator) is in agreement with published data that assure the continued vitality of skin cells after storage under similar conditions [265].

Looking into the storage at the ambient temperature, 24 h showed elevated iAOC due to two reasons. First, the antioxidant impact of the skin flora, assuming the occurrence of the flora sprout during the storage, that resulted in a marked increase in the AOC. This assumption became a theory, as the literature confirmed the AOC of some skin flora [266]. In addition, room temperature is a highly favourable condition for bacterial growth than cold weather [267], and tape stripping is one of the applicable methods for collecting skin flora for bacterial studies [268]. The second cause for the higher iAOC during storage is the generation of the lactic acid due to the post-mortem changes that occur 4-6 h after porcine slaughtering [228]. It has been shown that lactic acid has a concentration-dependent AOC [48], and its production in the skin rises at room temperature because of the enhanced skin breakdown under such condition.

According to the findings of this section, fresh ears storage in the refrigerator for no longer than 48 h, was adopted as an efficient storage condition for all the *ex-vivo* studies in this thesis.

4.2.2.2. storage conditions of the tapes

In the last stage of this study, the stability of the antioxidants in the tapes was investigated, as this is a crucial topic in the field of antioxidants research. These substances are susceptible to oxidation, photoreaction, and hydrolysis. For this reason, their stability was investigated under a variety of situations and time frames. **Figure 52** displays the findings, also expressed as the % change of the iAOC relative to freshly analysed samples.

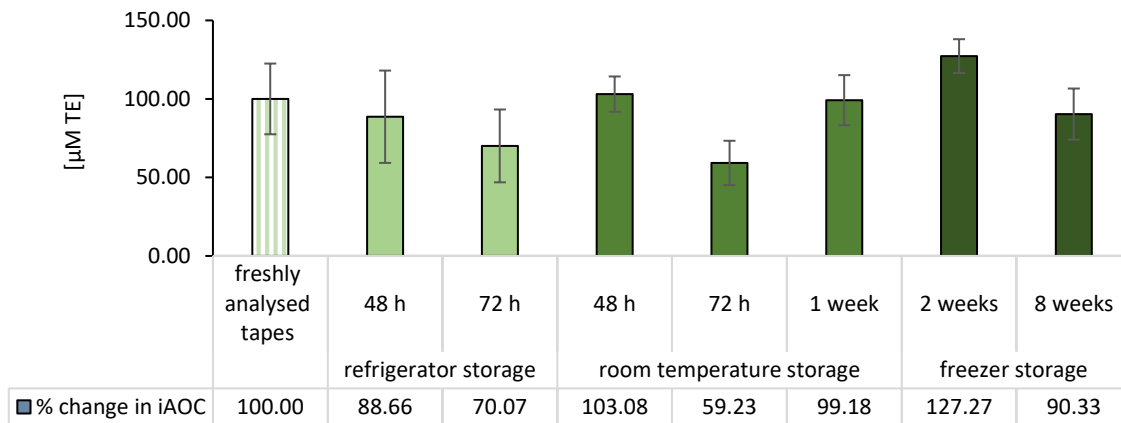


Figure 52: Influence of tapes storage on the iAOC for up to 8 weeks

After storing the tapes in a refrigerator and at ambient temperature for up to 48 h, insignificant changes in iAOC were detected (89% and 103%, respectively). Then, a major decline occurred, and a value of 70% for the samples that were held in the refrigerator, and 59% for those stored at the ambient temperature were detected. In a longer-term study, a week of ambient temperature storage increased the iAOC to almost the same level as the newly analysed samples (99%). While the longest storage for up to eight weeks at -20 °C, revealed no major fluctuation in the iAOC in the frozen tapes.

When compared to the newly analysed samples, the storage was, overall, promising. For up to 48 h, it did retain the iAOC effectively, which offers a very good window for extended analysis time in future research. The storage beyond this period impacted the measured iAOC, although the skin storage in the refrigerator is routinely followed [269, 270]. However, the storage of the entire skin seemed to be completely different from storing the separated skin on tapes, since the skin already lost its consistency and became more fragile.

The iAOC has been boosted after the additional storage at room temperature for up to one week, which is consistent with the findings from the third phase of this investigation. The main difference in this situation, is that the increment was observed after an entire week, not after 24 h. This change can be explained by the preservation of the normal physiology of the skin, which supported the growth of microorganisms in the case of storing intact ears. But in

the tapes, each SC layer has adhered to a particular tape, and only limited flora growth and skin decomposition are expected to occur.

The literature review indicated the use of variable storage conditions in skin antioxidant studies, including -70 °C in a study by Grazul-Bilska *et al.* [271], 4 °C for biopsy samples in other studies [124, 264], and -20 °C for the separated epidermis, biopsies, and excised skin in the work of others [272–274]. Furthermore, a temperature of -20 °C demonstrated efficacy for the storage of tapes following tape stripping in penetration experiments.[275].

Concluding the findings of this section, it was determined that storing the tapes in the freezer is the effective method for preserving skin antioxidants over the long term. It inhibited further reactivity of the skin's enzymatic and non-enzymatic antioxidants, for up to eight weeks without a substantial decrease in the AOC.

The outcomes from the first section of this study have been ensured the assay standards and suitability to be used to assess skin samples. Then, the second part demonstrated the high accuracy of the developed model to anticipate the oxidative changes in porcine skin, as it revealed the inter- and intra-individual differences. Furthermore, the storage conditions in the third section were adjusted, to provide greater repeatability and efficacy in future investigations.

So, according to the studies of this section which were recently published in peer-review literature [135], the suggested *ex-vivo* model is ready to be utilised for further extensive applications, with the advantages of being sensitive, versatile and simple to use as a standard model in skin-antioxidants research.

4.2.3. Treatment impact on skin antioxidant capacity—topical antioxidants

The application of various antioxidants to the skin to enhance its oxidative state is well-established approach in the literature. However, the final effect of these antioxidants on skin health cannot be guaranteed, as under certain conditions, they act as pro-oxidants, such as in case of the high concentration and in the presence of metals ions [276]. There is a lack of current knowledge on this point, and there are no studies on this effect in the *in-vivo* setting.

The main aim of this study was, therefore, to validate the ORAC model when used as a measurement tool to evaluate the impact of delivering topical antioxidants to the skin. The dominant antioxidants in skin are the same ones that are frequently used in cosmetics, and hence, they were chosen for this study: ascorbic acid, vitamin E and CoQ10. Two additional derivatives were selected to study the impact of the physicochemical differences: ascorbyl palmitate and TPGS, as vitamin C and vitamin E analogues, respectively. Moreover, the extensive effect of PEG was also studied as hydrophilic vehicle (**Figure 53**). Multiple concentrations were used in this study to investigate the accuracy of the method and the effect of the different concentrations on the net skin AOC.

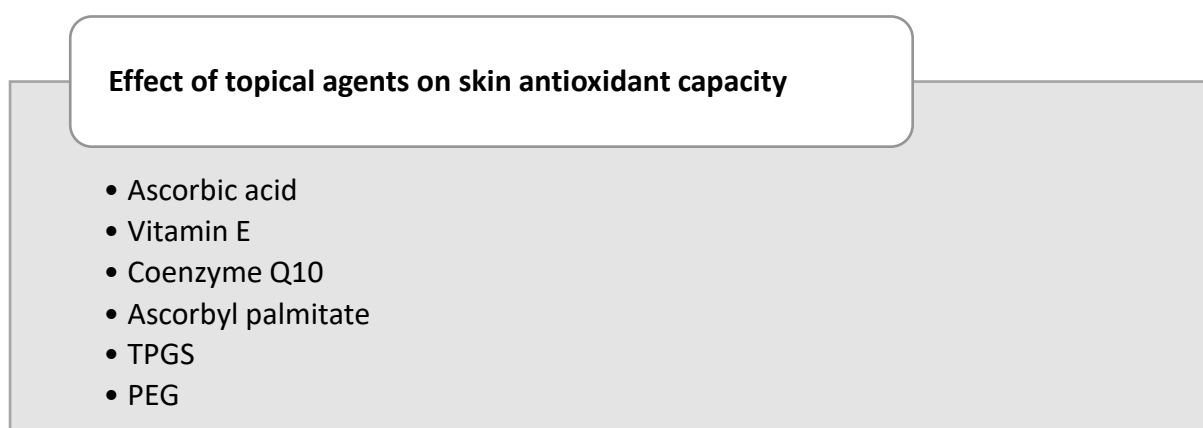


Figure 53: Study outline of current section

4.2.3.1. Ascorbic acid

Ascorbic acid is an essential molecule in skin, and it is also one of the most used antioxidants in cosmeceuticals. Many studies confirm its rising popularity as collagen expression and wound healing enhancer, photoprotective and anti-pigmentary [74, 277].

For these reasons, ascorbic acid was chosen as the first antioxidant to be applied and studied when using this model. **Figure 54** shows the chemical structure of L-ascorbic acid as a water-soluble weak acid. It is easily degraded by oxygen, light or temperature changing to L-dehydroascorbic acid, which makes its formulation challenging. Many strategies are used to overcome this issue, such as the use of more stable derivatives and formulation modifications.

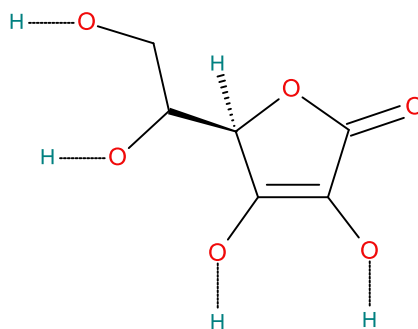


Figure 54: The chemical structure of L-ascorbic acid

It has poor oral bioavailability, which results in an inadequate supply for peripheral organs such as skin. Consequently, the local route is the main route to provide the skin with this resource for the promotion and preservation of its overall health. In cosmetic formulations, ascorbic acid and its derivatives are used in varying concentrations, from 5% up to 30%. However, 30% is associated with a higher incidence of skin irritation [74].

in-vitro studies

The antioxidant capacity (AOC) of ascorbic acid solutions (1%–30% (w/v)) were investigated via DPPH and ORAC assays. The results revealed a concentration-dependent AOC, as illustrated in **Table 15** and **Figure 55**.

Table 15: Values of the *in-vitro* AOC studies of ascorbic acid solutions

Ascorbic acid solutions (w/v)	DPPH (IC 50 [mg/mL])	ORAC (AOC [μ M TE])
1%	$1.61 \times 10^{-2} \pm 2.15 \times 10^{-3}$	$2.25 \times 10^4 \pm 4.92 \times 10^2$
5%	$3.42 \times 10^{-3} \pm 3.48 \times 10^{-4}$	$1.16 \times 10^5 \pm 7.50 \times 10^3$
10%	$1.88 \times 10^{-3} \pm 2.58 \times 10^{-4}$	$1.45 \times 10^5 \pm 1.90 \times 10^4$
20%	$8.32 \times 10^{-4} \pm 4.19 \times 10^{-5}$	$3.11 \times 10^5 \pm 3.56 \times 10^4$
30%	$5.27 \times 10^{-4} \pm 2.74 \times 10^{-5}$	$2.11 \times 10^5 \pm 2.92 \times 10^4$

They showed a linear correlation of $r = 0.97$ up to 20%, but then the 30% solution expressed a lower AOC by a two-third fold. The DPPH assay did not detect this decrease in AOC. The most possible reason for that is the difference in the measurement approach of each assay. The fluorometry provides greater sensitivity and specificity than spectrophotometry, which eventually leads to more precise and accurate readings using ORAC [153–155]. This pattern is applied to all results obtained by these two assays in this section.

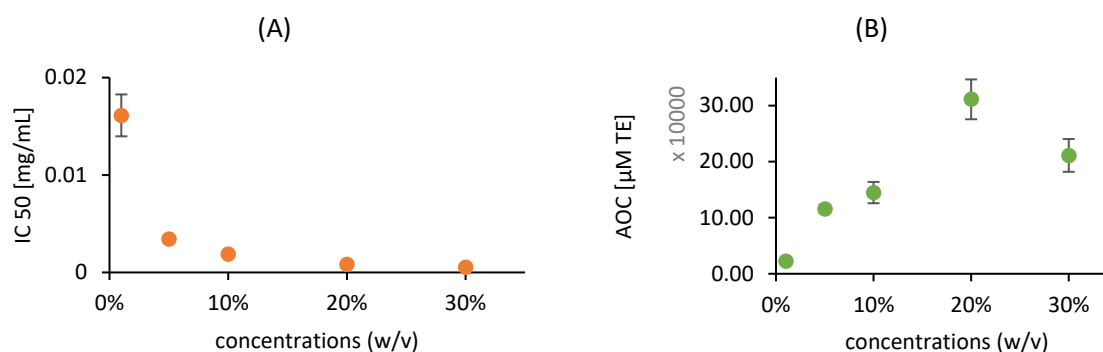


Figure 55: *in-vitro* AOC values of ascorbic acid solutions (A) using DPPH assay expressed as IC 50 [mg/mL], and (B) using ORAC assay expressed as AOC [μM TE]

The concentration-dependent *in-vitro* AOC behaviour of this molecule is already established since 1986 [278]. Furthermore, it has been found recently that even in an animal study, the clinical outcomes were dependent on the applied concentrations [279]. The results in this study are therefore totally in line with the literature. However, the exact AOC values cannot be compared to other studies due to the difference in the used chemicals and devices.

ex-vivo studies

Biophysical skin properties

The used porcine skin showed normal barrier functions and hydration. Trans epidermal water loss (TEWL) was 9.93 ± 2.21 g/hm² while hydration was 28.73 ± 15.11 .

Removed SC by tape stripping

In this study, stratum cornea (SC) was removed by tape stripping and then extracted and analysed. The IR-D values were measured for each tape. The cumulative values were employed to establish the average thickness of the SC that had been removed and used for

the AOC studies. Subsequently, the average SC removed from the three porcine ears was calculated as $5.98 \pm 0.56 \mu\text{m}$. This represents the depth that was reached by the tape stripping, and represents about 75% of the whole SC of $7.96 \mu\text{m}$ reported in the literature for porcine skin [138].

In detail, the average thickness of each of the three levels was as follows:

- 1st 10-layers equalling $2.42 \pm 0.29 \mu\text{m}$
- 2nd 10-layers equalling $2.00 \pm 0.22 \mu\text{m}$
- 3rd 10-layers equalling $1.57 \pm 0.20 \mu\text{m}$

The first ten layers removed larger amounts of corneocytes. This pattern was observed in all the studies using tape stripping and reported in this thesis. Moreover, the literature revealed similar observations when using this approach; corneocytes amount per strip decreased with the increased stripping depth [139, 280]. A likely explanation was reported by Jacobi *et al.* which is the higher cohesion force between the corneocytes with the increased tape stripping depth into the SC [280].

Small SDs of the average thickness values of the three ears confirm the uniformity of tape stripping procedure. It also indicates the high level of physiological similarities between the ears, as reflected in the thickness of the SC layers removed.

Skin AOC after treatment

Application of the solutions influenced the skin AOC significantly (**Figure 56**). The increased AOC was detected linearly up to 20%, and then there was a decline for the 30% treated area, which had almost the same AOC as the area treated with 10%. This particular result was in line with the *in-vitro* studies. It appears that at 30% the solution undergoes an *in-vitro* pro-oxidation reaction due to the high concentration, which consequently, decreases AOC and the *ex-vivo* effect.

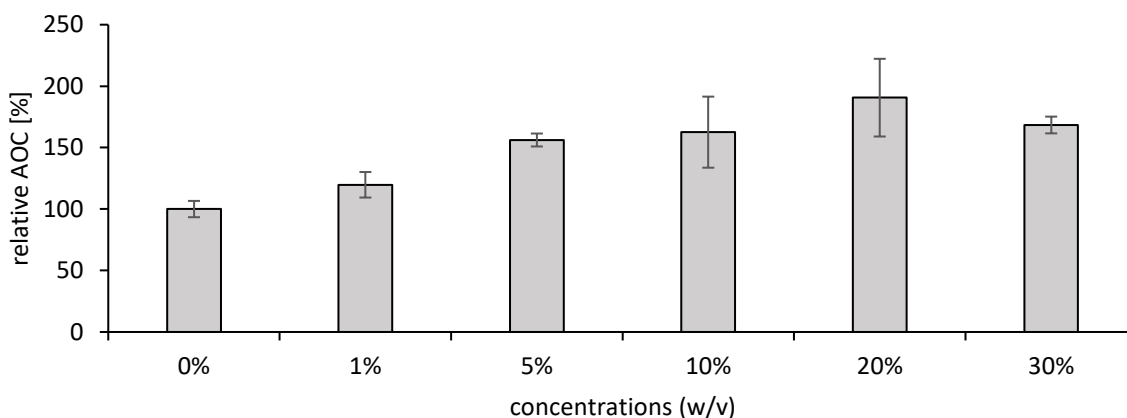


Figure 56: Relative AOC of the skin after treatment with ascorbic acid solutions (1 - 30% (w/v)), expressed as relative AOC [%] in relation to untreated skin

Several studies already reported this molecule's ability to increase skin resistance against oxidative stress and protect it from the environmental pro-oxidants by transfer of electrons and/or donation [74, 75]. However, only a particular study by Pinnell *et al.* studied the behaviour of several doses of up to 30% in pig skin by the detection of percutaneous absorption [281]. They found that it occurred in a dose-dependent manner, and the 20% formulation achieved maximal penetration. The higher doses of 25% and 30% were less effective in improving the cellular level of ascorbic acid, in full support to our findings.

The inability of the higher concentrations to further improve the skin AOC can be justified by the saturation of active and inactive permeation pathways of the ascorbic acid. According to reported data, sodium-ascorbate cotransporter-1 (SVCT1) is responsible for its active transportation in the epidermis tissue [75]. While the inactive transport can be estimated by the simple solvent drag mechanism as expressed by Kaushik *et al.* [229].

Interestingly, several points can be extrapolated from the responses obtained following treatment with ascorbic acid solutions in this study. First, the results indicated high sensitivity and accuracy of the method used to assess the effect of ascorbic acid on skin. The different concentrations had a detectable variable effect on skin AOC.

Second, the ability of this treatment to improve skin AOC was shown to be concentration-dependent, increasing up to 20%. However, it would be safe to apply a 30% solution, as it did not harm the skin or acted as pro-oxidant. The likely explanation for the lower AOC that resulted from this high concentration are the *in-vitro* pro-oxidative reaction and the saturation of the transport pathways

Last but not least, the highest concentration at which ascorbic acid can be used as a simple solution is 20%, with an improvement of $191\% \pm 32\%$ ($p = 0.0186$). For the future studies, it will be interesting to investigate the influence of the different vehicles on the AOC performance, as in this study a primary solution was used to rule out any other factors.

A deeper analysis was required to determine the extent of skin AOC improvement with the best formulation. For that, each layer of untreated skin and skin treated with 20% was separately analysed and plotted. As shown in **Figure 57**, the improvement in skin AOC occurred mainly in the first 10 layers of the SC. This result is fully in line with the known penetration profile of this antioxidant, as it is extremely hydrophilic and always challenging in dermal delivery.

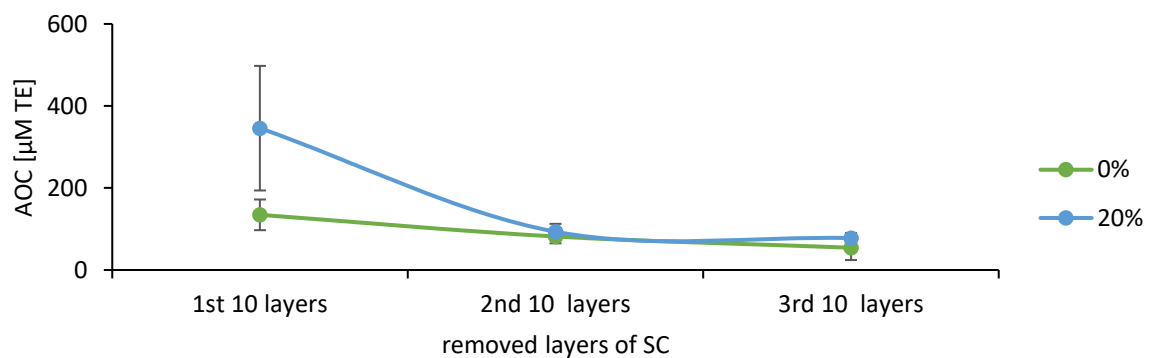


Figure 57: AOC of the skin layers after treatment with ascorbic acid solution (20% (w/v)), expressed as AOC [µM TE] compared to untreated skin

In the next step, data normalisation was done using the significant correlation between skin AOC and the corresponding protein absorption using IR-D. Normalisation was used to rule out the effect of the varying amounts of SC being removed via tape stripping, which may act as an influencing factor regardless of the procedure accuracy.

These results are illustrated in **Figure 58** and show a slightly different finding compared to the non-normalised data, where 5% ascorbic acid achieved the highest improvement in the skin AOC, with up to 200% \pm 23% ($p = 0.0047$). Although the 5% solution superiority, all the concentrations were able to improve skin AOC significantly, except for the 1% and 30%. Thus, normalisation may provide a more concrete effect and it can be used as a supportive analysis in the further studies. Again, the high safety potential of the dermal ascorbic acid for all concentrations up to 30% has been highlighted as none of the used solutions acted as pro-oxidant on skin. Moreover, their efficiency in enhancing the AOC of the SC, as an outer skin layer, have been proven, which thereby should expand the resistance to the environmental pro-oxidants.

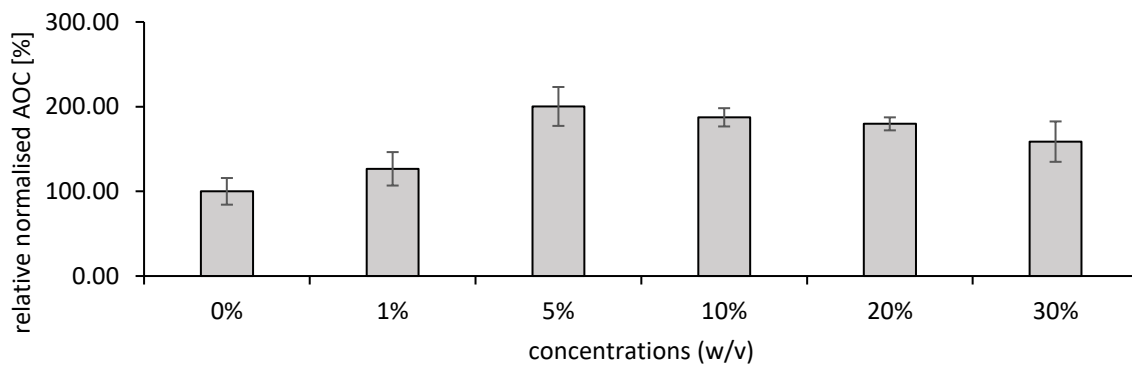


Figure 58: Relative normalised AOC of the skin after treatment with ascorbic acid solutions (1 - 30% (w/v)), expressed as relative AOC [%] in related to untreated skin

It is probable that this active ingredient underwent oxidation on the top of skin in the higher concentrations (10%, 20% and 30%), resulting in reduced AOC efficiency and a lowered skin

AOC after the application. However, this scenario was not noted for the non-normalised data, as the amount of the removed SC was not considered.

Improvement of AOC in all 30 SC layers has been found using normalised data, even in the deeper layers represented by the last SC layer after removal of 20 tapes (**Figure 59**). These highly significant ($p = 0.0005$) results are supported by the remarkable effect of ascorbic acid use in the clinical setting. Such as the double-blinded study by Humbert *et al.* which showed significant improvement in photodamaged skin after six months of daily application with 5% ascorbic acid [282].

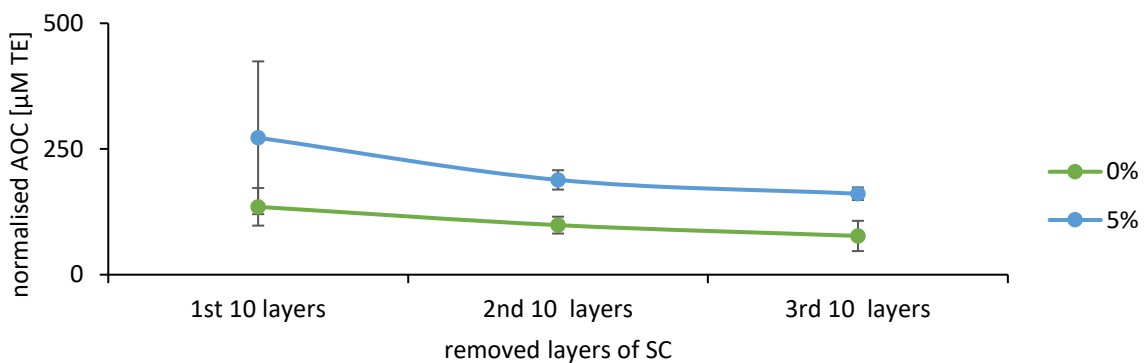


Figure 59: Normalised AOC of the skin layers after treatment with ascorbic acid solution (5% (w/v)), expressed as normalised AOC [µM TE] compared to untreated skin

The permeation of ascorbic acid is known to be poor and limited to the SC. This is especially true when it is present as charged molecules, as in this study's solutions. Many strategies are used to enhance its permeation and penetration, such as combining it with ferulic acid to lower the formulation's pH to keep the ascorbic acid uncharged [283]. Other strategies include the use of more lipophilic derivatives, although some of them did not show the same efficacy as ascorbic acid [284].

The findings of this study are of significant value in the field. Because the determination of ascorbic acid levels in skin tissue is not always possible and there is a gap in the literature

regarding this matter [74]. Thus, measuring it indirectly via our method could be a highly acceptable alternative method.

in-vitro and *ex-vivo* correlation study

The correlation studies are summarised in **Table 16**, as expressed by the Pearson correlation coefficient (r). The results disclosed a highly significant correlation between *in-vitro* AOC studies and the AOC of the skin obtained by tape stripping. The correlation was positive in the case of ORAC, while it was inverted in the case of the DPPH data, where the results were expressed as IC 50, which means that lower values had high AOC levels. Thereby, for the ascorbic acid solutions, it is possible to use these AOC assays to estimate the *ex-vivo* response. While ORAC and DPPH assay are already in use to assess the topical antioxidants formulations [285], further studies can be done to investigate if the correlation is still significant with the presence of more additives and excipients in the advanced cosmeceutical formulations.

Table 16: Values of the correlation studies between *in-vitro* and *ex-vivo* AOC using ascorbic acid solutions (1 - 30% (w/v))

	Average skin AOC	Average normalized AOC
ORAC assay (<i>in-vitro</i>)	$r = 0.9677$ ($p = 0.0069$)	$r = 0.4223$ ($p = 0.4788$)
DPPH assay (<i>in-vitro</i>)	$r = -0.9059$ ($p = 0.0342$)	$r = -0.7583$ ($p = 0.1374$)

4.2.3.2. Vitamin E

Vitamin E is one of the most dominant antioxidants in biological tissues. It is an essential component in the epidermal antioxidant barrier, mainly localised in the deeper skin layers. It protects the skin as a free radical scavenger, photoprotective and antitumorigenic agent. Several isomeric forms of this vitamin are present, and they are mainly divided into the tocopherols and the tocotrienols. In the skin, the prevalent forms are α -tocopherol ($\approx 90\%$) and γ -tocopherol ($\approx 10\%$) [2]. **Figure 60** shows the chemical structure of α -tocopherol, which is characterized by its highly lipophilic character, small molecular weight and a chromanol-ring structure [286].

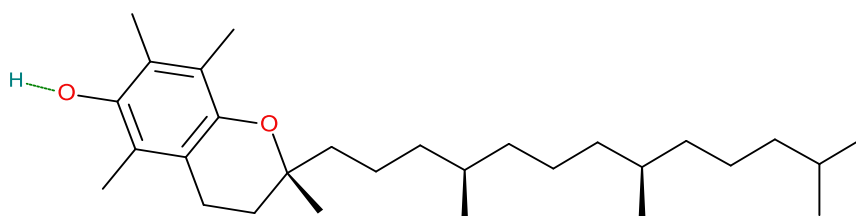


Figure 60: The chemical structure of α -tocopherol

In cosmetics, vitamin E is available in several forms, such as α -tocopherol, α -tocopherol acetate, Trolox, TPGS and mixed tocopherols oil, which were used in this section. Vitamin E in all its forms is used extensively as an antioxidant, as a formulation stabilizing antioxidant, and as a skin-conditioning agent, with or without ascorbic acid, in dosages from 2% to 36% [287].

in-vitro studies

The AOC results of vitamin E solutions in miglyol are illustrated in **Table 17** and showed a high antioxidant potential, although it is not more than the ascorbic acid. They revealed a similar pattern to that observed with ascorbic acid, in which concentration-dependency and higher

accuracy in AOC determination were obtained by ORAC (**Figure 61**). There was a linear correlation when using ORAC ($r = 0.93$) but a poor correlation when using DPPH ($r = 0.39$). This result is consistent with Im *et al.* study, who also described the concentration-dependent AOC of the tocopherols using six concentrations by the ABTS radical assay [288]. Interestingly, the most potent tocopherol was γ -tocopherol while β -tocopherol showed the lowest potency [288]. So, the *in-vitro* assays can be used efficiently to investigate the AOC of vitamin E formulations, including the use of ORAC and ABTS assays, and with lower accuracy, the DPPH assay.

Table 17: Values of the *in-vitro* AOC studies of vitamin E solutions

Vitamin E solutions (w/v)	DPPH (IC 50 [mg/mL])	ORAC (AOC [μ M TE])
1%	$4.46 \times 10^{-1} \pm 2.37 \times 10^{-2}$	$1.01 \times 10^4 \pm 1.61 \times 10^2$
5%	$4.14 \times 10^{-2} \pm 4.56 \times 10^{-3}$	$5.75 \times 10^4 \pm 3.43 \times 10^3$
10%	$1.81 \times 10^{-2} \pm 1.70 \times 10^{-3}$	$8.19 \times 10^4 \pm 1.02 \times 10^4$
20%	$9.70 \times 10^{-3} \pm 2.54 \times 10^{-4}$	$1.97 \times 10^5 \pm 1.38 \times 10^4$
30%	$6.14 \times 10^{-3} \pm 4.22 \times 10^{-4}$	$2.07 \times 10^5 \pm 1.87 \times 10^4$

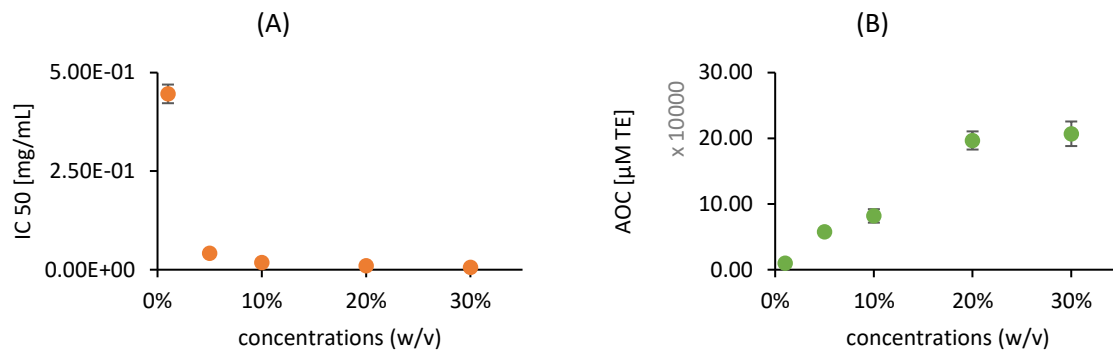


Figure 61: in-vitro AOC of vitamin E solutions (A) using DPPH assay expressed as IC 50 [mg/mL], and (B) using ORAC assay expressed as AOC [μM TE]

ex-vivo studies

Biophysical skin properties

Skin probes indicated a relatively impaired barrier function in the porcine skin that was used in this study, with a TEWL of 23.97 ± 6.32 g/hm². The skin hydration was in the normal range at 21.28 ± 4.31 .

According to an investigation done by Tsai *et al.*, defective barrier functions affect the percutaneous absorption of hydrophilic and amphipathic compounds only [258]. Therefore, the elevated TEWL was considered to have an irrelevant impact on the performance of this study.

Removed SC by tape stripping

IR-D studies revealed that $92\% \pm 3\%$ of the SC was stripped from the skin through this action, which was the equivalent of 7.36 ± 0.23 μm. The depth of each layer was as follows:

- 1st 10-layers equalling 3.26 ± 0.27 μm
- 2nd 10-layers equalling 2.34 ± 0.18 μm
- 3rd 10-layers equalling 1.76 ± 0.31 μm

The difference in the amount removed compared to the previous study can be explained by two factors. The first factor to be considered is the formulation effect. The solvent used here was miglyol, while water was used with the ascorbic acid. As already shown in the literature, the characteristics of the topical formulation may influence the tape stripping and modify the amount of removed corneocytes [289] because the formulation has the ability to modify the skin parameters, such as the hydration [227], and thus the cell adhesion and SC mechanical properties. Consequently, the use of tape stripping protocol after applying variable formulations can result in variable amounts of the removed SC.

The other factor is the physiological properties of skin, because it is naturally variable among pig species. Additionally, weather, including ultraviolet (UV) light and temperature, may influence skin even within the same animal from day to day. For this reason, the study was done using three ears obtained from the same farm and the same kind of pig. Moreover, the control sample had to be prepared individually for each experiment to ensure the accuracy of the results. Therefore, and because of these two factors, the skin used in a particular study cannot be directly compared to the skin used in another study which was done at a different time with a different formulation, i.e., ascorbic acid and this study.

Skin AOC after treatment

The application of vitamin E on skin resulted in improved skin AOC, of up to $130\% \pm 5\%$ for the 30% solution. Unexpectedly, there was an insignificant difference between all the results obtained (**Figure 62**). On comparing the results of the different solutions, unlike ascorbic acid, there was no clear concentration-dependent response.

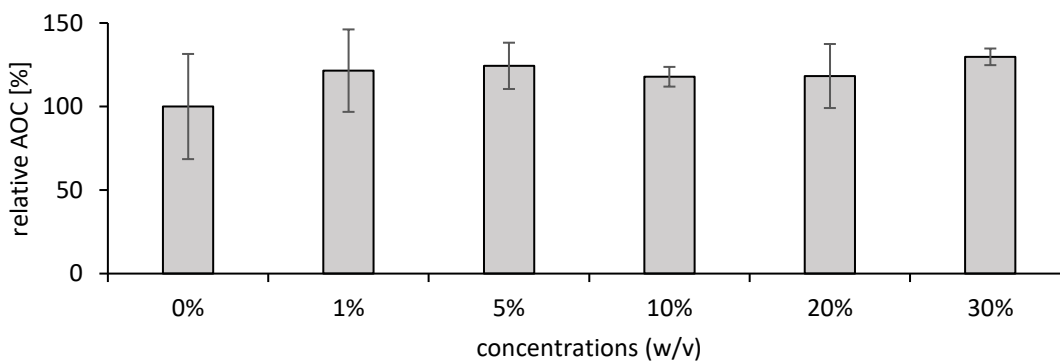


Figure 62: Relative AOC of the skin after treatment with vitamin E solutions (1 - 30% (w/v)), expressed as relative AOC [%] in relation to untreated skin

This finding can be explained by the biochemical nature of both antioxidants, where ascorbic acid is a charged hydrophilic molecule while vitamin E is a low molecular weight lipophilic one. According to known knowledge for dermal drug delivery of vitamin E, it is a permeable molecule, and thus, it is very likely that its effect in the skin will not be detected by tape stripping, where measurement is limited to SC.

The cumulative expertise is supporting these results, as the study of Traber *et al.* [290] in 1998 compared the distribution of the topical tocopherols into the skin layers and demonstrated their rapid penetration in 0.5 h. Most importantly, they found the largest portion in the deeper subcutaneous layers. Their likely explanation was the 'lipophilicity gradient', which made the molecules permeate rapidly toward the lipid secretory organ, sebaceous glands. This theory can be logical if we consider its low molecular weight, which will facilitate passive diffusion.

Another more recent study by Nada *et al.* [291] is supporting this argument. They failed to detect the α -tocopherol in SC after the repeated application with several formulations.

More reports assured the permeation of the tocopherols and their derivatives [287], but, however, there are no solid data describing the penetration ways into the skin and the precise reason for the vitamin E good penetration profile, as its profound hydrophobicity (calculated

as $\log P \approx 9$) should theoretically inhibit it. One interesting hypothesis to explain this phenomenon is the presence of α -tocopherol transfer protein (α -TTP) in skin [292]. This protein has been detected, mainly in hepatic tissue, as a special binding protein that transports α -tocopherol from the liver to the bloodstream to maintain its normal concentration [293]. Nevertheless, until now, it had not been identified in peripheral tissues like skin. Further understanding of the vitamin E pathways in skin is an interesting research area for an unresolved question.

The analysis of skin layers treated with 5% and 30% solutions is illustrated in **Figure 63**. It clearly shows AOC improvement in the second layer after 5% application, with improvements observed in both the first and second layers in the area treated with the 30% solution. The difference between these two formulations supports the anticipated penetration of vitamin E in skin. With the low concentration, the active ingredient penetrated the deeper layers and thus the elevated AOC was detected in the second layer only. With a higher concentration, the permeation pathway may become saturated, which allowed the vitamin to remain in the first layer. It is worth mentioning that the thickness of the first and second removed layers of SC by tape stripping in this study was higher than in the previous study ($5.6 \mu\text{m} \approx 76\%$ of the total removed SC), which means more corneocytes were removed and analysed. Therefore, the impact of this factor could be neutralised, and the normalised AOC needed to be calculated.

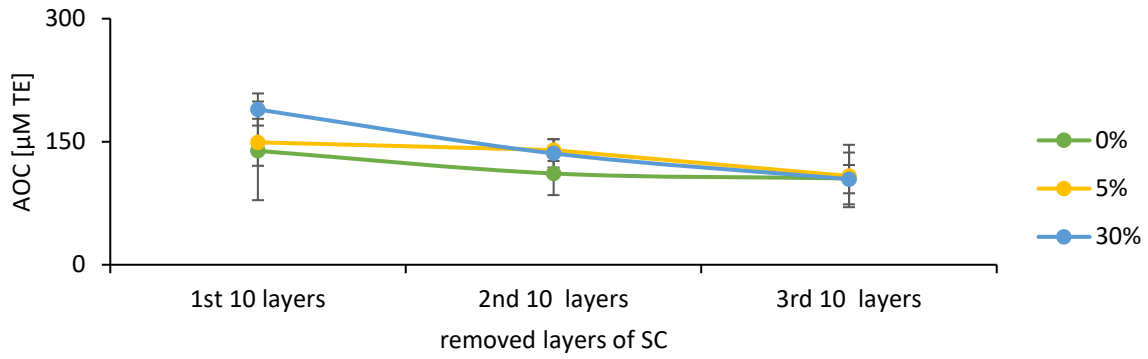


Figure 63: AOC of the skin layers after treatment with vitamin E solutions (5% and 30% (w/v)), expressed as AOC [$\mu\text{M TE}$] compared to untreated skin

The normalised AOC data delivered the same results as the earlier ones, where vitamin E improved the skin's AOC insignificantly and with a non-linear response. However, the 5% solution, as shown in **Figure 64**, achieved the highest AOC ($139\% \pm 33\%$). The high SD here can be explained by differences in the SC removal pattern due to initial biological variations in the porcine skin used.

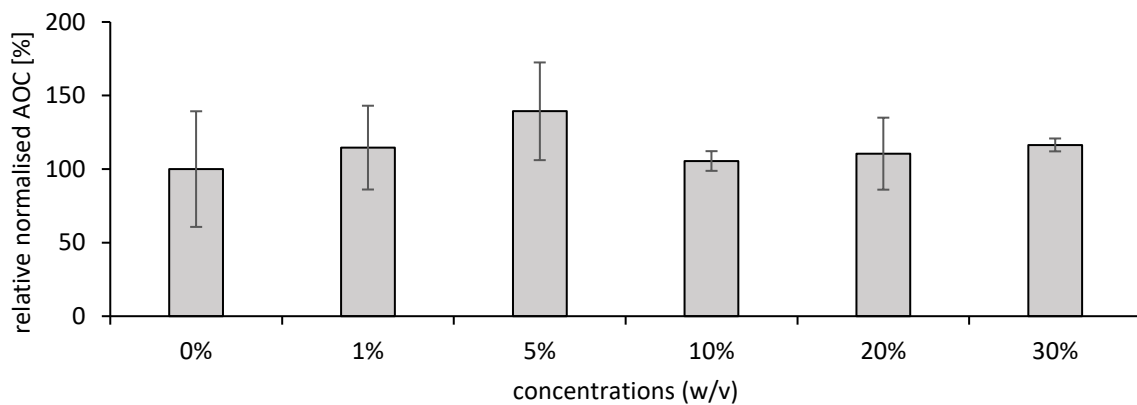


Figure 64: Relative normalised AOC of the skin after treatment with vitamin E solutions (1 - 30% (w/v)), expressed as relative normalised AOC [%] in relation to untreated skin

The assessment of normalised skin AOC of the separate layers presented almost the same findings (**Figure 65**). The 5% solution improved the deep layer only, but mild AOC improvement was obtained with the 30% formulation in the first and second layers. This effect can be due to the saturated pathways of the active ingredient through skin, or it may be due to the formulation difference between the 5% and the 30%, as the last one was more viscous, which prevents its optimal penetration. The formulation effect on the penetration is already well-known in the literature as a highly influencing factor [294].

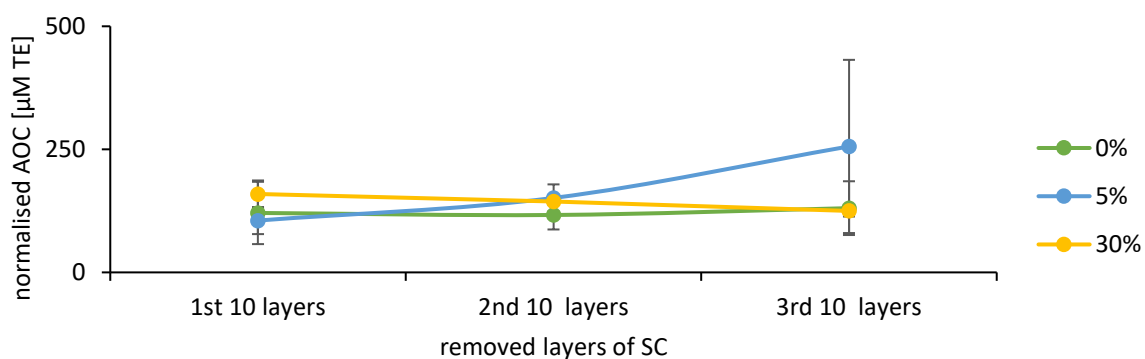


Figure 65: Normalised AOC of the skin layers after treatment with vitamin E solutions (5% and 30% (w/v)), expressed as normalised AOC [$\mu\text{M TE}$] compared to untreated skin

Although the current model has multiple advantages (easy to apply, cost-effective, versatile and possible to be used *in-vivo*), the obtained finding leads to the main limitation, which is the unlikely detection of the antioxidants with a high penetration profile: vitamin E is a classic example. Other actives with the same physicochemical properties are expected to show the same behaviour, such as ascorbyl palmitate and α -lipoic acid. This limitation is caused by the used technique; tape stripping, which is used to study only the SC. Therefore, the suggested model has been capable only to detect the effect that occurred in the SC, not beyond, as shown in **Figure 66**. Including another technique in addition to the tape stripping will

overcome this restriction, like the use of skin biopsy to be analysed by ORAC. Thus, the effect of the vitamin will be known on the SC and the deeper epidermis as well.

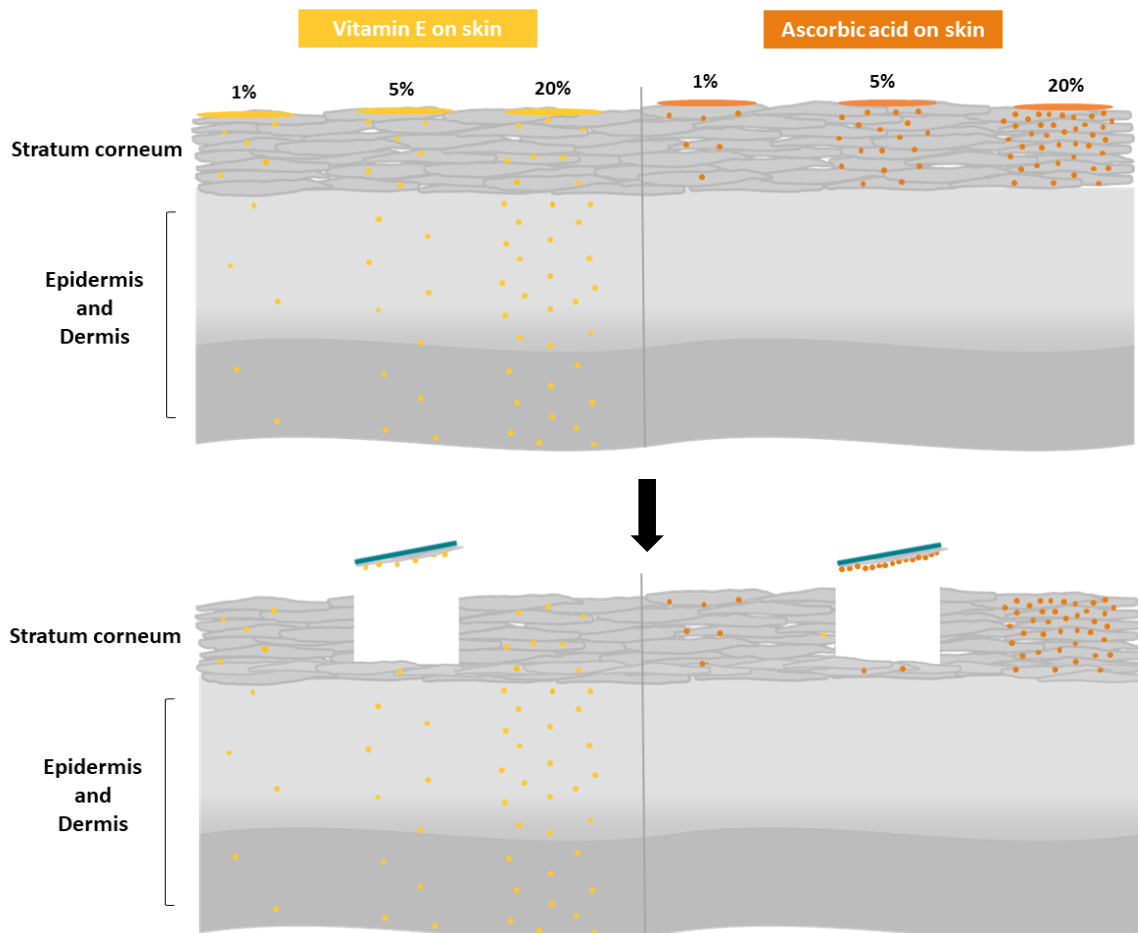


Figure 66: Hypothetical pathways for vitamin E and ascorbic acid in skin after the topical application of finite doses, followed by the tape stripping procedure which remove the SC layer in the treatment area; 30 tapes have been used and thus 30 SC layers were removed and analysed by ORAC assay

Nevertheless, the model is still with a very high value. The oxidative state of SC is reflected in the overall skin health, thereby, it is crucial to study and understand all the possible

influencing factors, including the use of topical antioxidants. Moreover, SC as the main protective skin layer with the antioxidant barrier is targeted in many treatment strategies, e.g., sunscreens and corneotherapy.

For further estimation of the model capabilities, more investigation was necessary to validate the method and to build the theory, which will be presented in the following sections using other compounds that are commonly used in the dermal formulations.

in-vitro and *ex-vivo* correlation study

As the effect of the vitamin E solutions on SC was not concentration-dependent, the *in-vitro* AOC studies cannot be used to predict the *ex-vivo* results for this model, as shown in **Table 18**. Similar findings can be predicted for the highly penetrating antioxidants, because they will not be retained in the SC and thus detected by the tape stripping. Anyhow, the correlation study can be promising if the deeper layers beyond the SC were included.

Table 18: Values of the correlation studies between *in-vitro* and *ex-vivo* AOC using with vitamin E solutions (1 - 30% (w/v))

	Average skin AOC	Average normalized AOC
ORAC assay (<i>in-vitro</i>)	r = -0.1362 (p = 0.8272)	r = -0.2707 (p = 0.6596)
DPPH assay (<i>in-vitro</i>)	r = 0.4827 (p = 0.4102)	r = -0.05591 (p = 0.9289)

4.2.3.3. Coenzyme Q10

Coenzyme Q10 (CoQ10) or Ubiquinone is one of the most dominant antioxidants in biological tissues, and it is characterized by quinone functional group. The reduced form of it is known by the name ubiquinol, while the oxidized form is called ubiquinone. Both are dominant in biological tissues, diet and cosmetics [295]. Number 10 in the name CoQ10 refers to the number of isoprene groups in the molecule, as illustrated in **Figure 67** [2].

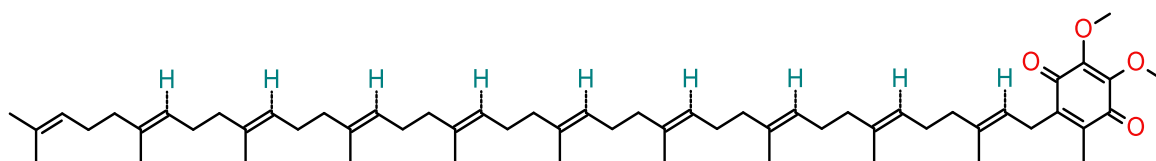


Figure 67: The chemical structure of CoQ10 (Ubiquinone)

CoQ10 is well-known for its major role in the electron transport chain in the mitochondria, cell membrane and low-density lipo-proteins. As can be expected from the structure, it is a highly lipophilic antioxidant with a large molecular weight (863.3 g/mol), which makes its delivery to biological tissue extremely challenging. However, it is frequently used in skin cosmetic products with proven efficacy and fair popularity. It is used in concentrations of 0.5-3% as an antiaging and topical antioxidant [296, 297].

in-vitro studies

The AOC of CoQ10 solutions was obtained by ORAC assay, as illustrated in **Table 19**. They showed a linear correlation with $r = 0.99$ (**Figure 68**).

Table 19: Values of the in-vitro AOC studies of CoQ10 solutions

CoQ10 solutions (w/v)	ORAC (AOC [$\mu\text{M TE}$])
0.5%	$1.21 \times 10^4 \pm 1.58 \times 10^2$
1%	$4.95 \times 10^4 \pm 5.81 \times 10^2$
2.5%	$1.36 \times 10^5 \pm 6.67 \times 10^3$
5%	$2.60 \times 10^5 \pm 2.78 \times 10^3$

However, it was not possible to use the DPPH assay for CoQ10 AOC determination, due to the formation of a reaction mixture that has high UV absorbance in the 517 nm area, where DPPH peak absorption is measured in the assay. Accordingly, the DPPH reading could not be distinguished, and the assay could not be performed.

The UV spectrum for the DPPH solution alone, CoQ10 alone, and the DPPH-CoQ10 chemical product are demonstrated in **Figure 69**.

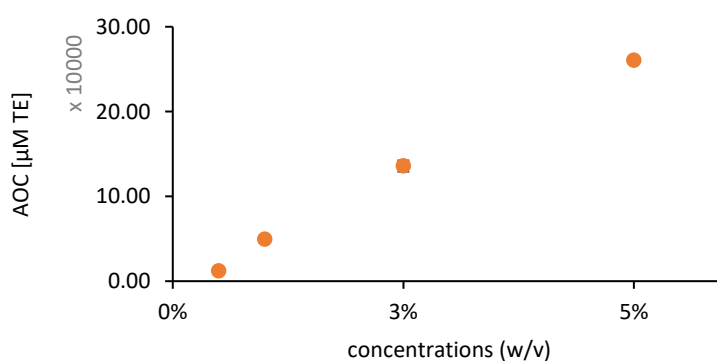


Figure 68: in-vitro AOC of CoQ10 solutions (0.5 - 5% (w/v)) using ORAC assay, expressed as AOC [$\mu\text{M TE}$]

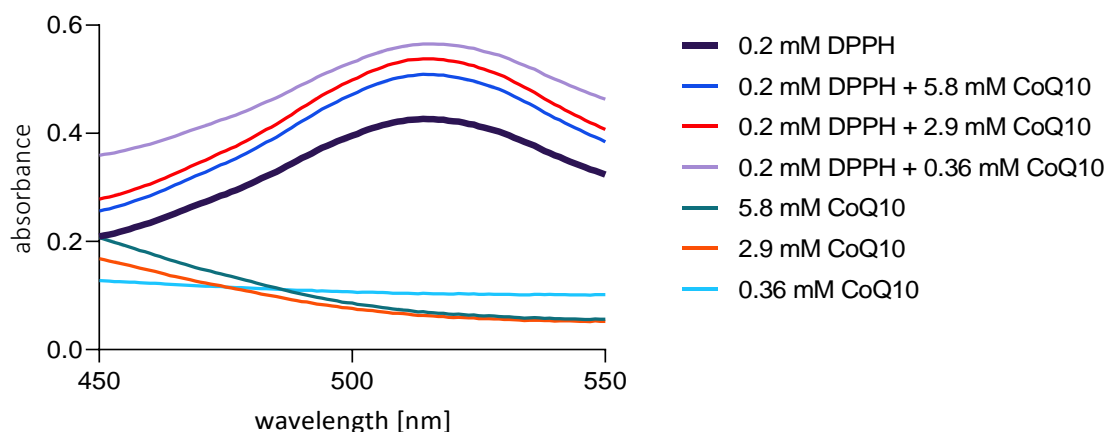


Figure 69: The UV spectrum (450 -550 nm) of 0.2 mM DPPH, CoQ10 solutions and mixtures of 0.2 mM DPPH with CoQ10 solutions to perform the DPPH assay

The spectrum of the DPPH showed high absorbance in the area of 450-550 nm, while the solutions of CoQ10 did not show similar absorbance in that area. Nevertheless, after the interaction with the DPPH for 30 min according to the assay protocol, the resulted solutions demonstrated very high absorption in the measurement area. For a higher concentration of the CoQ10, higher absorption was obtained i.e., higher than the values of the DPPH solution alone. This leads to the explanation of a reaction product between DPPH and CoQ10 building up in a concentration dependent manner and showing an absorbance overlapping with the pure DPPH. A similar overlapping has been observed with carotenoid-rich formulations in other studies, because they, too, have strong absorbance on the same wavelength as the DPPH [129, 168]. Accordingly, this overlapping shows that DPPH is an unsuitable assay for the AOC determination of CoQ10 formulations.

ex-vivo studies

Biophysical skin properties

Barrier functions and hydration status were within the normal range, with values of 5.49 ± 0.98 g/hm² and 21.97 ± 1.59 , respectively.

Removed SC by tape stripping

An average thickness of 6.46 ± 0.43 μ m was obtained from the SC of the three ears. This represents $81\% \pm 5\%$ of the complete SC layer, as mentioned in the literature. Each separate layer represented the following depth:

- 1st 10-layers equalling 2.83 ± 0.23 μ m
- 2nd 10-layers equalling 2.09 ± 0.17 μ m
- 3rd 10-layers equalling 1.53 ± 0.21 μ m

The same solvent used in the vitamin E study was used here (miglyol) and the amount of skin removed was $81\% \pm 5\%$ compared to $92\% \pm 3\%$ in that study which again emphasized the effect of the skin's physiological factors on tape stripping outcomes that mentioned previously. As in the current study, another group of pigs was used, and they experienced a different weather condition. The experimental notes reported sunny days before the pigs slaughtering and low relative humidity (28%) on the day of the study, which has proven to impact the SC thickness and epidermis properties [298].

Skin AOC after treatment

The CoQ10 solutions on skin are shown in **Figure 70**, while their effect is demonstrated in **Figure 71**. Surprisingly, the CoQ10 application increased the AOC initially, then decreased it, in a concentration-dependent pattern.

With the 0.5% dose, the AOC was significantly increased, by $126\% \pm 10\%$ ($p = 0.0439$). However, at the higher doses, CoQ10 acted as a pro-oxidant and decreased the skin's AOC linearly ($r = 0.93$). The 5% solution consumed almost one-half of the skin's antioxidant system compared to the untreated skin, with a significance of $p = 0.0012$.

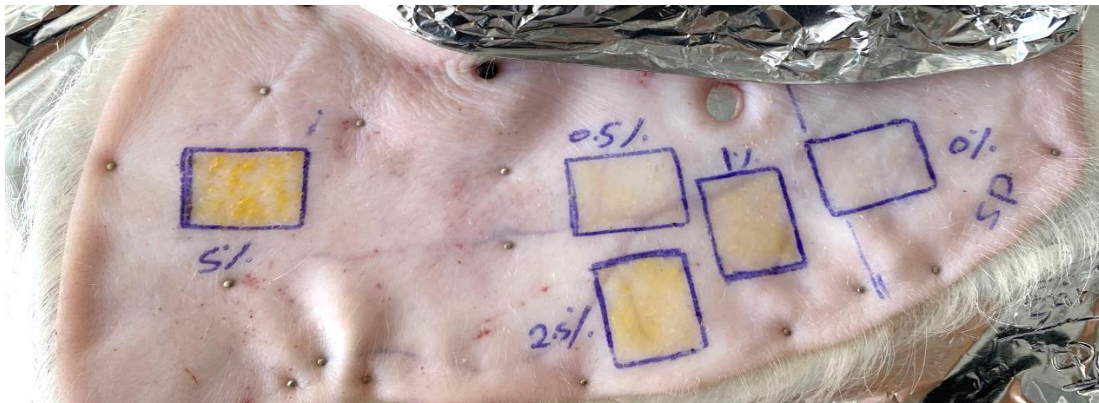


Figure 70: Porcine skin treated with the CoQ10 solutions (0.5 - 5% (w/v))

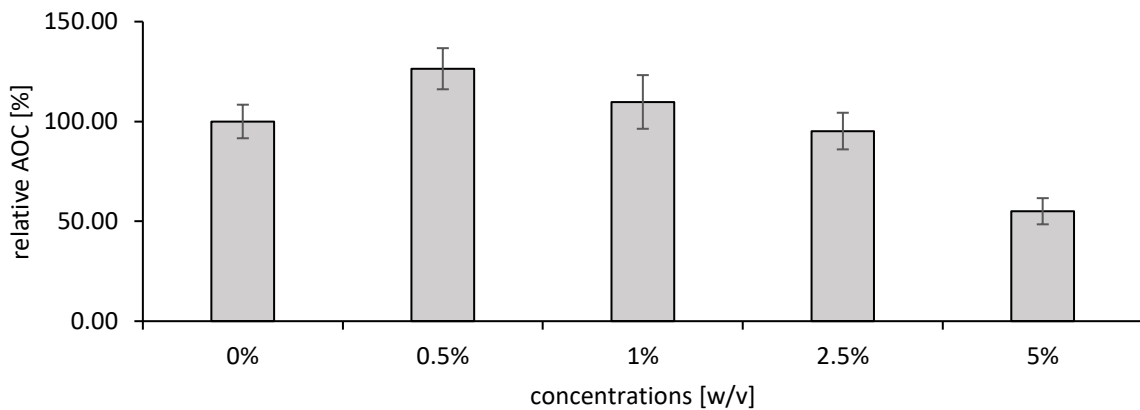


Figure 71: Relative AOC of the skin after treatment with Q10 solutions (0.5 - 5% (w/v)), expressed as relative AOC [%] in relation to untreated skin

The analysis of each removed skin layer indicated the extent of AOC change for treated areas with the lower and the higher concentrations; 0.5 and 5%. As illustrated in **Figure 72**, the antioxidant effect was mainly occurring in the superficial layer. This fits the known poor penetration profile of CoQ10 into the skin. Therefore, the AOC improvement was limited on the first layer because of the limited penetration of the active.

In contrast, pro-oxidative effect of 5% CoQ10 affected all skin layers with a high significance of $p < 0.0001$. This finding was unexpected, as this active ingredient does not have the ability to diffuse through the skin layers to impact them in this way. Therefore, the assumption can be made that this effect resulted from pro-oxidant stress in the top layer of skin, which depleted its antioxidants over the two hours of drug application. A close assessment of the literature has confirmed that, as H_2O_2 was generated on the skin upon the application of CoQ10 formulation [299]. This aggressive free radical has a very low molecular weight (34.015 g/mole) with the ability to permeate the skin and affect the whole epidermis [300]. Moreover, it is considered an inflammatory marker for multiple skin inflammatory diseases. From these data, we may acknowledge that the non-penetrating antioxidant can generate penetrating pro-oxidant with a serious negative impact.

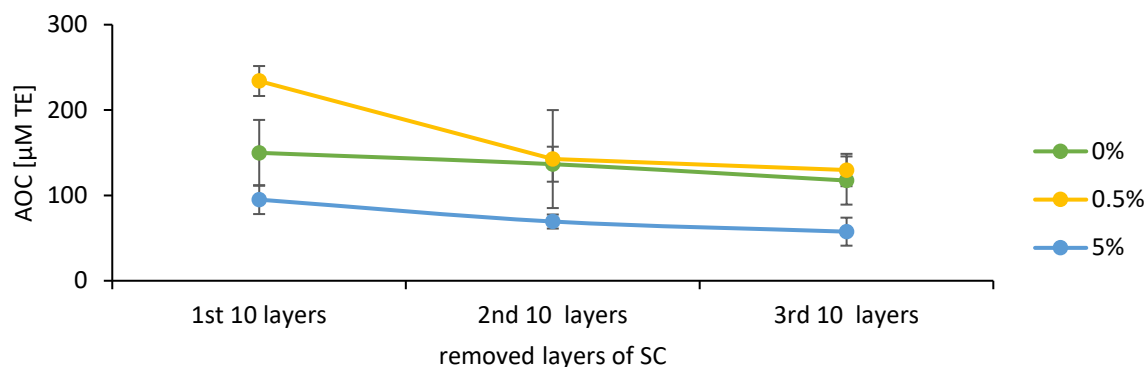


Figure 72: AOC of the skin layers after treatment with CoQ10 solutions (0.5% and 5% (w/v)), expressed as AOC [$\mu\text{M TE}$] compared to untreated skin

The normalised AOC provided the same results, as shown in **Figure 73** and **Figure 74**. but with a higher correlation coefficient (r) of 0.96. This linear response supports previous findings and the assumed theory. CoQ10 is an extremely lipophilic molecule with a high molecular weight, so it does not penetrate the skin. For this reason, our method was capable of an accurate evaluation of its AOC impact.

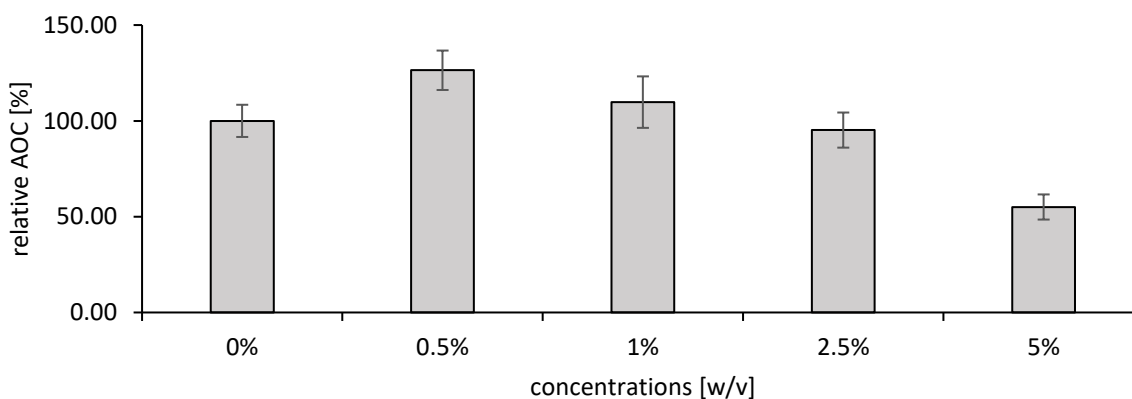


Figure 73: Relative normalised AOC of the skin after treatment with CoQ10 solutions (0.5 - 5% (w/v)), expressed as relative normalised AOC [%] in related to untreated skin

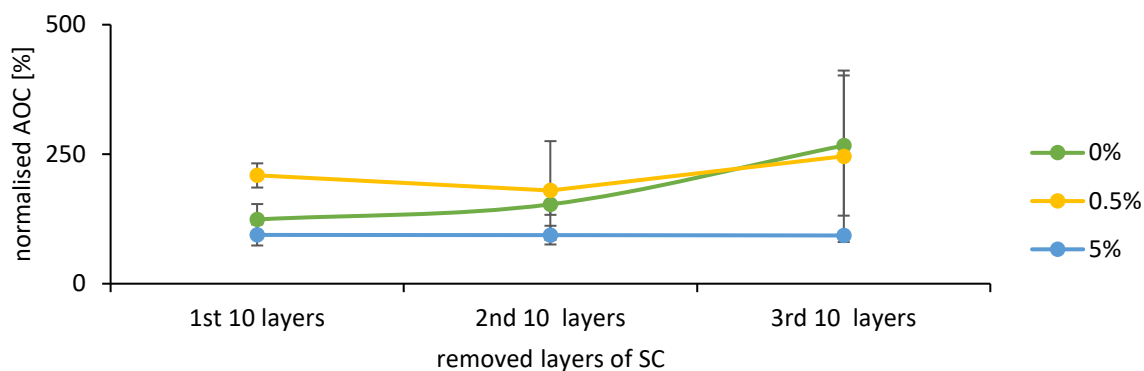


Figure 74: Normalised AOC of the skin layers after treatment with CoQ10 solutions (0.5% and 5% (w/v)), expressed as normalised AOC [$\mu\text{M TE}$] compared to untreated skin

The regular use of such cosmetics with pro-oxidative effects can harm the skin through the chronic depletion of its antioxidants. Serious skin conditions and diseases can develop, such as wrinkles, atopic dermatitis, vitiligo, psoriasis and cancer, as healthy skin is dependent on its ability to confront environmental factors by using its network of enzymatic and small molecule antioxidants.

In fact, the safety of this particular antioxidant has been questioned previously. Literature screening has revealed reported facial vitiligo in 15 patients triggered by CoQ10 antiaging products [299]. The doses were not reported, but the investigation confirmed the reason behind the disorder, which was the pro-oxidative effect, defined by the generation of H_2O_2 free radicals upon application.

According to the data obtained, the key factor determining the safety of CoQ10 cosmetic products is the applied dose. The statement can be made that a concentration $\geq 1\%$ is considered to be an unsafe dose for human skin in a simple solution. Further investigations may need to be done at the *in-vivo* level, but as the porcine skin used in this study has a high similarity to human skin, these results can be considered reliable data. However, animal cosmetic testing is banned in Europe [301], giving our suggested model a high value in this context.

The expert panel for cosmetic ingredient safety stated that most cosmetic formulations in the market containing CoQ10 are available in low concentrations of $\leq 0.05\%$ [295]. However, a market screening revealed a product with 2% [302], while most commercial products do not acknowledge the active ingredient dosage. Additionally, various dermal formulations in the literature have been formulated with concentrations up to 4.8% [297, 303].

We cannot state categorically that those formulations will have the same pro-oxidative impact on skin, because the role of the formulations has not yet been defined. Changing the formulation may or may not influence the oxidative effect of the antioxidant used, which requires precise testing of the individual products. Prospective studies on the role of the formulation warrant evaluation.

These results are of great interest from several perspectives. They confirmed the suitability of our model for the supposed purpose. So far, the results have yielded outstanding knowledge about the effect of antioxidants on skin that has not been noted before. More importantly, the efficacy and safety of certain antioxidant doses and formulations can be investigated via this model. This method can be used in the safety assessment of CoQ10 products as part of the pre-marketing evaluation to ensure the complete safety of the product.

***in-vitro* and *ex-vivo* correlation study**

Studies of the *in-vitro* AOC obtained by ORAC assay showed a significant inverse correlation with both average and normalised skin AOC; these values are presented in **Table 20**. The elevated AOC of the solutions did not improve the skin AOC, in contrast, they were associated with the dose-dependent pro-oxidative effect. Therefore, *in-vitro* AOC studies cannot be used to predict the efficacy or safety of CoQ10 in cosmeceutical formulations. More precise methods should be used, i.e., methods capable to estimate the biological settings.

Table 20: Values of the correlation studies between in-vitro and ex-vivo AOC using with CoQ10 solutions (0.5 - 5% (w/v))

	Average skin AOC	Average normalized AOC
ORAC assay (<i>in-vitro</i>)	$r = -0.9931$ $(p = 0.0069)$	$r = -0.9586$ $(p = 0.0414)$

4.2.3.4. Ascorbyl palmitate

For a proof of concept, ascorbyl palmitate was chosen for this section as a lipophilic analogue of vitamin C. It is synthesised by a condensation reaction between palmitoyl chloride and ascorbic acid in the presence of a dehydrochlorinating agent such as pyridine, as the ester of ascorbic acid and palmitic acid [304]. It is marketed as a vitamin C replacement under the name vitamin C ester. The chemical structure is shown in **Figure 75**.

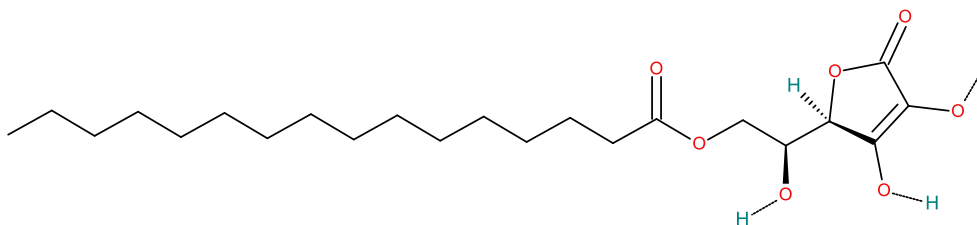


Figure 75: The chemical structure of ascorbyl palmitate

As ascorbic acid, it is used in cosmetics as an antioxidant, antiaging, and skin brightening agent. However, due to its chemical nature, this form of vitamin C ester has additional advantages over ascorbic acid. From a biophysical perspective, it is more stable, with higher resistance to oxidation and light [305]. Additionally, it can be used as a fragrance ingredient. From a biopharmaceutical point of view, it can penetrate through skin and reach deeper skin tissues [306].

The FDA has approved ascorbyl palmitate as a safe preservative for human consumption and as an excipient in approved drug formulations [307]. In cosmetics, it is used widely in skincare products and in colour products such as lipsticks in variable concentrations according to the aim of use.

in-vitro studies

The results of the *in-vitro* AOC testing with ascorbyl palmitate are shown in **Table 21** and **Figure 76**. The ORAC assay achieved a linear response with $r = 0.97$, while with the DPPH assay the linear correlation was poor. Compared to ascorbic acid, this active ingredient had lower AOC values at all concentrations, except for 30%. This result was expected, as it is known that ascorbic acid has the highest antioxidant performance among all its derivatives, as they lose part of their activity during their chemical processing [308]. Interestingly, the 30% ascorbyl palmitate did not show an *in-vitro* oxidation reaction as ascorbic acid did. The acid form is more reactive and less stable than the ester ascorbate.

Table 21: Values of the *in-vitro* AOC studies of ascorbyl palmitate solutions

Ascorbyl palmitate solutions (w/v)	DPPH (IC 50 [mg/mL])	ORAC (AOC [μ M TE])
1%	$2.37 \times 10^{-1} \pm 6.03 \times 10^{-3}$	$7.77 \times 10^3 \pm 9.18 \times 10^2$
5%	$5.71 \times 10^{-2} \pm 8.12 \times 10^{-3}$	$4.51 \times 10^4 \pm 4.12 \times 10^3$
10%	$2.17 \times 10^{-2} \pm 9.99 \times 10^{-4}$	$1.27 \times 10^5 \pm 1.94 \times 10^4$
20%	$2.03 \times 10^{-2} \pm 1.03 \times 10^{-3}$	$2.08 \times 10^5 \pm 1.74 \times 10^3$
30%	$1.29 \times 10^{-2} \pm 8.83 \times 10^{-4}$	$2.69 \times 10^5 \pm 4.71 \times 10^4$

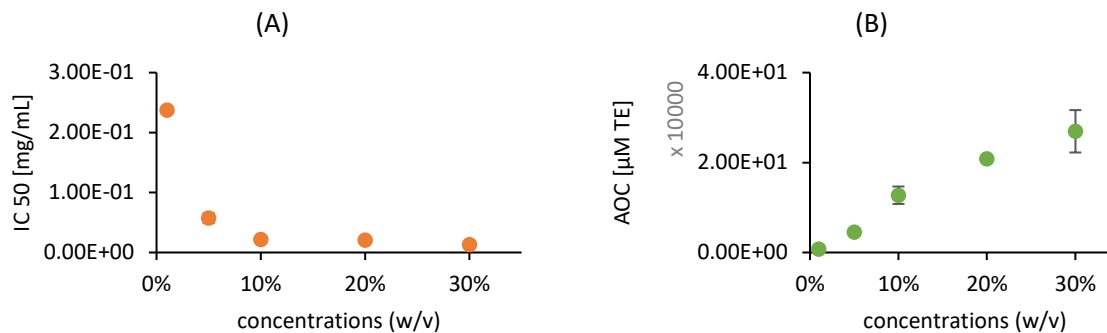


Figure 76: in-vitro AOC values of ascorbyl palmitate suspensions (A) using DPPH assay expressed as IC 50 [mg/mL], and (B) using ORAC assay expressed as AOC [μM TE]

ex-vivo studies

Biophysical skin properties

The used ears had good barrier function and a well-hydrated skin, as TEWL was 11.21 ± 7.76 g/hm² and hydration was 34.74 ± 8.64 .

Removed SC by tape stripping

IR-D studies revealed the complete removal of SC, with a removed thickness of 8.53 ± 0.58 μm. A large number of corneocytes were measured in the first layer, and the depth in each layer was:

- 1st 10-layer equalling 3.79 ± 0.25 μm
- 2nd 10-layer equalling 2.62 ± 0.25 μm
- 3rd 10-layer equalling 2.12 ± 0.19 μm

Skin AOC after treatment

The topical suspensions of ascorbyl palmitate improved skin AOC in a non-linear trend (**Figure 77**). The significant AOC improvement was only achieved after the application of the 30% concentration, which showed AOC of $145\% \pm 11\%$ and $p = 0.0389$. The other concentrations resulted in almost the same % of AOC increment (15 - 20%). Apparently, the 20% dose was enough to saturate transportation pathways and thus allowed AOC elevation in SC for the next doses: the 30%. Meaning, the increased dose above the 20% led to a higher concentration of ascorbyl palmitate in the SC that can be detected by the analysis.

We can assume that the active and inactive pathways allow a higher amount of this agent to permeate into the skin, more than the ascorbic acid because of its improved lipophilicity.

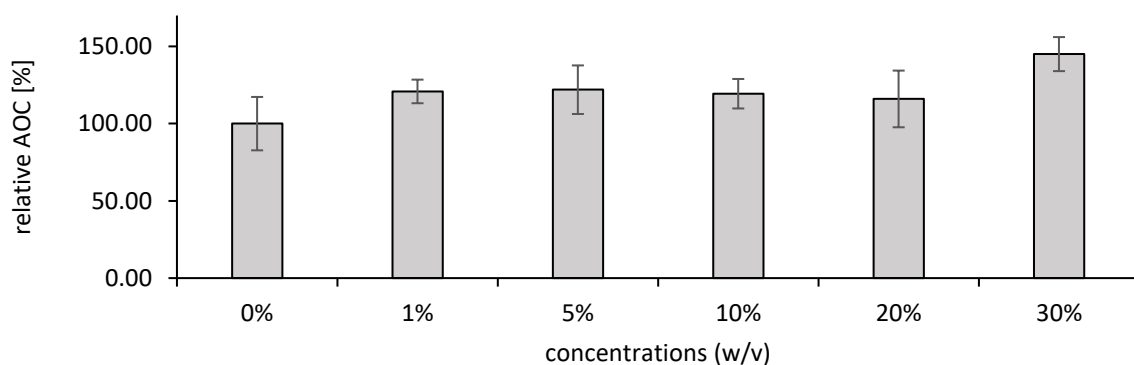


Figure 77: Relative AOC of the skin after treatment with ascorbyl palmitate suspensions (1 - 30% (w/v)), expressed as relative AOC [%] in relation to the AOC of untreated skin

These results fit well with the proposed concept and confirm our previous explanation for the ascorbic acid and vitamin E findings. Ascorbyl palmitate is known to penetrate in a more active way than ascorbic acid [13], as it has low molecular weight and higher lipophilicity of 414.5 g/mol and $\log p = 6.3$, respectively. Accordingly, its topical application led to higher

penetration, going deeper beyond the SC, and resulted in a non-linear detection by our model.

The detailed AOC analysis of each separate layer lends support to the earlier statement. This reflected AOC improvement in all layers, including the deepest layers of the treated skin, with the 30% suspension compared to the untreated skin, as illustrated in **Figure 78** ($p = 0.0093$).

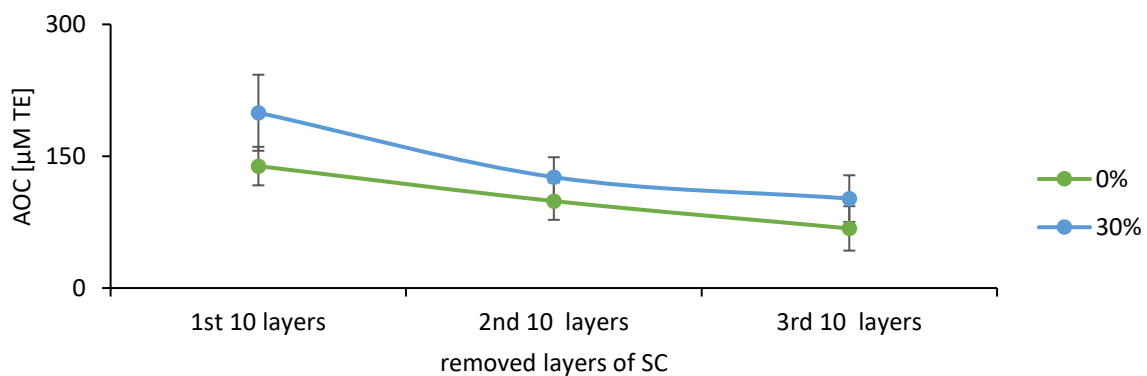


Figure 78: AOC of the skin layers after treatment with ascorbyl palmitate suspensions (30% (w/v)), expressed as AOC [µM TE] compared to untreated skin

The calculated normalised AOC is demonstrated in **Figure 79** and **Figure 80**. The same pattern was observed, where the 30% suspension led to the best AOC improvement after saturation of the transport pathways. The AOC of the individual layers also emphasized this improvement, which took place significantly in all layers ($p = 0.0349$).

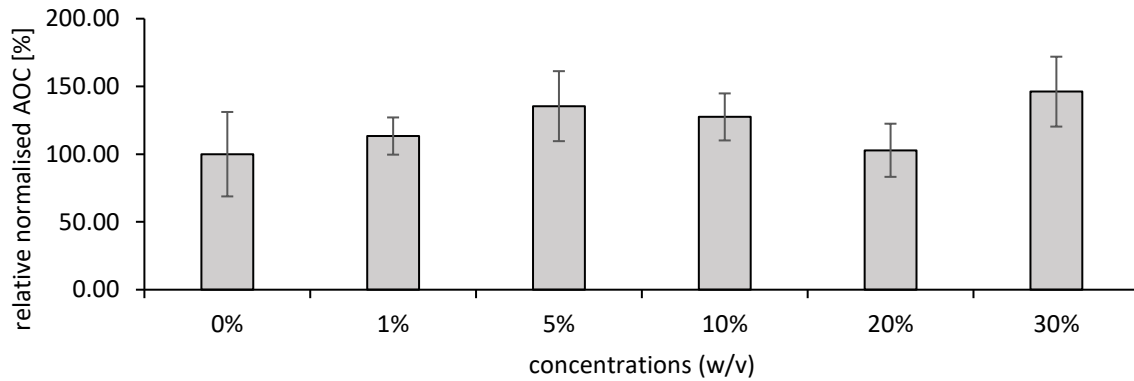


Figure 79: Relative normalised AOC of the skin after treatment with ascorbyl palmitate suspensions (1 - 30% (w/v)), expressed as relative normalised AOC [%] in relation to untreated skin

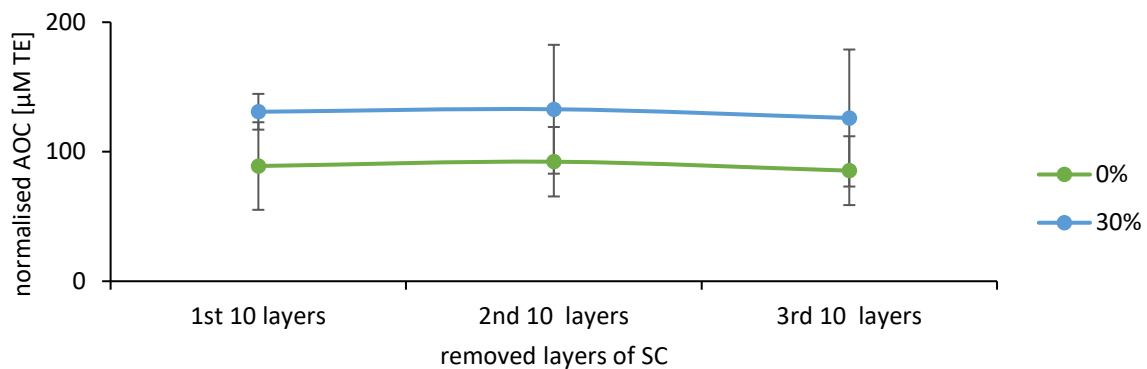


Figure 80: Normalised AOC of the skin layers after treatment with ascorbyl palmitate suspensions (30% (w/v)), expressed as normalised AOC [µM TE] compared to untreated skin

Literature screening did not reveal any direct recommendation in this matter, but according to the data from this study, a suggestion can be made regarding the use of vitamin C derivatives in cosmetics, which can be decided according to different purposes of the treatment. As a photoprotective agent, ascorbic acid will be an excellent choice that will

remain in the SC and prevents UV radiation damage, as will be shown in the next section of this thesis. On the other hand, the lipophilic ascorbyl derivatives will be the best option as antiaging agents by promoting collagen synthesis in the deeper skin layers. However, high doses may need to be used to ensure sufficient concentration in the upper SC as well. The study by Patrícia *et al.* supports our recommendation, where they compared the clinical effect of ascorbic acid to two lipophilic derivatives [284]. Interestingly, all actives enhance the SC but only the magnesium ascorbyl phosphate was able to alter the viscoelastic-to-elastic ratio due to its permeation into the deeper skin layer.

in-vitro and ex-vivo correlation study

As the skin AOC after the treatment indicated a non-linear pattern, the correlation results demonstrated a poor correlation, as shown in **Table 22**. A better correlation coefficient was found between *in-vitro* AOC by ORAC and average skin AOC, with $r = 0.6006$; however, it was not significant. This result may be extrapolated to include all the lipophilic ascorbic acid derivatives with the improved penetration profile, such as ascorbyl tetra isopalmitate and magnesium ascorbyl phosphate. Therefore, and also considering the results obtained in vitamin E study, the *in-vitro* AOC studies cannot be used effectively to predict the impact on the SC after treatment with the lipophilic compounds. However, they can be used to indicate the potency, as well as to confirm the activity.

Table 22: Values of the correlation studies between *in-vitro* and *ex-vivo* AOC using ascorbyl palmitate suspensions (1 - 30% (w/v))

	Average skin AOC	Average normalized AOC
ORAC assay (<i>in-vitro</i>)	$r = 0.6006$ ($p = 0.2841$)	$r = 0.2324$ ($p = 0.7068$)
DPPH assay (<i>in-vitro</i>)	$r = -0.2722$ ($p = 0.6578$)	$r = -0.3518$ ($p = 0.5615$)

4.2.3.5. TPGS on skin

As a water-soluble vitamin E derivative, the effect of α -tocopherol polyethylene glycol succinate (TPGS) on skin AOC was studied in this section for further proof of concept. It has a unique amphiphilic structure formed by the esterification reaction between PEG 1000 and vitamin E, as shown in **Figure 81**.

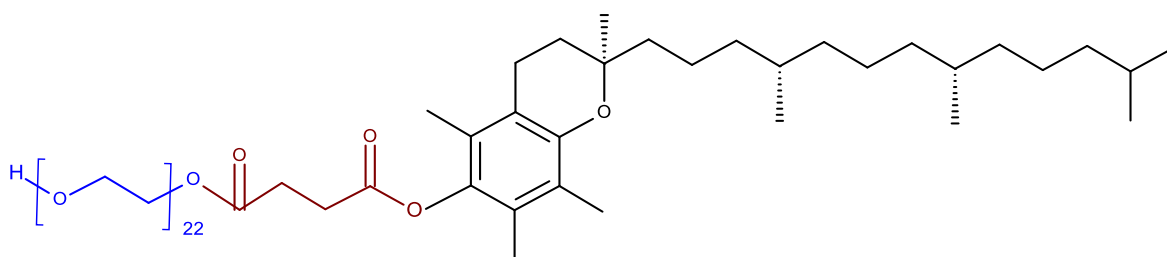


Figure 81: The chemical structure of TPGS which is composed of: vitamin E, succinic acid and PEG 1000

A range of 25 - 30% of d- α -tocopherol is available in TPGS according to the product information [309], with the advantage of many unique biochemical properties. As it has dual lipophilicity and hydrophilicity, surface-active properties and it is popularly used as a solubilizer, stabilizer and penetration enhancer [310]. Therefore, it is widely used as a vitamin E substitute in pharmaceuticals, food and cosmetics with a well-established safety profile [311].

in-vitro studies

The AOC of the TPGS solutions showed concentration-dependent behaviour, with correlation coefficient (r) of 0.98 using the ORAC assay and 0.92 for the DPPH assay (**Table 23** and **Figure 82**). However, as can be predicted, its AOC is far less than that of vitamin E, as it does

not contain pure tocopherols. For example, ORAC values for the 1% is only $224.33 \pm 28.17 \mu\text{M TE}$, which is almost only 2% of the vitamin E AOC of the same dose ($10057.32 \pm 161.43 \mu\text{M TE}$). This decline in activity can be explained by several factors. The first one is the decreased amount of vitamin E in the TPGS chemical structure. Second, is the slow non-enzymatic hydrolysis of the TPGS into vitamin E and succinate/ PEG [312]. Finally, are the chemical manufacturing steps of the compound which may require conditions that affect the vitamin activity, such are the exposure to heat and oxygen.

Table 23: Values of the in-vitro AOC studies of TPGS solutions

TPGS solutions (w/v)	DPPH (IC 50 [mg/mL])	ORAC (AOC [$\mu\text{M TE}$])
0.5%	10.84 ± 1.26	109.01 ± 2.25
1%	7.48 ± 0.03	224.33 ± 28.17
2.5%	5.72 ± 0.26	661.11 ± 88.26
5%	1.89 ± 0.03	1892.96 ± 332.61

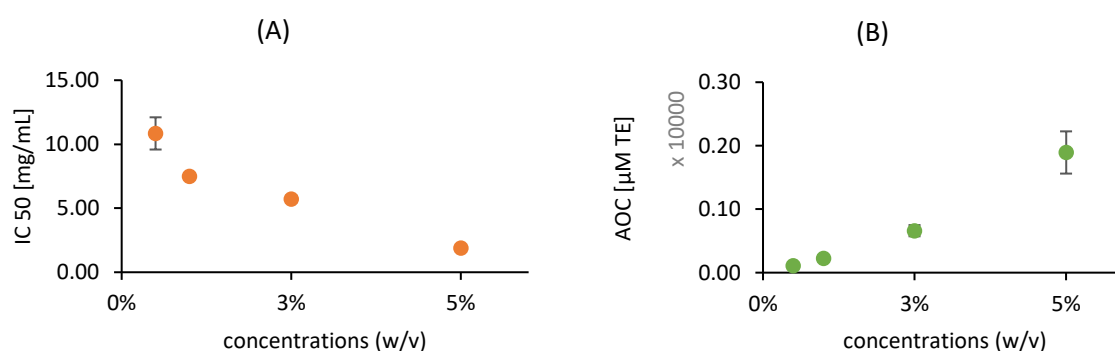


Figure 82: in-vitro AOC values of TPGS solutions (A) using DPPH assay expressed as IC 50 [mg/mL], and (B) using ORAC assay expressed as AOC [$\mu\text{M TE}$]

ex-vivo studies

Biophysical skin properties

The tested porcine skin showed normal average values for TEWL (8.34 ± 2.73 g/hm²) and relatively low hydration status of 16.48 ± 5.39 . From the study notes, this hydration status is possibly related to the sunny weather, which was dominant for six days before the experiment. The sun exposure may dry out the skin and subsequently be reflected in the corneometer measurements. However, this factor was considered neutralized because the control areas were used from the same ears.

Removed SC by tape stripping

Again, in this study, complete removal of SC occurred, with the thickness removed of 7.91 ± 1.05 μ m. The layers analysis showed variable thickness between layers, as follows:

- 1st 10-layers equalling 3.13 ± 0.62 μ m
- 2nd 10-layers equalling 2.70 ± 0.34 μ m
- 3rd 10-layers equalling 2.09 ± 0.21 μ m

Accordingly, the findings of this section reflect effects in the whole SC.

Skin AOC after treatment

The TPGS acted as a pro-oxidant and impacted skin AOC negatively in a concentration-dependent way, $r = 0.9$ (**Figure 83**). The most extreme effect was noted with 2.5% and 5% solutions, $p = 0.0425$ and 0.0333 , respectively. The depletion of skin antioxidants occurred despite the perceived *in-vitro* AOC and the profound safety of vitamin E on skin, which was demonstrated previously.

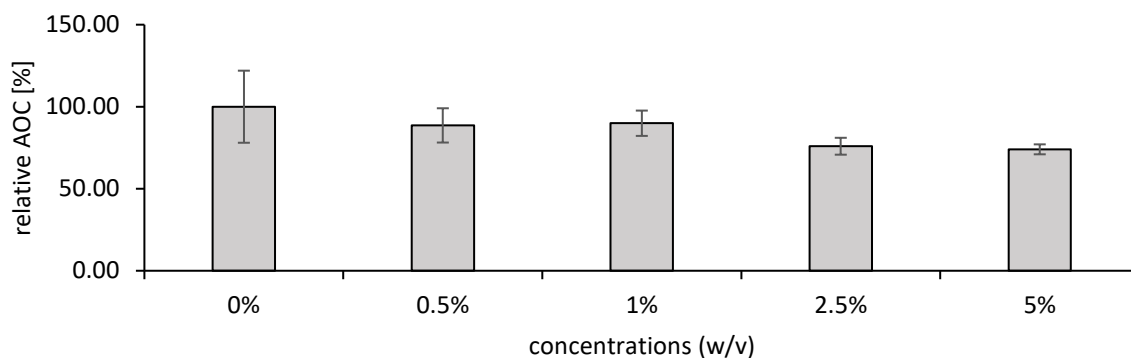


Figure 83 : Relative AOC of the skin after treatment with TPGS solutions (0.5 - 5% (w/v)), expressed as relative AOC [%] in relation to untreated area

This effect was unanticipated and has not been detected before. The most likely reason is the surface-active properties of TPGS, which expectedly leads to interaction with several skin components, such as proteins and lipids, which then enhances penetration and solubility [313]. There are no reported data linking TPGS with the declined skin AOC yet, but there are other interesting records that identified pro-oxidants compounds as by-products in the surfactant's formulation of Tween 80 and ethoxylated alcohols, which are also hydrophilic non-ionic surfactants [314, 315]. They were oxidized by-products such are peroxides, formaldehyde and carbonyl compounds. A similar investigation of the TPGS formulations is recommended and will be of much interest for future research.

In addition to the possibility of the presence of the pro-oxidant by-products, the amphoteric nature of this active ingredient and its activity as a permeation enhancer facilitated its manipulation of the skin. It interacted with the skin elements and impacted the oxidative state with a linear response.

In the literature review, the study of Sheu *et al.* confirmed the poor penetration of TPGS in skin after application [316]. They used several concentrations (0 – 20% (w/v)), and they suggested a specific mechanism for using TPGS in skin as a permeation enhancer. In order to decrease skin resistance to drug permeation, it reduces the interfacial tension and modifies

the interfacial barrier of the SC, which can be the mechanism of the pro-oxidative effect in the current study. On the same topic, it has already been reported that several non-ionic surfactants can disrupt the skin lipid matrix and alter the skin's wettability [317]. Accordingly, we can state that changes in the skin's barrier composition represent a major factor affecting the antioxidant barrier and the skin's detected AOC.

With similar performance to CoQ10, the pro-oxidative effect reached the deeper SC, as shown in **Figure 84**. The difference between 2.5% and 5% was small and only in the third layer, where the reduction equalled one-third of the original skin AOC ($p = 0.0425$ for the 2.5% and 0.0333 for the 5% solution).

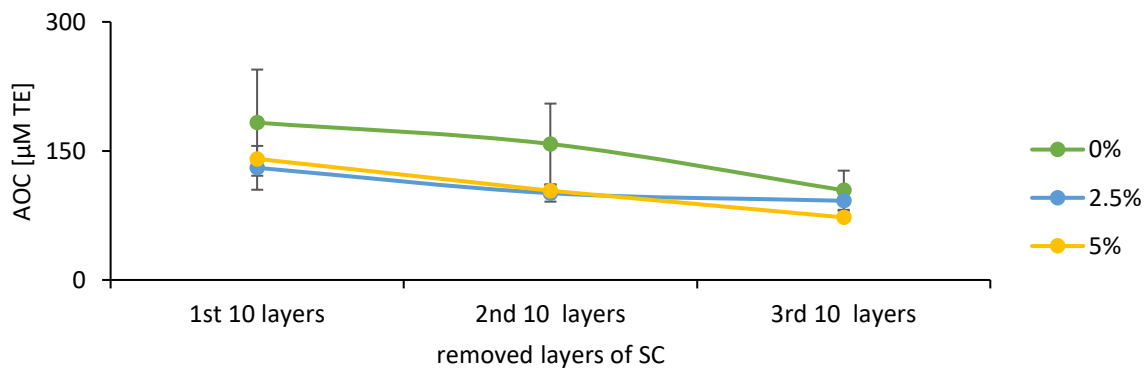


Figure 84: AOC of the skin layers after treatment with TPGS solutions (2.5% and 5% (w/v)), expressed as AOC [µM TE] compared to untreated skin

Examining the normalised AOC delivered interesting findings, as presented in **Figure 85**. The application of all concentrations reduced skin AOC. The most profound effect resulted from the lowest concentration (0.05%) by more than 40% with $p = 0.0069$.

A detailed assessment of the AOC of each skin layer showed the same trend observed previously (**Figure 86**). In general, a pro-oxidative effect was detected at all layers after treatment. However, a higher concentration (5%) of TPGS harmed the deep SC more by

consuming half the capacity of the second layer and more than one-third capacity of the last layer.

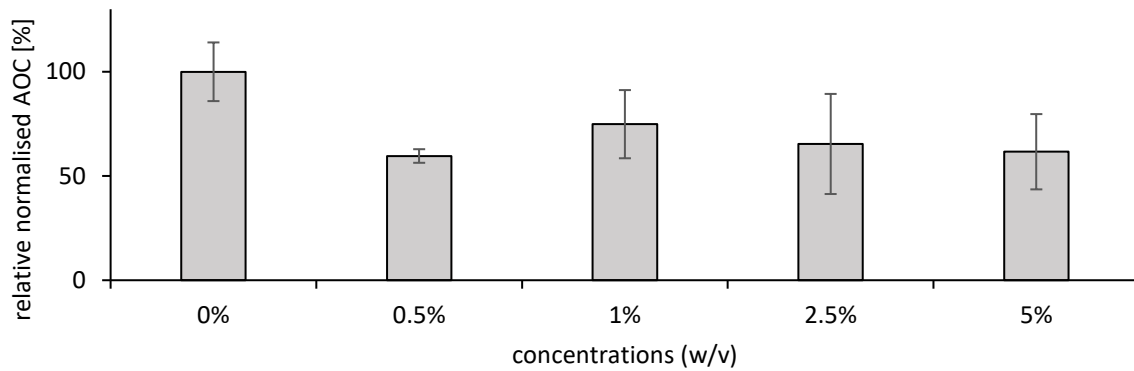


Figure 85: Relative normalised AOC of the skin after treatment with TPGS solutions (0.5 - 5% (w/v)), expressed as relative normalised AOC [%] in relation to untreated skin

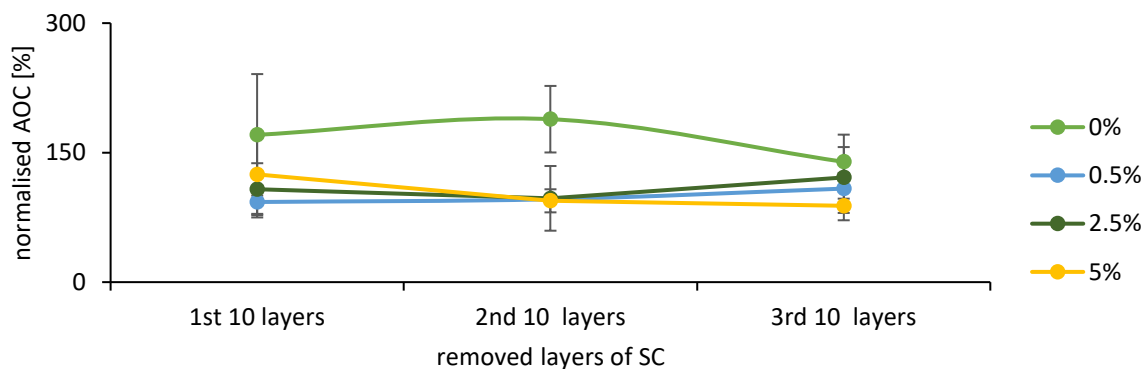


Figure 86: Normalised AOC of the skin layers after treatment with TPGS solutions (0.5%, 2.5% and 5% (w/v)), expressed as normalised AOC [μ M TE] compared to untreated skin

In summary, the use of TPGS solutions on skin leads to a pro-oxidative effect in the SC layer. This major effect occurred with a dose-dependent trend, which confirmed our previously

suggested theory; our model can indirectly detect the non-penetrating antioxidants effectively and accurately.

A similar pro-oxidative effect on skin was shown previously following the application of a high dose of CoQ10. The reported data shows that the same effect can be generated by the topical application of anthralin and benzyl peroxide [318, 319]. Those agents are known to mediate the production of free radicals in the skin and negatively affect skin AOC eventually.

Hence, the value of our model is of great interest in the field of skin health. If it is applied widely, the effect of different molecules (e.g., antioxidants, surfactants and drugs) on the epidermal antioxidant barrier can be determined simply and effectively. Specifically, the detailed effect of surfactants in leave-on products and soaps are worth a comprehensive assessment in the future.

***in-vitro* and *ex-vivo* correlation study**

The correlation studies are illustrated in **Table 24**. They indicated a good inverted correlation between the *in-vitro* assays and average skin AOC. As higher doses were associated with higher pro-oxidative stress on the skin. However, the normalised data was correlated with less meaningful values. As mentioned earlier, the most probable cause is the effect of the surface-active properties on the SC compositions and thickness after the application. Anyhow, more extensive studies are required to understand TPGS effect and the surfactants in general on skin AOC and tape stripping patterns as well.

Table 24: Values of the correlation studies between in-vitro and ex-vivo AOC using with TPGS solutions (0.5 - 5% (w/v))

	Average skin AOC	Average normalized AOC
ORAC assay (<i>in-vitro</i>)	r = -0.8213 (p = 0.1787)	r = -0.3347 (p = 0.6653)
DPPH assay (<i>in-vitro</i>)	r = 0.8446 (p = 0.1554)	r = 0.01787 (p = 0.9821)

4.2.3.6. PEGs

Vitamin E improved the skin AOC, while TPGS harmed it and used up its antioxidant system. To deepen our understanding, polyethylene glycols (PEGs) were also studied as a part of TPGS structure. This study was combined with a comprehensive biophysical skin evaluation before and after the treatment to investigate any possible factors that might influence skin AOC. Furthermore, the treatment duration was investigated using two different time frames: 2 and 4 hours and two different incubation conditions: 32°C and room temperature.

PEGs are polymeric mixtures of non-ionic, water-soluble oligomers. They are used widely in cosmetics as humectants, skin conditioners, solvents, emulsifiers, and surfactants with high levels of safety [320].

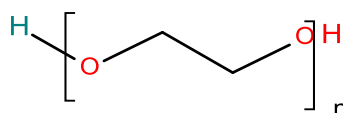


Figure 87: The basic chemical structure of polyethylene glycols

In this study, PEG 300 and PEG cream were chosen as two variable PEG types with different viscosities and MWs.

in-vitro studies

Both formulations showed AOC which was detected only by the ORAC assay. AOC values were $357.75 \pm 113.29 \mu\text{M TE}$ for PEG 300 and $332.45 \pm 34.24 \mu\text{M TE}$ for PEG cream. In comparison to the AOC of the 1% of vitamin E ($10057.32 \pm 161.43 \mu\text{M TE}$), their AOC can be considered insignificant.

ex-vivo studies

Biophysical skin properties

The studies revealed small differences in TEWL, hydration and stiffness influenced by treatment and incubation time. Although those changes are not significant, they reflect treatment impact and experimental conditions.

As shown in **Figure 88**, barrier functions were slightly decreased in the control and PEG cream-treated areas after 1 h at 32°C, and then improved again after 4 h. At room temperature, there was an improvement in all areas after 1 h, followed by a mild deterioration in the control and PEG cream-treated areas. However, compared to 0 h, the net effect was improved barrier function.

The data suggested a fair barrier protection effect by the PEG 300 after a 4 h usage, which is in agreement with the observation of Bárány *et al.* using a low molecular weight PEG derivative [321]. They detected the barrier improvement after the application of PEG-2 stearate and PEG-9 stearate on human skin [321]. The higher molecular weight derivative in contrast (PEG-40 stearate), did not show the same effect. In other studies, the barrier improvement effect of PEG-400 was observed with drugs reduced penetration rate [322–325].

The corneometer measurement reflected elevated skin moisture in all the areas tested after 4 h (**Figure 89**). However, the treated areas were more hydrated than the control after 1 h and 4 h. Higher hydration values were found after 4 h incubation at 32°C, as the closed space in the incubator increased the humidity (up to 53%) and affected all the areas by almost 2-fold.

The increased hydration with time in the control areas can be justified by the occurrence of the rigor mortis of the porcine skin, which started within 4–6 h after the pigs were slaughtered and lasted for 24–48 h [228]. During this phenomenon, tissue loses water and therefore more wetness will be detected on skin surfaces. As described by Keck *et al.* [228], this is combined with increased skin softness, and this was observed in the control sample at room temp (**Figure 90-B**).

Stiffness studies by indentometer showed lower values after 1 h for all areas at 32°C, followed by minor increments except for the PEG cream-treated area (**Figure 90**). At room temp, each sample showed a different trend: the control had decreased stiffness after 1 h and then increased after 4 h by 1.6-fold. The PEG 300 treated area kept almost the same value over the experimental time. Finally, the PEG cream-treated area showed increased values followed by a decrease overtime after 1 h and 4 h. The increased softness over time for the blank area is resulted by the rigor mortis changes at the open space. However, the treatment with the PEGs did not produce similar effect as they might prevent the water exchange, especially with PEG cream that has a high molecular weight counteracts its penetration [326]. This molecular weight dependent effect is more pronounced in the skin with healthy barrier functions, as in the skin in this study [327].

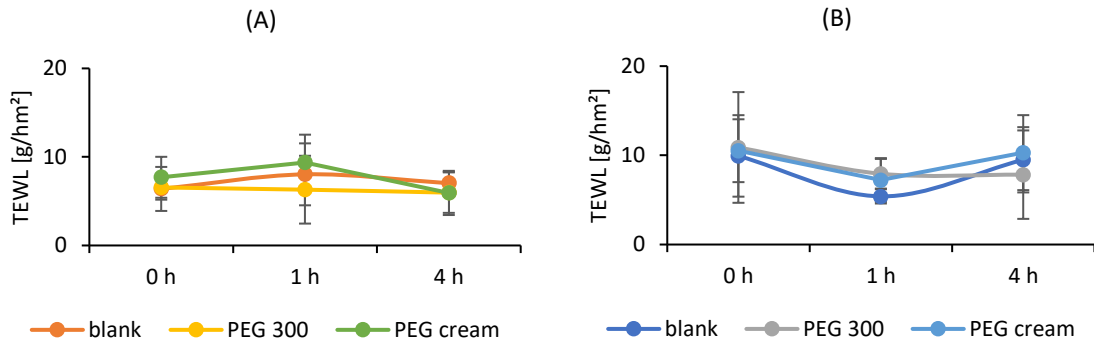


Figure 88: TEWL values at 0, 1 and 4 h (A) at 32 °C and (B) at room temp

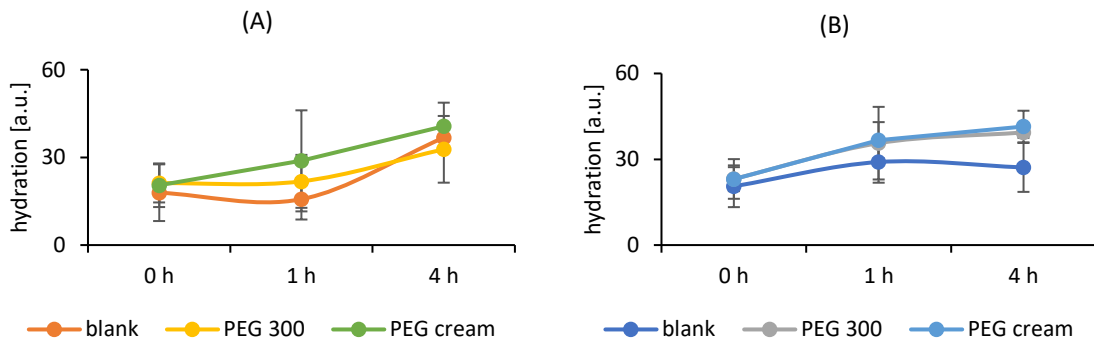


Figure 89: Hydration values at 0, 1 and 4 h (A) at 32 °C and (B) at room temp

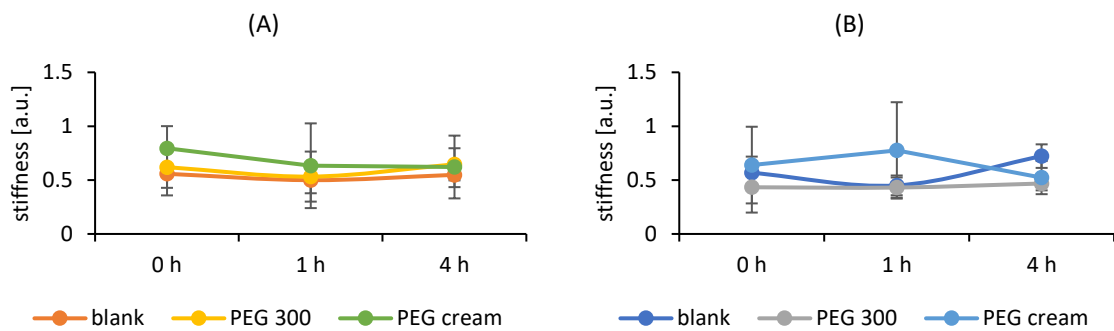


Figure 90: Stiffness values at 0, 1 and 4 h (A) at 32 °C and (B) at room temp

The available data clarified the significant role that experimental conditions can play, as changes in the incubation duration and conditions had a direct impact on both; the treated and control area. Therefore, tight control of these parameters must be done to assure reliable results.

Removed SC by tape stripping

Measurement of protein absorption via IR-D after tape stripping showed full SC removal for samples at 32°C, but only 79% ± 5% was removed from the skin stored at room temperature with estimated thicknesses of 8.63 ± 0.39 and 6.25 ± 0.39 µm, respectively. This difference in the removal pattern can be resulted from the incubation conditions, as the research papers showed that SC thickness is a sensitive marker to the different kinds of treatments and environmental temperature [273, 328]. In addition, another essential factor to be always considered is the physiological differences between the ears used for each study group, as each study was done using a different set of porcine ears and on different days. The values for each individually removed layer are described in the following table:

Table 25: The removed SC by tape stripping for each layer after treatment with PEGs formulations

	At 32 °C [µm]	At room temp [µm]
1st 10-layers equalling	3.40 ± 0.28	2.63 ± 0.28
2nd 10-layers equalling	3.01 ± 0.20	2.13 ± 0.16
3rd 10-layers equalling	2.22 ± 0.14	1.49 ± 0.22

Although there was a profound difference in the SC thickness between the two sets of ears, the relative ratio of each stripped layer to the removed SC thickness in the study is almost the

same. The 1st layer, for example, represents 39% in the first study and 42% in the second study. This finding ensures the reproducibility of the tape stripping procedure used, even in the case where different porcine ears are used.

Skin AOC after treatment

Despite their slight AOC, topical application of PEG formulations had an insignificant effect on the skin AOC, as shown in **Figure 91**. In the first study, at 32°C, the PEG cream slightly improved the skin AOC, especially after 4 h, to 123%, while PEG 300 resulted in almost no change. While at room temp, no marked differences were observed in the AOC.

The improvement in skin AOC upon cream application at 32°C can have resulted from its humectant effect, which may allow the preservation of the skin antioxidants during the incubation time. This effect was enhanced over time, leading to improved barrier functions, hydration, softness, and skin AOC. The obtained finding did not justify the TPGS pro-oxidative effect that was prescribed earlier, but on the opposite, it assured the safety of PEG vehicle to the skin antioxidant barrier. Therefore, the most probable cause of the depleted skin antioxidants by the TPGS is its surfactant properties. Accordingly, there is a fair possibility that the other PEG derivatives with the active-surface properties (e.g., PEG stearate) may show similar harmful effects. However, more studies should be performed to address this concern.

Despite the insignificant differences in these values, it draws attention to vehicles possible effects on skin oxidative state. They are extensively used in cosmetics and their impact is a vital issue for future research.

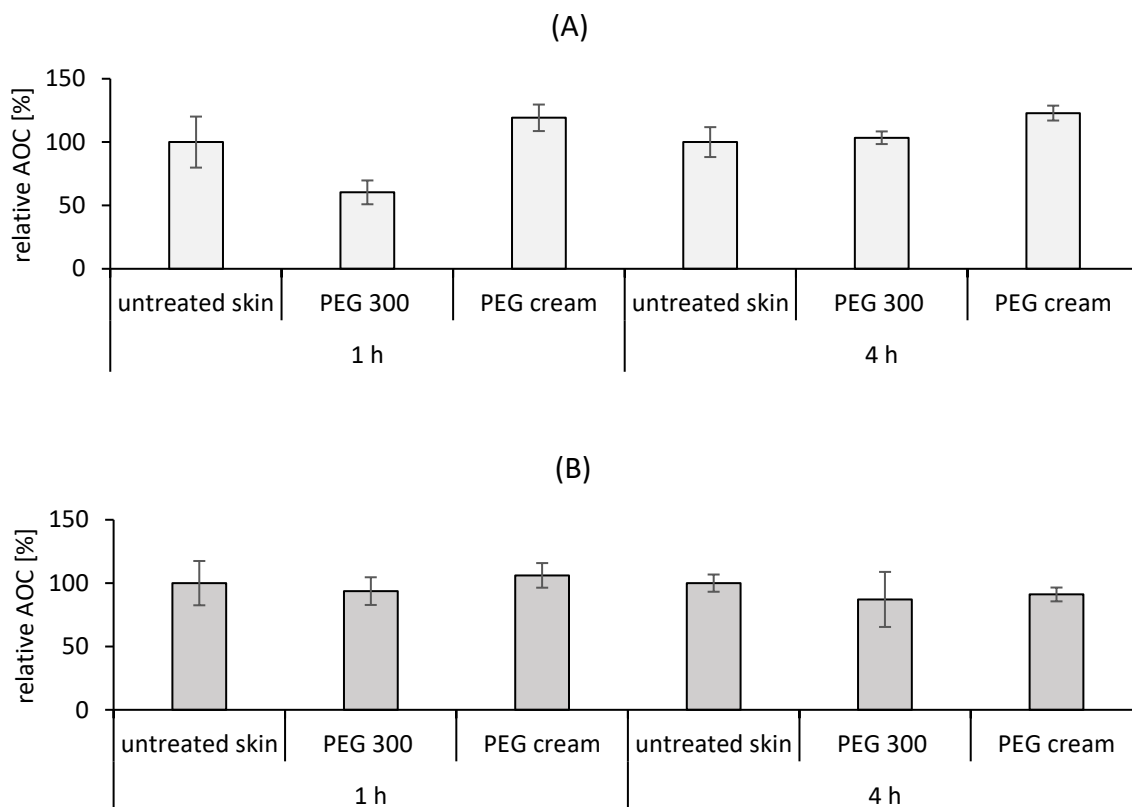


Figure 91: Relative AOC of the removed SC after treatment with PEG 300 and PEG cream, expressed as relative AOC [%] in relation to the AOC of untreated skin; (A) at 32 °C and (B) at room temp

The examination of AOC in the skin layers (**Figure 92**) shows slight changes that were detected in all layers for the PEG cream treatment areas at 32°C. However, for other areas treated with PEG 300, a mild decrease in AOC was detected in the first layers only.

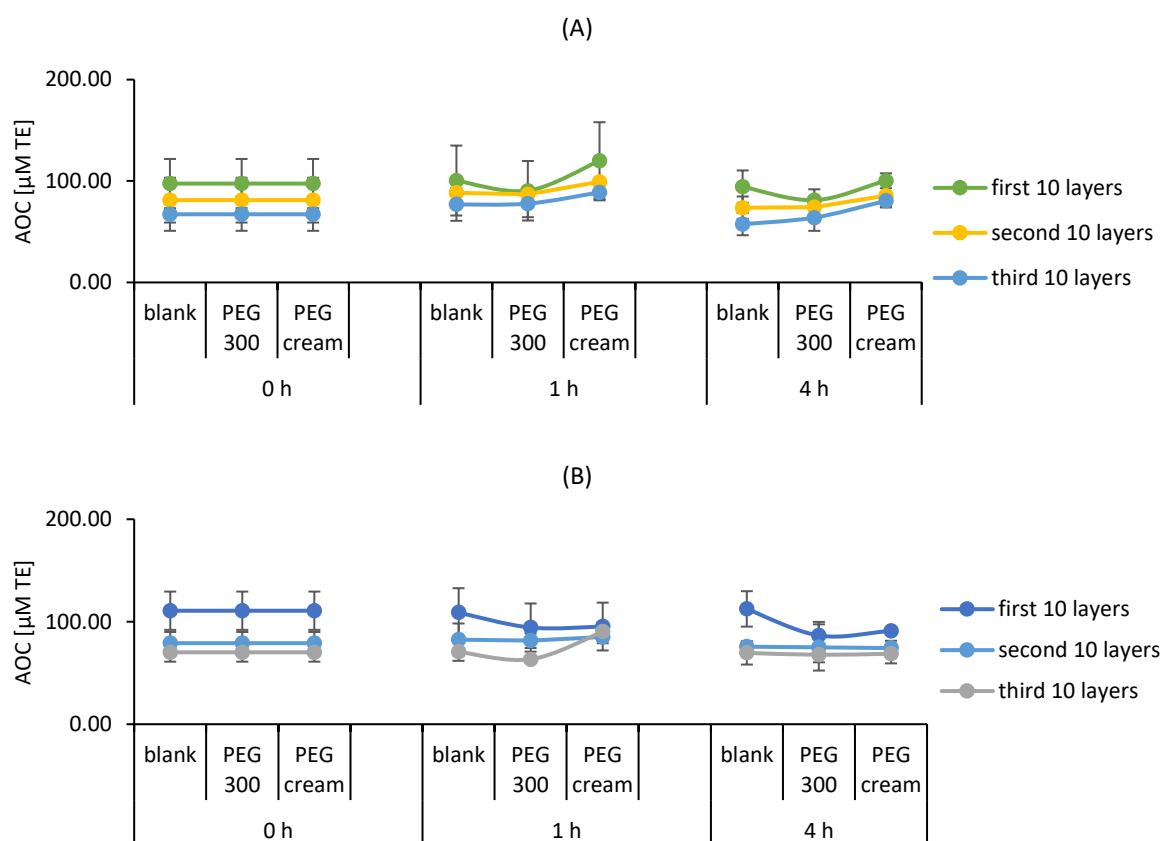


Figure 92: AOC of the SC layers (A) at 32 °C and (B) at room temp, expressed as AOC [µM TE] compared to untreated skin

Therefore, it can be concluded from this investigation that the experimental conditions were the main factor controlling the effect of the applied formulations. The active ingredient can improve skin AOC in some conditions but affect it in other conditions. For this reason, making adjustments in study conditions is a critical factor to be considered in skin studies; the aim must be to simulate human skin conditions to the maximum extent possible. In the current study, the first experiment was done at 32°C, which is the skin temperature; however, the closed space in the incubator did not provide a valid simulation for real skin *in-vivo*. Developing a more suitable condition is a persistent need to get a human skin-simulating model for prospective studies.

To sum up this study, a novel *ex-vivo* model was established for the indirect measurement of antioxidant penetration in the skin using six different molecules. The outcomes can be stated as the suitability of this approach to detect the effect of any molecule on the AOC of the SC. Moreover, accurate detection of the effect of the non-penetrating active ingredients in the SC can be provided simply and effectively, such as ascorbic acid and CoQ10.

The findings can be extrapolated and applied to other antioxidants that are used in cosmeceuticals formulations. Supported by the theory that has been built in this prolong study, we can assume that this model will provide accurate results for the measurement of the following poorly penetrating topical antioxidants:

- Arbutin
- β -carotene
- Curcumin
- Glutathione
- Lycopene

From another point of view, only limited detection for penetrating antioxidants in SC can be achieved, unless the method is adjusted and another technique to investigate the deeper skin layer is included, e.g.: extracts of skin biopsy. The other limitation is the use of the porcine *ex-vivo* skin model, which according to the recent data does not respond with reassembly as the living tissue due to the deficit of the oxygen supply chain [128, 329].

4.2.4. Treatment impact on skin antioxidant capacity—UV radiation

The *ex-vivo* model using ORAC and tape stripping was established, validated and applied to detect the changes in the stratum cornea (SC) oxidative state. In this section, further usage of the model is employed, by using ultraviolet (UV) radiation as the main pro-oxidant generator and underlying factor for skin aging and tumours in the recent decades.

Initially, the model's ability to detect negative impacts on skin was evaluated; then, the combined effects of exposure and the treatment with two cosmeceutical agents were assessed, as illustrated in **Figure 93**.

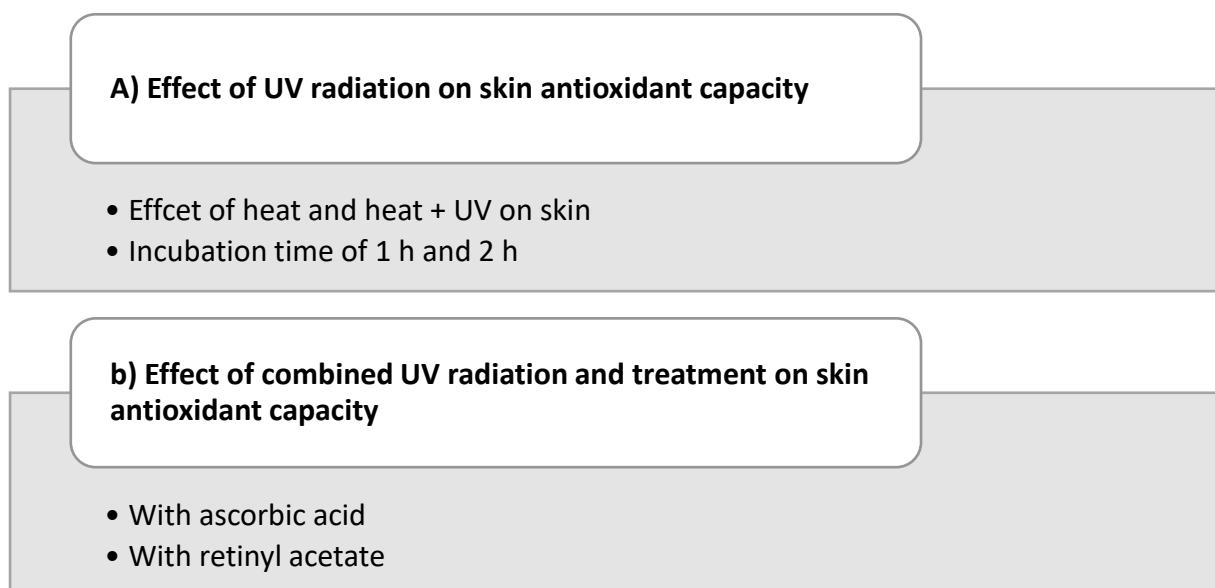


Figure 93: Study outline of current section

4.2.4.1. UV radiation

Biophysical skin properties

The utilised skin showed normal barrier functions, where the trans epidermal water loss (TEWL) was 9.76 ± 0.88 g/hm². Additionally, it was well-hydrated with an average hydration value of 41.87 ± 11.56 .

Removed SC by tape stripping

For the ears that were incubated for 1 h, the average removed SC of the six spots was 8.92 ± 0.67 μ m for the unexposed skin and 9.30 ± 0.60 μ m for the exposed skin. The ears incubated for 2 h had removed SC of 10.68 ± 0.82 and 11.23 ± 0.60 μ m for the unexposed and exposed skin, respectively.

Compared to the previous studies outlined in this thesis, the stripping depth in this study was deeper, and the calculated removed SC was much higher. The main expected cause for this is the impact of the heat and UV radiation on skin integrity and thereby the amount of corneocytes that were removed via tape stripping. As reflected in the experimental note, the skin was softer and weaker than usual after the exposure and the removal of the 30 SC layers, and the remaining skin was yellowish, indicated the complete absence of SC (**Figure 94**). Biniek *et al.* investigated this serious impact on SC, and showed a dramatic effect on the cell cohesion and mechanical integrity of human skin upon UV exposure [330].

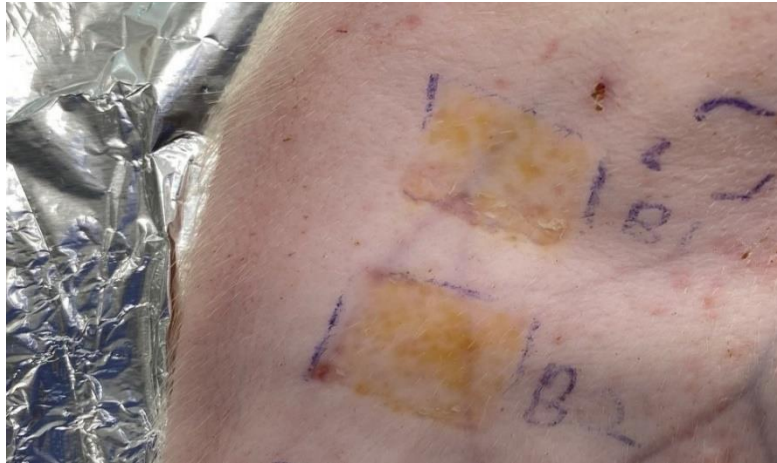


Figure 94: Porcine skin after the removal of 30 SC layers by tape stripping and the exposure to UV radiation

In the present study, the unexposed skin also underwent changes that resulted in high removal of SC, as the temperature inside the box containing the unexposed skin reached 37.50 °C after 1 h and 39.50 °C after 2 h. Logical theory could be assumed to explain this heat effect which is the drying out of the skin over the exposure time, which led to a weaker adhesion force between the corneocytes and thus a higher amount to be removed. A similar observation was made when dried skin tissues were compared to wet skin in a comparative tape stripping study, wherein higher removal was obtained using the dry skin [331]. In their review, Engebretsen *et al.* also reported the effect of high temperature in summer as altering the skin parameters and structure by increasing TEWL and hydration [332].

Thereby, the incubation condition of skin must be considered critical factor affecting the amount of the removed SC by tape stripping. In the current study, there is marked increase in the removed amount of SC, which must accordingly result in higher skin AOC to be detected; this correlation was previously confirmed [135], unless the effect of the solar radiation will overcome this correlation by altering the skin's oxidative state.

Skin AOC after treatment

The exposed skin was assessed after 1 and 2 h of the exposure and compared to unexposed skin that underwent the exact conditions. The results are illustrated in **Table 26** and **Figure 95**. The obtained values revealed the successful detection of the affected skin AOC, where the exposure for 1 h decreased it by 17% ($p = 0.0011$) and for 2 h by 30% ($p = 0.0064$). The calculated normalised AOC presented almost the same significant findings, even with the higher removed SC in this study.

Table 26: Skin AOC values upon the exposure to UV radiation for 1 and 2 h

		AOC [$\mu\text{M TE}$]	Normalised AOC [$\mu\text{M TE}$]
1 h	Unexposed skin	167.69 \pm 3.98	44.17 \pm 3.66
	Exposed skin	140.09 \pm 14.48	38.34 \pm 3.10
2 h	Unexposed skin	158.50 \pm 29.74	34.53 \pm 6.83
	Exposed skin	112.04 \pm 14.60	25.72 \pm 3.77

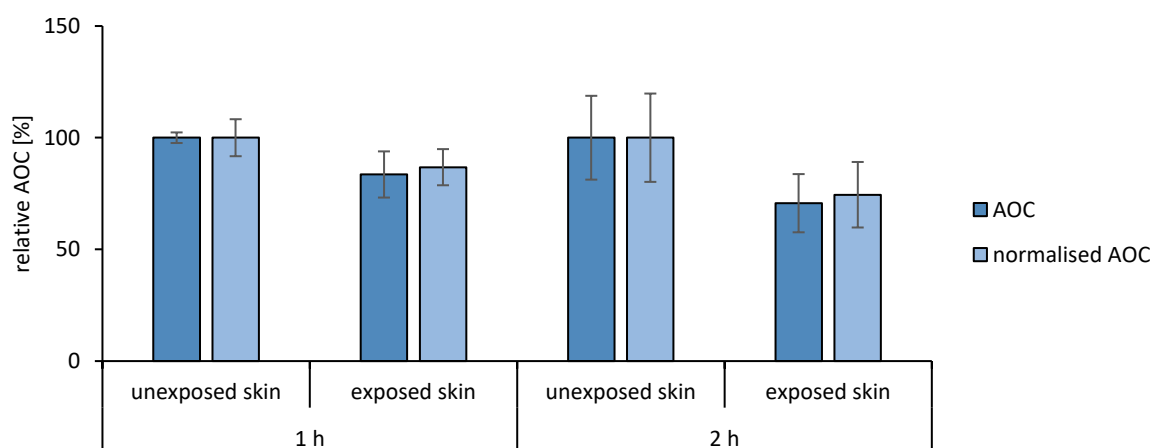


Figure 95: Relative AOC of the skin after the exposure to UV radiation for 1 and 2 h, expressed as relative AOC [%] in relation to unexposed skin

The impaired oxidative state caused by UV radiation has been extensively studied [57, 333–337]. Multiple well-documented conditions occur within the skin due to exposure, including photoaging, photo-immunosuppression and photo-carcinogenesis [2]. The effect of each type of radiation is closely related to its penetration depth into the skin—for example, UVB has short wavelengths (290–320 nm), and accordingly, its effects are usually limited to the SC, while UVA can penetrate till the mid layer of the epidermis due to its longer wavelengths (320–400 nm). Moreover, visible light can penetrate deeper into the dermis layer with much longer wavelengths (400–700 nm) [2]. Yet, UV radiation is of specific concern, as the resulting damage involves DNA modifications through UVB and photosensitisation through UVA which eventually generate free radicals and impair the oxidative balance [337]. However, other solar radiations (visible and infrared lights) have also been reported to induce erythema, thermal damage and even free-radical production upon exposure [2, 338].

The use of the porcine model to study the impact of solar radiation on skin has been established [339, 340]. Anyhow, in a considerable finding, Lohan *et al.* reported the formation of higher ROS in the *in-vivo* human skin compared to the *ex-vivo* porcine skin by a factor of 2.8 [338]. Thus, this factor should be kept into account, and the application of this model using living animals and/or human volunteers will produce more efficient and accurate outcomes. This step is highly applicable, as we implied a non-invasive procedure that has been used extensively with good acceptability, such as the recent clinical study that assess the SC biomarkers in order to determine the cancer prevalence [341]. Additionally, the results in this section indicate significant success for our model, which can be utilised effectively to assess the primary response in a time- and cost-effective manner.

4.2.4.2. Combined treatment and UV radiation

After establishing our method for UV related changes on skin oxidative state, further testing of the model's potential was performed using the combined effects of UV radiation as the

pro-oxidant agent, in addition to ascorbic acid as an antioxidant and photoprotective agent and retinol acetate as a contradictory agent. After that, we compared the obtained findings to the reported studies in the literature.

AOC *in-vitro* studies

Two different concentrations were prepared to be used in this study. Concentrations of 5% and 10% of the ascorbic acid because they are frequently used as vitamin C photoprotection studies [282, 342], and 0.01% and 1% for the retinol acetate as they are the lowest and the highest used dosages of this drug in cosmeceuticals [343]. ORAC assay was chosen as a sensitive AOC test to detect changes that might occur in the solutions at the specific conditions of the experiment; incubation at 32 °C, exposure to heat (39.5 °C) and UV radiation + heat (40.5 °C) for 2 h.

The results are illustrated in **Figure 96**, and showing comparable AOC values for the solutions. Therefore, the direct effects of the different conditions on the *in-vitro* AOC can be excluded, and any detectable effects upon the topical application of the solutions will then be due to the impact of the exposure only.

Unlike the retinol acetate's established good stability [344], the stability of ascorbic acid is always a matter of concern. It is easily prone to reversible oxidation to dehydroascorbic acid upon exposure to variable conditions such as heat and light, especially in the presence of metal ions and alkaline pH [345]. After the reversible oxidation, the reaction may further proceed into irreversible hydrolysis to develop 2,3-diketogulonic acid [345]. Despite these knowledges, in the obtained results there was no evidence supporting the loss of the original active form of the antioxidant in the tested solutions. Several reasons could be behind these findings, including the use of freshly prepared solutions, the absence of the transition metal ions in the media, the use of hydrophilic carrier with neutral pH and the use of low concentrations that do not exceed 10%; thus, the reactivity was minimised.

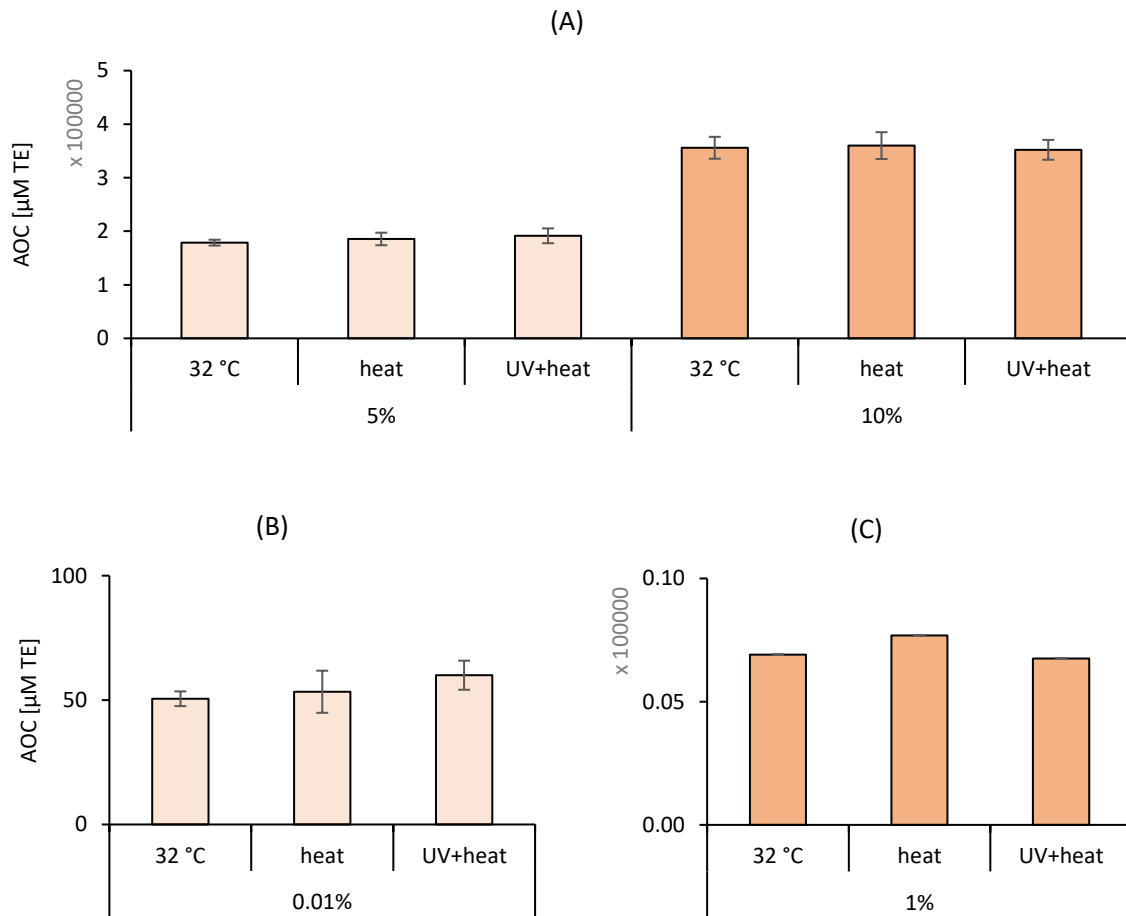


Figure 96: in-vitro AOC values of (A) ascorbic acid solutions (5% and 10% (w/v)), and (B and C) retinol acetate solutions (0.01% and 1% (w/v)), using ORAC assay and expressed as AOC [$\mu\text{M TE}$]

Given the assurance of the good stability and activity of the prepared solutions, the additional planned *ex-vivo* studies were performed using both agents.

ex-vivo studies

Ascorbic acid

This potent antioxidant was the first option to be studied with UV radiation, as it has proven photoprotective effects when applied on skin as pre- or post-exposure treatment.

Biophysical skin properties

The measured skin parameters indicated normal barrier functions of 12.72 ± 1.20 (g/hm²) and hydrated skin with a value of 56.92 ± 7.46 .

Skin AOC after treatment

The AOC of the exposed skin was compared to the AOC of unexposed skin that had undergone the exact same treatment with ascorbic acid as the exposed skin. **Figure 97** shows the results classified according to the applied concentration and type of exposure.

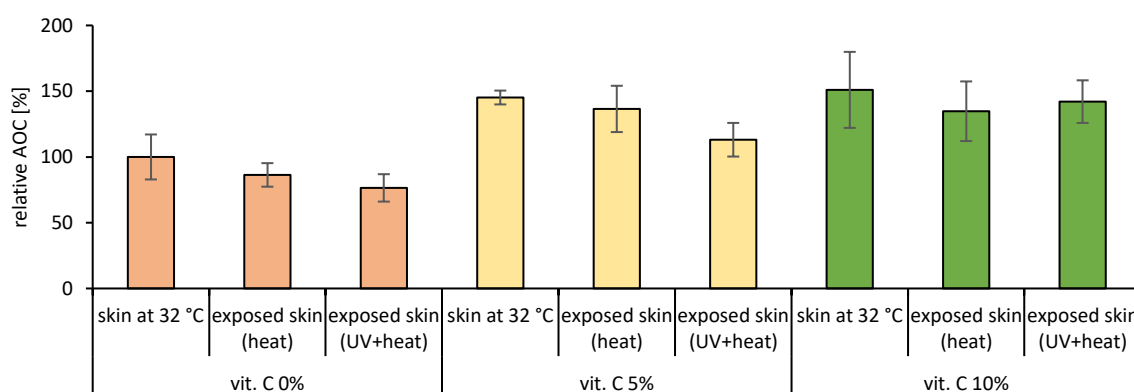


Figure 97: Relative AOC of the skin after the combined UV exposure and ascorbic acid treatment for 2 h, expressed as relative AOC [%] in relation to unexposed skin

The first data set presented pertains to skin treated with a blank solution that was maintained under three conditions for 2 h: incubation at 32 °C, exposure to heat and exposure to heat + UV radiation. Upon analysis, skin had descended relative AOC of 100.00% ± 17.11%, 86.34% ± 8.96% and 76.47% ± 10.43% due to the generation of free radicals upon exposure. As expected, the impact of heat alone was less significant than the impact of heat + UV radiation together.

The second data set is for the skin treated with the 5% solution. AOC was improved for all areas (145.20% ± 5.26%, 136.52% ± 17.60% and 113.10% ± 12.79%), but this improvement was less profound with exposure to UV radiation and heat together. Interestingly, the

concurrent treatment with the 5% solution appeared to have a very good impact, as it counteracted the pro-oxidative effects of heat and + UV radiation and acted as a photoprotective agent.

The last group revealed the treatment influence of the 10% ascorbic acid solution, resulting in almost the same elevated relative AOC for all skin areas ($150.99\% \pm 28.90\%$, $134.76\% \pm 22.66\%$, $142.07\% \pm 16.21\%$). The effects of the heat + UV radiation were completely neutralised; additionally, skin AOC was maintained and improved despite the pro-oxidative conditions. Thereby, we can summarise that, remarkably, the treatment with this particular formulation performed as photoprotective and antioxidant at the same time.

A detailed assessment of the skin exposed to heat + UV radiation is provided in **Figure 98**. It clearly reflects the dose-dependent protective effect of the ascorbic acid on the SC layers ($p < 0.0001$). In the absence of the antioxidant, the skin AOC was significantly affected, and the damage included all layers. On the contrary, the skin treated with both doses did not show these negative impacts; instead, it showed improved AOC, especially with the 10% ascorbic acid solution.

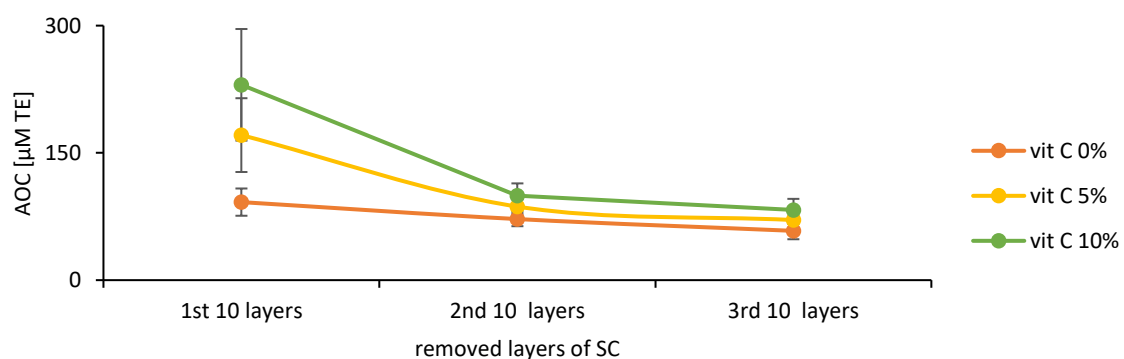


Figure 98: AOC of the skin layers after the combined exposure (UV + heat) and treatment with ascorbic acid solution (5% and 10% (w/v)), expressed as AOC [µM TE] compared to untreated skin

Unlike the current findings, our previous studies using ascorbic acid exhibited limited AOC effects on the deeper SC layers. The altered mechanical integrity of the skin upon exposure was the most likely reason for this, as it facilitates the penetration of such a poorly penetrating agent. The study by Hung *et al.* confirmed this theory, as they studied the cutaneous penetration pattern in photodamaged skin through the application of nanoparticles. They found that the barrier damage resulting from UVA exposure can increase the penetration of nanoparticles [346]. Other studies have also reported the same enhanced penetration upon exposure, using C₆₀-poly(vinylpyrrolidone) (PVP) dispersions [347] and titanium dioxide and zinc oxide nanoparticles [348]. Such change in skin parameters can be considered an advantage only in this case when it facilitates the topical delivery of antioxidants along with other antiaging agents to promote skin healing and recovery to a normal state after sunburn.

The outstanding outcomes of this analysis are in complete agreement with numerous reported studies [349–352], including the research paper by Kawashima *et al.* in scientific reports [350]. They proved the protective effect of ascorbic acid (doses of 10% and 20%) against UVB damage on the reconstituted human epidermis. Both pre- and post-exposure treatments were effective, but the pre-exposure treatment was more effective in preventing the induced UV damage. Another cytoprotective effect of ascorbic acid to UVA was observed by Gęgotek *et al.* Ascorbic acid was able to reduce the expression of the protein degradation in skin following exposure and prevent proinflammatory and proapoptotic signals. Later, the same researchers investigated the synergistic combination of ascorbic acid and rutin, and they achieving remarkable findings in the photoprotection from both UV radiations; A and B [351]. Notably, the combination of ascorbic acid and vitamin E has frequently been used for improved stability and efficacy, and it is thus also a highly effective mixture [353, 354].

As the photoprotective effect of the ascorbic acid is strongly linked to its antioxidant activity, research is expanding to investigate the potentials of other antioxidants. It has been found that several antioxidants can show similar advantages, as rutin [351], curcumin [355], vitamin E [356], resveratrol [357], α -lipoic acid [31].

Overall, this data implies two main points; first, the success of ascorbic acid as a photoprotective agent, and second, the high suitability of our model to study this effect. Further wide applications can be extrapolated and expected to add high value to the scientific field, such as the *ex-vivo* determination of the sunscreen protective effect upon UV exposure.

Retinyl acetate

Some existing data are suggesting possible photoprotective effect of retinyl acetate, while in contrast, other data are indicating its photosensitivity. Hence, this agent was selected for further testing in this section to investigate its net impact on skin AOC.

Biophysical skin properties

The average TEWL value was 11.37 ± 0.88 g/hm², and the hydration was 37.53 ± 13.34 ; both values indicated normal intact skin.

Skin AOC after treatment

Figure 99 shows the effects of the combined treatment and exposure on skin. At first glance, results showed no marked difference between the groups. The usage of both doses of retinyl acetate did not have any negative or positive impacts, as the relative AOC range was from $97.15\% \pm 8.23\%$ to $109.76\% \pm 11.35\%$.

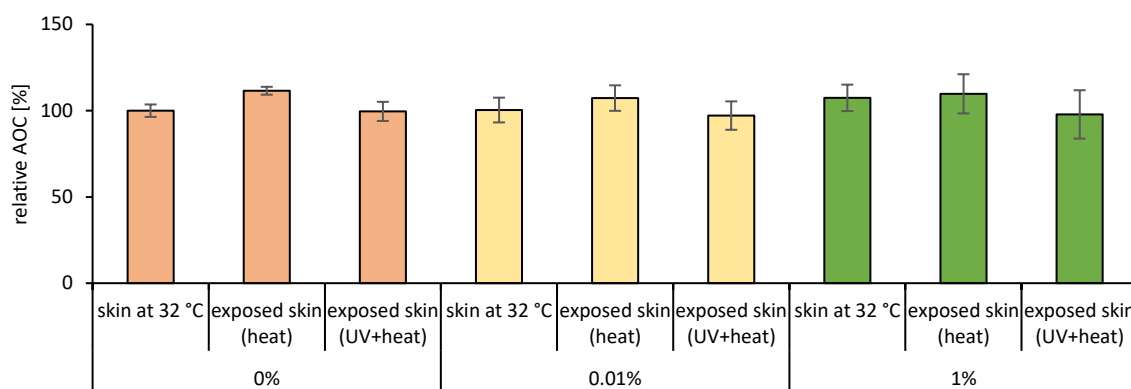


Figure 99: Relative AOC of the skin after the combined UV exposure and retinyl acetate treatment for 2 h, expressed as relative AOC [%] in relation to unexposed skin

But, upon closer investigation, a photoprotection effect could be observed in all treated areas, including the areas that were treated by the blank solution only (miglyol). Unexpectedly, this vehicle by itself was able to protect skin from damage by both UV radiation and heat. The average relative AOC values of all the blank-treated areas are presented in Table 27.

Table 27: The average relative AOC values for the blank-treated areas in variable incubation conditions for 2 h

Incubation condition	Relative AOC [%]
Skin at 32 °C	100.00 ± 3.61
Exposed skin (heat)	111.55 ± 2.28
Exposed skin (UV + heat)	99.58 ± 5.54

The same findings were confirmed by the analysis of SC layers that were exposed to the heat + UV for 2 h (Figure 100). No marked difference had been found between the skin treated with miglyol or with the two different concentrations of the retinyl acetate.

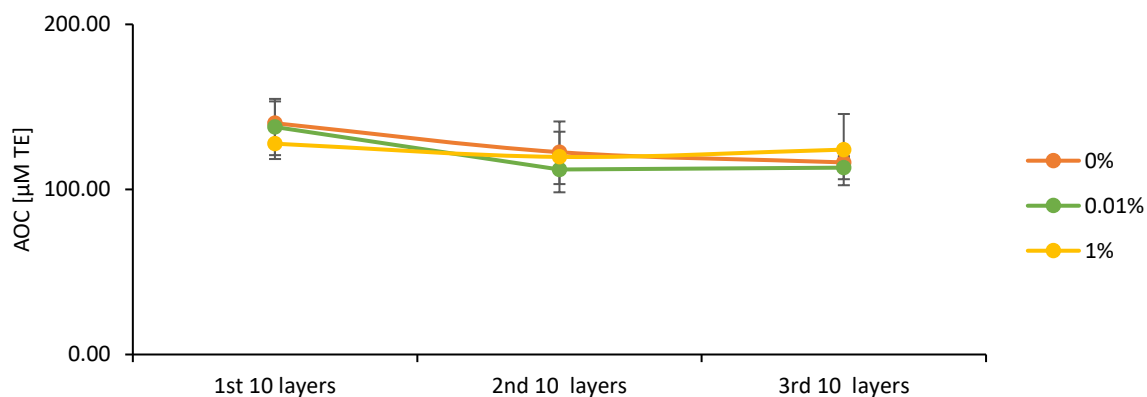


Figure 100: AOC of the skin layers after the combined exposure (UV + heat) and treatment with retinyl acetate suspensions (0.01% and 1% (w/v)), expressed as AOC [$\mu\text{M TE}$] compared to untreated skin

The obtained results are of great interest in many aspects: first, regarding the retinyl acetate, it belongs to the group of retinyl esters, which are reported to exhibit a photoprotective effect from UVB equivalent to a sunscreen with a sun protection factor (SPF) of 20 [358]. At the same time, however, other data has highlighted its photosensitivity, resulting in photodecomposition, including the production of oxidised products [359] that could, theoretically, affect the skin's oxidative state upon application. A possible reason for not observing this impact was the used vehicle in the present work that showed a good photoprotective activity, and thus, the photodecomposition of the retinyl acetate did not occur. However, considering the obtained findings and comparing the treated areas to the blank-treated areas, this agent did not have any effects on the skin's oxidative state.

This leads to the second aspect of the discussion; the great potential of miglyol as a photoprotective agent. The most likely mechanism for this activity was mentioned by Nikolic *et al.*, who investigated the synergistic effect between lipid vehicles and inorganic UV filters [360]. Interestingly, they reported a high UV absorbance in the area of 280–400 nm for several lipid formulations, including miglyol emulsion, which explained their obtained

photoprotective activity. Therefore, as suggested by the authors, these lipids would result in the scattering of UV radiation [360]. Accordingly, the vehicle used in the current study was forming an oily layer over the skin that was able to counteract the pro-oxidative damage caused by UV radiation by acting as a physical sun blocker.

Screening the literature confirmed the efficacy of many other lipid compounds as photoprotective agents, such as the polyunsaturated omega-3 [361], and the lipid extract of coffee beans [362]. As well, the study by Kaur *et al.* reported considerable SPF values for multiple fixed and essential oils, including coconut oil, olive oil and peppermint oil [363].

Prospective independent studies of miglyol are of much interest for further understanding of its photoprotection capabilities, as it is already an attractive vehicle in sunscreen formulations. Its main advantage is the lipophilicity, which allows carrying active ingredients and providing long-lasting effects on skin.

Application of the combined-therapy approach in this section has revealed the great potential of the model that was developed during the course of the study. This approach is expected to provide a result of high value, when applied for example, to the study of the effectiveness of sunscreen formulations. In this case, the main advantage is the ability to identify the net impact of all the critical factors on the skin's oxidative state and not simply the supposed potency as SPF which originally only indicate protection against UVB [59]. The considerable factors include UV radiation (type and intensity), active sunscreen ingredients, the formulation impact and the skin condition. Moreover, this model will be with a specific significance to deal with the major concerns which are raising in the scientific community regarding the induced free radicals generation upon UV exposure by sun-blocking agents [364], as they can cause extra stress in addition to UV radiation that may lead to a seriously impaired oxidative state. The use of a supporting method with this model is recommended especially if it is applied to undiscovered areas in skin research, which would reveal findings that cannot be compared with other studies in the literature.

Chapter 5. Summary

This thesis has been started by the characterisation of specific plants formulation “PlantsCrystals” regarding the antioxidant capacity and size analysis. After that, and using the same principle along with skin analysing techniques, the research is concluded by presenting a novel *ex-vivo* model to assess the skin's oxidative state using ORAC assay and tape stripping method. The developed model has been validated, standardised and then utilised for multiple applications.

The employed methodology included multiple antioxidant estimation assays, such as flavonoid and carotenoid content determination, Folin Ciocalteu, DPPH and ORAC assays. Furthermore, ORAC assay, tape stripping and the multi-probe adapter MPA 10 device were the main protocols that were used to develop and assess the porcine *ex-vivo* skin model.

Validation was done by the employment of the preliminary skin samples, afterwards, it was tested on a larger sample size using fresh porcine skin in a controlled lab climate. The numerical values of the antioxidant skin barrier were determined and expressed as the intrinsic AOC. Later, several treatments were applied and significant findings were obtained, as our model was able to detect the changes accurately in a good agreement with the reported data. The most common antioxidative agents in the cosmetics market were included as treatment agents: ascorbic acid, vitamin E, CoQ10 and ascorbyl palmitate, and their impact on the skin was investigated. In addition to the studies using the main pro-oxidative agent: UV radiation. Moreover, combined treatments were applied aiming to explore the potentials and the limits of this model, and interestingly, it proved its capability to reflect the net effect of multiple factors on the skin antioxidant barrier.

Unlimited practice can be applied using the model suggested in this thesis, in order to predict the impact of any kind of single or combined treatment on the skin, without the need to analyse the individual oxidative markers or the use of sophisticated devices.

Other relevant investigations have also been demonstrated in the current work, including the study on the novel PlantCrystals which was acting as the backbone of the later studies, mainly through the optimization and the validation of the AOC assays. In addition to the determination of the biophysical properties of intact and impaired porcine skin which was an important knowledge about the porcine *ex-vivo* model.

Therefore, this thesis is presenting a rapid, sustained, non-invasive, versatile, time- and cost-effective model to investigate the skin's oxidative state. Furthermore, it is revealing, for the first time, the mean values of the intrinsic AOC and the biophysical properties of the *ex-vivo* porcine skin.

Enormous research ideas can be recommended to be done based on the studies of the current work, initially on the impaired skin, including the utilising of the impaired skin model, the investigation of its iAOC and the treatment impact by applying anti- and pro-oxidative agents. Moreover, the model at this point is ready to be applied to living animals and/or human volunteers, to be part of the safety and efficacy pre-marking studies of the cosmeceutical formulations. This step is highly applicable, as we implied a simple and non-invasive procedure that has been used extensively with good acceptability.

Chapter 6. Zusammenfassung

Der Titel der Doktorarbeit lautet **„Einblicke in der antioxidativen Potenziale von Pflanzen und Haut“**.

Die Forschung begann mit der Charakterisierung der spezifischen Pflanzenformulierung „PlantsCrystals“ im Hinblick auf die antioxidative Kapazität und die Größenanalyse. Dann, und unter Verwendung des gleichen Prinzips kombiniert mit Hautanalysetechniken, präsentierte die Dissertation schließlich ein neuartiges Ex-vivo-Modell, um den oxidativen Zustand der Haut unter Verwendung von ORAC-Assay und Tape-Stripping-Verfahren zu beurteilen. Dieses Modell wurde validiert, standardisiert und anschließend für mehrere Anwendungen eingesetzt.

Die verwendete Methodik umfasste mehrere Assays zur Schätzung von Antioxidantien, wie die Bestimmung des Flavonoid- und Carotinoidgehalts, Folin Ciocalteu-, DPPH- und ORAC-Assays. Darüber hinaus waren der ORAC-Assay, die Tape-Stripping-Methode und das Multi-Sonden-Adapter-MPA-10-Gerät die Hauptmethoden, die zur Entwicklung und Bewertung des Ex-vivo-Hautmodells von Schweinen verwendet wurden.

Die Validierung erfolgte durch die Verwendung von vorläufigen Hautproben. Anschließend wurde eine größere Stichprobengröße mit frischer Schweinehaut in einem kontrollierten Laborklima untersucht. Die numerischen Werte der antioxidativen Hautbarriere wurden bestimmt und als intrinsische hauteigene Antioxidanskapazität “intrinsic Antioxidant Capacity” (iAOC) ausgedrückt. Danach wurden mehrere Behandlungen angewendet, und signifikante Ergebnisse erzielt, da das vorgeschlagene Modell die Änderungen in guter Übereinstimmung mit bereits veröffentlichten Daten bestimmen konnte. In den folgenden Schritten wurden die gängigsten Antioxidantien auf dem Kosmetikmarkt als Behandlungsmittel aufgenommen: Ascorbinsäure, Vitamin E, Coenzym Q10 und Ascorbylpalmitat und deren Wirkung auf die Haut untersucht. Neben dem Hauptprooxidat:

UV-Strahlung. Darüber hinaus wurden kombinierte Behandlungen mit dem Ziel angewendet, die Möglichkeiten und Grenzen dieses Modells zu erkunden. Interessanterweise bewies es seine Fähigkeit, die Nettowirkung mehrerer Faktoren auf die Antioxidanzbarriere der Haut widerzuspiegeln.

Das in dieser Arbeit vorgeschlagenen Modell kann unbegrenzt in der Praxis angewendet werden, um die Auswirkungen jeder Art von Einzel- oder Kombinationsbehandlung auf die Haut vorherzusagen, ohne dass die Notwendigkeit besteht, die einzelnen oxidativen Marker zu analysieren oder hoch entwickelte Geräte zu verwenden.

In der aktuellen Arbeit wurden auch andere relevante Untersuchungen demonstriert, darunter die Studie zu den neuartigen PlantCrystals, die als Rückgrat der späteren Studien diente, hauptsächlich durch die Optimierung und Validierung der AOC-Assays. Daneben ist die Bestimmung der biophysikalischen Eigenschaften von intakter und geschädigter Haut eine wesentliche Erkenntnis über das Ex-vivo-Hautmodell des Schweines.

Daher präsentiert diese Arbeit ein schnelles, nachhaltiges, nicht-invasives, vielseitiges, zeit- und kosteneffektives Modell zur Untersuchung des oxidativen Zustands der Haut. Darüber hinaus werden erstmals die Mittelwerte des iAOC und die biophysikalischen Eigenschaften der Ex-vivo-Schweinehaut offengelegt.

Basierend auf den Studien dieser Arbeit können umfangreiche Forschungsideen empfohlen werden, zunächst an der geschädigten Haut, einschließlich der Verwendung des Modells der geschädigten Haut, um ihre iAOC und die Wirkung der Anwendung von Anti- und Prooxidantien zu untersuchen. Darüber hinaus ist das Modell zu diesem Zeitpunkt bereit, an lebenden Tieren und/oder menschlichen Freiwilligen angewendet zu werden, um Teil der Sicherheits- und Wirksamkeitsstudien der Cosmeceutical-Formulierungen zu sein. Dieser Schritt ist sehr gut anwendbar, da wir ein einfaches und nicht-invasives Verfahren ausnutzen, das ausgiebig und mit guter Akzeptanz verwendet wurde.

Chapter 7. References

- [1] The first organism to use oxygen may have appeared surprisingly early. <https://www.science.org/content/article/first-organism-use-oxygen-may-have-appeared-surprisingly-early>. Accessed 15 August 2022.
- [2] McMullen, R. L. (2018), *Antioxidants and the skin*. CRC Press, Boca Raton.
- [3] Phaniendra, A., Jestadi, D. B., Periyasamy, L. (2015) Free radicals: properties, sources, targets, and their implication in various diseases, *Indian J Clin Biochem*, 30(1): p.11–26.
- [4] Gulcin, İ. (2020) Antioxidants and antioxidant methods: an updated overview, *Arch Toxicol*, 94(3): p.651–715.
- [5] Valko, M., Leibfritz, D., Moncol, J., et al. (2007) Free radicals and antioxidants in normal physiological functions and human disease, *Int J Biochem Cell Biol*, 39(1): p.44–84.
- [6] Singh, A., Kukreti, R., Saso, L., et al. (2019) Oxidative stress: a key modulator in neurodegenerative diseases, *Molecules*, 24(8).
- [7] Valko, M., Rhodes, C. J., Moncol, J., et al. (2006) Free radicals, metals and antioxidants in oxidative stress-induced cancer, *Chem Biol Interact*, 160(1): p.1–40.
- [8] Rasheed, A., Fathima Abdul Azeez, R. (2019), *A review on natural antioxidants, Traditional and complementary medicine*. IntechOpen, London.
- [9] Thiele, J., Elsner, P. (2001), *Oxidants and antioxidants in cutaneous biology. Current Problems in Dermatology*, v.29. KARGER, Basel.
- [10] Neha, K., Haider, M. R., Pathak, A., et al. (2019) Medicinal prospects of antioxidants: A review, *Eur J Med Chem*, 178: p.687–704.
- [11] Willcox, J. K., Ash, S. L., Catignani, G. L. (2004) Antioxidants and prevention of chronic disease, *Crit Rev Food Sci Nutr*, 44(4): p.275–295.
- [12] Graßmann, J. (2005) Terpenoids as Plant Antioxidants. *Plant hormones (Litwack G., Ed.), Vitamins and hormones : advances in research and applications v. 72, 0083-6729, Elsevier, Amsterdam, Boston: p.505–535.*
- [13] Stamford, N. P. J. (2012) Stability, transdermal penetration, and cutaneous effects of ascorbic acid and its derivatives, *J Cosmet Dermatol*, 11(4): p.310–317.

- [14] Shibuya, S., Sakaguchi, I., Ito, S., et al. (2017) Topical application of trisodium ascorbyl 6-palmitate 2-phosphate actively supplies ascorbate to skin cells in an ascorbate transporter-independent manner, *Nutrients*, 9(7).
- [15] Barra, P. A., Márquez, K., Gil-Castell, O., et al. (2019) Spray-drying performance and thermal stability of L-ascorbic acid microencapsulated with sodium alginate and gum arabic, *Molecules*, 24(16).
- [16] Comunian, T. A., Abbaspourrad, A., Favaro-Trindade, C. S., et al. (2014) Fabrication of solid lipid microcapsules containing ascorbic acid using a microfluidic technique, *Food Chem*, 152: p.271–275.
- [17] Khalid, N., Kobayashi, I., Neves, M. A., et al. (2013) Preparation and characterization of water-in-oil emulsions loaded with high concentration of l-ascorbic acid, *LWT*, 51(2): p.448–454.
- [18] Abubakar, A. R., Haque, M. (2020) Preparation of medicinal plants: basic extraction and fractionation procedures for experimental Purposes, *J Pharm Bioallied Sci*, 12(1): p.1–10.
- [19] Griffin, S., Tittikpina, N. K., Al-Marby, A., et al. (2016) Turning waste into value: nanosized natural plant materials of solanum incanum L. and pterocarpus erinaceus poir with promising antimicrobial activities, *Pharmaceutics*, 8(2).
- [20] Sarfraz, M., Griffin, S., Gabour Sad, T., et al. (2018) Milling the mistletoe: nanotechnological conversion of African mistletoe (*Loranthus micranthus*) into antimicrobial materials, *Antioxidants (Basel)*, 7(4): p.60.
- [21] Thiele, J. J., Schroeter, C., Hsieh, S. N., et al. (2001) The antioxidant network of the stratum corneum, *Curr Probl Dermatol*, 29(29): p.26–42.
- [22] Feingold, K. R., Elias, P. M. (2006), *Skin barrier*, ebrary, Inc. Taylor & Francis, New York.
- [23] Shindo, Y., Witt, E., Han, D., et al. (1994) Enzymic and non-enzymic antioxidants in epidermis and dermis of human skin, *J Invest Dermatol*, 102(1): p.122–124.
- [24] D'Aniello, C., Cermola, F., Patriarca, E. J., et al. (2017) Vitamin C in stem cell biology: impact on extracellular matrix homeostasis and epigenetics, *Stem Cells Int*, 2017: p.8936156.
- [25] Li, R., Bianchet, M. A., Talalay, P., et al. (1995) The three-dimensional structure of NAD(P)H:quinone reductase, a flavoprotein involved in cancer chemoprotection and chemotherapy: mechanism of the two-electron reduction, *Proc Natl Acad Sci U S A*, 92(19): p.8846–8850.
- [26] Schallreuter, K. U., Rokos, H., Chavan, B., et al. (2008) Quinones are reduced by 6-tetrahydrobiopterin in human keratinocytes, melanocytes, and melanoma cells, *Free Radic Biol Med*, 44(4): p.538–546.
- [27] Nandi, A., Yan, L.-J., Jana, C. K., et al. (2019) Role of catalase in oxidative stress- and age-associated degenerative diseases, *Oxid Med Cell Longev*, 2019: p.9613090.

- [28] Mugesh, G., Panda, A., Singh, H. B., et al. (2001) Glutathione peroxidase-like antioxidant activity of diaryl diselenides: a mechanistic study, *J Am Chem Soc*, 123(5): p.839–850.
- [29] Johnson, F., Giulivi, C. (2005) Superoxide dismutases and their impact upon human health, *Mol Aspects Med*, 26(4-5): p.340–352.
- [30] Schallreuter, K. U., Wood, J. M. (2001) Thioredoxin reductase — its role in epidermal redox status, *J Photochem Photobiol B: Biol*, 64(2-3): p.179–184.
- [31] Podda, M., Zollner, T. M., Grundmann-Kollmann, M., et al. (2001) Activity of alpha-lipoic acid in the protection against oxidative stress in skin, *Curr Probl Dermatol*, 29(29): p.43–51.
- [32] Gülçin, I. (2006) Antioxidant and antiradical activities of L-carnitine, *Life Sci*, 78(8): p.803–811.
- [33] Turkmen, D. (2020) Serum bilirubin and uric acid antioxidant levels in rosacea patients, *J Cosmet Dermatol*, 19(10): p.2717–2720.
- [34] Hoogduijn, M. J., Cemeli, E., Ross, K., et al. (2004) Melanin protects melanocytes and keratinocytes against H₂O₂-induced DNA strand breaks through its ability to bind Ca²⁺, *Exp Cell Res*, 294(1): p.60–67.
- [35] Darvin, M. E., Fluhr, J. W., Caspers, P., et al. (2009) In vivo distribution of carotenoids in different anatomical locations of human skin: comparative assessment with two different Raman spectroscopy methods, *Exp Dermatol*, 18(12): p.1060–1063.
- [36] Lademann, J., Köcher, W., Yu, R., et al. (2014) Cutaneous carotenoids: the mirror of lifestyle?, *Skin Pharmacol Physiol*, 27(4): p.201.
- [37] Warraich, U.-A., Hussain, F., Kayani, H. U. R. (2020) Aging - oxidative stress, antioxidants and computational modeling, *Heliyon*, 6(5): p.e04107.
- [38] Pisoschi, A. M., Pop, A., Iordache, F., et al. (2021) Oxidative stress mitigation by antioxidants - An overview on their chemistry and influences on health status, *Eur J Med Chem*, 209: p.112891.
- [39] Bowe, W. P., Patel, N., Logan, A. C. (2012) Acne vulgaris: the role of oxidative stress and the potential therapeutic value of local and systemic antioxidants, *J Drugs Dermatol*, 11(6): p.742–746.
- [40] Al-Shobaili, H. A., Alzolibani, A. A., Al Robaee, A. A., et al. (2013) Biochemical markers of oxidative and nitrosative stress in acne vulgaris: correlation with disease activity, *J Clin Lab Anal*, 27(1): p.45–52.
- [41] Al-Shobaili, H. A. (2014) Oxidants and anti-oxidants status in acne vulgaris patients with varying severity, *Ann Clin Lab Sci*, 44(2): p.202–207.
- [42] Simonetti, O., Bacchetti, T., Ferretti, G., et al. (2021) Oxidative stress and alterations of paraoxonases in atopic dermatitis, *Antioxidants (Basel)*, 10(5).

- [43] Bertino, L., Guarneri, F., Cannavò, S. P., et al. (2020) Oxidative stress and atopic dermatitis, *Antioxidants (Basel)*, 9(3).
- [44] Ji, H., Li, X.-K. (2016) Oxidative stress in atopic dermatitis, *Oxid Med Cell Longev*, 2016: p.2721469.
- [45] Obrador, E., Liu-Smith, F., Dellinger, R. W., et al. (2019) Oxidative stress and antioxidants in the pathophysiology of malignant melanoma, *Biol Chem*, 400(5): p.589–612.
- [46] Pizzimenti, S., Ribero, S., Cucci, M. A., et al. (2021) Oxidative stress-related mechanisms in melanoma and in the acquired resistance to targeted therapies, *Antioxidants (Basel)*, 10(12).
- [47] Narendhirakannan, R. T., Hannah, M. A. C. (2013) Oxidative stress and skin cancer: an overview, *Indian J Clin Biochem*, 28(2): p.110–115.
- [48] Bacchetti, T., Simonetti, O., Ricotti, F., et al. (2020) Plasma oxidation status and antioxidant capacity in psoriatic children, *Arch Dermatol Res*, 312(1): p.33–39.
- [49] Dobrică, E.-C., Cozma, M.-A., Găman, M.-A., et al. (2022) The involvement of oxidative stress in psoriasis: a systematic review, *Antioxidants (Basel)*, 11(2).
- [50] Pleńkowska, J., Gabig-Cimińska, M., Mozolewski, P. (2020) Oxidative stress as an important contributor to the pathogenesis of psoriasis, *Int J Mol Sci*, 21(17).
- [51] Rokos, H., Beazley, W. D., Schallreuter, K. U. (2002) Oxidative stress in vitiligo: photo-oxidation of pterins produces H₂O₂ and pterin-6-carboxylic acid, *Biochem Biophys Res Commun*, 292(4): p.805–811.
- [52] Xuan, Y., Yang, Y., Xiang, L., et al. (2022) The role of oxidative stress in the pathogenesis of vitiligo: a culprit for melanocyte death, *Oxid Med Cell Longev*, 2022: p.8498472.
- [53] Wang, Y., Li, S., Li, C. (2019) Perspectives of new advances in the pathogenesis of vitiligo: from oxidative stress to autoimmunity, *Med Sci Monit*, 25: p.1017–1023.
- [54] Radiation: Ultraviolet (UV) radiation. [https://www.who.int/news-room/questions-and-answers/item/radiation-ultraviolet-\(uv\)](https://www.who.int/news-room/questions-and-answers/item/radiation-ultraviolet-(uv)). Accessed 4 August 2022.
- [55] Masaki, H. (2010) Role of antioxidants in the skin: anti-aging effects, *J Dermatol Sci*, 58(2): p.85–90.
- [56] Bosch, R., Philips, N., Suárez-Pérez, J. A., et al. (2015) Mechanisms of photoaging and cutaneous photocarcinogenesis, and photoprotective strategies with phytochemicals, *Antioxidants (Basel)*, 4(2): p.248–268.
- [57] D'Orazio, J., Jarrett, S., Amaro-Ortiz, A., et al. (2013) UV radiation and the skin, *Int J Mol Sci*, 14(6): p.12222–12248.

- [58] Rittié, L., Fisher, G. J. (2015) Natural and sun-induced aging of human skin, *Cold Spring Harb Perspect Med*, 5(1): p.a015370.
- [59] Baki, G., Alexander, K. S. (2015), *Introduction to cosmetic formulation and technology*. Wiley, Hoboken, New Jersey.
- [60] Nakashima, Y., Ohta, S., Wolf, A. M. (2017) Blue light-induced oxidative stress in live skin, *Free Radic Biol Med*, 108: p.300–310.
- [61] Zastrow, L., Groth, N., Klein, F., et al. (2009) UV, sichtbares Licht, Infrarot. Welche Wellenlängen produzieren oxidativen Stress in menschlicher Haut?, *Hautarzt*, 60(4): p.310–317.
- [62] 9 out of 10 people worldwide breathe polluted air, but more countries are taking action. <https://www.who.int/news-room/detail/02-05-2018-9-out-of-10-people-worldwide-breathe-polluted-air-but-more-countries-are-taking-action>. Accessed 14 August 2022.
- [63] Mudway, I. S., Kelly, F. J., Holgate, S. T. (2020) Oxidative stress in air pollution research, *Free Radic Biol Med*, 151: p.2–6.
- [64] Lewtas, J. (2007) Air pollution combustion emissions: characterization of causative agents and mechanisms associated with cancer, reproductive, and cardiovascular effects, *Mutat Res*, 636(1-3): p.95–133.
- [65] Brook, R. D. (2008) Cardiovascular effects of air pollution, *Clin Sci*, 115(6): p.175–187.
- [66] Samet, J. M., Chen, H., Pennington, E. R., et al. (2020) Non-redox cycling mechanisms of oxidative stress induced by PM metals, *Free Radic Biol Med*, 151: p.26–37.
- [67] Valacchi, G., Pambianchi, E., Coco, S., et al. (2022) MicroRNA alterations induced in human skin by diesel fumes, ozone, and UV radiation, *J Pers Med*, 12(2): p.176.
- [68] Fussell, J. C., Kelly, F. J. (2020) Oxidative contribution of air pollution to extrinsic skin ageing, *Free Radic Biol Med*, 151: p.111–122.
- [69] Passeron, T., Zouboulis, C. C., Tan, J., et al. (2021) Adult skin acute stress responses to short-term environmental and internal aggression from exposome factors, *J Eur Acad Dermatol Venereol*, 35(10): p.1963–1975.
- [70] Mistry, N. (2017) Guidelines for formulating anti-pollution products, *Cosmetics*, 4(4): p.57.
- [71] Guo, Q., Liang, F., Tian, L., et al. (2019) Ambient air pollution and the hospital outpatient visits for eczema and dermatitis in Beijing: a time-stratified case-crossover analysis, *Environ Sci Process Impacts*, 21(1): p.163–173.
- [72] Abolhasani, R., Araghi, F., Tabary, M., et al. (2021) The impact of air pollution on skin and related disorders: A comprehensive review, *Dermatol Ther*, 34(2): p.e14840.

- [73] Azevedo Martins, T. E., Sales de Oliveira Pinto, C. A., Costa de Oliveira, A., et al. (2020) Contribution of topical antioxidants to maintain healthy skin—a review, *Sci. Pharm.*, 88(2): p.27.
- [74] Ravetti, Clemente, Brignone, et al. (2019) Ascorbic acid in skin health, *Cosmetics*, 6(4): p.58.
- [75] Wang, K., Jiang, H., Li, W., et al. (2018) Role of vitamin C in skin diseases, *Front Physiol*, 9: p.819.
- [76] Thiele, J. J., Hsieh, S. N., Ekanayake-Mudiyanselage, S. (2005) Vitamin E: critical review of its current use in cosmetic and clinical dermatology, *Dermatol Surg*, 31(7): p.805-13.
- [77] Zhang, M., Dang, L., Guo, F., et al. (2012) Coenzyme Q(10) enhances dermal elastin expression, inhibits IL-1 α production and melanin synthesis in vitro, *Int J Cosmet Sci*, 34(3): p.273–279.
- [78] Fuller, B., Smith, D., Howerton, A., et al. (2006) Anti-inflammatory effects of CoQ10 and colorless carotenoids, *J Cosmet Dermatol*, 5(1): p.30–38.
- [79] Boo, Y. C. (2021) Arbutin as a skin depigmenting agent with antimelanogenic and antioxidant properties, *Antioxidants (Basel)*, 10(7).
- [80] Saeedi, M., Khezri, K., Seyed Zakaryaei, A., et al. (2021) A comprehensive review of the therapeutic potential of α -arbutin, *Phytother Res*, 35(8): p.4136–4154.
- [81] Polouliakh, N., Ludwig, V., Meguro, A., et al. (2020) Alpha-arbutin promotes wound healing by lowering ROS and upregulating insulin/IGF-1 pathway in human dermal fibroblast, *Front Physiol*, 11: p.586843.
- [82] Vollono, L., Falconi, M., Gaziano, R., et al. (2019) Potential of curcumin in skin disorders, *Nutrients*, 11(9).
- [83] Akbik, D., Ghadiri, M., Chrzanowski, W., et al. (2014) Curcumin as a wound healing agent, *Life Sci*, 116(1): p.1–7.
- [84] Li, H., Gao, A., Jiang, N., et al. (2016) Protective effect of curcumin against acute ultraviolet B irradiation-induced photo-damage, *Photochem Photobiol*, 92(6): p.808–815.
- [85] Bae, J.-Y., Choi, J.-S., Choi, Y.-J., et al. (2008) (-)Epigallocatechin gallate hampers collagen destruction and collagenase activation in ultraviolet-B-irradiated human dermal fibroblasts: involvement of mitogen-activated protein kinase, *Food Chem Toxicol*, 46(4): p.1298–1307.
- [86] León, D., Buchegger, K., Silva, R., et al. (2020) Epigallocatechin gallate enhances MAL-PDT cytotoxic effect on PDT-resistant skin cancer squamous cells, *Int J Mol Sci*, 21(9): p.3327.
- [87] Kim, E., Hwang, K., Lee, J., et al. (2018) Skin protective effect of epigallocatechin gallate, *Int J Mol Sci*, 19(1): p.173.
- [88] Nichols, J. A., Katiyar, S. K. (2010) Skin photoprotection by natural polyphenols: anti-inflammatory, antioxidant and DNA repair mechanisms, *Arch Dermatol Res*, 302(2): p.71–83.

- [89] Hecker, A., Schellnegger, M., Hofmann, E., et al. (2022) The impact of resveratrol on skin wound healing, scarring, and aging, *Int Wound J*, 19(1): p.9–28.
- [90] Lin, M.-H., Hung, C.-F., Sung, H.-C., et al. (2021) The bioactivities of resveratrol and its naturally occurring derivatives on skin, *J Food Drug Anal*, 29(1): p.15–38.
- [91] Panche, A. N., Diwan, A. D., Chandra, S. R. (2016) Flavonoids: an overview, *J Nutr Sci*, 5: p.e47.
- [92] Xu, D.-P., Li, Y., Meng, X., et al. (2017) Natural antioxidants in foods and medicinal plants: extraction, assessment and resources, *Int J Mol Sci*, 18(1): p.96.
- [93] Yoder, S. C., Lancaster, S. M., Hullar, M. A., et al. (2015), *Diet-Microbe Interactions in the Gut. Gut Microbial Metabolism of Plant Lignans*. Academic Press.
- [94] Chung, K. T., Wong, T. Y., Wei, C. I., et al. (1998) Tannins and human health: a review, *Crit Rev Food Sci Nutr*, 38(6): p.421–464.
- [95] Box, J. D. (1983) Investigation of the Folin-Ciocalteu phenol reagent for the determination of polyphenolic substances in natural waters, *Water Res*, 17(5): p.511–525.
- [96] Pękal, A., Pyrzynska, K. (2014) Evaluation of aluminium complexation reaction for flavonoid content assay, *Food Anal Methods*, 7(9): p.1776–1782.
- [97] Orsavová, J., Sytařová, I., Mlček, J., et al. (2022) Phenolic compounds, vitamins C and E and antioxidant activity of edible honeysuckle berries (*Lonicera caerulea* L. var. *kamtschatica* Pojark) in relation to their origin, *Antioxidants (Basel)*, 11(2).
- [98] Rodriguez-Amaya, D. B. (2001), *A guide to carotenoid analysis in foods*. ILSI Press, Washington D.C.
- [99] Sist, P., Tramer, F., Lorenzon, P., et al. (2018) *Rhodiola rosea*, a protective antioxidant for intense physical exercise: An in vitro study, *JFF*, 48: p.27–36.
- [100] Xiao, Z., Zhang, Y., Chen, X., et al. (2017) Extraction, identification, and antioxidant and anticancer tests of seven dihydrochalcones from *Malus 'Red Splendor'* fruit, *Food Chem*, 231: p.324–331.
- [101] Rubio, C. P., Hernández-Ruiz, J., Martínez-Subiela, S., et al. (2016) Spectrophotometric assays for total antioxidant capacity (TAC) in dog serum: an update, *BMC Vet Res*, 12(1): p.166.
- [102] Huang, D., Ou, B., Prior, R. L. (2005) The chemistry behind antioxidant capacity assays, *J Agric Food Chem*, 53(6): p.1841–1856.
- [103] Prior, R. L., Wu, X., Schaich, K. (2005) Standardized methods for the determination of antioxidant capacity and phenolics in foods and dietary supplements, *J. Agric. Food Chem.*, 53(10): p.4290–4302.

- [104] Cao, G., Alessio, H. M., Cutler, R. G. (1993) Oxygen-radical absorbance capacity assay for antioxidants, *Free Radic Biol Med*, 14(3): p.303–311.
- [105] Munteanu, I. G., Apetrei, C. (2021) Analytical methods used in determining antioxidant activity: a review, *Int J Mol Sci*, 22(7).
- [106] Somogyi, A., Rosta, K., Pusztai, P., et al. (2007) Antioxidant measurements, *Physiol Meas*, 28(4): p.R41-55.
- [107] Miller, N. J., Rice-Evans, C., Davies, M. J., et al. (1993) A novel method for measuring antioxidant capacity and its application to monitoring the antioxidant status in premature neonates, *Clin Sci*, 84(4): p.407–412.
- [108] Benzie, I. F., Strain, J. J. (1996) The ferric reducing ability of plasma (FRAP) as a measure of "antioxidant power": the FRAP assay, *Anal Biochem*, 239(1): p.70–76.
- [109] Foti, M. C., Daquino, C., Geraci, C. (2004) Electron-transfer reaction of cinnamic acids and their methyl esters with the DPPH(*) radical in alcoholic solutions, *J Org Chem*, 69(7): p.2309–2314.
- [110] Frankel, E. N., Meyer, A. S. (2000) The problems of using one-dimensional methods to evaluate multifunctional food and biological antioxidants, *J. Sci. Food Agric.*, 80(13): p.1925–1941.
- [111] Mendoza, D. J., Maliha, M., Raghuwanshi, V. S., et al. (2021) Diethyl sinapate-grafted cellulose nanocrystals as nature-inspired UV filters in cosmetic formulations, *Mater Today Bio*, 12: p.100126.
- [112] Singh, S., Lohani, A., Mishra, A. K., et al. (2019) Formulation and evaluation of carrot seed oil-based cosmetic emulsions, *J Cosmet Laser Ther*, 21(2): p.99–107.
- [113] Nandy, A., Lee, E., Mandal, A., et al. (2020) Microencapsulation of retinyl palmitate by melt dispersion for cosmetic application, *J Microencapsul*, 37(3): p.205–219.
- [114] Pawłowicz, K., Paczkowska-Walendowska, M., Osmatek, T., et al. (2022) Towards the preparation of a hydrogel from lyophilisates of the *aloe arborescens* aqueous extract, *Pharmaceutics*, 14(7).
- [115] Martinez, R. M., Pinho-Ribeiro, F. A., Steffen, V. S., et al. (2016) Topical formulation containing hesperidin methyl chalcone inhibits skin oxidative stress and inflammation induced by ultraviolet B irradiation, *Photochem Photobiol Sci*, 15(4): p.554–563.
- [116] Manosroi, A., Chutoprapat, R., Sato, Y., et al. (2011) Antioxidant activities and skin hydration effects of rice bran bioactive compounds entrapped in niosomes, *J Nanosci Nanotechnol*, 11(3): p.2269–2277.
- [117] Ratz-Lyko, A., Arct, J., Pytkowska, K. (2012) Methods for evaluation of cosmetic antioxidant capacity, *Skin Res Technol*, 18(4): p.421–430.
- [118] Herrling, T., Zastrow, L., & Groth, N. (1998) Classification of cosmetic products : The radical protection factor (RPF).

- [119] Herrling, T., Jung, K. (2012) The Radical Status Factor (RSF): a novel metric to characterize skin products, *Int J Cosmet Sci*, 34(4): p.285–290.
- [120] Katerji, M., Filippova, M., Duerksen-Hughes, P. (2019) Approaches and methods to measure oxidative stress in clinical samples: research applications in the cancer field, *Oxid Med Cell Longev*, 2019: p.1279250.
- [121] Herrling, T., Jung, K., Fuchs, J. (2006) Measurements of UV-generated free radicals/reactive oxygen species (ROS) in skin, *Spectrochim Acta A Mol Biomol Spectrosc*, 63(4): p.840–845.
- [122] Fujita, H., Hirao, T., Takahashi, M. (2007) A simple and non-invasive visualization for assessment of carbonylated protein in the stratum corneum, *Skin Res Technol*, 13(1): p.84–90.
- [123] Matsumoto, M., Ogai, K., Aoki, M., et al. (2018) Changes in dermal structure and skin oxidative stress in overweight and obese Japanese males after weight loss: a longitudinal observation study, *Skin Res Technol*, 24(3): p.407–416.
- [124] Hagens, R., Khabiri, F., Schreiner, V., et al. (2008) Non-invasive monitoring of oxidative skin stress by ultraweak photon emission measurement. II: biological validation on ultraviolet A-stressed skin, *Skin Pharmacol Physiol*, 14(1): p.112–120.
- [125] Camera, E., Mastrofrancesco, A., Fabbri, C., et al. (2009) Astaxanthin, canthaxanthin and beta-carotene differently affect UVA-induced oxidative damage and expression of oxidative stress-responsive enzymes, *Exp Dermatol*, 18(3): p.222–231.
- [126] Haag, S. F., Bechtel, A., Darvin, M. E., et al. (2010) Comparative study of carotenoids, catalase and radical formation in human and animal skin, *Skin Pharmacol Physiol*, 23(6): p.306–312.
- [127] Ekanayake-Mudiyanselage, S., Tavakkol, A., Polefka, T. G., et al. (2005) Vitamin E delivery to human skin by a rinse-off product: penetration of alpha-tocopherol versus wash-out effects of skin surface lipids, *Skin Pharmacol Physiol*, 18(1): p.20–26.
- [128] Lohan, S., Lauer, A.-C., Arndt, S., et al. (2015) Determination of the antioxidant status of the skin by in vivo-electron paramagnetic resonance (EPR) spectroscopy, *Cosmetics*, 2(3): p.286–301.
- [129] Abraham, A. M., Alnemari, R. M., Jacob, C., et al. (2020) PlantCrystals-nanosized plant material for improved bioefficacy of medical plants, *Materials (Basel)*, 13(19).
- [130] Abraham, A. M., Alnemari, R. M., Brüßler, J., et al. (2021) Improved antioxidant capacity of black tea waste utilizing plantcrystals, *Molecules*, 26(3).
- [131] Abraham, A. M., Quintero, C., Carrillo-Hormaza, L., et al. (2021) Production and characterization of sumac PlantCrystals: influence of high-pressure homogenization on antioxidant activity of sumac (*Rhus coriaria* L.), *Plants (Basel)*, 10(6).

- [132] Romero, G. B., Keck, C. M., Müller, R. H. (2016) Simple low-cost miniaturization approach for pharmaceutical nanocrystals production, *Int J Pharm*, 501(1-2): p.236–244.
- [133] Ordoñez A.A.L., Gomez J.D., M.A. Vattuone M.A., Isla M.I. (2006) Antioxidant activities of *Sechium edule* (Jacq.) Swartz extracts, *Food Chem*, 97(3): p.452–458.
- [134] Ou, B., Hampsch-Woodill, M., Prior, R. L. (2001) Development and validation of an improved oxygen radical absorbance capacity assay using fluorescein as the fluorescent probe, *J Agric Food Chem*, 49(10): p.4619–4626.
- [135] Alnemari, R. M., Brüßler, J., Keck, C. M. (2022) Assessing the oxidative state of the skin by combining classical tape stripping with ORAC assay, *Pharmaceuticals*, 15(5): p.520.
- [136] Bouwman-Boer, Y., Fenton-May, V., Le Brun, P. (2015), *Practical pharmaceuticals: an international guideline for the preparation, care and use of medicinal products*. Springer, Cham.
- [137] Pelikh, O., Stahr, P.-L., Huang, J., et al. (2018) Nanocrystals for improved dermal drug delivery, *Eur J Pharm Biopharm*, 128: p.170–178.
- [138] Klang, V., Schwarz, J. C., Hartl, A., et al. (2011) Facilitating in vitro tape stripping: application of infrared densitometry for quantification of porcine stratum corneum proteins, *Skin Pharmacol Physiol*, 24(5): p.256–268.
- [139] Voegeli, R., Heiland, J., Doppler, S., et al. (2007) Efficient and simple quantification of stratum corneum proteins on tape strippings by infrared densitometry, *Skin Res Technol*, 13(3): p.242–251.
- [140] Shraim, A. M., Ahmed, T. A., Rahman, M. M., et al. (2021) Determination of total flavonoid content by aluminum chloride assay: A critical evaluation, *LWT*, 150: p.111932.
- [141] Pertuzatti, P. B., Barcia, M. T., Rodrigues, D., et al. (2014) Antioxidant activity of hydrophilic and lipophilic extracts of Brazilian blueberries, *Food Chem*, 164: p.81–88.
- [142] Chandra, S., Khan, S., Avula, B., et al. (2014) Assessment of total phenolic and flavonoid content, antioxidant properties, and yield of aeroponically and conventionally grown leafy vegetables and fruit crops: a comparative study, *Evid Based Complement Alternat Med*, 2014: p.253875.
- [143] Granato, D., Shahidi, F., Wrolstad, R., et al. (2018) Antioxidant activity, total phenolics and flavonoids contents: Should we ban in vitro screening methods?, *Food Chem*, 264: p.471–475.
- [144] Chaaban, H., Ioannou, I., Chebil, L., et al. (2017) Effect of heat processing on thermal stability and antioxidant activity of six flavonoids, *J Food Process Preserv*, 41(5): p.e13203.
- [145] Elhamirad, A. H., Zamanipoor, M. H. (2012) Thermal stability of some flavonoids and phenolic acids in sheep tallow olein, *Eur. J. Lipid Sci. Technol.*, 114(5): p.602–606.

- [146] Council of Europe (2016), European pharmacopoeia, Ninth edition. Council of Europe, Strasbourg.
- [147] Ford, L., Theodoridou, K., Sheldrake, G. N., et al. (2019) A critical review of analytical methods used for the chemical characterisation and quantification of phlorotannin compounds in brown seaweeds, *Phytochem Anal*, 30(6): p.587–599.
- [148] Luis, C-H., Ana M R., Camilo Q-O., et al (2016) Comprehensive characterization and antioxidant activities of the main biflavonoids of *Garcinia madruno*: A novel tropical species for developing functional products, *JFF*, 27: p.503–516.
- [149] Davalos, A., Gomez-Cordoves, C., Bartolome, B. (2004) Extending applicability of the oxygen radical absorbance capacity (ORAC-fluorescein) assay, *J Agric Food Chem*, 52(1): p.48–54.
- [150] Zulueta, A., Esteve, M. J., Frígola, A. (2009) ORAC and TEAC assays comparison to measure the antioxidant capacity of food products, *Food Chem*, 114(1): p.310–316.
- [151] Carrillo-Hormaza, L., Ramírez, A. M., Quintero-Ortiz, C., et al. (2016) Comprehensive characterization and antioxidant activities of the main biflavonoids of *Garcinia madruno* : A novel tropical species for developing functional products, *JFF*, 27: p.503–516.
- [152] Huang, D., Ou, B., Hampsch-Woodill, M., et al. (2002) Development and validation of oxygen radical absorbance capacity assay for lipophilic antioxidants using randomly methylated beta-cyclodextrin as the solubility enhancer, *J. Agric. Food Chem.*, 50(7): p.1815–1821.
- [153] Khetan, D., Gupta, N., Chaudhary, R., et al. (2019) Comparison of UV spectrometry and fluorometry-based methods for quantification of cell-free DNA in red cell components, *Asian J Transfus Sci*, 13(2): p.95–99.
- [154] Choosing the Best Detection Method: Absorbance vs. Fluorescence. <https://www.biocompare.com/Bench-Tips/173963-Choosing-the-Best-Detection-Method-Absorbance-vs-Fluorescence/>. Accessed 17 November 2021.
- [155] Eleftherios P. Diamandis, Theodore K. Christopoulos (1996), *Immunoassay. Fluorescence immunoassays*. Academic Press.
- [156] Nutrient Data Laboratory (2010), USDA database for the oxygen radical absorbance capacity (ORAC) of selected foods. U.S. dept. of agriculture.
- [157] Wu, X., Beecher, G. R., Holden, J. M., et al. (2004) Lipophilic and hydrophilic antioxidant capacities of common foods in the United States, *J. Agric. Food Chem.*, 52(12): p.4026–4037.
- [158] Griffin, S., Alkhayer, R., Mirzoyan, S., et al. (2017) Nanosizing *Cynomorium*: Thumbs up for Potential Antifungal Applications, *Inventions*, 2(3): p.24.

- [159] Akram, M., Riaz, M., Munir, N., et al. (2020) Chemical constituents, experimental and clinical pharmacology of *Rosa damascena*: a literature review, *J Pharm Pharmacol*, 72(2): p.161–174.
- [160] Mahboubi, M. (2016) *Rosa damascena* as holy ancient herb with novel applications, *J Tradit Complement Med*, 6(1): p.10–16.
- [161] Boskabady, M. H., Shafei, M. N., Saberi, Z., et al. (2011) Pharmacological effects of *rosa damascena*, *Iran J Basic Med Sci*, 14(4): p.295–307.
- [162] Niazi, M., Hashempur, M. H., Taghizadeh, M., et al. (2017) Efficacy of topical Rose (*Rosa damascena* Mill.) oil for migraine headache: A randomized double-blinded placebo-controlled cross-over trial, *Complement Ther Med*, 34: p.35–41.
- [163] Kürkçüoğlu, M., Abdel-Megeed, A., Başer, K. (2013) The composition of Taif rose oil, *J Essent Oil Res*, 25(5): p.364–367.
- [164] Abdel-Hameed, E.-S. (2012) Total phenolics and antioxidant activity of defatted fresh Taif rose, Saudi Arabia, *BJPR*, 2(3): p.129–140.
- [165] Galal, T. M., Al-Yasi, H. M., Fawzy, M. A., et al. (2022) Evaluation of the Phytochemical and Pharmacological Potential of Taif's Rose (*Rosa damascena* Mill var. *trigintipetala*) for Possible Recycling of Pruning Wastes, *Life (Basel)*, 12(2): p.273.
- [166] Huang, F.-C., Horváth, G., Molnár, P., et al. (2009) Substrate promiscuity of RdCCD1, a carotenoid cleavage oxygenase from *Rosa damascena*, *Phytochemistry*, 70(4): p.457–464.
- [167] Nayebi, N., Khalili, N., Kamalinejad, M., et al. (2017) A systematic review of the efficacy and safety of *Rosa damascena* Mill. with an overview on its phytopharmacological properties, *Complement Ther Med*, 34: p.129–140.
- [168] Knoth, D., Alnemari, R. M., Wiemann, S., et al. (2021) Fingerprint of nature—skin penetration analysis of a stinging nettle PlantCrystals formulation, *Cosmetics*, 8(1): p.21.
- [169] Slavov, A., Vasileva, I., Stefanov, L., et al. (2017) Valorization of wastes from the rose oil industry, *Rev Environ Sci Biotechnol*, 16(2): p.309–325.
- [170] Griffin, S., Sarfraz, M., Farida, V., et al. (2018) No time to waste organic waste: Nanosizing converts remains of food processing into refined materials, *J Environ Manage*, 210: p.114–121.
- [171] Top countries for Dates Production - Source FAO. <https://www.nationmaster.com/nmx/ranking/dates-production>. Accessed 6 July 2022.
- [172] Homayouni, A., Azizi, A., Keshtiban, A. K., et al. (2015) Date canning: a new approach for the long time preservation of date, *J Food Sci Technol*, 52(4): p.1872–1880.

- [173] Saafi, E. B., Louedi, M., Elfeki, A., et al. (2011) Protective effect of date palm fruit extract (*Phoenix dactylifera* L.) on dimethoate induced-oxidative stress in rat liver, *Exp Toxicol Pathol*, 63(5): p.433–441.
- [174] Saafi-Ben Salah, E. B., El Arem, A., Louedi, M., et al. (2012) Antioxidant-rich date palm fruit extract inhibits oxidative stress and nephrotoxicity induced by dimethoate in rat, *J Physiol Biochem*, 68(1): p.47–58.
- [175] Samad, M. A., Hashim, S. H., Simarani, K., et al. (2016) Antibacterial properties and effects of fruit chilling and extract storage on antioxidant activity, total phenolic and anthocyanin content of four date palm (*Phoenix dactylifera*) cultivars, *Molecules*, 21(4): p.419.
- [176] Rock, W., Rosenblat, M., Borochoy-Neori, H., et al. (2009) Effects of date (*Phoenix dactylifera* L., Medjool or Hallawi Variety) consumption by healthy subjects on serum glucose and lipid levels and on serum oxidative status: a pilot study, *J. Agric. Food Chem.*, 57(17): p.8010–8017.
- [177] Al-Alawi, R. A., Al-Mashiqri, J. H., Al-Nadabi, J. S. M., et al. (2017) Date palm tree (*Phoenix dactylifera* L.): natural products and therapeutic options, *Front Plant Sci*, 8: p.845.
- [178] Hamad, I., AbdElgawad, H., Al Jaouni, S., et al. (2015) Metabolic analysis of various date palm fruit (*Phoenix dactylifera* L.) cultivars from Saudi Arabia to assess their nutritional quality, *Molecules*, 20(8): p.13620–13641.
- [179] Al-Farsi, M., Alasalvar, C., Morris, A., et al. (2005) Comparison of antioxidant activity, anthocyanins, carotenoids, and phenolics of three native fresh and sun-dried date (*Phoenix dactylifera* L.) varieties grown in Oman, *J. Agric. Food Chem.*, 53(19): p.7592–7599.
- [180] Kikuchi, N., Miki, T. (1978) The separation of date (*Phoenix dactylifera*) sterols by liquid chromatography, *Mikrochim Acta*, 69(1-2): p.89–96.
- [181] Thompson, L. U., Boucher, B. A., Liu, Z., et al. (2006) Phytoestrogen content of foods consumed in Canada, including isoflavones, lignans, and coumestrol, *Nutr Cancer*, 54(2): p.184–201.
- [182] Warnasih, S., Salam, S., Hasanah, U., et al. (2019) Total phenolic, flavonoid content and metabolite profiling of methanol extract of date (*Phoenix dactylifera*) seeds by LC-QTOF-MS, *ICICS*: p.30029.
- [183] Gutiérrez, R. M. P., Mitchell, S., Solis, R. V. (2008) *Psidium guajava*: a review of its traditional uses, phytochemistry and pharmacology, *J Ethnopharmacol*, 117(1): p.1–27.
- [184] Díaz-de-Cerio, E., Verardo, V., Gómez-Caravaca, A. M., et al. (2017) Health effects of *Psidium guajava* L. leaves: an overview of the last decade, *Int J Mol Sci*, 18(4): p.897.
- [185] Nair, R., Chanda, S. (2007) In-vitro antimicrobial activity of *Psidium guajava* L. leaf extracts against clinically important pathogenic microbial strains, *Braz. J. Microbiol.*, 38(3): p.452–458.

- [186] Fernandes, M., Dias, A., Carvalho, R. R., et al. (2014) Antioxidant and antimicrobial activities of *Psidium guajava* L. spray dried extracts, *Ind Crops Prod*, 60: p.39–44.
- [187] Deguchi, Y., Miyazaki, K. (2010) Anti-hyperglycemic and anti-hyperlipidemic effects of guava leaf extract, *Nutr Metab (Lond)*, 7: p.9.
- [188] Birdi, T., Daswani, P., Brijesh, S., et al. (2010) Newer insights into the mechanism of action of *Psidium guajava* L. leaves in infectious diarrhoea, *BMC Complement Altern Med*, 10: p.33.
- [189] Luo, Y., Peng, B., Liu, Y., et al. (2018) Ultrasound extraction of polysaccharides from guava leaves and their antioxidant and antiglycation activity, *Process Biochem*, 73: p.228–234.
- [190] Kumar, M., Tomar, M., Amarowicz, R., et al. (2021) Guava (*Psidium guajava* L.) leaves: nutritional composition, phytochemical profile, and health-promoting bioactivities, *Foods*, 10(4).
- [191] Wang, L., Wu, Y., Bei, Q., et al. (2017) Fingerprint profiles of flavonoid compounds from different *Psidium guajava* leaves and their antioxidant activities, *J Sep Sci*, 40(19): p.3817–3829.
- [192] Hassan, E. M., El Gendy, A. E.-N. G., Abd-ElGawad, A. M., et al. (2020) Comparative chemical profiles of the essential oils from different varieties of *Psidium guajava* L, *Molecules*, 26(1).
- [193] Soliman, F. M., Fathy, M. M., Salama, M. M., et al. (2016) Comparative study of the volatile oil content and antimicrobial activity of *Psidium guajava* L. and *Psidium cattleianum* Sabine leaves, *Bull Fac Pharm*, 54(2): p.219–225.
- [194] Adrian, J. A. L., Arancon, N. Q., Mathews, B. W., et al. (2015) Mineral composition and soil-plant relationships for common guava (*Psidium guajava* L.) and yellow strawberry guava (*Psidium cattleianum* var. *lucidum*) tree parts and fruits, *Commun Soil Sci Plant Anal*, 46(15): p.1960–1979.
- [195] JM Freire, CM Patto de Abreu, S Maris da Silveira Duarte, FB Araujo de Paula, AR Lima, RAZ Lima, DA Rocha, AA Simao (2014) Nutritional characteristics of guava leaves and its effects on lipid metabolism in hypercholesterolemic rats, *Afr. J. Biotechnol.*, 13 (46): p.4289–4293.
- [196] Vernon, L. P., Seely, G. R. (1966), *The chlorophylls*. Elsevier Science, Burlington.
- [197] Zhou, B., Tan, M., Lu, J.-F., et al. (2012) Simultaneous determination of five active compounds in *chimonanthus nitens* by double-development HPTLC and scanning densitometry, *Chem Cent J*, 6(1): p.46.
- [198] Yassin, D. A., Nasim, M. J., Abraham, A. M., et al. (2021) Upcycling culinary organic waste: production of plant particles from potato and carrot peels to improve antioxidative capacity, *CNT*, 2(1): p.62–70.
- [199] GATES, R. R., ZIMMERMANN, A. A. (1953) Comparison of skin color with melanin content, *Journal of Investigative Dermatology*, 21(6): p.339–348.

- [200] Ortonne, J. P. (2012) Normal and abnormal skin color, *Annales de Dermatologie et de Vénéréologie*, 139: p.S125-S129.
- [201] Campiche, R., Curpen, S. J., Lutchmanen-Kolanthan, V., et al. (2020) Pigmentation effects of blue light irradiation on skin and how to protect against them, *Int J Cosmet Sci*, 42(4): p.399–406.
- [202] Kimball, A. B., Kaczvinsky, J. R., Li, J., et al. (2010) Reduction in the appearance of facial hyperpigmentation after use of moisturizers with a combination of topical niacinamide and N-acetyl glucosamine: results of a randomized, double-blind, vehicle-controlled trial, *Br J Dermatol*, 162(2): p.435–441.
- [203] Carpentier, P. H., Satger, B., Poensin, D., et al. (2013) La chromamétrie, une technique prometteuse pour la quantification de l'atteinte cutanée dans l'insuffisance veineuse chronique, *J Mal Vasc*, 38(4): p.236–242.
- [204] WALKER, G. T. (1961) The pH of the skin, *Drug Cosmet Ind*, 89: p.585.
- [205] Rovenský, J., Micánek, Z., Najbrt, V. (1968) Význam aktuálního pH kůže u dětí, *Cesk Dermatol*, 43(4): p.224–228.
- [206] Blank, I. H. (1939) Measurement of pH of the skin surface, *J Invest Dermatol*, 2(5): p.231–234.
- [207] Meyer, W., Neurand, K., Bartels, T. (1991) Der "Säureschutzmantel" der Haut unserer Haustiere, *Dtsch Tierarztl Wochenschr*, 98(5): p.167–170.
- [208] Yosipovitch, G., Tur, E., Morduchowicz, G., et al. (1993) Skin surface pH, moisture, and pruritus in haemodialysis patients, *Nephrol Dial Transplant*, 8(10): p.1129–1132.
- [209] Schmid-Wendtner, M.-H., Korting, H. C. (2006) The pH of the skin surface and its impact on the barrier function, *Skin Pharmacol Physiol*, 19(6): p.296–302.
- [210] Proksch, E. (2018) pH in nature, humans and skin, *J Dermatol*, 45(9): p.1044–1052.
- [211] Ali, S. M., Yosipovitch, G. (2013) Skin pH: from basic science to basic skin care, *Acta Derm Venereol*, 93(3): p.261–267.
- [212] Werner, Y. (1986) The water content of the stratum corneum in patients with atopic dermatitis. Measurement with the Corneometer CM 420, *Acta Derm Venereol*, 66(4): p.281–284.
- [213] Werner, Y., Lindberg, M. (1985) Transepidermal water loss in dry and clinically normal skin in patients with atopic dermatitis, *Acta Derm Venereol*, 65(2): p.102–105.
- [214] Berardesca, E., Maibach, H. I. (1990) Transepidermal water loss and skin surface hydration in the non invasive assessment of stratum corneum function, *Derm Beruf Umwelt*, 38(2): p.50–53.

- [215] Berardesca, E., Fideli, D., Borroni, G., et al. (1990) In vivo hydration and water-retention capacity of stratum corneum in clinically uninvolved skin in atopic and psoriatic patients, *Acta Derm Venereol*, 70(5): p.400–404.
- [216] Rehbinder, E. M., Advocaat Endre, K. M., Lødrup Carlsen, K. C., et al. (2020) Predicting skin barrier dysfunction and atopic dermatitis in early infancy, *J Allergy Clin Immunol Pract*, 8(2): p.664-673.
- [217] Klotz, T., Ibrahim, A., Maddern, G., et al. (2022) Devices measuring transepidermal water loss: A systematic review of measurement properties, *Skin Res Technol*, 28(4): p.497–539.
- [218] Clarys, P., Barel, A. O. (2017), *Agache's Measuring the Skin. Measurement of Skin Surface Hydration*. Springer, Cham.
- [219] Choi, Y., Oh, S. J., Lee, J. H. (2021) Novel technology at hand to measure skin hydration by Biodisplay smartphone touch screen panel, *Sci Rep*, 11(1): p.19410.
- [220] Stark, H. L. (1980) An interpretation of the initial low stiffness phase of the in vivo load extension relationship for human skin, *Eng Med*, 9(4): p.184–188.
- [221] Burton, J. L. (1982) Thick skin and stiff joints in insulin-dependent diabetes mellitus, *Br J Dermatol*, 106(3): p.369–371.
- [222] Kikuchi, I., Inoue, S., Hamada, K., et al. (1985) Stiff skin syndrome, *Pediatr Dermatol*, 3(1): p.48–53.
- [223] Bader, D. L., Bower, P. (1983) Mechanical characteristics of skin and underlying tissues in vivo, *Biomaterials*, 4(4): p.305–308.
- [224] Batisse, D., Bazin, R., Baldeweck, T., et al. (2002) Influence of age on the wrinkling capacities of skin, *Skin Res Technol*, 8(3): p.148–154.
- [225] Runel, G., Cario, M., Lopez-Ramirez, N., et al. (2020) Stiffness measurement is a biomarker of skin ageing in vivo, *Exp Dermatol*, 29(12): p.1233–1237.
- [226] Yang, Y., Qiu, L., Wang, L., et al. (2019) Quantitative assessment of skin stiffness using ultrasound shear wave elastography in systemic sclerosis, *Ultrasound Med Biol*, 45(4): p.902–912.
- [227] Wiemann, S., Keck, C. M. (2021) Are lipid nanoparticles really superior? A holistic proof of concept study, *Drug Deliv Transl Res*, 12(6): p.1433–1444.
- [228] Keck, C. M., Abdelkader, A., Pelikh, O., et al. (2022) Assessing the dermal penetration efficacy of chemical compounds with the ex-vivo porcine ear model, *Pharmaceutics*, 14(3): p.678.
- [229] Kaushik, V., Ganashalingam, Y., Schesny, R., et al. (2021) Influence of massage and skin hydration on dermal penetration efficacy of Nile red from petroleum jelly-an unexpected outcome, *Pharmaceutics*, 13(12).

- [230] Abruzzo, A., Parolin, C., Corazza, E., et al. (2021) Influence of lactobacillus biosurfactants on skin permeation of hydrocortisone, *Pharmaceutics*, 13(6).
- [231] Herrero-Fernandez, M., Montero-Vilchez, T., Diaz-Calvillo, P., et al. (2022) Impact of water exposure and temperature changes on skin barrier function, *J Clin Med*, 11(2).
- [232] Nakamura, T., Yoshida, H., Haneoka, M., et al. (2022) Season- and facial site-specific skin changes due to long-term mask wearing during the COVID-19 pandemic, *Skin Res Technol*, 28(5): p.749–758.
- [233] Mohd Ariffin, N. H., Hasham, R. (2020) Assessment of non-invasive techniques and herbal-based products on dermatological physiology and intercellular lipid properties, *Heliyon*, 6(5): p.e03955.
- [234] Fluhr, J. W., Menzel, P., Schwarzer, R., et al. (2022) Acidic skin care promotes cutaneous microbiome recovery and skin physiology in an acute stratum corneum stress model, *Skin Pharmacol Physiol*, 35(5): p.266–277.
- [235] Lim, S., Shin, J., Cho, Y., et al. (2019) Dietary patterns associated with sebum content, skin hydration and pH, and their sex-dependent differences in healthy korean adults, *Nutrients*, 11(3).
- [236] Ivanova, Z., Aleksiev, T., Dobrev, H., et al. (2022) Use of a novel Indentometer to evaluate skin induration in localized scleroderma and psoriasis vulgaris, *Skin Res Technol*, 28(2): p.317–321.
- [237] Ajito, T., Suzuki, K., Okumura, J., et al. (2001) Skin pH of Domestic Animals, *Jpn. J. Vet. Clinics*, 24(1): p.9–12.
- [238] Hamilton, D. W., Walker, J. T., Tinney, D., et al. (2022) The pig as a model system for investigating the recruitment and contribution of myofibroblasts in skin healing, *Wound Repair Regen*, 30(1): p.45–63.
- [239] Chilcott, R. P., Stubbs, B., Ashley, Z. (2001) Habituating pigs for in-pen, non-invasive biophysical skin analysis, *Lab Anim*, 35(3): p.230–235.
- [240] Gabard, B., Treffel, P., Charton-Picard, F., et al. (1995) Irritant reactions on hairless micropig skin: a model for testing barrier creams?, *Curr Probl Dermatol*, 23: p.275–287.
- [241] Ranamukhaarachchi, S. A., Lehnert, S., Ranamukhaarachchi, S. L., et al. (2016) A micromechanical comparison of human and porcine skin before and after preservation by freezing for medical device development, *Sci Rep*, 6: p.32074.
- [242] Summerfield, A., Meurens, F., Ricklin, M. E. (2015) The immunology of the porcine skin and its value as a model for human skin, *Mol Immunol*, 66(1): p.14–21.
- [243] Jacobi, U., Kaiser, M., Toll, R., et al. (2007) Porcine ear skin: an in vitro model for human skin, *Skin Pharmacol Physiol*, 13(1): p.19–24.

- [244] Moy, A. J., Tunnell, J. W. Imaging in dermatology. Diffuse reflectance spectroscopy and imaging. Hamblin, Avci et al. (Ed.) 2016 – : p.203–215.
- [245] Sherwood, E. R., Toliver-Kinsky, T. (2004) Mechanisms of the inflammatory response, *Best Pract Res Clin Anaesthesiol*, 18(3): p.385–405.
- [246] Nadworny, P. L., Wang, J., Tredget, E. E., et al. (2008) Anti-inflammatory activity of nanocrystalline silver in a porcine contact dermatitis model, *Nanomedicine*, 4(3): p.241–251.
- [247] Gao, Y., Wang, X., Chen, S., et al. (2013) Acute skin barrier disruption with repeated tape stripping: an in vivo model for damage skin barrier, *Skin Res Technol*, 19(2): p.162–168.
- [248] Levin, J., Maibach, H. (2008) Human skin buffering capacity: an overview, *Skin Res Technol*, 14(2): p.121–126.
- [249] Yoo, M. A., Kim, S. H., Han, H. S., et al. (2022) The effects of wearing a face mask and of subsequent moisturizer use on the characteristics of sensitive skin, *Skin Res Technol*, 28(5): p.714–718.
- [250] Herman, T. F., Bordoni, B. (2022), *Wound classification*, StatPearls Publishing, Treasure Island (FL).
- [251] <https://www.woundcaresurgeons.org>, Different types of wounds - wound care surgeons. <https://www.woundcaresurgeons.org/blogs/know-about-different-types-of-wounds>. Accessed 22 August 2022.
- [252] Mehta W., A., Emmett, M. (2009), *Primer on kidney disease. Approach to acid-base disorders*. Elsevier Inc, Amsterdam.
- [253] Dabboue, H., Builles, N., Frouin, É., et al. (2015) Assessing the impact of mechanical damage on full-thickness porcine and human skin using an in vitro approach, *Biomed Res Int*, 2015: p.434623.
- [254] Mazzarello, V., Piu, G., Ferrari, M., et al. (2019) Efficacy of a topical formulation of sodium bicarbonate in mild to moderate stable plaque psoriasis: a randomized, blinded, inpatient, controlled study, *Dermatol Ther (Heidelb)*, 9(3): p.497–503.
- [255] Suchonwanit, P., Triyangkulsri, K., Ploydaeng, M., et al. (2019) Assessing biophysical and physiological profiles of scalp seborrheic dermatitis in the thai population, *Biomed Res Int*, 2019: p.5128376.
- [256] Mazzarello, V., Ferrari, M., Ena, P. (2018) Werner syndrome: quantitative assessment of skin aging, *Clin Cosmet Investig Dermatol*, 11: p.397–402.
- [257] Kmieć, M. L., Pajor, A., Broniarczyk-Dyła, G. (2013) Evaluation of biophysical skin parameters and assessment of hair growth in patients with acne treated with isotretinoin, *Postepy Dermatol Alergol*, 30(6): p.343–349.

- [258] Tsai, J. C., Sheu, H. M., Hung, P. L., et al. (2001) Effect of barrier disruption by acetone treatment on the permeability of compounds with various lipophilicities: implications for the permeability of compromised skin, *J Pharm Sci*, 90(9): p.1242–1254.
- [259] Ilyasov, I. R., Beloborodov, V. L., Selivanova, I. A. (2018) Three ABTS•+ radical cation-based approaches for the evaluation of antioxidant activity: fast- and slow-reacting antioxidant behavior, *Chem Pap*, 72(8): p.1917–1925.
- [260] Klang, V., Schwarz, J. C., Lenobel, B., et al. (2012) In vitro vs. in vivo tape stripping: validation of the porcine ear model and penetration assessment of novel sucrose stearate emulsions, *Eur J Pharm Biopharm*, 80(3): p.604–614.
- [261] Hoppel, M., Baurecht, D., Holper, E., et al. (2014) Validation of the combined ATR-FTIR/tape stripping technique for monitoring the distribution of surfactants in the stratum corneum, *Int J Pharm*, 472(1-2): p.88–93.
- [262] Turner, N. J., Pezzone, D., Badylak, S. F. (2015) Regional variations in the histology of porcine skin, *Tissue Eng Part C Methods*, 21(4): p.373–384.
- [263] Denat, L., Kadekaro, A. L., Marrot, L., et al. (2014) Melanocytes as instigators and victims of oxidative stress, *J Invest Dermatol*, 134(6): p.1512–1518.
- [264] Maibam, U., Hooda, O. K., Sharma, P. S., et al. (2018) Differential level of oxidative stress markers in skin tissue of zebu and crossbreed cattle during thermal stress, *Livest Sci*, 207: p.45–50.
- [265] Silvestre, M., Saeed, A., Cervera, R., et al. (2003) Rabbit and pig ear skin sample cryobanking: effects of storage time and temperature of the whole ear extirpated immediately after death, *Theriogenology*, 59(5-6): p.1469–1477.
- [266] Andersson, T., Ertürk Bergdahl, G., Saleh, K., et al. (2019) Common skin bacteria protect their host from oxidative stress through secreted antioxidant RoxP, *Sci Rep*, 9(1): p.3596.
- [267] Ketter, P. M., Kamucheka, R., Arulanandam, B., et al. (2019) Platelet enhancement of bacterial growth during room temperature storage: mitigation through refrigeration, *Transfusion*, 59(S2): p.1479–1489.
- [268] Ogai, K., Nagase, S., Mukai, K., et al. (2018) A Comparison of techniques for collecting skin microbiome samples: swabbing versus tape-stripping, *Front Microbiol*, 9: p.2362.
- [269] Rosenquist, M. D., Cram, A. E., Kealey, G. P. (1988) Skin preservation at 4 °C: A species comparison, *Cryobiology*, 25(1): p.31–37.
- [270] Zhu, Z. M. (1989) Optimal conditions for the storage of split-thickness skin at 4C, *CJS*, 27(3): p.169-72, 190.

- [271] Grazul-Bilska, A. T., Bilski, J. J., Redmer, D. A., et al. (2009) Antioxidant capacity of 3D human skin EpiDerm model: effects of skin moisturizers, *Int J Cosmet Sci*, 31(3): p.201–208.
- [272] Abla, M. J., Banga, A. K. (2013) Quantification of skin penetration of antioxidants of varying lipophilicity, *Int J Cosmet Sci*, 35(1): p.19–26.
- [273] Pelikh, O., Eckert, R. W., Pinnapireddy, S. R., et al. (2021) Hair follicle targeting with curcumin nanocrystals: Influence of the formulation properties on the penetration efficacy, *J Control Release*, 329: p.598–613.
- [274] Patel, S. R., Zhong, H., Sharma, A., et al. (2009) Controlled non-invasive transdermal iontophoretic delivery of zolmitriptan hydrochloride in vitro and in vivo, *Eur J Pharm Biopharm*, 72(2): p.304–309.
- [275] Zhao, X., Schaffzin, J. K., Carson, J., et al. (2020) Analysis of chlorhexidine gluconate in skin using tape stripping and ultrahigh-performance liquid chromatography-tandem mass spectrometry, *J Pharm Biomed Anal*, 183: p.113111.
- [276] Sotler, R., Poljšak, B., Dahmane, R., et al. (2019) Prooxidant activity of antioxidanta and their impact on health, *Acta Clin Croat*, 58(4): p.726–736.
- [277] Kishimoto, Y., Saito, N., Kurita, K., et al. (2013) Ascorbic acid enhances the expression of type 1 and type 4 collagen and SVCT2 in cultured human skin fibroblasts, *Biochem Biophys Res Commun.*, 430(2): p.579–584.
- [278] Wayner, D., Burton, G. W., Ingold, K. U. (1986) The antioxidant efficiency of vitamin C is concentration-dependent, *BBA*, 884(1): p.119–123.
- [279] Olofinnade, A. T., Onaolapo, A. Y., Onaolapo, O. J. (2021) Concentration-dependent effects of dietary L-ascorbic acid fortification in the brains of healthy mice, *Cent Nerv Syst Agents Med Chem*, 21(2): p.104–113.
- [280] Jacobi, U., Weigmann, H.-J., Ulrich, J., et al. (2005) Estimation of the relative stratum corneum amount removed by tape stripping, *Skin Res Technol*, 11(2): p.91–96.
- [281] Pinnell, S. R., Yang, H., Omar, M., et al. (2001) Topical L-ascorbic acid: percutaneous absorption studies, *Dermatol Surg*, 27(2): p.137–142.
- [282] Humbert, P. G., Haftek, M., Creidi, P., et al. (2003) Topical ascorbic acid on photoaged skin. Clinical, topographical and ultrastructural evaluation: double-blind study vs. placebo, *Exp Dermatol*, 12(3): p.237–244.
- [283] Lin, F.-H., Lin, J.-Y., Gupta, R. D., et al. (2005) Ferulic acid stabilizes a solution of vitamins C and E and doubles its photoprotection of skin, *J Invest Dermatol*, 125(4): p.826–832.

- [284] Campos, P. M. B. G. M., Gonçalves, G. M. S., Gaspar, L. R. (2008) In vitro antioxidant activity and in vivo efficacy of topical formulations containing vitamin C and its derivatives studied by non-invasive methods, *Skin Res Technol*, 14(3): p.376–380.
- [285] Ratz-Lyko, A., Arct, J., Pytkowska, K. (2012) Methods for evaluation of cosmetic antioxidant capacity, *Skin Res Technol*, 18(4): p.421–430.
- [286] Eitenmiller, R. R., Lee, J. (2004), *Food chemistry, composition and analysis. Vitamin E. Food science and technology*, 137. Marcel Dekker; London : Taylor & Francis, New York.
- [287] Fiume, M. M., Bergfeld, W. F., Belsito, D. V., et al. (2018) Safety assessment of tocopherols and tocotrienols as used in cosmetics, *Int J Toxicol*, 37(2): p.61S-94S.
- [288] Im, S., Nam, T. G., Lee, S. G., et al. (2014) Additive antioxidant capacity of vitamin C and tocopherols in combination, *Food Sci Biotechnol*, 23(3): p.693–699.
- [289] Lademann, J., Jacobi, U., Surber, C., et al. (2009) The tape stripping procedure--evaluation of some critical parameters, *Eur J Pharm Biopharm*, 72(2): p.317–323.
- [290] Traber, M. G., Rallis, M., Podda, M., et al. (1998) Penetration and distribution of alpha-tocopherol, alpha- or gamma-tocotrienols applied individually onto murine skin, *Lipids*, 33(1): p.87–91.
- [291] Nada, A., Krishnaiah, Y. S. R., Zaghoul, A.-A., et al. (2011) In vitro and in vivo permeation of vitamin E and vitamin E acetate from cosmetic formulations, *Med Princ Pract*, 20(6): p.509–513.
- [292] Lennarz, W. J. and Lane, M. D., Eds., (2013) *Encyclopedia of biological chemistry*. Elsevier, Amsterdam.
- [293] Lim, Y., Traber, M. G. (2007) Alpha-tocopherol transfer protein (alpha-TTP): insights from alpha-tocopherol transfer protein knockout mice, *Nutr Res Pract*, 1(4): p.247–253.
- [294] Kim, B., Cho, H.-E., Moon, S. H., et al. (2020) Transdermal delivery systems in cosmetics, *biomed dermatol*, 4(1).
- [295] Krista (2020) Safety assessment of ubiquinone ingredients as used in cosmetics. CIR Report Data Sheet.
- [296] mattilsynet, Risk profile CoQ10 and Idebenone. https://www.mattilsynet.no/kosmetikk/stoffer_i_kosmetikk/risk_profile_of_coq10_and_idebenone_0110.11369/binary/Risk%20Profile%20of%20CoQ10%20and%20Idebenone%200110. Accessed 28 October 2021.
- [297] Ryu, K.-A., Park, P. J., Kim, S.-B., et al. (2020) Topical delivery of coenzyme Q10-loaded microemulsion for skin regeneration, *Pharmaceutics*, 12(4): p.332.
- [298] Pearse, A. D., Gaskell, S. A., Marks, R. (1987) Epidermal changes in human skin following irradiation with either UVB or UVA, *J Invest Dermatol*, 88(1): p.83–87.

- [299] Schallreuter, K. U. (2013) Q10-triggered facial vitiligo, *Br J Dermatol*, 169(6): p.1333–1336.
- [300] Jankovskaja, S., Labrousse, A., Prévau, L., et al. (2020) Visualisation of H₂O₂ penetration through skin indicates importance to develop pathway-specific epidermal sensing, *Mikrochim Acta*, 187(12): p.656.
- [301] Internal Market, Industry, Entrepreneurship and SMEs, Ban on animal testing. https://ec.europa.eu/growth/sectors/cosmetics/ban-animal-testing_en. Accessed 17 November 2021.
- [302] Care, T. S., Coenzyme Q10 Serum. <https://www.timelessha.com/products/coenzyme-q10-serum-1-oz>. Accessed 17 November 2021.
- [303] Junyaprasert, V. B., Teeranachaideekul, V., Souto, E. B., et al. (2009) Q10-loaded NLC versus nanoemulsions: stability, rheology and in vitro skin permeation, *Int J Pharm*, 377(1-2): p.207–214.
- [304] Alfonso R. Gennaro (1985), *Remington's Pharmaceutical Sciences*, Book Review, 74. Mack Publishing Co, Easton.
- [305] Špiclin, P., Gašperlin, M., Kmetec, V. (2001) Stability of ascorbyl palmitate in topical microemulsions, *Int J Pharm*, 222(2): p.271–279.
- [306] Elmore, A. R. (2005) Final report of the safety assessment of L-ascorbic acid, calcium ascorbate, magnesium ascorbate, magnesium ascorbyl phosphate, sodium ascorbate, and sodium ascorbyl phosphate as used in cosmetics, *Int J Toxicol*, 24(2): p.51–111.
- [307] Johnson W, Boyer IJ, Bergfeld WF, et al (2022) Safety assessment of ethers and esters of ascorbic acid as used in cosmetics, *Int J Toxicol*, 41(2_suppl): p.57S-75S.
- [308] Liu, Y., Liu, C., Li, J. (2020) Comparison of vitamin C and its derivative antioxidant activity: evaluated by using density functional theory, *ACS Omega*, 5(39): p.25467–25475.
- [309] Vitamin E TPGS, Tocofersolan. <http://www.parmentier.de/gpfneu/english/tpgs.php>. Accessed 18 November 2021.
- [310] Tavares Luiz, M., Di Delello Filippo, L., Carolina Alves, R., et al. (2021) The use of TPGS in drug delivery systems to overcome biological barriers, *Eur Polym J*, 142: p.110129.
- [311] Rowe, R. C., Sheskey, P. J., Quinn, M. E. (2009), *Handbook of pharmaceutical excipients*. Pharmaceutical Press, London.
- [312] Yan, A., Bussche, A. von dem, Kane, A. B., et al. (2007) Tocopheryl polyethylene glycol succinate as a safe, antioxidant surfactant for processing carbon nanotubes and fullerenes, *Carbon N Y*, 45(13): p.2463–2470.
- [313] Alonso, C., Lucas, R., Barba, C., et al. (2015) Skin delivery of antioxidant surfactants based on gallic acid and hydroxytyrosol, *J Pharm Pharmacol*, 67(7): p.900–908.

- [314] Bergh, M., Magnusson, K., Nilsson, J. L., et al. (1997) Contact allergenic activity of Tween 80 before and after air exposure, *Contact Derm*, 37(1): p.9–18.
- [315] Bodin, A., Shao, L. P., Nilsson, J. L., et al. (2001) Identification and allergenic activity of hydroxyaldehydes - a new type of oxidation product from an ethoxylated non-ionic surfactant, *Contact Derm*, 44(4): p.207–212.
- [316] Sheu, M.-T., Chen, S.-Y., Chen, L.-C., et al. (2003) Influence of micelle solubilization by tocopheryl polyethylene glycol succinate (TPGS) on solubility enhancement and percutaneous penetration of estradiol, *JCR*, 88(3): p.355–368.
- [317] Lemery, E., Briançon, S., Chevalier, Y., et al. (2015) Surfactants have multi-fold effects on skin barrier function, *Eur J Dermatol*, 25(5): p.424–435.
- [318] Thiele, J. J., Rallis, M., Izquierdo-Pullido, M., et al. (1998) Benzoyl peroxide depletes human stratum corneum anti-oxidants, *J Dermatol Sci*, 16: p.S202.
- [319] Lange, R. W., Germolec, D. R., Foley, J. F., et al. (1998) Antioxidants attenuate anthralin-induced skin inflammation in BALB/c mice: role of specific proinflammatory cytokines, *J Leukoc Biol*, 64(2): p.170–176.
- [320] Fruijtjer-Pöllöth, C. (2005) Safety assessment on polyethylene glycols (PEGs) and their derivatives as used in cosmetic products, *Toxicology*, 214(1-2): p.1–38.
- [321] Bárány, E., Lindberg, M., Lodén, M. (2000) Unexpected skin barrier influence from nonionic emulsifiers, *Int J Pharm*, 195(1-2): p.189–195.
- [322] Degim, I., Pugh, W., Hadgraft, J. (1998) Effect of ion complexants on the iontophoresis of salbutamol, *Int J Pharm*, 167(1-2): p.229–231.
- [323] Hatanaka, T., Shimoyama, M., Sugibayashi, K., et al. (1993) Effect of vehicle on the skin permeability of drugs: polyethylene glycol 400-water and ethanol-water binary solvents, *JCR*, 23(3): p.247–260.
- [324] Sarpotdar, P. P., Gaskill, J. L., Giannini, R. P. (1986) Effect of polyethylene glycol 400 on the penetration of drugs through human cadaver skin in vitro, *J Pharm Sci*, 75(1): p.26–28.
- [325] Valia, K. H., Chien, Y. W., Shinal, E. C. (1984) Long-term skin permeation kinetics of estradiol (I): effect of drug solubilizer-polyethylene glycol 400, *Drug Dev Ind Pharm*, 10(7): p.951–981.
- [326] Tsai, J.-C., Shen, L.-C., Sheu, H.-M., et al. (2003) Tape stripping and sodium dodecyl sulfate treatment increase the molecular weight cutoff of polyethylene glycol penetration across murine skin, *Arch Dermatol Res*, 295(4): p.169–174.
- [327] Tsai, J. C., Hung, P. L., Sheu, H. M. (2001) Molecular weight dependence of polyethylene glycol penetration across acetone-disrupted permeability barrier, *Arch Dermatol Res*, 293(6): p.302–307.

- [328] Forst, T., Caduff, A., Talary, M., et al. (2006) Impact of environmental temperature on skin thickness and microvascular blood flow in subjects with and without diabetes, *Diabetes Technol Ther*, 8(1): p.94–101.
- [329] Albrecht, S., Elpelt, A., Kasim, C., et al. (2019) Quantification and characterization of radical production in human, animal and 3D skin models during sun irradiation measured by EPR spectroscopy, *Free Radic Biol Med*, 131: p.299–308.
- [330] Biniek, K., Levi, K., Dauskardt, R. H. (2012) Solar UV radiation reduces the barrier function of human skin, *Proc Natl Acad Sci U S A*, 109(42): p.17111–17116.
- [331] Schwarz, J. C., Klang, V., Hoppel, M., et al. (2012) Corneocyte quantification by NIR densitometry and UV/Vis spectroscopy for human and porcine skin and the role of skin cleaning procedures, *Skin Pharmacol Physiol*, 25(3): p.142–149.
- [332] Engebretsen, K. A., Johansen, J. D., Kezic, S., et al. (2016) The effect of environmental humidity and temperature on skin barrier function and dermatitis, *J Eur Acad Dermatol Venereol*, 30(2): p.223–249.
- [333] Brand, R. M., Wipf, P., Durham, A., et al. (2018) Targeting mitochondrial oxidative stress to mitigate UV-induced skin damage, *Front Pharmacol*, 9: p.920.
- [334] Birch-Machin, M. A., Russell, E. V., Latimer, J. A. (2013) Mitochondrial DNA damage as a biomarker for ultraviolet radiation exposure and oxidative stress, *Br J Dermatol*, 169 Suppl 2: p.9–14.
- [335] Birch-Machin, M. A., Swalwell, H. (2010) How mitochondria record the effects of UV exposure and oxidative stress using human skin as a model tissue, *Mutagenesis*, 25(2): p.101–107.
- [336] Meinke, M. C., Busch, L., Lohan, S. B. (2021) Wavelength, dose, skin type and skin model related radical formation in skin, *Biophys Rev*, 13(6): p.1091–1100.
- [337] Amaro-Ortiz, A., Yan, B., D'Orazio, J. A. (2014) Ultraviolet radiation, aging and the skin: prevention of damage by topical cAMP manipulation, *Molecules*, 19(5): p.6202–6219.
- [338] Lohan, S. B., Müller, R., Albrecht, S., et al. (2016) Free radicals induced by sunlight in different spectral regions - in vivo versus ex vivo study, *Exp Dermatol*, 25(5): p.380–385.
- [339] Brozyna, A., Chwirot, B. W. (2006) Porcine skin as a model system for studies of ultraviolet a effects in human skin, *J Toxicol Environ Health Part A*, 69(12): p.1155–1165.
- [340] Brozyna, A., Wasilewska, K., Wesierska, K., et al. (2009) Porcine skin as a model system for studies of adverse effects of narrow-band UVB pulses on human skin, *J Toxicol Environ Health Part A*, 72(13): p.789–795.

- [341] Keurentjes, A. J., Jakasa, I., John, S. M., et al. (2020) Tape stripping the stratum corneum for biomarkers of ultraviolet radiation exposure at sub-erythemal dosages: a study in human volunteers, *Biomarkers*, 25(6): p.490–497.
- [342] Darr, D., Combs, S., Dunston, S., et al. (1992) Topical vitamin C protects porcine skin from ultraviolet radiation-induced damage, *Br J Dermatol*, 127(3): p.247–253.
- [343] www.paulaschoice.de, Welcher Retinol-Anteil ist am besten für meine Haut? | Paula's Choice. <https://www.paulaschoice.de/de/wie-finde-ich-die-richtige-retinol-staerke>. Accessed 28 May 2022.
- [344] Chilcote, M. E., Guerrant, N. B., Ellenberger, H. A. (1949) Stability of vitamin A acetate under laboratory conditions, *Anal Chem*, 21(8): p.960–963.
- [345] Yin, X., Chen, K., Cheng, H., et al. (2022) Chemical stability of ascorbic acid integrated into commercial products: a review on bioactivity and delivery technology, *Antioxidants (Basel)*, 11(1).
- [346] Hung, C.-F., Chen, W.-Y., Hsu, C.-Y., et al. (2015) Cutaneous penetration of soft nanoparticles via photodamaged skin: Lipid-based and polymer-based nanocarriers for drug delivery, *Eur J Pharm Biopharm*, 94: p.94–105.
- [347] Souto, G. D., Pohlmann, A. R., Guterres, S. S. (2015) Ultraviolet A irradiation increases the permeation of fullerenes into human and porcine skin from C₆₀-poly(vinylpyrrolidone) aggregate dispersions, *Skin Pharmacol Physiol*, 28(1): p.22–30.
- [348] Monteiro-Riviere, N. A., Wiench, K., Landsiedel, R., et al. (2011) Safety evaluation of sunscreen formulations containing titanium dioxide and zinc oxide nanoparticles in UVB sunburned skin: an in vitro and in vivo study, *Toxicol Sci*, 123(1): p.264–280.
- [349] Gęgotek, A., Domingues, P., Skrzydlewska, E. (2020) Natural exogenous antioxidant defense against changes in human skin fibroblast proteome disturbed by UVA radiation, *Oxid Med Cell Longev*, 2020: p.3216415.
- [350] Kawashima, S., Funakoshi, T., Sato, Y., et al. (2018) Protective effect of pre- and post-vitamin C treatments on UVB-irradiation-induced skin damage, *Sci Rep*, 8(1): p.16199.
- [351] Gęgotek, A., Ambrożewicz, E., Jastrząb, A., et al. (2019) Rutin and ascorbic acid cooperation in antioxidant and antiapoptotic effect on human skin keratinocytes and fibroblasts exposed to UVA and UVB radiation, *Arch Dermatol Res*, 311(3): p.203–219.
- [352] Rijnkels, J. M., Moison, R. M. W., Podda, E., et al. (2003) Photoprotection by antioxidants against UVB-radiation-induced damage in pig skin organ culture, *Radiat Res*, 159(2): p.210–217.

- [353] Murray, J. C., Burch, J. A., Streilein, R. D., et al. (2008) A topical antioxidant solution containing vitamins C and E stabilized by ferulic acid provides protection for human skin against damage caused by ultraviolet irradiation, *JAAD*, 59(3): p.418–425.
- [354] Moison, R. M. W., van Beijersbergen Henegouwen, G. M. J. (2002) Topical antioxidant vitamins C and E prevent UVB-radiation-induced peroxidation of eicosapentaenoic acid in pig skin, *Radiat Res*, 157(4): p.402–409.
- [355] Deng, H., Wan, M., Li, H., et al. (2021) Curcumin protection against ultraviolet-induced photo-damage in Hacat cells by regulating nuclear factor erythroid 2-related factor 2, *Bioengineered*, 12(2): p.9993–10006.
- [356] Krol, E. S., Kramer-Stickland, K. A., Liebler, D. C. (2000) Photoprotective actions of topically applied vitamin E, *Drug Metab Rev*, 32(3-4): p.413–420.
- [357] Aziz, M. H., Afaq, F., Ahmad, N. (2005) Prevention of ultraviolet-B radiation damage by resveratrol in mouse skin is mediated via modulation in survivin, *Photochem Photobiol*, 81(1): p.25–31.
- [358] Antille, C., Tran, C., Sorg, O., et al. (2003) Vitamin A exerts a photoprotective action in skin by absorbing ultraviolet B radiation, *J Invest Dermatol*, 121(5): p.1163–1167.
- [359] Tolleson, W. H., Cherng, S.-H., Xia, Q., et al. (2005) Photodecomposition and phototoxicity of natural retinoids, *Int J Environ Res Public Health*, 2(1): p.147–155.
- [360] Nikolić, S., Keck, C. M., Anselmi, C., et al. (2011) Skin photoprotection improvement: synergistic interaction between lipid nanoparticles and organic UV filters, *Int J Pharm*, 414(1-2): p.276–284.
- [361] Pilkington, S. M., Watson, R. E. B., Nicolaou, A., et al. (2011) Omega-3 polyunsaturated fatty acids: photoprotective macronutrients, *Exp Dermatol*, 20(7): p.537–543.
- [362] Wagemaker, T. A. L., Carvalho, C. R. L., Maia, N. B., et al. (2011) Sun protection factor, content and composition of lipid fraction of green coffee beans, *Ind Crops Prod*, 33(2): p.469–473.
- [363] Kaur, C. D., Saraf, S. (2010) In vitro sun protection factor determination of herbal oils used in cosmetics, *Pharmacognosy Res*, 2(1): p.22–25.
- [364] Schneider, S. L., Lim, H. W. (2019) A review of inorganic UV filters zinc oxide and titanium dioxide, *Photodermatol Photoimmunol Photomed*, 35(6): p.442–446.

Chapter 8. Curriculum vitae

Personal data

Name	Reem Mohammed Alnemari
Nationality	Saudi Arabian
Contact	ph.dreem@hotmail.com

Education

2004 - 2009	Doctor of Pharmacy (Pharm.D) King Abdulaziz University, Jeddah, Saudi Arabia
2012 - 2015	Master of Pharmacy Sciences, in major Pharmaceutics King Abdulaziz University, Jeddah, Saudi Arabia

Current work

2009 – Current	Lecturer in the Pharmaceutics and Pharmaceutical Technology department, Pharmacy College, Taif University, Saudi Arabia
2018 - Current	PhD Candidate at the department of Pharmaceutical Technology and Biopharmaceutics, Philips-Marburg University, Germany

Chapter 9. Publications

Original papers

- 1- Abraham, A.M.; Alnemari, R.M.; Jacob, C.; Keck, C.M. (2020) ***PlantCrystals—nanosized plant material for improved bioefficacy of medical plants***, *Materials*, 13, 4368.
- 2- Knoth, D.; Alnemari, R.M.; Wiemann, S.; Keck, C.M.; Brüßler, J. (2021) ***Fingerprint of nature—skin penetration analysis of a stinging nettle plantCrystals formulation***. *Cosmetics*, 8, 21.
- 3- Abraham, A.M.; Alnemari, R.M.; Brüßler, J.; Keck, C.M. (2021) ***Improved antioxidant capacity of black tea waste utilizing PlantCrystals***. *Molecules* 26, 592.
- 4- Keck, C.M.; Abdelkader, A.; Pelikh, O.; Wiemann, S.; Kaushik, V.; Specht, D.; Eckert, R.W.; Alnemari, R.M.; Dietrich, H.; Brüßler, J. (2022) ***Assessing the dermal penetration efficacy of chemical compounds with the ex-vivo porcine ear model***. *Pharmaceutics* 14, 678.
- 5- Alnemari, R.M.; Brüßler, J.; Keck, C.M. (2022) ***Assessing the oxidative state of the skin by combining classical tape stripping with ORAC assay***. *Pharmaceutics* 15, 520.

Oral presentations

- 1- Alnemari, R., Keck, C.M. J., Brüßler, J., (2020) ***Novel ex-vivo model to study skin antioxidants***. The 22nd international conference on oxidative stress reduction, redox homeostasis and antioxidants (Paris Redox 2020), Paris/France, 8-9 October.
- 2- Alnemari, R.M., J., Brüßler, J., Keck, C.M. (2021) ***Oxidative changes in porcine skin model using UV radiation and ascorbic acid***. Annual meeting of the German pharmaceutical society (DPhG), Leipzig/Germany, 28 September – 1 October.

Poster presentations

- 1- Alnemari, R., Carrillo-Hormaza L., Pinnapireddy, S.R., Keck, C.M. (2019) **Determination of antioxidant capacity in skin using ORAC assay**. Annual meeting of the German pharmaceutical society (DPhG), Heidelberg/Germany, 01-04 September.
 - 2- Abraham, A., Alnemari, R., Keck, C.M. (2019) **Sustainable nano products: production and characterization of PlantCrystals from the waste of black tea as a source of antioxidant phenolic compounds**. Annual meeting of the German pharmaceutical society (DPhG), Heidelberg/Germany, 01-04 September
 - 3- Abraham, A.; Alnemari, R.; Keck, CM. (2019) **PlantCrystals a novel principle for the formulation of natural cosmetics**. Annual SEPAWA congress, Berlin/Germany, 28.- 30. October.
 - 4- Abraham, A.; Alnemari, R.; Keck, CM. (2019) **Improved antioxidant capacity through Nano-Nutraceuticals: production and characterization of black tea PlantCrystals**. 46th Annual meeting of controlled release society (CRS), Valencia/Spain, 21.- 24. July.
 - 5- Alnemari, R., Azizi. S., Macht, J., Brüßler, J., Keck, C.M. (2020) **Novel model to detect antioxidant capacity of cosmeceuticals in skin**. Controlled release society (CRS) virtual annual meeting, June 29 - July 3.
 - 6- Alnemari, R.M., J., Brüßler, J., Keck, C.M. (2021) **Antioxidant and pro-oxidant effect of antioxidants on skin**. 13th Central European symposium on pharmaceutical technology (CESPT), Gdańsk/Poland, 16-18 September.
-